# Modulation of tactile and visuotactile perception by transcranial alternating current stimulation

### Dissertation

zur Erlangung des akademischen Grades eines Doktors der Medizin (Dr. med.)

an der

Medizinischen Fakultät der Universität Hamburg

vorgelegt von

Darius Zokai

aus

Frankfurt am Main

Betreuer:in / Gutachter:in der Dissertation: Prof. Dr. Andreas K. Engel

Gutachter:in der Dissertation: PD Dr. Gregor Leicht

Vorsitz der Prüfungskommission: PD Dr. Gregor Leicht

Mitglied der Prüfungskommission: PD Dr. Bastian Cheng

Mitglied der Prüfungskommission: PD Dr. Thomas Sauvigny

Datum der mündlichen Prüfung: 17.10.2025

## **TABLE OF CONTENT**

1.	GEN	NERAL INTRODUCTION	6
1.1.	Α	im of this thesis	6
1.2.	N	Notion perception	6
1.2	2.1.	Ambiguous tactile apparent motion perception	9
1.2	2.2.	Unambiguous visuotactile apparent motion perception	16
1.3.	N	leural oscillations	19
1.4. cohe		leural synchronization and coherence: binding-by-synchrony and communication- through-	21
1.5.	G	amma oscillations and bistable perception	23
1.6.	N	Ion-invasive brain stimulation and transcranial alternating current stimulation (tACS)	25
2.	GEN	NERAL OVERVIEW OF THE METHODOLOGY	34
2.1.	P	articipants	34
2.2.	T	actile stimuli	35
2.3.	T	ACS protocol	36
2.4.	D	ata and statistical analyses	41
3.	МО	DULATION OF AMBIGUOUS TACTILE APPARENT MOTION PERCEPTION BY TACS	5. 41
3.1.	lr	ntroduction	41
3.2.	N	Naterials and methods	43
3.2	2.1.	Participants	43
3.2	2.2.	Experimental paradigm and tactile SAM stimulus	43
3.2	2.3.	TACS protocol	
3.2	2.4.	Pupillometry and gaze data	54
3.2	2.5.	Hypothesis	55
3.3.	S	tatistical analyses and results	56
3.3	3.1.	Normalized percept time (NPT)	59
3.3	3.2.	Button press per minute (BPM)	78

3.3.3	Analyses of cumulative gamma distribution functions (gCDF) of NPTs	85
3.3.4	l. Exploratory analyses of pupil dilatation	102
3.4.	Discussion	109
3.4.1	Phase specific <i>tACS</i> effect on normalized percept time (NPT)	110
3.4.2	Phase specific tACS effect on button press per minute (BPM)	114
3.4.3	Analyses of cumulated gamma distribution functions	115
3.4.4	Pupil dilation is indicative prior to perceptual formation	118
3.4.5	Ch	•
cond	lition	119
3.5.	Conclusion	120
	MODULATION OF UNAMBIGUOUS VISUOTACTILE APPARENT MOTION PER	122
4.2.	Materials and methods	122
4.2.1	L. Participants	122
4.2.2	2. Visuotactile stimuli	122
4.2.3	B. Experimental paradigm of the unambiguous visuotactile apparent motion stimulus (F	igure 41) 124
4.2.4	I. TACS protocol	129
4.2.5	5. Hypothesis	133
4.3.	Statistical analyses and results	133
4.3.1	Accuracies	134
4.3.2	2. Reaction times	139
4.3.3	3. Rate Correct Score	146
4.3.4	I. Signal Detection Theory parameters: sensitivity (d') and bias (c)	152
4.3.5	Non-parametric permutational statistical analyses of reaction time distributions	160
4.4.	Discussion	166
4.4.1 sensi	No phase specific <i>tACS</i> effect for accuracies (ACC), reaction times (RT), Rate Correct S itivity index (d') and decision boundary (criterion c)	• •
4.4.2	Phase specific tACS effect for correct reaction time data	170
4.5.	Conclusion	171
5. G	ENERAL DISCUSSION	172

ь.	GENERAL SUMMARY	. 1/6
7.	SUPPLEMENTARY MATERIAL – TABLES	. 180
7.1.	Modulation of ambiguous tactile apparent motion perception by tACS	180
7.2.	Modulation of unambiguous visuotactile apparent motion perception by tACS	199
8.	LIST OF ABBREVIATIONS	. 212
9.	LIST OF ILLUSTRATIONS	. 214
10.	LIST OF TABLES	. 218
11.	BIBLIOGRAPHY	. 220
12.	DECLARATION OF THE PERSONAL CONTRIBUTION	. 231
13.	EIDESSTATTLICHE VERSICHERUNG	. 232
14.	ACKNOWLEDGEMENT	. 233

#### 1. General Introduction

#### 1.1. Aim of this thesis

The present thesis aims to expand our understanding of transcranial alternating current stimulation (tACS) as an instrument for modulating sensory perception and processing in humans. Specifically, the principal objective of this dissertation is to analyze and investigate the potential neuromodulatory effects of tACS on ambiguous tactile and unambiguous visuotactile apparent motion perception in humans. This research seeks to contribute to the existing body of knowledge on the use of tACS as a neuromodulatory device.

#### 1.2. Motion perception

Perception and its underlying neural processes have been a significant focus under investigation in neuroscientific research for decades (Engel & Fries, 2016; Kandel et al., 2012: 449 – 711). The interplay between anatomical structures and physiological functions, which ultimately lead to a conscious perception of ourselves, and our environment have neither been finally clarified, nor fully understood (Crick & Koch, 2003; Engel & Fries, 2016). In recent years, however, our understanding of the neural basis of perceptual functions in different modalities has increased significantly (Crick & Koch, 2003; Engel & Fries, 2016; Kandel et al., 2012: 449 – 711). In particular, the scientific dissection of sensory, perceptual, and cognitive subfunctions and their neural foundations form an elementary component in explaining specific perceptual and cognitive states as well as different states of consciousness (Crick & Koch, 2003; Engel & Fries, 2016; Kandel et al., 2012: 449 – 711).

Recent neurocognitive frameworks emphasize a distinction between sensation and perception (Aggelopoulos, 2015; Goldstein, 2009: 1011-1013). In neuroscientific terminology, sensation refers to the early stages of sensory processing in which sensory receptors detect, transmit and transduce environmental stimuli to the central nervous system (Goldstein, 2009: 1011-1013). The concept describes a bottom-up or data-driven approach to processing sensory information in which raw sensory data is analyzed, extracted, and encoded into neural signals that are transmitted to the central nervous system (Aggelopoulos, 2015; Goldstein, 2009: 1011–1013). Bottom-up processing lays the foundation for subsequent stages of perceptual processing and provides initial input for constructing higher-level perceptions (Goldstein, 2009: 1011–1013).

Perception, in contrast to sensation, entails the organization, interpretation, and conscious experience of those sensations, encoded in neuronal signals (Aggelopoulos, 2015; Goldstein, 2009: 1011-1013). Perception is therefore assumed to be an active and dynamic process of information evaluation and interpretation, primarily conducted by cortical areas. Sensation, on the other hand, characterizes the initial stage of receiving environmental information, which subsequently undergoes neural coding within the respective sensory modalities (Aggelopoulos, 2015; Goldstein, 2009: 1011-1013). Associated with the concept of perception is the reference to top-down processing (Aggelopoulos, 2015; Goldstein, 2009: 1011-1013). Top-down processing states that perception and its neural cortical underpinnings involve a constant process of actively comparing stimulus patterns with previously stored neural representations and further actively inferring and predicting upcoming stimuli patterns based on prior knowledge and neural network activity configurations (Aggelopoulos, 2015; Goldstein, 2009: 1011-1013). This concept highlights the integrative nature of perception, where the brain actively engages in top-down processes to shape and refine the interpretation of sensory information, leveraging internal models and cognitive factors to generate meaningful perceptual experiences. The perception of coherent motion is considered to be a fundamental property of human sensory experience, allowing us to effectively navigate and interact with our environment. For neuroscientific researchers, investigations of motion perception are of special interest, as they may provide insights into the complex interaction of the neural mechanisms underlying our perception of the dynamic world around us. The perception of coherent motion may be one of the major challenges and an essential function accomplished by our perceptive systems (Goldstein, 2009: 571 – 583; Kandel et al., 2012: 449 - 711; Vitello, 2010). From an evolutionary perspective, motion perception may be critical for identifying moving animals and thus generating attention and vigilance towards a potential threat and predicting a potentially adverse outcome (Goldstein, 2009: 571 – 583; Vitello, 2010). Moreover, during locomotion, motion perception could provide the perceiving organism with critical information about the object itself as well as about the spatial relationship between the stationary and non-stationary environment (Goldstein, 2009: 571 – 583; Vitello, 2010).

In summary, the ability to extract meaningful motion information from our sensory inputs and integrate them into a coherent perceptual representation is essential for our understanding of the environment and for effective behavioral responses. Regarding everyday life situations, the visual modality seems to provide the most accurate information about motion perception (Goldstein, 2009:

571 – 583; Kandel et al., 2012: 449 – 711; Soto-Faraco & Väljamäe, 2012). This assumption is reflected in decades of intense investigations regarding motion perception in the visual domain (Goldstein, 2009: 571 - 583; Soto-Faraco & Väljamäe, 2012). Motion perception in the domain of the somatosensory system as well as the auditory system is far less investigated and comprehended in relation to visual motion perception (Soto-Faraco & Väljamäe, 2012; Vitello, 2010). In the early stages of neurocognitive research basic stimuli have been used to assess and investigate fundamental properties of coherent motion perception (Goldstein, 2009: 469 – 472; van Schiller, 1933). As the fields of neuroscience and psychology have evolved, various stimulus designs have employed the phenomenon of apparent motion patterns to dissect the cognitive subfunctions underlying motion perception (Goldstein, 2009: 469-472). In general, apparent motion can be understood as one of the most common types of illusory motion perception: static stimuli, which are presented in a predefined temporal and spatial sequence, are subjectively perceived as coherent motion patterns (Goldstein, 2009: 571 – 583). This elementary phenomenon seems to be ubiquitous in everyday life situations: e.g., the rapid presentation of static images creates the illusion of movement and moving scenery in a film. Especially, in recent decades the understanding of visual motion perception was further expanded. A major contribution to this field is the two-stream hypothesis proposed by Goodale and Milner in 1992. This model synthesizes neuroanatomical and neurophysiological evidence to suggest the existence of two distinct neural processing streams within the central nervous system (Goodale & Milner, 1992). According to this hypothesis a ventral and a dorsal neural processing stream represent specific neural pathways for distinct cognitive operating mechanisms (Goodale & Milner, 1992). Both streams originate in the primary visual cortex (Goodale & Milner, 1992). The dorsal stream propagates towards the parietal lobe, whereas the ventral stream propagates to the temporal lobe (Goodale & Milner, 1992). The ventral stream is primarily associated with a functional role in cognitive processes concerning recognition and identification, whereas, regarding the distinct subfunction of motion perception, the dorsal stream seems to have a prominent function (Goodale & Milner, 1992). Notably, research findings indicate that the middle temporal area (MT) within the extrastriate cortex exhibits a high concentration of neurons sensitive to the direction of motion (J. H. Maunsell & van Essen, 1983). This area is believed to serve as an integration hub for the processing of complex and even multimodal visual motion signals (van Kemenade et al., 2014). Interestingly, neurons of the MT area are believed to comprise of receptive fields, that cross the vertical meridian (Rose, 2005). In addition, anatomical

marker studies have revealed direct neuronal interaction links between contralateral MT areas (J. H. R. Maunsell & van Essen, 1987). These properties may be advantageous for integrating visual motion signals, that span across both visual hemifields and are represented across both hemispheres (Rose, 2005). The question of whether the perception of motion as a general mechanism is represented by a supramodal mechanism comprising neural signal integration in superior cortical brain areas, or whether every distinct modality has its own motion-perceiving module represented within the respective primary neural cortical area, remains unresolved. To date, the nature of motion perception as a universal mechanism remains elusive, raising questions of its neural representation (Harrar et al., 2008; Sanchez et al., 2020). One hypothesis proposes the existence of a supramodal mechanism by which neural signals from various sensory modalities are integrated within higher-level cortical areas (Harrar et al., 2008; Sanchez et al., 2020). This supramodal perspective suggests that motion perception is not confined to a specific sensory modality, but rather involves the convergence of information from different sensory channels in higher cortical brain areas (Lewis et al., 2000; Harrar et al., 2008; Sanchez et al., 2020). On the other hand, an alternative hypothesis proposes that each sensory modality has its own module for the perception of motion, localized within the respective primary cortical area responsible for processing that modality (Harrar et al., 2008). According to this theory, different neural circuits within the primary sensory cortices process the perception of motion in their respective sensory domains (Harrar et al., 2008).

#### 1.2.1. Ambiguous tactile apparent motion perception

Principally, sensory systems are limited in their capacity to represent the full range of physical environmental information (Kandel et al., 2012: 449 – 711). In everyday situations, human sensory organs are often confronted with incomplete and inherent ambiguity of (natural) stimuli (Kandel et al., 2012: 449 – 711; Kersten et al., 2004; Vitello, 2010). These ambiguities and restrictions of sensory input necessitate adaptation, extrapolation, and reconstruction processes (top-down processes) of incomplete environmental information performed by perceptual systems in order to form coherent and meaningful interpretations of our environment (Kersten et al., 2004; Kornmeier & Mayer, 2014). In neuroscientific research, extreme instances of ambiguous stimulus patterns have attracted sizeable interest as perceptual and cognitive stimuli (Blake & Logothetis, 2002; Schwartz et al., 2012). Famous examples of such stimuli of pronounced ambiguity and multistable perceptual states include the

Necker cube and Borings old and young women (Necker, 1832; Boring, 1930). These stimuli elicit multiple and shifting perceptual interpretations. Another prominent version of multistability arises by exposing distinct visual stimuli separately to each eye (Blake & Logothetis, 2002). The conscious perceptual state spontaneously alternates between the two images presented (Blake & Logothetis, 2002). This phenomenon is known as binocular rivalry (Blake & Logothetis, 2002).

Predominantly, ambiguous perception has been studied in the visual modality (Schwartz et al., 2012). Nevertheless, the auditory, olfactory, visual, and tactile domain have been observed to exhibit features of multistable and bistable perceptual phenomena (Schwartz et al., 2012). Semantic bistability has even been reported in speech perception (Schwartz et al., 2012). This broad range of sensory modalities exhibiting such phenomena highlights the universality and complexity of ambiguous perception. The popularity of ambiguous stimuli is founded in the fact, that the objective physical stimulation remains constant over time, whereas the conscious subjective perceptual state alternates between distinct and valid interpretations of the sensory stimulus (Blake & Logothetis, 2002; Schwartz et al., 2012). Consequently, the resulting distinctive neural activity measured during the respective perceptual state can be attributed and interpreted as representing the respective distinct conscious perceptual state (Blake & Logothetis, 2002; Schwartz et al., 2012). Interestingly, general principles regarding ambiguous and multistable stimuli can be derived (Blake & Logothetis, 2002; Schwartz et al., 2012; Liaci et al., 2016). First, reported perceptual transitions show a probabilistic profile that can be approximated by a gamma distribution (Brascamp et al., 2005). Secondly, depending on the ambiguity of the stimulus, perceptual alternations are often perceived as distinct and mutually exclusive (Conrad et al., 2012). Finally, the timing and occurrence of perceptual alternations can be influenced by volition (Kornmeier et al., 2009). Nevertheless, it should be considered that a major pitfall of these types of stimuli may be their inherent subjective nature (Blake & Logothetis, 2002). Consequently, experimental settings utilizing ambiguous or multistable stimulus settings are entirely dependent on the trustworthiness of participants' subjective responses (Blake & Logothetis, 2002). Therefore, for some experimental designs, it may be crucial that participants are not enlightened by the specific hypotheses of the study (Blake & Logothetis, 2002).

In the visual domain, von Schiller (1933) introduced the ambiguous stroboscopic alternative motion (SAM) stimulus. This stimulus design consists of two diagonally paired light dots, presented at opposite corners of an imaginary rectangular frame (Schiller, 1933). Subsequent temporal activation of the

opposing diagonal light dots results in a coherent perception of a moving stimulus (Chaudhuri & Glaser, 1991; Hock et al., 2005; Schiller, 1933). Furthermore, continuous stimulation streams of the light dots cause participants to spontaneously alternate between two distinct perceptual states: the apparent direction of motion is perceived as a *horizontal* or a *vertical* anti-parallel *motion direction* (Chaudhuri & Glaser, 1991).

This apparent motion stimulus is also referred to as the "apparent motion quartet" (Carter et al., 2008). Interestingly, the perception of the orientation of the apparent motion can be modulated by adjusting the aspect ratio, which is defined as the ratio of *vertical* distance to *horizontal* distance of the light dots:

$$AR(aspect\ ratio) = \frac{vertical\ distance}{horizontal\ distance}$$
 (Chaudhuri & Glaser, 1991).

Further investigations revealed a sigmoidal psychometric relationship between the aspect ratio and the proportion of perceived direction in the apparent motion pattern, at least for the visual modality (Chaudhuri & Glaser, 1991). Small aspect ratios, reflected in relatively large horizontal distances, bias the perceptual state towards a vertical perception of apparent motion, whereas large aspect ratios (reflected in relatively small horizontal distances) result in a biased perception towards a horizontal direction of apparent motion (Chaudhuri & Glaser, 1991; Hock et al., 2005). Interestingly, at an aspect ratio of 1, a typical predominance of vertical perception is observed (Chaudhuri & Glaser, 1991; Hock et al., 2005). While an aspect ratio of approximately 1,2 results in a peak of ambiguity and instability of an apparent motion direction perception reflected in a peak of perceptual switching rates (Chaudhuri & Glaser, 1991; Hock et al., 2005). Interestingly, the vertical motion perception bias observed for equidistant horizontal and vertical visual token distances disappears, if all four diagonal visual dots are presented within a single visual hemifield (Chaudhuri & Glaser, 1991). This phenomenon may imply the involvement of transcallosal neuronal information processing in the described perceptual bias (Rose, 2005). This hypothesis is supported by animal studies demonstrating that synchronized gamma band activity across the hemispheres abolished when the corpus callosum is transected (Engel et al., 1991). In addition, visual perception of apparent horizontal motion appears to be impaired in patients with surgical division of the corpus callosum (Gazzaniga, 1987). These results provide further indication for the critical function of interhemispheric communication in modulating apparent motion perception. The distinctive characteristics of the visual SAM stimulus were postulated to result from interhemispheric integration (Rose, 2005; Helfrich et al., 2014). As an explanation of the empirical evidence, the interhemispheric integration hypothesis was established.

In summary, this theory suggests that as the right and left visual hemifields are represented in opposite hemispheres of the brain, vertical motion is represented within one hemisphere, whereas horizontal motion requires integration of processed information between hemispheres. Therefore, encoded horizontal motion may be more challenging and a less favored resolution during metastable and ambiguous states of perception. (Chardhuri & Glaser et al., 1991; Helfrich et al., 2014; Strüber et al., 2014). The phenomenon of ambiguous apparent motion perception extends beyond the visual domain and has been demonstrated in the tactile modality (Carter et al., 2008; Conrad et al., 2012; Darki & Rankin, 2021; Harrar & Harris, 2007; Harrar et al., 2008; Liaci et al., 2016; Vitello 2010). Harrar and Harris (2007) explicitly demonstrated that the grouping principles of gestalt theory and tactile ambiguity also apply to the tactile domain (Harrar & Harris, 2007). They developed a tactile version of the "Pikler-Ternus effect", consisting of sequential streams of tactile stimulation (Harrar & Harris, 2007). Depending on the inter stimulus interval, the apparent motion pattern of the stimuli is likely to be perceived as either a "group motion" pattern or an "element motion" pattern (Harrar & Harris, 2007). Additionally, they designed experimental conditions, that entailed unimodal visual ambiguous stimuli as well as bimodal visuotactile ambiguous stimuli (Harrar & Harris, 2007). The perceptual principles of the tactile sense were discovered to operate in a fundamentally similar manner compared to the visual modality (Harrar & Harris, 2007, Harrar et al., 2008). Nevertheless, perceptual alterations were reported to be less dynamic compared to the visual modality (Harrar & Harris, 2007). Moreover, further investigations regarding the bimodal experimental version suggested a distinct intersensory grouping mechanism for the tactile, visual, and bimodal domains (Harrar & Harris, 2007; Harrar et al., 2008). Carter et al. (2008) postulated the initial evidence that bistable perceptual states can be produced by a tactile version of the SAM stimulus (Carter et al., 2008). By applying successive alternating streams of tactile stimulation to the fingertip with an experimental array of approximately one cm2 in size, participants reported spontaneous reversals of their perceptual states in the direction of either a vertical or horizontal apparent tactile motion pattern (Carter et al., 2008). Interestingly, variations in aspect ratio did not have a pronounced effect on the perceptual disambiguation of the tactile stimulus (Carter et al., 2008). Furthermore, it should be noted that the quality of tactile motion perception was described as a smooth physical transition across the fingertip, even though the

stimulus consisted of discrete stimulation points with a separated inter-stimulus interval of 300 ms (Carter et al., 2008). Another extended variation of the tactile version of the SAM stimulus was investigated by Conrad et al. (Conrad et al., 2012). They designed a visuotactile experiment consisting of four small LEDs attached to four coin-sized tactile vibration stimuli placed on an imaginary rectangle on the medial side of each index finger of each corresponding hand (Conrad et al., 2012). This design allowed for spatially and temporally coupled presentation of the visuotactile stimuli (Conrad et al., 2012).

The experimental procedure consisted of a *unimodal* tactile condition, a *unimodal* visual condition, and a bimodal condition involving *congruent* or *incongruent* visuotactile stimulation (Conrad et al., 2012). In addition, the experimental procedure included three different fixed distances between the index fingers, which allowed them to test for aspect ratio dependencies (Conrad et al., 2012). In the *congruent* visuotactile and *unimodal* tactile stimulation condition, it was observed that the dynamic reversals of the coherent motion percept were reduced, suggesting a more stable percept of coherent motion for the tactile modality (Conrad et al., 2012). In particular, the perceived direction of coherent motion could be represented as a function of the inter index finger distance, also referred to as the "horizontal" or "between finger distance" (Conrad et al., 2012). For small inter-finger distances (AR = 0.5), the dominant *perceived motion direction* was primarily *horizontal*, whereas for large inter-finger distances (AR = 2), the *vertical* motion percept prevailed (Conrad et al., 2012). For intermediate inter finger distances (AR = 1) approximately equal motion percept patterns were observed (Conrad et al., 2012). Nevertheless, compared to the visual version of the SAM stimulus, the disambiguation effect of the aspect ratio on the SAM stimulus for the tactile modality is much less pronounced, even for more extreme aspect ratios (Conrad et al., 2012).

Correspondingly, comparable results were observed by Vitello (Vitello, 2010). In a similar manner to Conrad et al., tactile stimulation patterns were applied to the medial side of the index finger, and the aspect ratio was systematically varied in categories of 0.25, 0.5, 1, 2, and 4. The experimental investigation revealed that the perception of the tactile *motion direction* could be described as a linear function depending on the independent variable of the aspect ratio (Vitello, 2010). In other words, smaller inter index finger distances (between finger distances) biased participants' perceptions towards a *horizontal* motion perception, whereas larger inter index finger distances resulted in a biased participants' perception towards a *vertical* perception (Vitello, 2010). Interestingly, more

extreme aspect ratios did not reveal a pronounced shift of the perceived tactile motion direction (Vitello, 2010). Furthermore, it should be noted that the linear relationship between the aspect ratio and the SAM stimulus stands in contrast to the visual SAM stimulus, which is rather described as a sigmoidal shaped psychometric function (Conrad et al., 2012, Liaci et al., 2016; Vitello, 2010). Liaci et al. further investigated the role of the aspect ratio of the SAM stimulus in the tactile modality (Liaci et al., 2016). In addition, they investigated the perception of tactile apparent motion perception through the premise of "endogenous-" and "exogenous reference frames" (Liaci et al., 2016). The authors characterize the "endogenous reference frame" as a "somatotopic" or "skin-based reference frame" to which the spatial information of a tactile stimulus can be referenced (Liaci et al., 2016). Furthermore, the tactile stimulation can be mapped "to an exogenous space-based" or "world-based reference frame" (Liaci et al., 2016). Regarding the "endogenous reference frame" Liaci et al. further elaborate that encoded stimuli are represented in relation to an individual "body surface", whereas the "exogenous reference frame" refers to encoded stimuli referenced to external (world) representation (Liaci et al., 2016). Considering that only the "exogenous reference frame" is accessible in the visual modality, the authors speculated that, the small disambiguation effect of the aspect ratio in the tactile domain might be attributable to integrating conflicting information regarding these two "reference frames" (Liaci et al., 2016). Another aspect which might contribute to the diminished influence of the AR for the tactile SAM stimulus "may be a different spatial scaling" in the tactile modality compared to the visual domain (Liaci et al., 2016). To further investigate these hypotheses two pairs of tactile stimulators were placed on an imaginary rectangle on each forearm of each participant (Liaci et al., 2016). By systematically manipulating the aspect ratio towards more extreme values than previously investigated by Vitello (2010) and Conrad et al. (2012), they observed only a minimal effect on the disambiguation of perceptual states compared to the visual modality (Liaci et al., 2016). Interestingly, the "exogenous reference frame" can be systematically manipulated by rotating forearm positions (e.g., crossed forearm posture) (Liaci et al., 2016). Shared characteristics of the visual and tactile domains are observed in the dependence of the perceived direction of the apparent motion on the aspect ratio (Liaci et al., 2016). These findings are consistent with previous studies of tactile ambiguous motion perception (Conrad et al., 2012; Vitello, 2010). Furthermore, there appears to be a general bias for the perceived direction of vertical tactile apparent motion (Liaci et al., 2016). Nevertheless, differences between modalities are also emphasized (Liaci et al., 2016). The tactile

stimulus differs considerably compared to the visual modality in aspects of stimulus size, timing and inter stimulus intervals (Liaci et al., 2016). Compared to the visual domain, even substantial alterations of the visual SAM stimulus, such as stimulus size and inter stimulus interval, do not alter the perception of apparent motion patterns or the influence of the aspect ratio (Liaci et al., 2016). This clearly robustness of the SAM highlights the visual stimulus (Liaci et al., 2016). Furthermore, another explanation of the differences in modalities may be attributed by reconciling conflicting information of the "endogenous" and "exogenous reference frames" (Liaci et al., 2016). A long-standing debate revolves around the existence of a supramodal common mechanism with a potentially common neural source resolving ambiguity (Liaci et al., 2016). This question refers to the aforementioned concepts of bottom-up and top-down processing in cognitive neuroscience. The bottom-up approach suggests that the effect of disambiguation develops at low levels of information processing in the respective modality, whereas the top-down view presumes a perceptual and cognitive supramodal resolving mechanism represented in neural networks and higher order brain areas (Liaci et al., 2016). Regarding the common features of the tactile and visual SAM stimulus, the hypothesis of interhemispheric integration has been proposed to explain the vertical bias in the apparent motion direction given aspect ratios close to one (Chaudhuri & Glaser, 1991; Helfrich et al., 2016). According to this hypothesis, the visual hemifields are neurally processed in contralateral brain areas (Chaudhuri & Glaser, 1991; Helfrich et al., 2016). Consequently, the perception of vertical motion direction is processed within hemispheres, whereas the perception of a coherent motion direction of a horizontal pattern requires integration across both hemispheres (Helfrich et al., 2016; Rose, 2005). As a result, the perception of horizontal motion direction may require more resources and thus be less "preferred" due to the disambiguation effect of a given aspect ratio close to one (Chaudhuri & Glaser, 1991; Helfrich et al., 2016).

Correspondingly, the same rationale might be applied to the tactile modality (Liaci et al., 2016). The "endogenous reference frame" may be founded in the neuronal somatotopic representation of the body surface (Liaci et al., 2016). The right forearm is neurally represented in the left hemisphere, whereas the left forearm is neurally represented in the right hemisphere. Consequently, withinforearm (intra-forearm, *vertical*) motion could be processed within one hemisphere, whereas between-forearm (inter-forearm, *horizontal*) motion could be processed by integrating the perceptual information between the hemispheres in order to form a coherent motion perception (Liaci et al.,

2016). Consequently, this theory could explain a *vertical* bias for the tactile modality (Liaci et al., 2016). In summary, ambiguous apparent motion stimuli appear to be suited to study bistable perceptual processes in visual and tactile modalities (Liaci et al., 2016). Investigations regarding the visual SAM stimulus depict a sigmoidal dependence of the perceived apparent *motion direction* from the aspect ratio (Chaudhuri & Glaser, 1991; Liaci et al., 2016). The magnitude of the disambiguation effect is clearly enhanced by increasing or decreasing the aspect ratio to extreme values (Chaudhuri & Glaser, 1991, Hock et al., 2005). Intermediate aspect ratios (around one) elicit bistable apparent motion percepts, altogether with a *vertical* perceptual bias for aspect ratios of one (Chaudhuri & Glaser, 1991; Rose, 2005). In the tactile domain, the scientific basis is less well founded (Liaci et al., 2016). This is reflected in a diminished disambiguation effect for extreme aspect ratios and the linear relationship between the aspect ratio and the perceived direction of the apparent motion (Liaci et al., 2016). Overall, the bistability of the SAM stimulus can be considered as generally comparable for the different modalities (Liaci et al., 2016). Nevertheless, evidence for a postulated role of a central supramodal disambiguation mechanism seems rather unlikely (Liaci et al., 2016).

#### 1.2.2. Unambiguous visuotactile apparent motion perception

In situations we encounter in our daily lives, we are continuously presented with a variety of natural stimuli. These stimuli naturally activate our receptive organs in more than just one sensory modality. For example, when we perceive an object, the visual system encodes its color, shape, height, and length, while tactile and proprioceptive organs process information about its texture and weight. In addition, the object may have a distinct smell and taste, stimulating olfactory and gustatory senses, and it may produce specific sounds, activating the auditory system. This example illustrates that perception in natural settings can generally be understood as a multisensory process, requiring an integrative mechanism by our central nervous system in order to give rise to coherent and meaningful interpretations of the environmental world around us (Calvert et al., 2004; Kandel et al., 2012). Often, it is only in the case of functional failures that we realize the significance of these fundamental properties for perception. But not only functions like perception are highly influenced by multisensory processes. Also, cognitive functions and learning processes are significantly impacted by multisensory mechanisms (Calvert et al., 2004).

Coherent multisensory motion perception, although evidently one of the most important fundamentals of perception, has received rather less attention in the past by neuroscientific researchers regarding multisensory integration. Furthermore, many investigations in cognitive neuroscience studying multisensory integrational properties applied rather static than dynamic stimuli (Calvert et al., 2004). In this section further investigations will be explored that examine multisensory interaction effects of apparent motion phenomena.

Interestingly, early studies combining auditory and visual apparent motion streams did not reveal significant differences in performance levels when the motion direction of the bimodal pattern was congruent or incongruent (Calvert et al., 2004). Nevertheless, it should be highlighted that in in these early investigations, auditory and visual stimuli were presented in a spatially (but not temporally) decoupled relationship (Calvert et al., 2004). More recent studies have provided evidence for the existence of cross-modal effects on the perception of motion patterns (Calvert et al., 2004). For example, in ambiguous visual motion settings, participants showed a tendency to perceive the directional visual motion pattern of an unambiguous presented auditory motion stimulus (Calvert et al., 2004). Another variation of multisensory apparent motion perception task in the visual and auditory domains has been explored by introducing spatially and temporally coupled auditory and visual stimuli to participants (Soto-Faraco et al., 2002). Bimodal stimuli were presented in a congruent or incongruent horizontal (left to right versus right to left) motion direction, as well as a synchronous or asynchronous pattern. In this context, synchronous and asynchronous refer to visual light dots, which are presented in a temporally interval of 0 ms or 500 ms, whereas congruence refers to the directional pattern of the bimodal stimulus (Soto-Faraco et al., 2002). Participants were instructed to ignore the visual modality and just reported their perception of the auditory direction pattern (Soto-Faraco et al., 2002). The results of this experiment showed that in the synchronously congruent condition, participants reached the highest performance levels, whereas in the synchronous incongruent (conflicting) trials participants performed at chance levels (Soto-Faraco et al., 2002). Interestingly, in the asynchronous trials no effect of congruency could be observed, and participants reported all auditory direction patterns accurately, regardless of the factor of congruent or incongruent trials (Soto-Faraco et al., 2002). This finding is consistent with evidence of audiovisual integration, which suggests that multisensory integration aborts for asynchronies greater than approximately 200 ms (Soto-Faraco et al., 2002). The authors speculate that these results may reflect the dominance of

the visual modality over the auditory modality in terms of *motion direction* patterns (Soto-Faraco et al., 2002). Another possible explanation could be that visual stimuli induce an illusory reversal of the directional patterns of the auditory motion stimulus, leading to a phenomenon known as the "capture effect". A concrete instance of visual capture can be illustrated when a sound, usually perceived as moving from left to right, coincides with the observation of a visual stimulus moving from right to left (Soto-Faraco et al., 2002). This results in the perception that both stimuli (the auditory stimulus and the visual stimulus) are moving from right to left. This interpretation is supported by the qualitative feedback provided by the participants regarding their perception during the experiment (Soto-Faraco et al., 2002). An extension of this experiment using confidence ratings of participants revealed that, confidence levels remained high even for the *incongruent* trials (Calvert et al., 2004). However, it is not clearly established, whether these bimodal interaction effects evolve from decisional, or post perceptual processes or if they represent a perceptual cross-modal interaction effect during an early step of sensory processing (Calvert et al., 2004; Soto-Faraco et al., 2002).

Evidence for multisensory integration of apparent motion stimuli has been incomplete and sometimes leaves central methodological questions unanswered (Calvert et al., 2004). Early investigations often presented stimuli in a spatially or temporally decoupled manner, thereby reducing potential cross-modal integration effects (Calvert et al., 2004). Another aspect regards the importance of the dynamic characteristics of stimuli. Accumulating evidence in recent years suggests, that dynamic properties of continuous and apparent motion stimuli exhibit features of cross modal effects, which exceed multisensory stimulus processing with static stimuli features (Calvert et al., 2004).

Furthermore, it remains rather unclear on which level multisensory integration effects occur. Most likely cognitive (post-perceptional) and decisional inferences may be involved as well as perceptual processes at an early level of informational processing of dynamic events (Calvert et al., 2004). Nevertheless, post-perceptual cognitive processes may not be specifically related to the integration of multisensory dynamic motion stimuli (Calvert et al., 2004). Isolating the individual components of the different levels of multisensory motion processing proves to be a difficult undertaking. However, recent evidence suggests, in correspondence with other multisensory phenomena, that primary perceptive multimodal processes play fundamental role in the integration of dynamic motion perception (Calvert et al., 2004; Soto-Faraco et al., 2004). In addition, effects of modality dominance for dynamic interactions have been observed (Soto-Faraco et al., 2002; Soto-Faraco et al., 2004). The

visual modality appears to significantly influence the perception of auditory motion perception, while the reverse effect could not be clearly established (Soto-Faraco et al., 2002; Soto-Faraco et al., 2004). These results have been consistently replicated under different experimental conditions and methods (Calvert et al., 2004; Soto-Faraco et al., 2002; Soto-Faraco et al., 2004). In general, it may be inferred that the visual domain has greater influence than other sensory modalities regarding the perception of motion (Soto-Faraco et al., 2002; Soto-Faraco et al., 2004). Nevertheless, the assumed visual effect may not be explained by mere dominance (Soto-Faraco et al., 2002; Soto-Faraco et al., 2004). The relationship between cross modal interactions of dynamic motion stimuli appears to be flexible in nature and may be based on higher cognitive factors such as the allocation of attention or expectancy effects and modality specific characteristics (Soto-Faraco et al., 2002; Soto-Faraco et al., 2004).

#### 1.3. Neural oscillations

The scientific breakthroughs regarding the neural basis of human and non-human cognitive functions and perceptual states have been in close association with the advancement of approaches of assessing and operationalizing brain activity. A significant milestone in this field was the introduction of the electroencephalogram (EEG) by Hans Berger in 1929, which had a profound impact on neuroscientific research (Berger, 1929; Herrmann et al., 2016). Initially, the EEG was used as clinical diagnostic tool to identify abnormalities in patients by recording evoked potentials (Herrmann et al., 2016). Nevertheless, since the 1980s, the EEG, established itself as a fundamental component in neuroscience due to its capability of recording oscillatory neural signals (Herrmann et al., 2016). In the context of cognitive neuroscience, these oscillatory signals recorded by the EEG have become an important key method for understanding cognitive processes and perceptual states (Engel & Fries, 2016; Herrmann et al., 2016). In general, neural oscillations are believed to display rhythmic synchronization patterns of neuronal excitatory and inhibitory states and comprise of five phenomenological distinct frequency ranges: delta (0.5-3.5 Hz), theta (4-7 Hz), alpha (8-12 Hz), beta (13-30 Hz) and gamma (> 30 Hz) (Engel & Fries, 2016; Herrmann et al., 2016). Since their discovery, these frequency bands have been correlated to a diverse collection of cognitive functions, underscoring their importance in comprehending brain processes (Herrmann et al., 2016). Delta oscillations appear to span a wide range of neural cortical and subcortical networks (Herrmann et al., 2016). These types of oscillations are particularly pronounced during primary development periods, during slow-wave sleep, and during the

activation of motivational processes and the brain's reward systems. (Knyazev, 2012). In the cognitive domain, they appear to have an important, presumably inhibitory role in modulating attentional processes (Harmony, 2013; Herrmann et al., 2016). Theta oscillations are believed to regulate other brain areas by inhibiting their activity (Herrmann et al., 2016). Furthermore, they appear regularly in memory formation and learning processes (Buzsáki, 2002). In addition, it is believed that theta oscillations span neural networks projecting to hippocampal regions (Buzsáki, 2002; Herrmann et al., 2016; Herweg et al., 2020). One of the first categorized oscillation bands are alpha oscillations (Berger, 1929). This frequency band typically prevails during a state of wakeful rest without the presence of external physical stimulation (Engel & Fries, 2016). They are assumed to have a broad role in sensory perception, attentional processes, and memory formation processes (Clayton et al., 2018; Herrmann et al., 2016; Klimesch, 2012). Interestingly, experiments examining alpha functions often show invers correlative relations with cognitive performance tasks (Herrmann et al., 2016). In addition, they are believed to elicit cognitive functions of suppression, selection, and expectation (Clayton et al., 2018; Herrmann et al., 2016; Klimesch, 2012).

Beta oscillations are prominently observed in sensorimotor tasks (Engel & Fries, 2010). In the motor system, beta oscillations appear to represent the preservation and stability of a current selected motor program (Engel & Fries, 2010). Regarding the perceptual and cognitive functions, it is proposed that beta oscillations are linked with endogenous top-down influences that maintain the stability of a sensorimotor state by attenuating the impact of a potentially unexpected event (Engel & Fries, 2010). Interestingly, patients with Parkinson's disease exhibit an abnormal augmentation of beta oscillations, which is likely associated to clinical symptoms and cognitive functions seen in these patients (Engel & Fries, 2010). Recently, the functional significance of beta band oscillations has been expanded (Spitzer & Haegens, 2017). Rather than simply preserving a current cognitive or sensorimotor state, it has been suggested that the beta frequency band is correlated with dynamic and content-specific, activations and reactivations of functional neuronal networks between and within cortical brain areas and therefore allowing for dynamic adaptations of sensorimotor requirements (Spitzer & Haegens, 2017). Initially seen in animal experiments, gamma band oscillations in a range of > 30 Hz, appear to exert a particularly fundamental excitatory function in neuronal networks (Herrmann et al., 2016). Today it is assumed that local gamma band oscillations arise due to balanced excitatory and inhibitory feedback mechanisms between cortical pyramidal cells and GABAergic interneurons (Siegel et al., 2012). Increases in gamma band oscillations are observed in awake states and in REM Sleep, while they are absent during deep sleep states and under anesthesia (Engel et al., 2001). Interestingly, gamma band oscillations are a widespread pattern observed across species, occurring in sensory and motor systems, as well as in higher association areas of the central nervous system and during memory formation processes (Engel & Fries, 2016). Particularly, processes such as attention, expectation, language, visual awareness, and tasks involving memory formation and conscious perception show pronounced gamma band modulations (Herrmann et al., 2010, Herrmann et al., 2016). At a behavioral level, gamma band responses have been found to have predictive value for performance measures such as reaction time and accuracy in cognitive and perceptual tasks (Herrmann et al., 2010). Interestingly, the amount of gamma band activity appears to be positively associated with increased cognitive and attentional demands (Engel & Fries, 2016; Fries, 2009). In general, numerous investigations revealed a pronounced relationship between cognitive and perceptual functions and gamma band oscillations (Engel & Fries, 2016; Hermann et al., 2016).

The high temporal precision of EEG and MEG has proven to be advantageous for studying the temporal dynamics of brain function (Herrmann et al., 2016). In particular, the EEG has emerged as a robust measurement approach in the search for neural correlates of cognitive processes and consciousness in the context of fast, dynamic oscillatory patterns (Siegel et al., 2012).

# 1.4. Neural synchronization and coherence: binding-by-synchrony and communication-through-coherence

Advancements in characterizing neural activity in the framework of neuronal oscillations reveal fundamental questions about the understanding of information processing and information integration (Engel & Fries, 2016). Regarding neural oscillations central concepts have been proposed (Engel, 2012; Engel & Fries, 2016). The conceptions of binding-by-synchrony and communication-through-coherence suggest that neural synchrony and coherence of oscillatory activity play critical roles in the integration and coordinated processing of information represented by locally distributed neural activity across brain regions (Engel, 2012; Engel & Fries, 2016). The binding-by-synchrony hypothesis refers to the conception that oscillatory synchronous neural activity plays a fundamental role in integrating information from locally separated brain regions into a coherent percept or representation (Engel, 2012; Engel & Fries, 2016). This model suggests that synchronized oscillatory

activity in different brain regions which are involved in processing distinct features of an object or a stimulus, allows to bind these features together to form a unified perceptual conscious experience (Engel, 2012; Engel & Fries, 2016). Several lines of evidence support these assumptions (Engel, 2012; Engel & Fries, 2016). The hypotheses states that coherent and coupled oscillations dynamically and flexibly bind groups of neurons that are involved in the same cognitive process to form an assembly (von der Malsburg, 1995; Engel & Singer, 1997; Engel & Singer, 2001; Varela et al., 2001). The concept of neural assemblies has been shown to be supported by experimental approaches in animals and humans investigating synchronous neural oscillations (Engel & Singer, 2001; Engel & Fries, 2016). Research has demonstrated that synchronized rhythmic neural oscillatory activity, particularly in the gamma frequency band (around 30-80 Hz), are correlated with binding and the integration of different visual features (Fries, 2015). For example, studies investigating visual object recognition have demonstrated increased gamma-band synchrony between visual areas involved in processing specific features (e.g., color, shape) (Fries, 2015; Engel & Fries, 2016). This synchronization of gamma activity is thought to facilitate the integration of neural representations, leading to the perception of a unified conscious object (Fries, 2015; Engel & Fries, 2016).

In addition to binding and the assembly model, neural synchrony and oscillatory coherence are also believed to facilitate communication between brain regions, enabling the coordinated transmission, gating of information, and the integration of distributed cognitive processes (Fries, 2015; Engel & Fries, 2016). This concept, known as communication-through-coherence, implies that coherent oscillatory activity serves as a mechanism for establishing functional connections and facilitating information exchange between brain regions (Fries, 2015; Engel & Fries, 2016). Coherent oscillations provide the possibility of precisely coordinating the states of neuronal excitability fluctuations to establish rhythmic communication windows for the exchange of information between neuronal populations (Fries, 2005; Siegel et al., 2012). Studies utilizing functional connectivity measures have revealed that coherent oscillatory activity can reflect the strength of functional connections between brain regions (Engel & Fries, 2016). Coherence measures, derived from EEG, MEG, or intracranial recordings, have provided insights into the synchronized activity patterns that support efficient communication within neural networks (Engel & Fries, 2016). Furthermore, coherence measures have been related to specific cognitive functions, such as attention, memory, and language processing, suggesting that communication-through-coherence plays a critical role in establishing cognitive processes (Engel &

Fries, 2016). In addition, these conceptions also account for top-down influences (such as attention, predictions, and prior knowledge) which exert modulatory functions and consequently further determine perceptual states (Engel et al., 2001; Engel & Fries, 2016). Neural synchronization may facilitate the selection of functionally significant neural activity because neural oscillations that are temporally concurrent are more robustly captured by different neural assemblies than neural signals that are temporally disseminated (Fries, 2009; Fries, 2015; Engel & Fries, 2016; Siegel et al., 2012). Activity patterns with strongly coupled temporal signatures are functionally effective and globally available, making them fundamental for information sharing across different brain regions (Engel & Fries, 2016). This process is influenced by bottom-up factors and top-down factors, leading to competition between different assemblies and resulting in dynamic, functionally relevant changes in synchrony and thus perceptual or cognitive states (Fries, 2015; Engel & Fries, 2016).

Recently, two independent coupling modes have been introduced to approach synchronization processes between neural oscillatory signals (Siegel et al., 2012; Engel et al., 2013). The first mode, referred to as phase coherence or phase coupling, quantifies a fixed relationship of the phase alignment of two oscillatory signals (Siegel et al., 2012). The second measure of synchronization is the amplitude correlation of oscillations within a frequency or between oscillatory signals of different frequencies (Siegel et al., 2012; Engel et al., 2013). The functional role of this second coupling mechanism is still largely speculative (Siegel et al., 2012; Engel et al., 2013).

In conclusion, the concepts of neural synchrony and coherence provide valuable insights and approaches into the mechanisms underlying the dynamic coordination of brain activity. Neural coherence and synchronization processes are believed to facilitate the consolidation, organization, filtering, and transmission of functionally relevant neural information, thereby influencing the contents of perceptual and cognitive systems, as well as conscious states (Engel & Fries, 2016).

#### 1.5. Gamma oscillations and bistable perception

Long before neural oscillations were understood as meaningful processes and mechanisms for neural communication, cognition, perception, and conscious states, they were dismissed as a phenomenon of "background noise" (Herrmann et al., 2016). In recent decades, however, further investigations suggest that they are specifically and reproducibly associated with a variety of cognitive brain functions (Engel & Fries, 2016; Helfrich et al., 2014, Herrmann et al., 2016). In particular, gamma oscillations,

characterized by high-frequency neural activity in the range of 30-80 Hz, have been the focus of extensive research in the field of neuroscience due to their repeated associations with various cognitive processes and perceptual phenomena, including bistable perception (Engel & Fries, 2016; Rose 2005; Helfrich et al., 2016). As outlined above, bistable perception refers to the observation that an ambiguous stimulus can be perceptual experienced in multiple, mutually exclusive ways, with the perception spontaneously oscillating over time. Bistable and multistable phenomena allow for the association of neuronal oscillatory activity patterns with selective perceptual states, which in turn allows for inferences about the relevance of the respective neuronal activity for perceptual and cognitive functions (Kornmeier & Bach, 2012, Helfrich 2014). A special research emphasis was taken in processes regarding communication and coupling modes of distinct neural networks, which are presumably of crucial importance for the determination of distinct perceptual states (Helfrich et al., 2014; Helfrich et al., 2016; Hipp et al., 2011). For instance, Rose (2005) investigated a series of visual SAM stimulus settings while recording electroencephalographic data from human participants (Rose, 2005). The investigated neurophysiological data demonstrated for the first time the relevance of functional oscillatory coupling for ambiguous apparent motion percepts (Rose, 2005). Subjective horizontal perceptual states relative to vertical perceptual states were significantly associated with increased functional coupling in the gamma band of 30-50 Hz (Rose, 2005). Oscillatory gamma bang coupling was most pronounced at extrastriate visual electrodes, involving the human MT area, located above the respective hemispheres (Rose, 2005). The experiment provides data in favor for the hypotheses, that binding by synchrony may be the underlying mechanisms for formatting distinct communicating neural assemblies in perceptually ambiguous stimulus settings (Rose, 2005). Helfrich et al. (2016) constructed an expanded experimental version of the visual SAM stimulus by correlating electroencephalographic data of human participants while performing the visual bistable SAM task (Helfrich et al., 2016). In addition to the study by Rose (2005), an emphasis was placed on investigating source space coupling properties in large-scale cortical networks (Helfrich et al., 2016). In general, this study further demonstrates that correlated neuronal synchronization patterns of spatially distributed task-relevant cortical networks are significantly associated with the conscious perceptual state of a bistable visual apparent motion stimulus (Helfrich et al., 2016). Furthermore, correlated neuronal interaction patterns could be dissected into distinct features (Helfrich et al., 2016). Specifically, oscillations in the alpha band, spanning from parietal to occipital

areas appear to determine interhemispheric communication and subsequent apparent motion perception (Helfrich et al., 2016). Increased phase synchronization in the gamma band via the dorsal pathway of the visual stream appear to represent a neuronal mechanism of information integration (Helfrich et al., 2016). Consistent with the findings from Rose (2005), it should be emphasized that, increased functional coupling between electrodes spanning over both MT areas was observed at the sensor lever (Helfrich et al., 2016). Nevertheless, the hypothesized increased gamma coupling between bilaterally hMT and occipital cortex could not be established in source level analyses (Helfrich et al., 2016). Since the studies described so far have primarily provided correlative evidence for the functional relevance of gamma band synchronization processes, an emerging field of studies has aimed to establish experimental designs, to allow for casual associations of gamma band synchronization and subsequent perceptual states by applying transcranial electrical stimulation. One methodological approach to investigate causal relationships between neural oscillations and cognitive, perceptual, and conscious states is to apply non-invasive neuromodulatory approaches, such as transcranial stimulation experiments (Bland & Sale, 2019; Herrmann et al., 2016). In the following section, non-invasive transcranial electrical stimulation approaches are introduced and summarized.

1.6. Non-invasive brain stimulation and transcranial alternating current stimulation (*tACS*) One of the central aims of neuroscientific research is to understand the complex spatiotemporal dynamics and mechanisms of the central nervous system, that are believed to give rise to the various powerful cognitive functions and conscious states of the human mind (Bland & Sale, 2019; Engel & Fries, 2016). Historically, most researchers have investigated brain activity while participants were engaged in a cognitive or perceptual task (Bland & Sale 2019; Herrmann et al., 2016). Thus, the traditional paradigm defined the cognitive process as the independent variable and the corresponding neural activity as the dependent variable (Herrmann et al., 2016). Consequently, strictly speaking through the lens of the traditional paradigm, the observed relationship between a specific cognitive and perceptual process or a conscious state and an empirically observed brain activity is only correlative in nature (Bland & Sale 2019; Herrmann et al., 2016). In recent years many neuroscientific laboratories attempt to inverse the traditional paradigm, to obtain a better understanding of neural correlates of perceptive states and cognitive functions by directly manipulating neural activity (Bland & Sale 2019; Herrmann et al., 2016).

The approach of directly manipulating brain activity inverts the traditional experimental concept by redefining neural activity as the independent variable in this new framework, while the variations observed in cognitive processes become the dependent variable (Herrmann et al., 2016). This inversion provides the opportunity to establish a causal relationship between the observed brain activity and specific cognitive and behavioral outputs, as well as conscious states, using non-invasive brain stimulation (Herrmann et al., 2016).

Based on this concept, many methods have been introduced and refined to influence brain activity (Bikson et al., 2019; Herrmann et al., 2016).

A well-established approach to modulate neural oscillations is the repetitive stimulation with a sensory stimulus, which consequently induces a characteristic steady state evoked potential, measured by the EEG (Regan, 1977). The underlying idea behind this method is to drive the oscillatory neural activity with a specific frequency of the sensory stimulation to enhance the amplitude of that frequency and directly influence the presumed associated cognitive process (Hermann et al., 2016). The concept behind this mechanism is termed entrainment (Hermann et al., 2016). Furthermore, the phenomenon of entrainment leads to the synchronization and alignment of ongoing neural oscillations with an entrained frequency (Hermann et al., 2016). In other words, the external stimulation "entrains" or aligns the brain's natural oscillatory activity to match the external stimulated frequency (Hermann et al., 2016).

EEG-neurofeedback represents an alternative method for manipulating oscillatory neural activity and subsequent cognitive functions (Hermann et al., 2016). By direct visualization of oscillatory activity, participants can learn the ability to endogenously modulate their own oscillatory activity and thereby influence the associated cognitive function (Hermann et al., 2016). The application of rhythmic magnetic pulses, also known as repetitive transcranial magnetic stimulation (rTMS), is yet another approach believed to regulate and entrain neural oscillatory activity and subsequent cognitive function by briefly inducing focal currents and direct action potentials in the brain (Thut et al., 2012).

The final group of non-invasive neural stimulation method is characterized by transcranial electric stimulation (tES) (Bikson et al., 2019; Herrmann et al., 2016).

The aim of this approach is to manipulate neural activity via the application of an electric current through the intact scalp by placing electrodes on the scalp (Bikson et al., 2019; Bland & Sale, 2019; Herrmann et al., 2016). Given the advancements in recent research many different protocols and

modifications of tES have been established (Bikson et al., 2019). By applying a direct electrical field through the scalp via adjustable electrodes, the electric current is believed to flow between a positively charged anode to a negatively charged cathode (Bikson et al., 2019; Bland & Sale, 2019; Herrmann et al., 2016). This form of non-invasive electrical stimulation is called transcranial direct current stimulation (tDCS) (Bikson et al., 2019; Bland & Sale, 2019; Herrmann et al., 2016). The effects of tDCS are believed to involve widespread subthreshold depolarization and resulting excitation of nerve cells in the proximity of the anode, while hyperpolarization of nerve cells and decreased neural excitability is believed to occur in proximity of the cathode (Bikson et al., 2019; Bland & Sale, 2019). It is assumed that ongoing oscillations of cortical and subcortical neural networks are modulated by the applied electric field, even without directly manipulating neuronal firing rates (Bikson et al., 2019; Bland & Sale, 2019). However, the effect of tDCS and tES in general are complicated by the complex anatomic orientation and folding patterns of the cortical layers (Bland & Sale, 2019).

Another popular form of tES is transcranial alternating current stimulation (tACS), which is generally defined as the application of sinusoidal electrical stimulation using electrodes positioned on the intact surface of the head (Bikson et al., 2019; Bland & Sale, 2019; Herrmann et al., 2016). The orientation of the stimulation field alternates periodically, with the anode and cathode shifting in each half period (Bikson et al., 2019). The precise mechanisms underlying the effects of tACS are not fully understood (Bikson et al., 2019; Bland & Sale, 2019; Herrmann et al., 2016). Nevertheless, there is accumulating evidence that provides possible explanations. There are two primary types of suggested tACS effects: online effects observed during the stimulation period and offline or after-effects that endure beyond the stimulation period (Bland & Sale, 2019). Either type of effect encompasses the entrainment of neural oscillatory activity to the frequency of the external current and the modulation of large-scale neural coupling mechanisms (Schwab et al., 2019; Weinrich et al., 2017). Due to the oscillatory properties of neural activity the application of a sinusoidal electrical current has been considered a promising approach to modulate the ongoing rhythmic brain activity (Bland & Sale, 2019; Herrmann et al., 2016; Vosskuhl et al., 2018). Furthermore, this approach aims to modulate neural oscillations in a pattern that is specific to both phase and frequency. (Bland & Sale, 2019; Herrmann et al., 2016; Vosskuhl et al., 2018). Importantly, the approach seeks to achieve this modulation without impacting the actual rate of action potentials, capitalizing on the oscillatory properties of neural activity (Bland & Sale, 2019; Herrmann et al., 2016; Vosskuhl et al., 2018). The administration of alternating currents

induces oscillatory changes in the membrane potential of cortical neurons' cell bodies as well as dendrites (Vöröslakos et al., 2018). The alternating fluctuation in membrane potential is believed to modulate the membrane potential towards depolarization or hyperpolarization, which consequently result in alternations of the likelihood of neurons firing action potentials (Antal & Herrmann, 2016; Vöröslakos et al., 2018). Consequently, tACS is believed to manipulate the ongoing rhythmicity of action potentials in a phase-specific and frequency-specific manner via subthreshold depolarization and hyperpolarization (Antal & Herrmann, 2016; Bland & Sale, 2019; Krause et al., 2019; Herrmann et al., 2016; Vöröslakos et al., 2018). By applying alternating currents to the scalp, tACS is believed to induce an electric field in neural tissue that influences oscillatory neural activity (Wischnewski et al., 2023). The induced oscillatory electric fields can impact neural spike timing, synaptic plasticity, and long-range coherence, leading to changes in brain oscillatory power, frequency, and phase connectivity (Wischnewski et al., 2023). This modulation of neural activity through tACS has implications for cognitive and behavioral processes (Wischnewski et al., 2023). Nevertheless, in correspondence to tDCS the stimulation is not considered robust enough to directly alter the firing rate of action potentials (Reato et al., 2010; Vosskuhl et al., 2018). Therefore, tACS is considered a form of subthreshold stimulation that does not directly induce neuronal spikes (Bland & Sale, 2019; Krause et al., 2019; Herrmann et al., 2016; Vöröslakos et al., 2018). In more detail, recent studies investigating effects of tACS reveal, that aligned pyramidal cells in primarily cortical layer V exhibit the most sensitive changes in response to the induced electric fields (Radman et al., 2009; Fröhlich, 2014). One reason for that feature may be their elongated somatodendritic extensions (Radman et al., 2009; Fröhlich, 2014) as well as their neuroplastic activity, and cortico-cortical projections (Kim et al., 2015; Spruston, 2008; Ulrich, 2002). Consequently, by stimulating these neurons long-term effects, and extensive oscillatory cortical connectivity may be induced (Kasten et al., 2016; Zaehle et al., 2010). Recent evidence indicates the existence of discrete neural mechanisms underlying tACS effects, spanning from cellular to global network levels (Liu et al., 2018).

The first mechanism is described as stochastic resonance: different neurons modulated by *tACS* exhibit varying and stochastically fluctuating polarization or hyperpolarization of the membrane potential, which consequently leads to varying temporary probabilities to generate action potentials (Liu et al., 2018). The second mechanism is described as rhythmic resonance: this process comes into effect if the frequency of tACS aligns with the frequency of the endogenous oscillation (Liu et al., 2018). This

alignment allows the oscillatory current to convene with the endogenous wave at a similar phase during each cycle (Liu et al., 2018). The third mechanism involves the temporal stimulation component. The timing of neuronal spikes is governed by the interplay between the externally applied current and the intrinsic oscillatory neural activity (Liu et al., 2018). This collaboration potentially activates the same set of neurons in each period of stimulation (Liu et al., 2018). The fourth mechanism accounts for the concept of network entrainment: For entraining the naturally erratic neural activity an external oscillating current of appropriate amplitude may be essential (Liu et al., 2018). Lastly, the imposed pattern mechanism suggests that the strongest stimulation amplitudes are needed to override the endogenous regular oscillations and initiate new oscillations (Liu et al., 2018). These processes contribute to the description provided by Vosskuhl et al. regarding the global network level influence of tACS (Vosskuhl et al., 2018). It is proposed that the online and offline effects of tACS are causally explained by synergistic processes of entrainment and neuroplasticity (Vosskuhl et al., 2018). As outlined above, entrainment refers to the process in which an external rhythmic system influences a naturally oscillating system, causing it to synchronize with the external frequency (Vosskuhl et al., 2018). In the case of tACS, the externally applied current induces the intrinsic neural oscillations to align with the phase and frequency of the extrinsic non-invasive stimulation (Vosskuhl et al., 2018). Regarding the phenomenon of neuroplasticity, the mechanism of long-term potentiation (LTP) and long-term depression (LTD), as well as spike-timing dependent plasticity (STDP) are considered relevant factors (Feldman, 2012). LTP refers to the strengthening of synaptic connectivity when the presynaptic action potential precedes the postsynaptic potential (Feldman, 2012). In contrast, LTD involves synaptic weakening when a presynaptic action potential follows a postsynaptic action potential (Feldman, 2012). These processes are believed to be essential in generating effects of tACS by modulating neuronal synchrony (Vosskuhl et al., 2018). Numerous studies have provided evidence supporting this explanation (Vossen et al., 2015; Zaehle et al., 2010). Moreover, this hypothesis may explain the persistence of tACS offline effects for a duration extending to several minutes (Kasten et al., 2016). Given these characteristics of tACS mechanisms, it is one of the only techniques (alongside rTMS) principally capable of influencing phase coherence and, consequently, establishing and testing causal relationships in line with the communication through coherence hypotheses (Bland & Sale, 2019; Fries, 2005; Fries, 2015). For instance, Helfrich et al. applied a bihemispheric HD-tACS protocol at a frequency of 40 Hz (Helfrich et al., 2014). This study discovered that tACS influenced

interhemispheric functional coupling in a phase-specific manner (Helfrich et al., 2014). *In-phase* stimulation augmented neuronal coupling, whereas *anti-phase* stimulation diminished neural synchronization in the targeted brain areas (Helfrich et al. 2014). Interestingly, these changes in coupling patterns were functionally correlated with corresponding changes in the participants' perceptual state during an apparent visual motion paradigm (visual SAM): *in-phase* stimulation increased the perception times of a *horizontal* percept, while *anti-phase* stimulation resulted in an increase of *vertical* motion percept times (Helfrich et al., 2014). These findings support the functional importance of neural coupling processes in cognitive and perceptual mechanisms (Helfrich et al., 2014).

The effects of tACS are influenced by a wide range of parameters, including the selected amplitude and frequency of stimulation (Bland & Sale, 2019). Furthermore, the effects of tACS can also be influenced by an individual's cortical folding and the resulting current penetration, which are determined by their three-dimensional orientation (Radman et al., 2009). The intensity of different stimulus protocols conventionally refers to a peak-to-peak scope (Bikson et al. 2019). Most of noninvasive electric stimulation studies apply a current strength of ≤ 2 mA peak-to-peak, to avoid the empirical observation that higher intensities often result in pinching, burning, itching and painful sensations on the skin underneath the electrode (Bikson et al., 2019; Bland & Sale, 2019; Fertonani et al., 2015). Even with intensity ranges of  $\leq 2$  mA, these sensations may be experienced by some participants. Another argument for using lower intensities is the possibility to implement specific sham stimulation conditions in experimental designs (Bikson et al., 2019; Bland & Sale, 2019). Furthermore, besides current intensities, sensations due to the transcranial nature of the electrical application seem to be determined by the specific features and characteristics of the electric stimulation and tES montage like waveform, frequency, electrode type and location as well as impedance of the scalp (Bland & Sale, 2019; Fertonani et al., 2015). Nevertheless, a few studies managed to implement higher stimulation intensities with and without applying anesthetizing creme on the scalp in advance of the electrical stimulation (Asamoah et al., 2019; Vöröslakos et al., 2018). Higher intensities of applied current are usually believed to result in higher field intensities, generally measured in mV/mm or V/m in the neural tissue (Bland & Sale, 2019). Animal studies suggest that in order to modulate ongoing endogenous neural network oscillations, field strengths exceeding 1 V/m are necessary (Bland & Sale, 2019; Fröhlich & McCormick, 2010; Vöröslakos et al., 2018). Furthermore, increasing the frequency of

stimulation may also require higher stimulation intensities to influence neural susceptibility to membrane polarization (Anastassiou et al., 2010; Bland & Sale, 2019). Nevertheless, recent evidence suggests that by adjusting the applied frequency to the inherent frequency of the oscillation of the neural network via tACS, spike timing modulation and entrainment can be established, even at low electric field strengths of 0,2 - 0,3 V/m (Krause et al., 2019). The specific question of how much intensity is required to successfully generate a sufficient field strength to modulate ongoing neural oscillations is still a relevant aspect of current debate (Bland & Sale, 2019). Further investigations regarding the most commonly used stimulation intensities, typically applied in the range of  $\sim 1-2$  mA peak-to-peak, showed that the resulting field strength ranged from 0,1 - 0,8 V/m (Vöröslakos et al., 2018, Krause et al., 2019). The high variability of the observed field intensity in different studies can be attributed to factors such as individual anatomy, type of electrode montage and other stimulation modalities (Alekseichuk et al., 2019). It should be noted that inducing detectable muscle activity in the primary motor cortex typically necessitates a field intensity ranging from 100 to 200 V/m (Bland & Sale 2019). Comparing these relations, tACS induced electrical field intensities in the brain appear to be of minimal amount, just enough to induce minimal changes (Bland & Sale, 2019). Despite these minimal changes, many recent experiments, and investigations during the last decade in human and animal studies reveal a vast amount of behavioral and neurophysiological evidence regarding the induced effect of tACS (Schutter & Wischnewski, 2016; Herrmann & Strüber, 2017; Veniero et al., 2019). Regarding the transcutaneous nature of the applied current in tES, the issue of current shunting arises (Bland & Sale, 2019). The applied current penetrates the skin, skull, cerebrospinal fluid before propagating to the targeted layers of gray and white matter of the brain (Asamoah et al., 2019). Considerably, the majority of the electrical current (~ 75%) is attenuated by the various layers that include the integument, cranial bones, and cerebrospinal fluid (Asamoah et al. 2019). Efforts to optimize the focality and intensity of stimulation sites have resulted in high density montages (Helfrich et al. 2014, Cancelli et al. 2016).

Furthermore, evidence suggests that the shunting proportion may be directly dependent on the proximity of the anode and cathode (Asamoah et al. 2019). In general, some heuristic rules may be applied for the tES montages (Bland & Sale 2019). By increasing the distance between the anode and cathode the fraction of current shunting trough the soft tissue, bone and cerebrospinal fluid will also decrease, while the intensity of the resulting electric field will increase, at the expense of a loss of

focality in the targeted brain area (Bland & Sale 2019). In recent years a focus on indirect effects of tACS has evolved (Asamoah et al., 2019). When tACS is applied within conventional intensity ranges in the alpha and beta frequency bands, tACS can induce visual phenomena known as phosphenes, particularly in occipital and frontal electrode montages (Kanai et al., 2008). Early experiments suggested that the interaction between tACS and endogenous neural oscillations in visual areas of the brain contributed to the emergence of phosphenes (Kanai et al., 2008). Nevertheless, subsequent investigations advocated rather for a retinal source of tACS induced phosphenes (Schutter, 2016). Interestingly, retinal electric stimulation and resulting phosphenes have the ability to entrain neural oscillations in visual cortex and may therefore modulate cognitive and perceptive processes, in the fashion of repetitive sensory stimulation (Schutter, 2016, Bland & Sale 2019). Strictly speaking this type of neural modulation would be considered as indirect sensory stimulation (Bland & Sale, 2019). Due to the transcutaneous nature of tACS and tES, the first layer that the applied current must penetrate is the skin, and as a result, most of the electric field strength is attenuated at the skin barrier, affecting the skin itself (Alekseichuk et al., 2019; Asamoah et al., 2019). The intensity levels of the electric field can significantly exceed the threshold of stimulating peripheral nerves and skin receptors (Alekseichuk et al., 2019; Asamoah et al., 2019). To further elucidate the role of peripheral nerve stimulation some investigators conducted experiments by blocking peripheral nerve signals with topical anesthetizing creme (Asamoah et al., 2019). Interestingly, some electrophysiological and behavioral effects suggest that the entrainment effect on central neurons is more likely explained by repetitive peripheral nerve stimulation rather than by a direct modulatory influence on the cortex (Asamoah et al., 2019). Similar to repetitive stimulation of the retina, repetitive stimulation of the skin and its embedded peripheral nerves and receptors by tACS appears to be able to indirectly entrain and modulate neural oscillatory networks, by providing rhythmic input to the central nervous system (Asamoah et al., 2019, Bland & Sale, 2019). These experiments have led to competing hypotheses regarding the modulatory effect observed by tACS (Vieira et al., 2020). One hypothesis suggests that tACS effects are explained by repetitive transcutaneous stimulation (Asamoah et al., 2019). The counter hypothesis argues that tACS effects are explained by the influence of the applied electrical field on central neuronal cells (Asamoah et al., 2019, Vieira et al., 2020). A recent study in alert monkeys found contradictory results to the peripheral entrainment hypotheses, suggesting the influence of a direct tACS effect on endogenous network

oscillations (Vieira et al., 2020). Furthermore, another aspect regarding the mechanisms of tACS effects has been introduced. Even if the penetrating direct electric field reaches the intracranial neural tissues, the observed effects could at least possibly also be generated by affecting neural glial cells, which may act as a mediating component (Monai & Hirase, 2018). In conclusion, it seems that much more research is needed to further understand and elucidate the causal relationship on how tACS effects are generated. One approach to achieve this goal is to combine ongoing tACS/tES with concurrent recordings of neural activity, such as MEG and EEG (Helfrich et al., 2014). Nevertheless, several complex factors need to be considered in this regard. Since the electrical stimulation is in the same modality, as the recording of the neural oscillatory activity, artifacts are generated, that greatly exceed the amplitudes of the measured inherent neural activity (Kasten & Herrmann, 2019). Furthermore, in many experiments the stimulation frequency and the frequency of interest captured by MEG and EEG are equivalent, potentially contaminating the analysis (Bland & Sale, 2019). As the mechanisms of tACS effects are believed to predominantly occur during stimulation ("online effects"), researchers have investigated methods to remove these tACS artifacts (Noury et al., 2016).

In a sequence of experiments Noury et al. demonstrated, that the artifact produced by *tACS* exhibits a non-linear structure, which complicates artifact removal efforts considerably (Noury et al., 2016; Noury & Siegel 2017; Noury & Siegel, 2018). Rhythmic physiological processes such as respiration and heartbeat have been shown to modulate impedances, leading to concurrent non-linear modulations of *tACS* artifact amplitudes in EEG/MEG recordings (Noury et al., 2016; Noury & Siegel, 2017). Extracting artifact-free components from measured EEG/MEG online activity has proven to be a difficult task (Noury et al., 2016). Conventional published methods for the removal of the artefact have been indicated to violate core assumptions, resulting in the possibility to mistake the artifact for a genuine neural activity (Noury et al., 2016, Noury & Siegel, 2017). Furthermore, it should be noted that that tES applications are generally controlled by the applied current of the stimulation, which might have direct impact on the amplitude modulations of physiological perturbations (Noury & Siegel, 2017). The current controlled stimulation feature of tES, results in the consequential adjustment of the applied voltage, if respective changes in impedances of electrodes occur (Bland & Sale, 2019). Two variations in impedance over time are intuitively plausible: at the onset of stimulation, impedance levels are generally assumed to be higher and decrease over time (Bland & Sale, 2019). However, the

evaporation of conducting gels over time may also lead to higher impedances (Bland & Sale, 2019). Due to the profound theoretical and practical complexities of artifact removal, which can potentially contaminate online tACS and EEG/MEG recordings, many researchers have shifted their experimental designs to focus on tACS effects immediately following stimulation periods (referred to as "aftereffects" or "offline effects"), assuming that these effects persist beyond the stimulation epoch (Bland & Sale, 2019). As described above, online effects of tACS are often believed to be established through the mechanism of entrainment (Bland & Sale, 2019; Vosskuhl et al., 2018). In addition, tACS effects are also attributed to spike timing dependent changes in the plasticity of the neural networks (Bland & Sale, 2019; Vosskuhl et al., 2018). It should be noted that most researchers believe that the mechanisms of tACS effects operate through entrainment of neural oscillatory networks during stimulation, while the presumed long-lasting aftereffects are probably caused by changes in the plasticity of cortical and subcortical networks (Bland & Sale, 2019; Vosskuhl et al., 2018). Evidence supporting the entrainment mechanism of tACS includes observations that its efficacy is enhanced by increasing the stimulation magnitude and adapting the frequency to the aimed inherent neural oscillatory signal (Schutter & Wischnewski, 2016; Bland & Sale, 2019). However, there is currently a mixed pattern of evidence regarding the specificity of frequency and phase dependence of tACS (Bland & Sale, 2019). Despite the significant pitfalls and limitations of tES and tACS, non-invasive brain stimulation remains a potential fascinating and promising approach to modulate ongoing endogenous neural oscillatory network activity in humans and animals. Consequently, tES in general and tACS in specific provide the powerful potential to establish a causal relationship between empirically observed neural activity and cognitive and perceptual processes, as well as conscious states (Herrmann et al., 2016).

#### 2. General Overview of the Methodology

#### 2.1. Participants

The study subjects were recruited exclusively from the University Medical Center in Hamburg, Germany. Written informed consent was obtained from all participants. Financial compensation was provided for voluntary participation in this study.

This investigation adhered to the guidelines outlined in the Declaration of Helsinki and received approval from the local ethics committee of the medical association in Hamburg, Germany, (IRB number: PV4908).

Visual, auditory, and somatosensory functions were reported to be normal. All participants were unmedicated and none reported a presence or history of any neurological or psychiatric disease. Additionally, all subjects reported being right-handed and having a dominant right foot.

#### 2.2. Tactile stimuli

The tactile stimuli consisted of four vibrotactile C-2 tactors (Engineering and Acoustics Inc., 406 Live Oak Blvd, Casselberry, FL 32707, USA; Figure 1). The C-2 tactors are linear transducing actuators contained in a housing with a vibration frequency range of 200-300 Hz and an optimum vibration frequency of 250 Hz, which was used as the tactile stimulation frequency for both experiments. The vibration frequency corresponds to the peak sensitivity of the body's phasic Pacinian corpuscle, which is most sensitive to vibrational stimuli (Biswas et al., 2015; Skedung et al., 2013). One C-2 tactor has a height of 0.31 inch, a total diameter of 1.2 inch, the diameter of the actuator is 0.3 inch and each C-2 tactor has a total weight of 17 grams (Engineering and Acoustics Inc., 406 Live Oak Blvd, Casselberry, FL 32707, USA). The exposed material, in contact with human skin consists of anodized aluminum and polyurethane (Engineering and Acoustics Inc., 406 Live Oak Blvd, Casselberry, FL 32707, USA). The vibration burst settings were controlled by a customized MATLAB (MATLAB, R2016b (9.1.0), The MathWorks Inc., Natick, MA, USA) script running on a Microsoft computer, which was located outside the experimental chamber, where the participant was seated. The specifications of the activation of the C-2 tactors were adjusted to match optimal drive and driver recommendations (sine wave bursts with a frequency of 250 Hz at 0.25 A, amplifier of 0.5 W). The activation of vibrational bursts of the C-2 tactors produces an ambient sound every instant the tactile stimulus gets activated. To dimmish potential auditory interference on the perception of a motion pattern, white noise was delivered via in-ear noise isolating headphones to mask the ambient sound. The volume level of the white noise, required to suppress the ambient sound of the C-2 tactors, was adjusted prior to the beginning of the experiments to the individual threshold for each subject.

Figure 1 – C-2 tactor used in both experiments.



C-2 tactor used in both experiments (Engineering and Acoustics Inc., 406 Live Oak Blvd, Casselberry, FL 32707, USA, <a href="https://eaiinfo.com/product/c2/">https://eaiinfo.com/product/c2/</a>).

#### 2.3. *TACS* protocol

Similar *tACS* protocol configurations were used for both experimental settings. Differences between the protocols are highlighted in the appropriate sections. While performing the experimental tasks, transcranial current stimulation was applied bilaterally at 40 Hz by two accumulator powered stimulators (DC-Stimulator plus, NeuroConn, neuroCare Group GmbH, Munich, Germany; Figure 2). The electrical current was continuously applied during the whole experimental task through ten Ag/AgCl electrodes (12 mm diameter, EASYCAP GmbH, Herrsching, Germany; Figure 3) in a 4-in-1 electrode configuration for each electrical stimulation site respectively (Misselhorn et al., 2019; Patel et al., 2009; Saturnino et al., 2017; Figure 4). The stimulation parameters of the alternating current were controlled by a customized MATLAB script running on a Microsoft computer. The DC-Stimulators

were configured to function in external mode, which enabled exact control of the current output through the voltage input. The voltage signal was generated by a customized MATLAB script and produced physically by an NI-DAQ device using Labview (NI USB 6343, National Instruments, Texas, USA).

Prior to the non-invasive electrical stimulation, a standard realistic three-shell brain model, targeting the bihemispheric primary somatosensory cortex (S1) was established (Misselhorn et al., 2019, Nolte & Dassios, 2005).

Therefore, the bihemispheric target areas were chosen in accordance with metanalytic evidence regarding target coordinates of primary somatosensory cortex (S1) in MNI-space (Holmes & Tamè, 2019). The electrode locations for the 4-in-1 configurations were selected to maximize the electric field strength in the hand-knob area of the primary somatosensory cortex (S1).

Therefore, electric current densities (V/m) were estimated by constructing an inverse model of exact low-resolution electromagnetic tomography (eLORETA) (Pascual-Marqui et al., 2011).

In addition, the estimation included a cortical grid based in MNI-space (MNI 152), which was accomplished by resampling the Freesurfer model to a 10.000 MNI-space grid (Desikan et al., 2006; Misselhorn et al., 2019).

The calculation of the electric field intensity introduced at location  $\vec{x}$  was conducted based on "linear weighting of the lead field matrix  $\vec{L}$ " with the induced currents  $\alpha i$ , where i represents the indices of the ten electrodes used for electric stimulation, as follows (Misselhorn et al., 2019):

$$\vec{E}(\vec{x}) = \sum i (\vec{L}(\vec{x})\alpha i)$$

The 4-in-1 electrode montages allowed for targeted current flow under the central stimulation electrode and increased the focality of the propagating electric field generated by the alternating current stimulation (Misselhorn et al., 2019; Saturnino et al., 2017; Figure 4). The electrodes for stimulation were fabricated using an abrasive electrolyte contact gel (Abralyt 2000, Easycap, Herrsching, Germany). The impedances of the stimulation electrodes were measured by an impedance meter from BrainAmp (Brain Products GmbH, Gilching, Germany; Figure 3). The combined impedance and the individual impedance measured between the central electrode and the peripheral electrodes for each side of the 4-in-1 configuration of the tACS electrodes, were maintained below 15 k $\Omega$ . In

addition, the individual impedances for each participant were set not to deviate greater than 10 k $\Omega$ , in order to maintain approximately constant applied electric fields within subjects and allow for comparable impedances between subjects. Since the modeled electric field strengths are based on similar impedances, impedance control is essential (Misselhorn et al., 2019).

Regarding *in-phase* stimulation the identical synchronized sinusoidal waveforms for each 4-in-1 stimulation sites were applied. Whereas regarding *anti-phase* stimulation, one sinusoidal waveshape was rephased by 180°.

Electrical stimulation intensity was ramped up (from zero to maximum intensity) sinusoidally for a tensecond-long segment, that preceded the start of the actual (visuo-) tactile stimulation in order to accustom participants to the electrical stimulation.

The *sham* stimulation condition consisted of a ramp up segment for ten seconds immediately followed by a ramp out segment for ten seconds.

After the experiment, participants were debriefed and completed a qualitative questionnaire regarding the perceived possible sensations and side effects of the electrical stimulation.

Due to significant methodological limitations regarding the compatibility of online *tACS* and EEG recordings, the experimental design was established as a behavioral experiment, without any online recordings of electroencephalographic data.

Figure 2 – DC-Stimulator plus



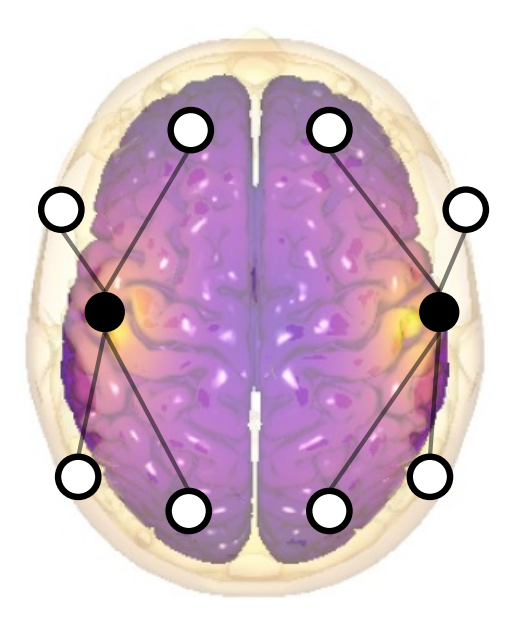
For both experiments two accumulator powered stimulators were applied for each stimulation site respectively (DC-Stimulator plus, NeuroConn, neuroCare Group GmbH, Munich, Germany, <a href="https://www.neurocaregroup.com/de/dc-stimulator-plus">https://www.neurocaregroup.com/de/dc-stimulator-plus</a>).

Figure 3 – EASYCAP Equipment



The EASYCAP Equipment was used as a placeholder for the Ag/AgCl tAC-Stimulation electrodes (Easycap GmbH, Am Anger 5, D-82237, Woerthsee-Etterschlag, <a href="https://www.easycap.de/wp-content/uploads/2019/10/Partial\_PRODUCT-OVERVIEW-08-2019.pdf">https://www.easycap.de/wp-content/uploads/2019/10/Partial\_PRODUCT-OVERVIEW-08-2019.pdf</a>, M64) . The electrical current field densities estimation with the specific *tACS* electrode configuration can be derived from figure 4.

Figure 4 – *tACS* setup (*in-phase* modeled current)



All experiments involved a two-sided, multi-electrode setup for bilateral *tACS*. The black and white dots represent stimulation electrodes at different polarities. The sinusoidal stimulation frequency was set to 40 Hz for both experimental setups. An estimation of the maximum current intensities on the cortical surface was conducted (see section 2.3.). Subjects received bihemispheric *in-phase* and *anti-phase* alternating current stimulation, via two symmetrical adjusted 4-in-1 configurations over somatosensory cortices.

The model of the cortical folding is color-coded to represent the calculated extreme field strength in V/m.

### 2.4. Data and statistical analyses

The acquired data in all experiments were analyzed using SPSS (IBM Corp. Released 2016. IBM SPSS Statistics for macos, Version 24.0. Armonk, NY: IBM Corp), MATLAB (MATLAB, R2016b (9.1.0), The MathWorks Inc., Natick, MA, USA), and JASP (JASP Team (2022). JASP (Version 0.16.3) [Computer software]). Statistical analyses were conducted with parametrical statistical procedures as well as non-parametric permutation tests if requirements for parametric procedures were not fulfilled. A comprehensive account of the statistical procedures used in each experiment can be found in their respective methods and results sections.

# 3. Modulation of ambiguous tactile apparent motion perception by tACS

#### 3.1. Introduction

This exploratory, within-subject designed experiment aims to expand the understanding of tACS effects on ambiguous tactile apparent motion perception. Therefore, a tactile stimulus design was established in correspondence to the experiment specified by Liaci et al. (Liaci et al., 2016). Four vibrotactile elements (C-2 tactors) were attached on the ventral side of each forearm (Liaci et al., 2016). Both forearms were held in parallel alignment so that the vibrotactile elements formed an imaginary rectangle (Liaci et al., 2016). Stimulation streams of subsequent diagonal activation caused participants to spontaneous alternate between two mutually exclusive perceptual states: the tactile stimulus could be perceived as an antiparallel horizontal or vertical apparent motion pattern (Liaci et al., 2016). Originally, the stimulus design was established in the visual modality by van Schiller in 1933 and was described as Stroboscopic Alternative Motion (SAM) stimulus (Schiller, 1993). As outlined in the general introduction, the visual stimulus consists of two diagonally arranged light dots on an imaginary rectangular frame (Schiller, 1993). Alternating sequential diagonal activation of these light dots causes participants to perceive a visual apparent motion either in a horizontal or a vertical direction (Rose, 2005; Schiller, 1993). In recent years, many researchers in the field of neuroscience found new interest in this rather basic tactile version of the SAM stimulus (Carter et al., 2008; Conrad et al., 2012; Helfrich et al., 2014; Liaci et al., 2016; Strüber et al., 2014). As outlined above, a significant advantage of bistable stimuli is that, although the physical stimulus remains constant over time, the subjective percept changes into different mutually exclusive states (Conrad et al., 2012; Helfrich et al., 2014). Many

scientists take advantage of this fact because it allows to associate specific neuronal activity patterns to conscious perceptual patterns (Blake & Logothetis, 2002; Helfrich et al., 2016).

In non-bistable stimulus settings, variations in neuronal activity could be explained by variations in the stimulus setting, which, depending on the scientific hypothesis, could confound the interpretation of association patterns between perceptual states and neural activity (Helfrich et al., 2016).

For the visual modality, the study by Helfrich et al. (2014) showed that interhemispheric functional connectivity and corresponding correlated perceptive states are modulated by *tACS* in parieto-occipital regions in a phase-specific way (Helfrich et al., 2014).

Accordingly, the present investigation has been designed to explore the role of *tACS* in the modulation of apparent tactile motion perception. By applying bihemispheric, frequency- and phase specific sinusoidal *tACS* to targeted brain regions involved in tactile processing, this investigation aims to uncover whether the manipulation of neural oscillations can influence the perception of ambiguous tactile apparent motion perception. Understanding the impact of *tACS* on this perceptual phenomenon could shed light on the neural mechanisms that govern the integration and interpretation of tactile stimuli in the brain.

The experimental setup involves bihemispheric, symmetrical 4-in-1 montages over the somatosensory cortices, allowing for targeted current flow and increased focality of the propagating electric field. This behavioral experimental investigation aims to replicate and extend the principal idea of bistable motion perception in the tactile modality.

Furthermore, this study aims to elucidate the impact of phase- and frequency specific *tACS* targeting somatosensory cortices on tactile bistable perception.

Measuring pupil data has become increasingly popular in neuro-scientific experiments because it provides insights into cognitive, perceptual, and emotional processes (De Gee et al., 2014; Einhäuser et al., 2008; Kloosterman et al., 2015). Pupil diameter is modulated by changes in the autonomic nervous system and is sensitive to alterations in cognitive effort, decision making processes, and attentional allocation (De Gee et al., 2014; Kraus et al., 2023). It is also sensitive to emotional arousal and perceptual alterations (Einhäuser et al., 2008; Kloosterman et al., 2015).

The integration of pupil measurements can provide supporting evidence for *tACS* effects on tactile perception. Alterations in pupil size have been shown to be partially associated with variations in neural activity (Kraus et al., 2023; Larsen & Waters, 2018).

In perceptual rivalry, pupillometry and eye tracking can provide insights into the mechanisms underlying spontaneous perceptual alterations (Einhäuser et al., 2008).

For example, Einhäuser et. al., found a significant increase in pupil diameter preceding the perceptual switch for visual and auditory ambiguous stimuli. Furthermore, they observed that that the relative magnitude of the pupil dilation could be identified as a significant positive predictor of the subsequent perceptual duration (Einhäuser et al., 2008).

Consequently, the authors hypothesized that autonomous brainstem systems such as the locus coeruleus and its associated neurotransmitter norepinephrine, may influence neural networks of perceptual selection and perceptual alteration (Einhäuser et al., 2008; Larsen & Waters, 2018).

To this end, we utilized pupillometry and eye tracking data to explore and investigate possible relationships between *tACS*, pupil dilation, and perceptual stability in human tactile ambiguous motion perception.

The comprehensive approach, combining *tACS* as a neuromodulatory tool and pupil measurements as an objective indicator, provides valuable insights into the dynamic interplay between modulated brain oscillations and tactile perception.

#### 3.2. Materials and methods

#### 3.2.1. Participants

In total eighteen healthy subjects (n = 18, 10 females, 8 males, age range = 20-35 years, mean age = 26.3889 years, standard deviation = 3.8370) were recruited (Table 1).

### 3.2.2. Experimental paradigm and tactile SAM stimulus

Participants were comfortably seated in a sound and light attenuated and electrotonically shielded chamber within the laboratory area of the department of neurophysiology and pathophysiology of the university medical center in Hamburg (Germany).

To induce an ambiguous tactile perception of apparent motion, four vibrotactile elements (C-2 tactors, vibration frequency at 250 Hz, detailed description in section 2.2.) were attached on the ventral side of each forearm. Both forearms were placed in a supinated straight parallel position on a rectangular wooden frame, which was placed on a table in front of the participant. The wooden frame was marked with an adjustable strip, that predefined the between forearm (horizontal) distances for the C-2

tactors. The specific within (vertical) and between (horizontal) forearm distances were individually predefined for each participant to match an aspect ratio of approximately 1,25. Consistent with the investigations conducted by Liaci et al. (2016) distances for the tactile stimulation sites on the respective forearm were defined in relation to the total forearm length for each participant (Liaci et al., 2016). This procedure was adopted to control for individual variability in forearm length (Liaci et al., 2016).

Furthermore, both forearms were concealed with a visual cover to avoid potential visual influences on the perception of the different distances of the C-2 tactors.

Stimulation streams of simultaneous activation of the C-2 tactors on diagonal corners and alternating subsequent activation of the C-2 tactors at the opposite corners caused participants to spontaneously switch between a tactile *horizontal* apparent motion percept and a tactile *vertical* apparent motion percept.

In this context, the tactile *horizontal* apparent motion percept can be described as between forearm motion, whereas the tactile *vertical* apparent motion percept can be referred to as within forearm motion (Liaci et al., 2016). The corresponding descriptions of motion patterns in the tactile domain can be explained by theoretical considerations (Liaci et al., 2016). In the visual modality a three-dimensional stimuli space is projected to a two-dimensional retinal space (Liaci et al., 2016). Consequently, motion patterns in the *vertical* trajectory and motion patterns along the anterior-posterior and cranio-caudal axis might be represented by the same cognitive and neuronal mechanism (Liaci et al., 2016). Regarding the concept of the "endogenous" and "exogenous reference frames", the constellation of this design allows for the alignment of the two "reference frames", since within forearm motion is equivalent to the concept of *vertical* motion and between forearm motion is equivalent to *horizontal* motion (Liaci et al., 2016).

During the task, participants are instructed to report their current tactile perception by activating one of two keys on a response device. (Cedrus Response Pad, RB844, Cedrus Corporation, San Pedro, CA 90734, USA) with their right foot, with the right (or left) button is representing a *horizontal* percept, whereas the left (or right) button is representing a *vertical* percept. The indication of the response direction patterns was counterbalanced between participants. If the participant did not perceive a clear current tactile perceptual state of either a *horizontal* or *vertical* pattern, the subject was instructed to release all buttons. Prior piloting of the experiment revealed that the amplitude of the

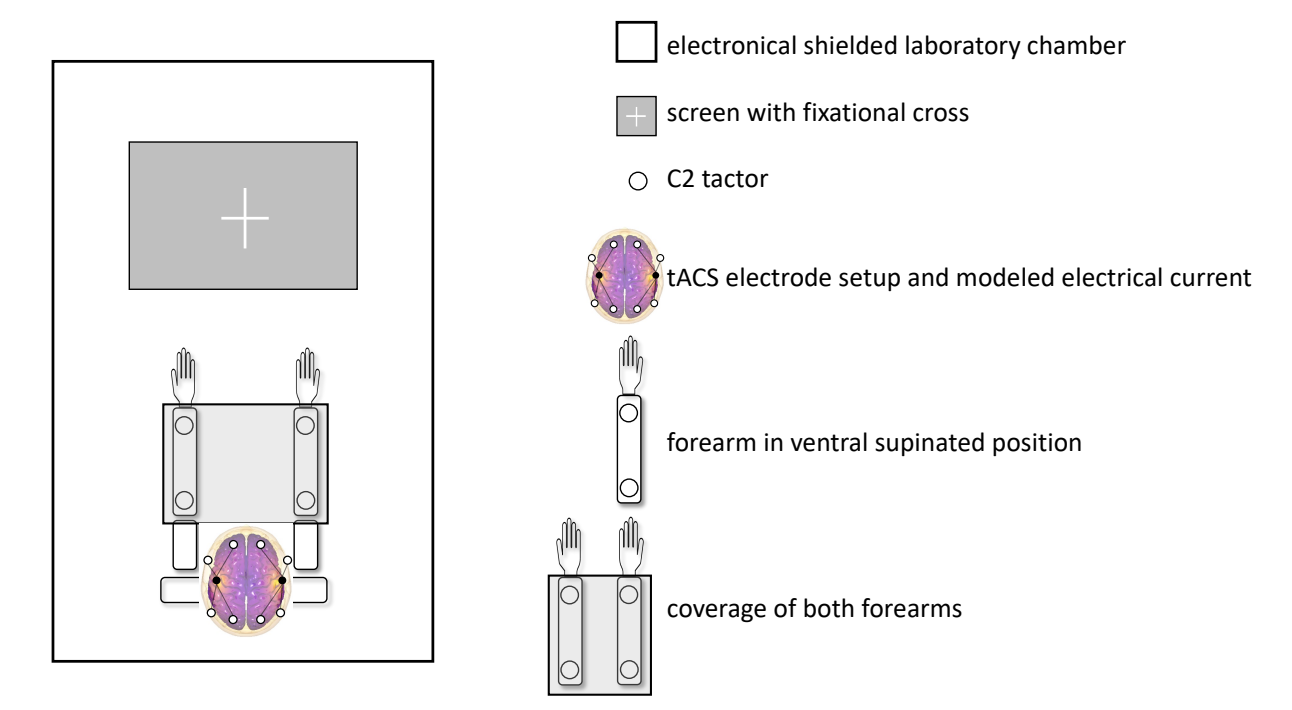
intensities for the proximal tactile stimulation sites of the C-2 actuators at maximum tactile stimulation intensity were perceived more clearly than the distal stimulation sites in proximity to the wrist. Consequently, the intensities for all four stimulation sites were individually adjusted so that the intensity of the tactile sensation was perceived to be identical at all four stimulation sites (distal C-2 tactors intensity [range 0-1]: mean amplitude: 0.986 arbitrary units [ $\pm$  0.283 standard deviation], proximal C-2 tactors intensity: 0.686 arbitrary units [ $\pm$  0.357 standard deviation]). In addition, a central fixation cross (1.6 cm x 1.6 cm,  $1.528^\circ$  visual angle) was displayed on a BenQ XL2420T screen (1.9206 x 1.080, 120 Hz), mounted in approximately 60 cm distance in front of the participant. Participants were required to maintain fixation on the cross for the whole duration of the experiment. To ensure compliance, each subject was provided with glasses that integrated pupil and eye tracking functions (Pupil Labs GmbH, Sanderstr. 28, 12047, Berlin, Germany), which were calibrated prior to the start of the experiment (Kassner & Patera, 2012).

Prior to the actual ambiguous tactile stimulus configurations, a proceeding unambiguous horizontal or unambiguous vertical tactile start configuration was introduced. This unambiguous configuration would switch to the ambiguous configuration after a random time jitter time ranging from 12,5 seconds to 17,5 seconds. The random jitter phase was adjusted within and between every participant in order to ensure for equal sensory stimulation time periods for each condition and sub condition. The unambiguous stimulus configurations functioned as a control condition to keep participants' attention and focus on their tactile apparent motion perception and to allow for an objective control throughout the duration of the experiment. In addition, the rationale for introducing the variable jitter range of the unambiguous configuration was to decrease the possibility of expectational effects by participants. The directional motion pattern of the unambiguous start configuration was randomly assigned for the specific trial but counterbalanced to be equally matched across the whole experiment for each participant. In total, the experiment comprised of 10 trials with equally randomized and counterbalanced preassigned start configuration of the unambiguous start configuration. A trial consisted of tactile stimulation streams with a duration of 100 seconds in total. All trials in the respective tACS condition were performed in one continuous run. The simultaneous activation of the C-2 tactor lasted for 300 ms with an interstimulus interval of 200 ms. Before commencing the experiment, participants received information regarding the bistable nature of the tactile stimulus and

underwent approximately ten minutes of training to familiarize themselves with the *unambiguous* and ambiguous stimulus configurations.

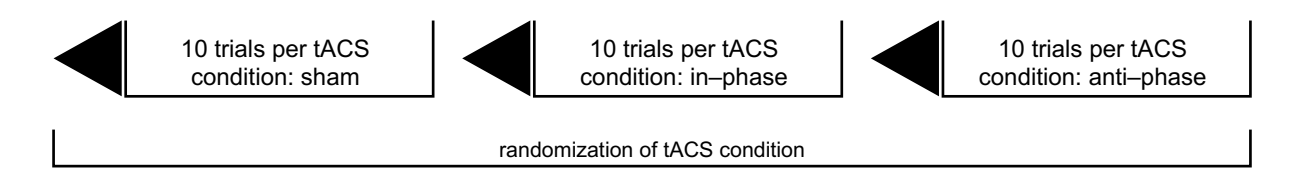
All participants were blinded with respect to the different non-invasive brain stimulation conditions and concrete scientific hypotheses. The sequence of the experimental *tACS conditions* was randomly preassigned and counterbalanced within and between participants. All experimental conditions were performed consecutively in a single session. One participant (subject 14, male) accidently pressed the two buttons of the reponse box simultaneously for a total duration of 96,2776 seconds in the *sham* condition. Consequently, time frames of this period were excluded from all further analyses.

Figure 5 – Schematic representation of the experimental design (tactile SAM)



Schematic representation of the experimental design for the tactile SAM stimulus. Subjects in the experiment were positioned within a laboratory room designed to minimize electronic interference, control light exposure, and dampen sound levels. C-2 tactors were attached at relative distances to the forearms of each participant, which were placed in a ventral and supinated position. In order to diminish possible visual influences, forearms were visually shielded with a cover.

Figure 6 – Schematic representation of tACS conditions and study concept (tactile SAM)



Schematic representation of *tACS conditions* and study concept. The black triangles represent the ramp up segment of the *tACS* protocol. All three *tACS conditions* were preassigned to participants and administered consecutively within the same day. It should be noted that the ramp up segment was only used at the beginning of a *tACS* block prior to the actual tactile stimulation (and therefore prior to the start of the first trial). After the ramp up segment, *tACS* was applied continuously throughout all trials within the specific *tACS condition*.

Figure 7 – Detailed trial description (tactile SAM)

	1 trial (100 seconds)		
tACS ramp up segment (10 seconds)	continuous tACS application (sham, in – phase, anti – phase) frequency of 40 Hz intensity of 4 mA peak-to-peak		
	unambiguous tactile configuration (12.5 – 17.5 secs)	ambiguous tactile configuration (87.5 – 82.5 secs )	

10 trials per tACS condition (1000 seconds ~ 16.7 minutes)

Each trial in the experiment consisted of 100 seconds of tactile (and electrical) stimulation. The onset of each trial consisted of either a *horizontal* or *vertical unambiguous* stimulus configuration. The *motion direction* was randomly assigned and counterbalanced within subjects. To avoid expectancy effects, the duration of the *unambiguous* tactile configuration was also randomized (12.5 – 17.5 seconds). In total, there were 5 trials with an *unambiguous vertical* start condition and 5 trials with an *unambiguous horizontal* start condition. In addition, the time frame of the *unambiguous* tactile stimulus configuration served as a control condition. Following the *unambiguous* tactile condition, the tactile stimulation changed to the *ambiguous* tactile configuration (87.5 seconds – 82.5 seconds). A total of 10 trials were conducted per *tACS condition* (3 x 10 trials). Accordingly, the experiment lasted

1000 seconds (~16.7 minutes) for a *tACS* block in total. Throughout the tactile stimulation, bilateral *tACS* was applied continuously. It should be mentioned that the ten second ramp up segment was used only for the first trial. The tactile stimulation commenced when the maximum intensity of the electrical stimulation was reached.

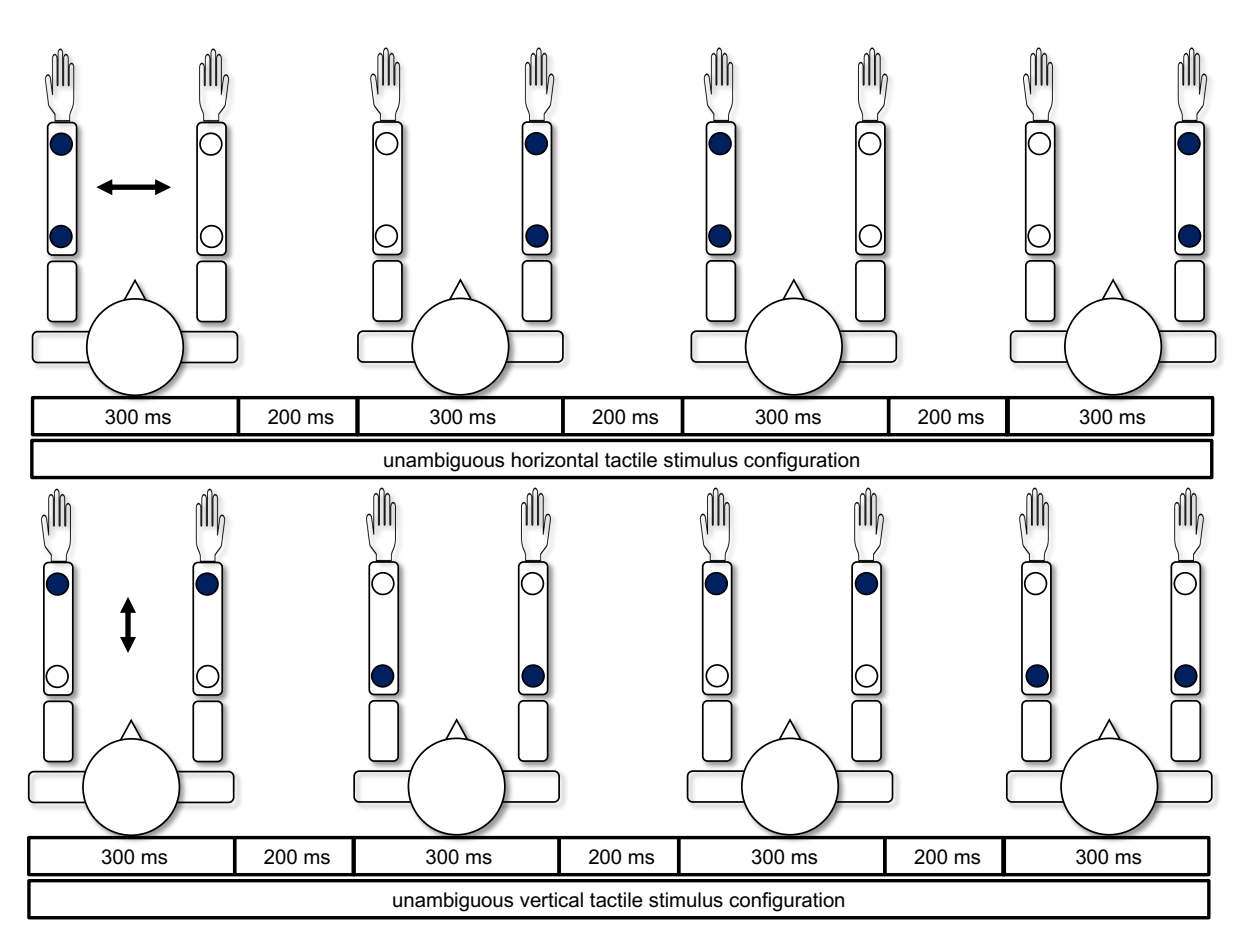
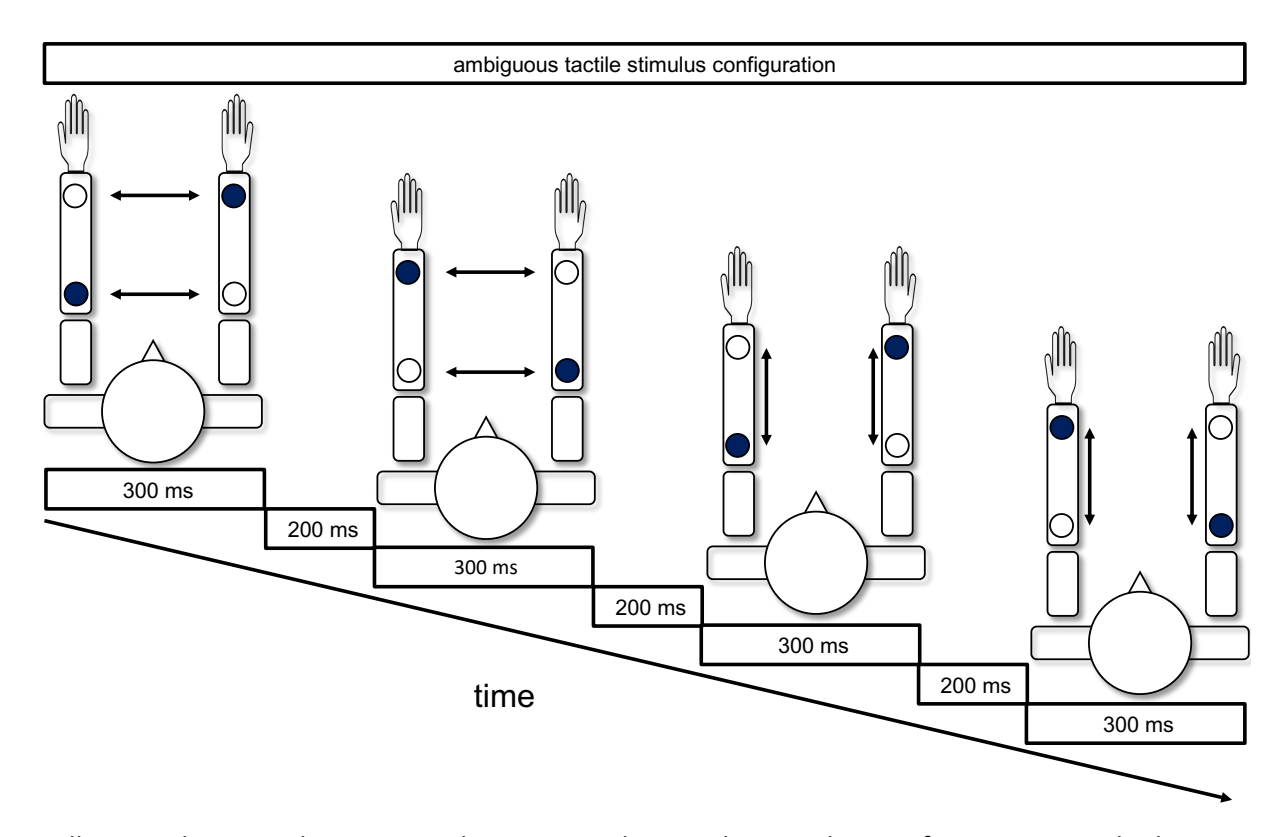


Figure 8 – *Unambiguous* tactile stimulus configuration (tactile SAM)

A trial started with the *unambiguous* tactile stimulus configuration, which consisted of either an *unambiguous horizontal* or an *unambiguous vertical* tactile *motion direction*. *Unambiguous motion directions* were randomized and balanced within subjects. C-2 tactors were activated for 300 ms with an interstimulus interval of 200 ms. Timeframes of *unambiguous* stimulus configurations were used as a control condition in order to keep subjects' attentional focus on the tactile motion perception. Blue filled circles indicate an activated C-2 tactor.

Figure 9 – Ambiguous tactile stimulus configuration (tactile SAM)



Following the *unambiguous* tactile pattern, the tactile stimulus configuration switched to an *ambiguous* configuration. As described in the main text, the *ambiguous* tactile configuration produces an apparent tactile antiparallel *horizontal* or *vertical* motion perception. C-2 tactors were activated for 300 ms with an interstimulus interval of 200 ms. Blue filled circles indicate an activated C-2 tactor.

### 3.2.3. TACS protocol

While performing the *ambiguous* tactile apparent motion perception task, transcranial current stimulation was bilaterally applied by two accumulator powered stimulators (DC-Stimulator plus, NeuroConn, neuroCare Group GmbH, Munich, Germany). The current was continuously applied via ten Ag/AgCl electrodes (12 mm diameter, EASYCAP GmbH, Herrsching, Germany) in a 4-in-1 electrode configuration for each stimulation site respectively. The frequency and intensity of the alternating current stimulation was controlled by a customized MATLAB (MATLAB, R2016b (9.1.0), The MathWorks Inc., Natick, MA, USA) script and adjusted to a frequency of 40 Hz and a stimulation magnitude of 4 mA peak-to-peak.

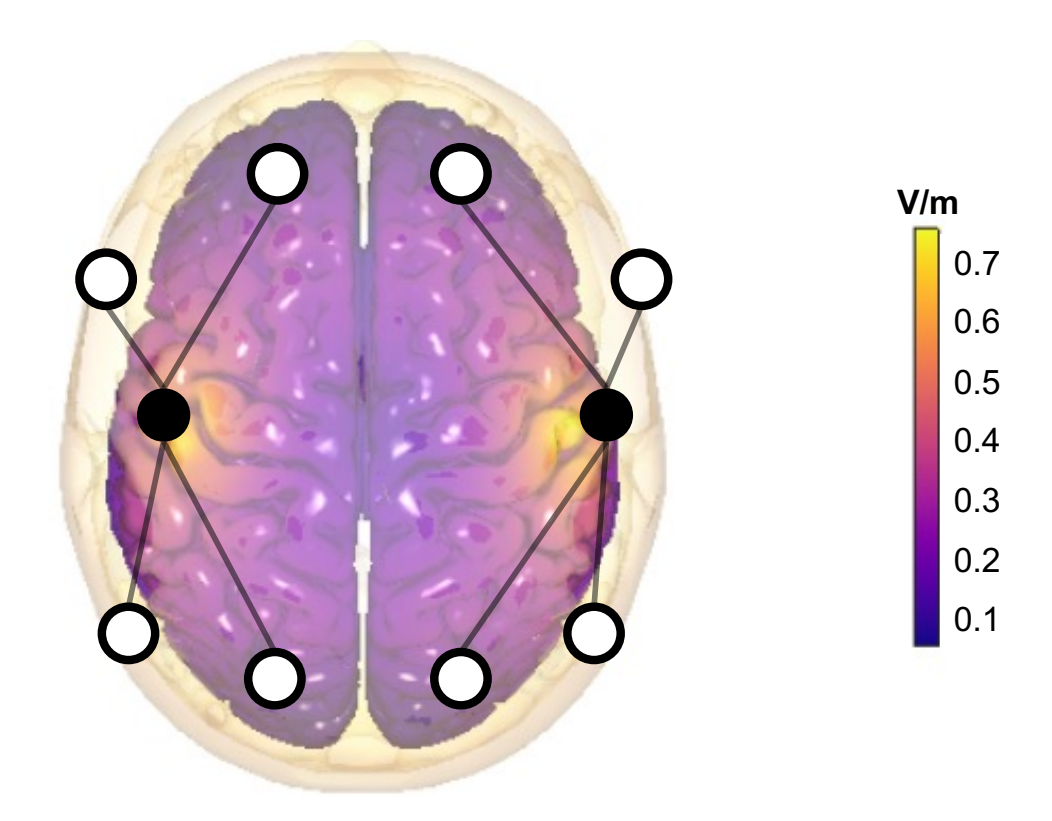
Because of the relatively high intensity of 4 mA peak-to-peak used in this study, the skin of the participants' head was locally anesthetized by applying a topical anesthetic cream (EMLA, 25 mg/g Lidocain + 25 mg/g Prilocain, Creme, Aspen Germany GmbH, Munich, Germany), in accordance with the application manual of the topical pharmaceutic. The anesthetic effect of this procedure was tested individually for each subject prior to the beginning of the experiment to dimmish possible discomforting or painful sensations evolving from the non-invasive electrical stimulation.

TACS was administered in a block wise experimental design, and the tACS conditions were preassigned and counterbalanced across and within participants. At the beginning of the *in-phase* and *anti-phase* tACS conditions, the electrical stimulation intensity was increased sinusoidally (from 0 mA to the maximum of 4 mA intensity) for a ten-second-long segment preceding the onset of the tactile SAM stimulus in order to accustom participants to the electrical stimulation. The *sham* stimulation condition consisted of a ten-second-long ramp up segment immediately followed by a ten-second-long ramp down segment.

After the experiment, participants received a debriefing and completed a questionnaire regarding the perceived possible sensations and side effects of the electrical stimulation. Subjects were able to phenomenologically discriminate between the two stimulating conditions and the *sham* condition. Nevertheless, they were not able to distinguish between the *in-phase* or *anti-phase* condition.

Phenomenologically, the majority of participants reported perceiving the tactile activation patterns as distinct antiparallel motion patterns in either *horizontal* or *vertical* direction. Nevertheless, some participants described the quality of the tactile percept as a smooth transitional wave, switching in antiparallel fashion between a *horizontal* and *vertical* direction pattern.

Figure 10 – tACS setup (in-phase modeled current, tactile SAM)



The experiment involved a two-sided, 4-in-1 electrode setup for bilateral *tACS*. The black and white dots represent stimulation electrodes at different polarities. The sinusoidal magnitude of the electrical stimulation was adjusted to 4 mA peak-to-peak at a frequency of 40 Hz. An estimation of the maximum current intensities on the cortical surface was conducted (see section 2.3.). Subjects received bihemispheric *in-phase* and *anti-phase* alternating current stimulation, via two symmetrically adjusted 4-in-1 montages over somatosensory cortices. The modeled cortical surface is color-coded to represent the simulated maximum field strength in V/m (4 mA peak-to-peak).

Figure 11 – Electrical stimulation parameters – anti-phase tACS condition (tactile SAM)

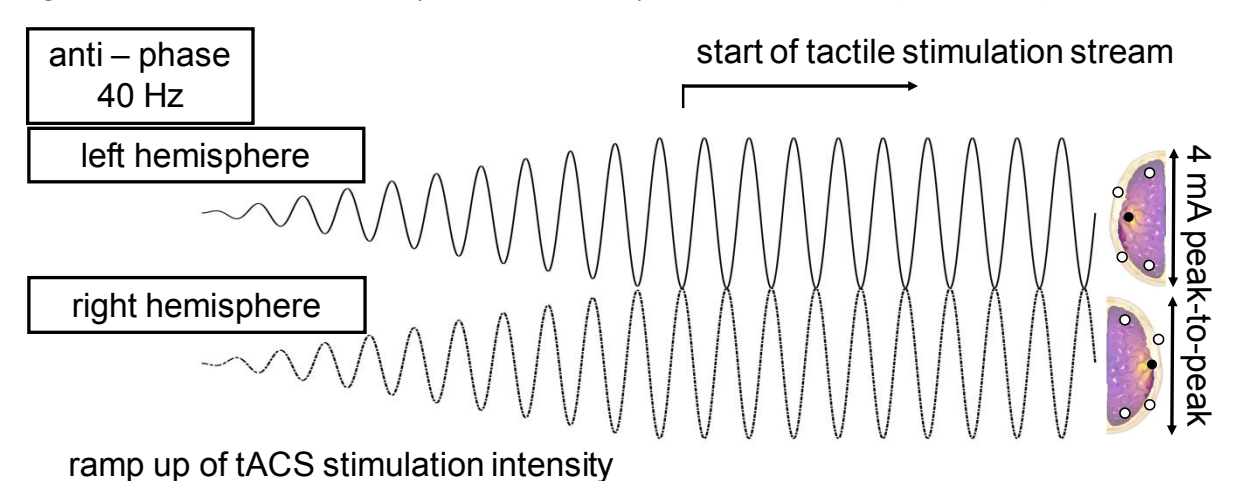


Figure 12 – Electrical stimulation parameters – *in-phase tACS condition* (tactile SAM)

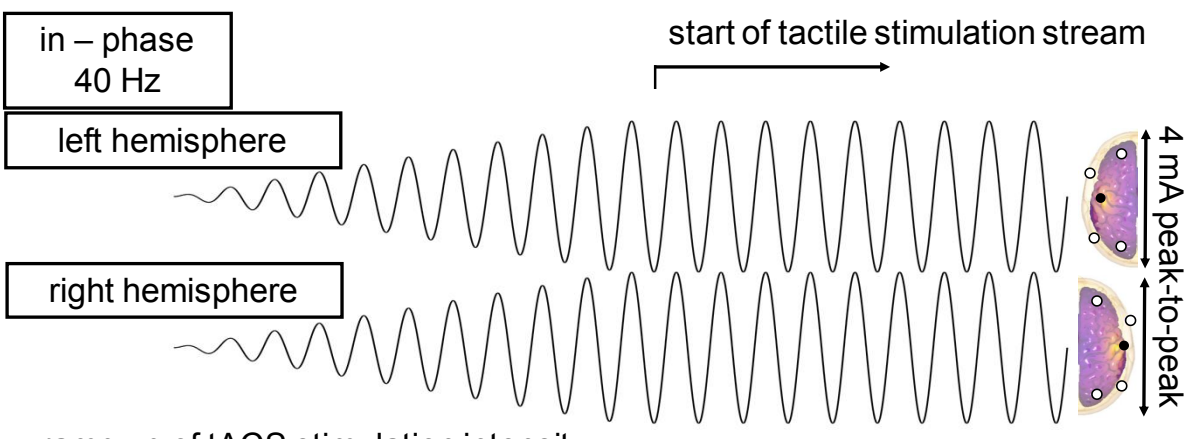


Figure 13 – Electrical stimulation parameters – *sham* condition (tactile SAM)

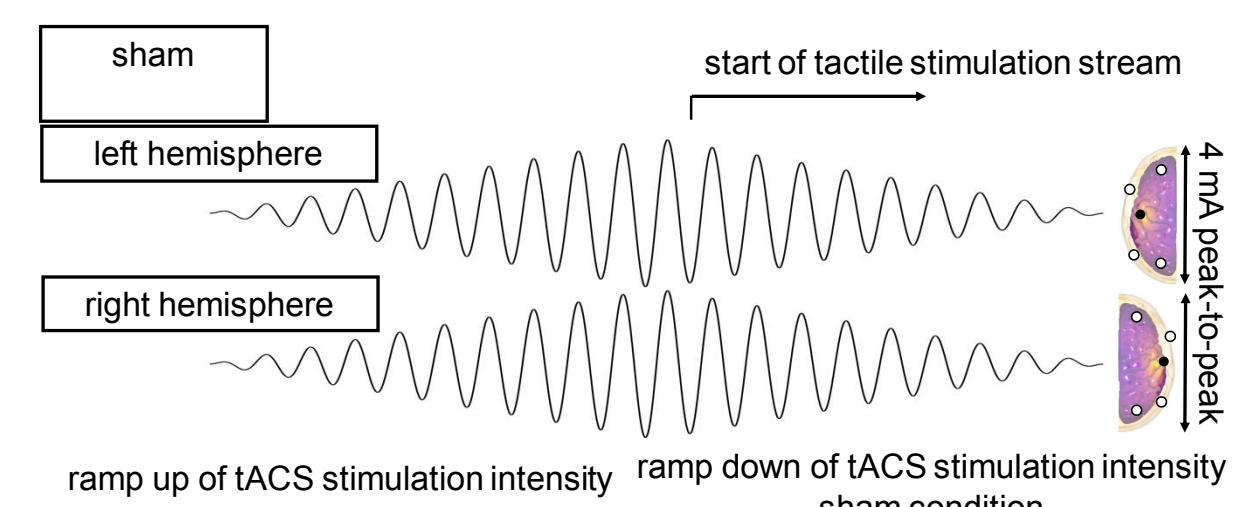


Figure 11-13. Electrical stimulation parameters – tACS conditions (tactile SAM).

Bilateral electrical stimulation was applied to participants while they performed the tactile apparent ambiguous motion task. The magnitude of electrical stimulation was adjusted to 4 mA peak-to-peak and a frequency of 40 Hz. The ramp up segment was fixed for 10 seconds before reaching maximum intensity, followed by the tactile ambiguous stimulation.

sham condition

For the *anti-phase* condition (Figure 11), sinusoidal alternating electrical stimulation is applied to both hemispheres with opposite phases. Specifically, when one hemisphere experiences a positive phase, the other hemisphere experiences a negative phase. This approach is hypothesized to disrupt the interhemispheric communication, resulting in potential improvements in *vertical* motion perception or impairments in *horizontal* motion perception.

For the *in-phase* condition (Figure 12), alternating current with identical phase is administered to both hemispheres of the brain. The objective, as detailed in the main text, is to synchronize neural activity between hemispheres in order to improve coordination and communication. This synchronization is speculated to enhance the perception of *horizontal* tactile motion, which may necessitate interhemispheric cooperation. *In-phase tACS* may enhance the integration of information between the left and right hemispheres, leading to potential improvements in *horizontal* motion perception or impairments in *vertical* motion perception.

Regarding the *sham* condition (Figure 13), the electrical stimulation of the ramp up segment was subsequently continued by a ramp down segment of 10 seconds. It should be noted that a lower sinusoidal frequency was used in this figure for clarity.

## 3.2.4. Pupillometry and gaze data

Gaze position data and pupil diameter data were recorded as part of the experiment. The measured data served two purposes: to control for saccades/micro-saccades and to measure pupil size for further exploratory analyses.

Therefore, *horizontal* and *vertical* gaze positions and the pupil areas of both eyes were registered for each participant using specialized Pupil-labs software and hardware (<a href="https://pupil-labs.com/">https://pupil-labs.com/</a> products/core/, Pupil Labs GmbH, Sanderstr. 28, 12047, Berlin).

The sampling rate of the recordings was 60 Hz, and calibration was performed before the beginning of each experimental block. For blink detection the Pupil-labs software as well as a customized MATLAB (MATLAB, R2016b (9.1.0), The MathWorks Inc., Natick, MA, USA) script was used. Therefore, identified blinks were padded by 200 ms and linearly interpolated. In the following step, a fourth-order Butterworth low-pass filter with a cutoff frequency of 4 Hz was applied to the interpolated pupil time courses. In the next step, the filtered data was z-scored for each trial based on the mean and standard deviation of the individual time courses. To account for the impact of blinks and saccades on the pupil behavior, we employed a deconvolution technique and eliminated these components from the pupil measurements through linear regression, following the methodology specified in Urai et al., 2017 (Urai et al., 2017).

The time courses of pupil diameter were obtained by identifying the moment of a button press that indicated the onset of a current percept. Subsequently, a period of 10 seconds prior to and following the identified timepoint was extracted from the pupil time course for further analysis. This time series was referred to as the *pressed* condition. As a *control* condition, the time point with the maximum temporal distance to the onset of a *horizontal* or *vertical* percept (indicated by a button press) was identified. In the subsequent step, the pupil time course 10 seconds prior to and following to that time point was extracted. Additionally, it was ensured that data from the extracted time course did not overlap with data from the *pressed* time series.

This approach allowed for a detailed investigation and statistical comparison of the pupil's response to the perceptual task over a substantial period of time. For further analysis of the overall pupil amplitude (positive or negative) in temporal relation to the current perceptual state, a linear projection procedure of the individual pupil time course was performed as described by De Gee et al., 2014 and Kloostermann et al., 2015 (De Gee et al., 2014; Kloostermann et al., 2015).

The linear projection procedure is well established as a reliable method for computing the amplitude of functional magnetic resonance imaging (fMRI) responses (Ress et al., 2000). It is formulated as:

$$A_i = \frac{R_i * \overline{R}}{\left| \left| \overline{R} \right| \right|^2}$$

where  $A_i$  represents the scalar amplitude estimate for the identified pupil time course  $i.\ R_i$  encompasses the pupil response time course of that individual trial.  $\overline{R}$  denotes the average pupil response time course over all trials and all conditions for a specified participant (De Gee et al., 2014; Kloostermann et al., 2015). This approach has the advantage of condensing each individual pupil's time series within each trial into a scalar quantity of pupil response amplitude (De Gee et al., 2014; Kloostermann et al., 2015). This is achieved by calculating the dot product between the time series of the pupil response of each trial and the normalized mean response of each individual participant. (De Gee et al., 2014; Kloostermann et al., 2015). This method provides reliable measurements of the amplitude for each trial (De Gee et al., 2014; Kloostermann et al., 2015). Furthermore, the measurement of amplitude modulation considers the normalized mean response of each individual participant, accounting for individual variations in the pupil evoked response function in a data-based manner (De Gee et al., 2014; Kloostermann et al., 2015).

#### 3.2.5. Hypothesis

Three different *tACS conditions* were defined as the independent variables: *in-phase* stimulation, *anti-phase* stimulation and *sham* stimulation. In accordance with the hypotheses of bihemispheric integration for the visual SAM stimulus, we hypothesize that the specific directional pattern of perceived *horizontal* and *vertical* tactile apparent motion is correlated with specific interand intrahemispheric characteristic brain states. Moreover, the *tACS* design aims to causally and phase-specifically modulate these neural brain states and the corresponding behavioral outcomes.

In concrete terms, it is anticipated that the application of 40 Hz *in-phase tACS* will enhance *horizontal* tactile perception, as evidenced by longer *horizontal* percept times. In contrast, it is hypothesized that 40 Hz *anti-phase tACS* will enhance *vertical* tactile perception, resulting in longer *vertical* percept times. Conversely, it is hypothesized that 40 Hz *in-phase tACS* will impair *vertical* tactile perception, as evidenced by a reduction in *vertical* percept times. Similarly, 40 Hz *anti-phase tACS* is hypothesized to impair *horizontal* tactile perception, resulting in a reduction in *horizontal* percept times. In addition to the behavioral data, an exploratory investigation of pupil diameter measurements will be conducted for the distinct *tACS conditions*. Potential differences in response patterns of pupil data between the *tACS conditions* may reflect distinct *tACS* induced modulations of neural processing and subsequent tactile motion perception.

## 3.3. Statistical analyses and results

The primary dependent variables were normalized percept time (NPT) and the button press rate, reflected in button pressed per minute (BPM). The dependent variables were calculated separately for each subject in each trial and each condition. In the statistical analyses, only trial times of the ambiguous stimulus configuration lasting more than one second were included. To objectively track participants' attention to the perceived tactile direction pattern, the *unambiguous start configurations* preceding the actual ambiguous stimulus configurations were used as a control condition. For the presented time of the *unambiguous horizontal* direction pattern, the control condition revealed that 0,8619 (mean ± 0,1087, standard deviation) of the time frames were accurately indicated as a *horizontal* percept across all participants. During the time of the *vertical unambiguous* stimulus configuration 0,7006 (mean, ± 0,1638, standard deviation) of the time frames were correctly indicated across all participants. Furthermore, the overall button presses per minute rate for perceiving a *vertical* or *horizontal* motion pattern related to the ambiguous stimulus configuration was 1,8566 (mean, ± 0,8897, standard deviation). The mean overall button presses per minute rate related to the ambiguous stimulus configuration for a motion percept was 0,9283 (mean, ± 0,5233, standard deviation).

For statistical analysis and comparisons, two separate 3x2x2 repeated measures analysis of variance (RM-ANOVA) were constructed for the dependent variables of normalized percept time (NPT) and button press per minute (BPM). The RM-ANOVAs contained the factors of *tACS condition* (3: [sham, in-

phase, anti-phase]), perceived motion direction (2: [horizontal percept, vertical percept]) and start configuration of the unambiguous stimuli (2: [horizontal unambiguous, vertical unambiguous]).

Furthermore, a more detailed exploratory statistical analysis of the normalized percept times (NPTs) was conducted using a 3x4x2 RM-ANOVA model. To that end, individual data of the normalized percept time were sorted and statistically analyzed depending on the preceding percept for every participant.

This allowed for the categorization of perceptual alternations or non-alterations and their subsequent normalized percept times, thus enabling the analysis of four possible combinations:

- 1 preceding horizontal percept → subsequent horizontal percept,
- 2 preceding *horizontal* percept → subsequent *vertical* percept,
- 3 preceding *vertical* percept → subsequent *horizontal* percept,
- 4 preceding *vertical* percept → subsequent *vertical* percept.

The subsequent normalized percept times (NPTs) in dependence of the preceding percept were statistically analyzed. For statistical comparison, a 3x4x2 RM-ANOVA design was implemented consisting of three factors: tACS condition (3: [sham, in-phase, anti-phase]), perceptual alteration (4: [horizontal-to-horizontal, vertical-to-vertical, vertical-to-horizontal, vertical-to-vertical]), and start configuration of the unambiguous stimuli (2: [horizontal unambiguous, vertical unambiguous]).

In order to resolve for complex interactions effects of the 3x4x2 RM-ANOVA, a following statistical analyses composing of four nested RM-ANOVAs were conducted. Therefore, the factors tACS condition (3: [sham, in-phase, anti-phase]), and start configuration of the unambiguous stimuli (2: [horizontal unambiguous, vertical unambiguous]) were analyzed within each of the four distinct perceptual alteration conditions. For all reported RM-ANOVA analyses and results the Greenhouse-Geisser correction as well as Bonferroni-corrected post hoc analyses were used where appropriate.

Figure 14 – Normalized percept time (NPT) in dependence of the preceding percept (tactile SAM)

button press	button release	button press
preceding horizontal percept	no percept	subsequent horizontal percept
preceding horizontal percept	no percept	subsequent vertical percept
preceding vertical percept	no percept	subsequent horizontal percept
preceding vertical percept	no percept	subsequent vertical percept
		analyzed time frame of NPTs

For a more detailed exploratory analyses, the NPTs were categorized in dependence of the preceding *perceived motion direction* pattern. This classification resulted in four possible combinations, as shown in this figure.

For further analyses, gamma cumulative distribution functions were calculated and assessed based on NPTs. For statistical comparison and evaluation of distribution differences between experimental conditions, non-parametric permutational statistical comparisons based on condition differences were performed. For this purpose, confidence intervals (CIs) were calculated based on a factorial design consisting of the factors of *tACS condition* (3: [sham, in-phase, anti-phase]), perceived motion direction (2: [horizontal percept, vertical percept]), and start configuration of the unambiguous stimuli (2: [horizontal unambiguous, vertical unambiguous]). This approach provides a robust method for examining even minor alterations in distribution shape that may not be automatically apparent as significant mean differences in RM-ANOVAs (Misselhorn et al., 2019). It is important to note, that the calculated confidence intervals were adjusted for multiple comparisons by considering the count of condition-wise contrasts and the global spread of NPT values. Therefore, condition differences that exceeded the corrected confidence interval were considered statistically significant.

Pupillometry data were statistically evaluated using non-parametric permutational statistical comparisons. For this purpose, pupil data from the *pressed* conditions und *control* conditions for the respective *tACS* sub conditions were statistically evaluated based on condition differences of *pressed* and *control* conditions.

To evaluate statistical differences correction for multiple comparisons by considering the number of condition wise comparisons and the range of the pupil data time course was applied.

Finally, correlation patterns regarding the predictive value of the pupil amplitude modulation in the different *tACS conditions* were assessed using Spearman's correlation between the variables of amplitude modulation and NPTs.

All detailed information regarding the analyses and procedures performed for the dependent variables are described in the following sections.

### 3.3.1. Normalized percept time (NPT)

NPTs were defined for the *horizontal* and *vertical* motion pattern distinctly as:

$$NPT_{(horizontal \,|\, vertical)} = \frac{perceived \; motion \; time \; in \; seconds}{total \; time \; of \; ambiguous \; stimulus \; configuration \; in \; seconds}$$

The overall mean NPT for perceiving a *vertical* or *horizontal* motion pattern related to the ambiguous stimulus configuration was 0.8829 (mean,  $\pm\,0.1149$  standard deviation). The mean overall percept time related to the ambiguous stimulus configuration for a motion percept was 0.4414 (mean  $\pm\,0.2204$ , standard deviation).

3.3.1.1. Normalized percept time (NPT) – 3x2x2 RM-ANOVA (Figure 15-17; Table 2-4)

tACS condition (3: [sham, in-phase, anti-phase])

perceived motion direction (2: [horizontal percept, vertical percept])

start configuration of the unambiguous stimuli (2: [horizontal unambiguous, vertical unambiguous])

A significant effect for the main factor *tACS condition* (F = 5.595, df = 2, p = 0.008,  $\eta_p^2 = 0.248$ , n = 18) and the main factor of *perceived motion direction* (F = 8.430, df = 1, p = 0.010,  $\eta_p^2 = 0.331$ , n = 18) was observed. The main factor *start configuration of unambiguous motion direction* showed no significant difference (F = 1.626, df = 1, p = 0.219,  $\eta_p^2 = 0.087$ , n = 18).

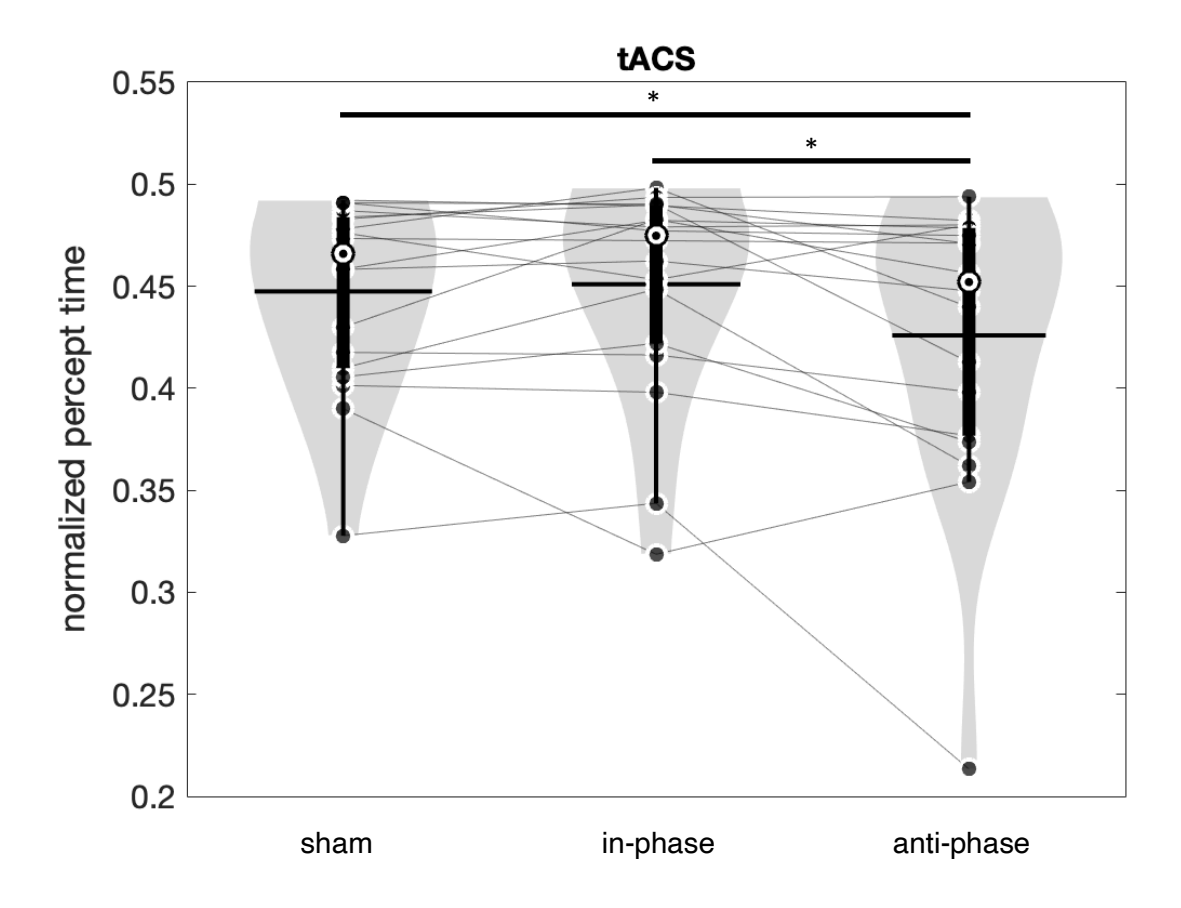
Finally, the interaction effect of *tACS* condition and perceived motion direction (F = 0.736, df = 2, p = 0.487,  $\eta_p^2 = 0.041$ , n = 18), the interaction effect of *tACS* condition and unambiguous start configuration (F = 0.454, df = 2, p = 0.639,  $\eta_p^2 = 0.026$ , n = 18), the interaction effect of perceived motion direction and unambiguous start configuration (F = 0.075, df = 1, p = 0.787,  $\eta_p^2 = 0.004$ , n = 18) and the

interaction effect of tACS condition, perceived motion direction and unambiguous start configuration  $(F=0.344, df=2, p=0.712, \eta_p^2=0.020, n=18)$  revealed no significant effect (Table 2 and 3). Bonferroni-corrected post hoc comparisons for the tACS conditions revealed a significant difference between the *in-phase* condition and *anti-phase* condition  $(t=3.090, p_{bonf}=0.012, Cohen's d=-0.018, n=18)$ , as well as a significant difference between the *sham* condition and *anti-phase* condition  $(t=2.655, p_{bonf}=0.036, Cohen's d=0.110, n=18)$ . No significant difference could be observed for the

comparison of the sham condition and in-phase condition (t = -0.436,  $p_{bonf} = 1$ , Cohen's d = 0.128, n = 0.128

18) (Table 4).

Figure 15 – Violin plot – 3x2x2 RM-ANOVA Normalized percept time (NPT) – post hoc comparisons of *tACS conditions* (tactile SAM)

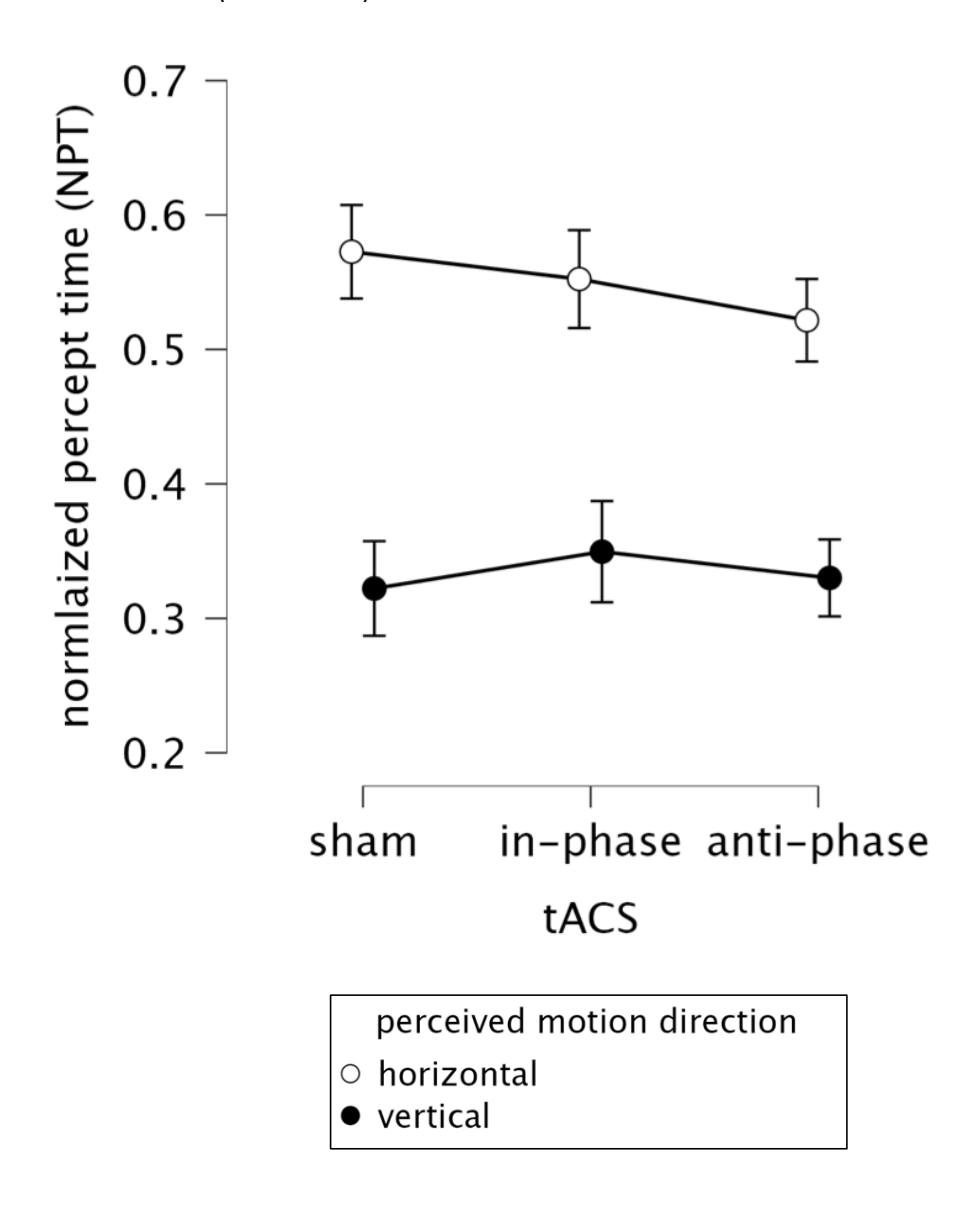


Effects of *tACS conditions* on normalized percept time (NPT). The main factor of *tACS* revealed a highly significant effect of the *tACS conditions*. Post hoc analyses indicated significantly longer normalized percept time in the *sham* and *in-phase tACS condition* in relation to the *anti-phase* condition (sham - anti-phase:  $p_{bonf} = 0.036$ ; in-phase - anti-phase:  $p_{bonf} = 0.012$ ) (Table 4).

Black dots represent each subject in the respective condition. The solid black horizontal lines indicate the mean value for the respective condition, the circular white marker with the inner black dot indicates the median value for the respective condition.

Note. Results are averaged over the levels of perceived motion direction and unambiguous start configuration.

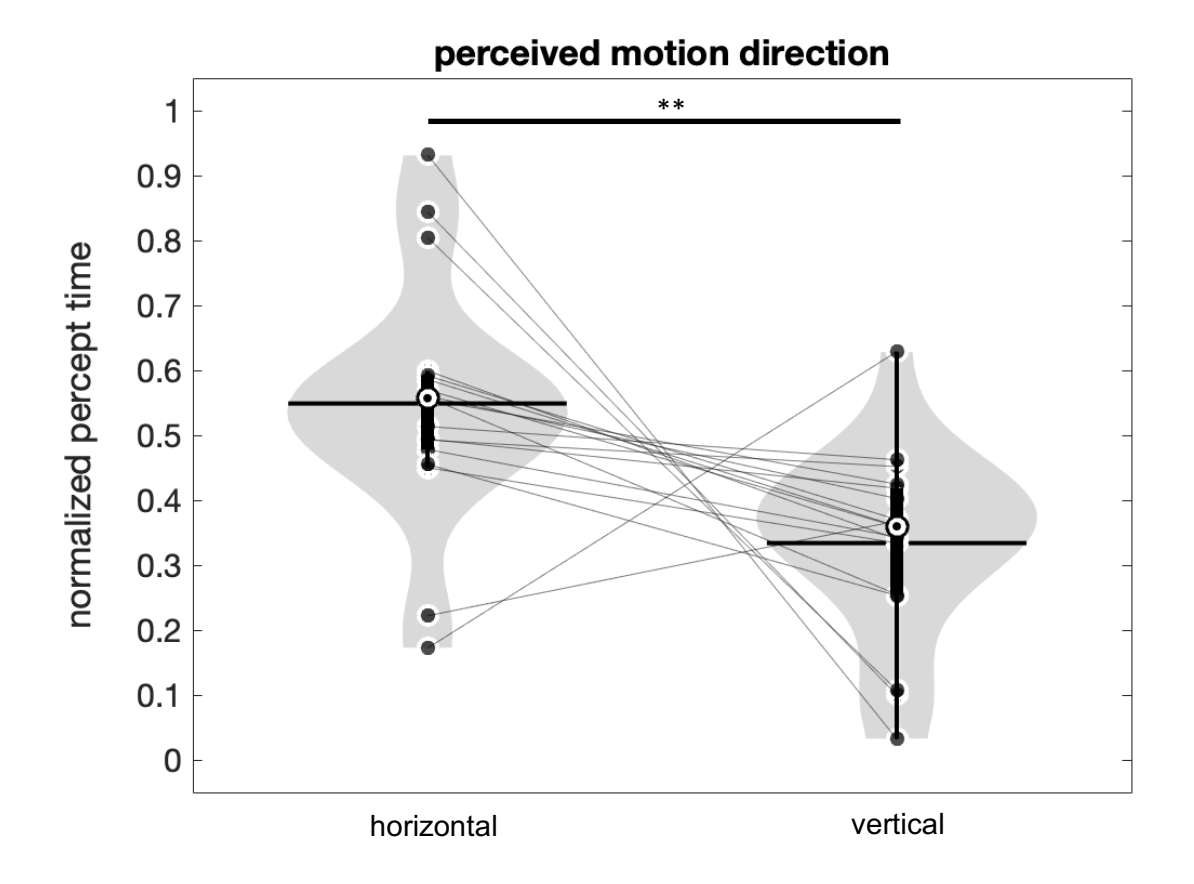
Figure 16 – Line plot – 3x2x2 RM-ANOVA Normalized percept time (NPT) – Interaction of *tACS* and *perceived motion direction* (tactile SAM)



Interaction effect of tACS and perceived motion direction on normalized percept time (NPT). The interaction effect did not reach significance (p = 0.487) (Table 2). Error bars indicate the standard error of means. The filled black dots indicate the mean values across participants for the vertical perceived motion direction, whereas the white dots indicate the mean values across participants for the vertical vertica

*Note.* Results are averaged over the levels of *unambiguous start configuration*.

Figure 17 – Violin plot – 3x2x2 RM-ANOVA Normalized percept time (NPT) – *perceived motion direction* (tactile SAM)



Effects of *perceived motion direction* on normalized percept time (NPT). The normalized percept time of a *horizontal* (between forearm) motion pattern was significantly longer in relation to the normalized percept time for a *vertical* (within forearm) motion percept (p = 0.01) (Table 2). Black dots represent each subject in the respective condition. The solid black horizontal lines indicate the mean value for the respective condition, the circular white marker with the inner black dot indicates the median value for the respective condition.

*Note.* Results are averaged over the levels of *tACS* and *unambiguous start configuration*.

3.3.1.2. Normalized percept time (NPT) – 3x4x2 RM-ANOVA (Figure 18-21; Table 5-8)

tACS condition (3: [sham, in-phase, anti-phase])

perceptual alteration (4: [horizontal-to-horizontal, vertical-to-vertical, vertical-to-horizontal, vertical-to-vertical])

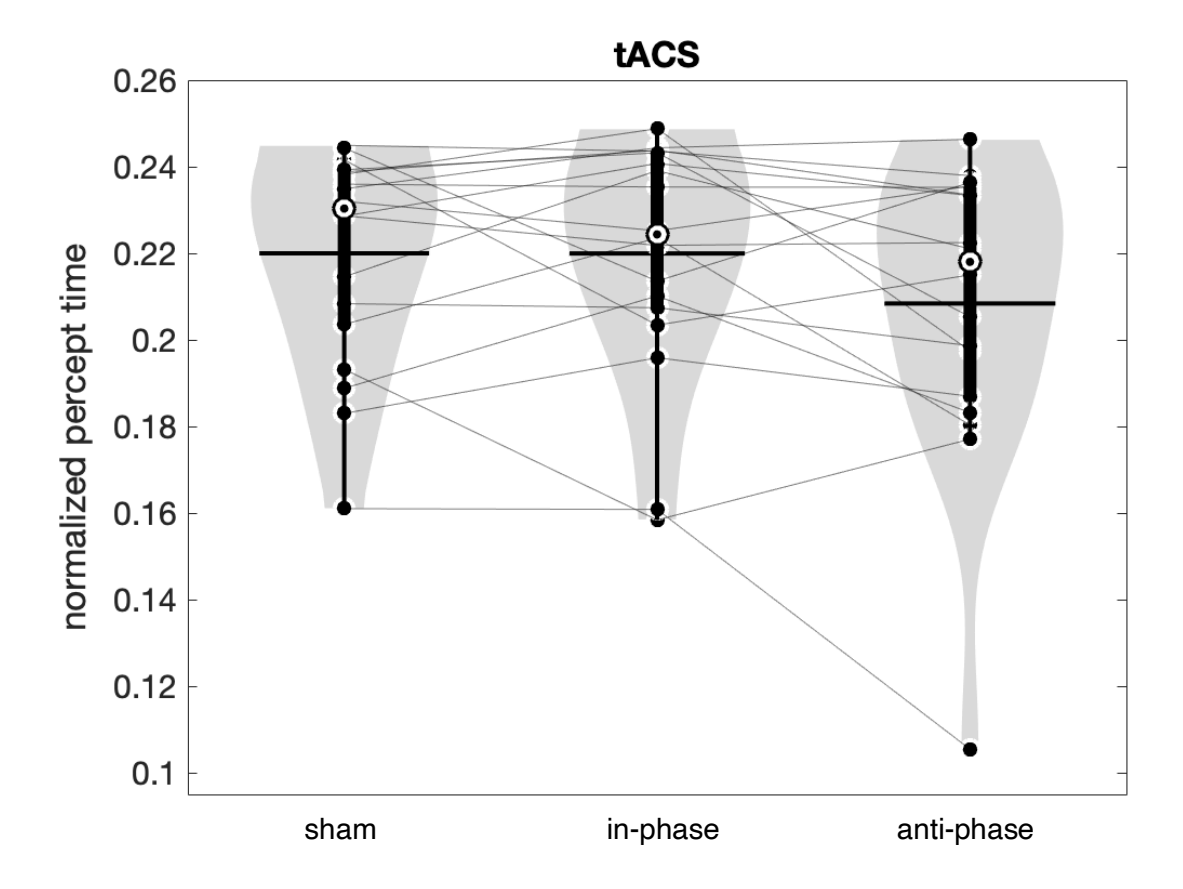
start configuration of the unambiguous stimuli (2: [horizontal unambiguous, vertical unambiguous])

The exploratory 3x4x2 factorial RM-ANOVA of NPTs in dependence on perceptual alteration revealed a significant main effect for tACS (F = 4.025, df = 2, p = 0.027,  $\eta^2 p = 0.191$ , n = 18). Bonferroni-corrected post hoc analyses did not reveal any significant differences. Nevertheless, a trend toward significance was observed between the sham and in-phase conditions (t = 2.453,  $p_{bonf} = 0.058$ , Cohen's d = 0.070, n= 18), as well as the sham and anti-phase condition (t = 2.462,  $p_{bonf} = 0.057$ , Cohen's d = 0.070, n = 18) (Table 7). The main factor of perceptual alteration showed a significant effect (Greenhouse-Geisser corrected, F = 12.485, df = 2.119, p < 0.001,  $\eta^2 p = 0.423$ , n = 18). Subsequent Bonferroni-corrected post hoc analyses revealed significant effects between horizontal-to-horizontal and vertical-to-horizontal (t = -4.058,  $p_{bonf}$  = 0.001, Cohen's d = -1.170, n = 18), as well as vertical-to-vertical and horizontal-tovertical (t = -3.362,  $p_{bonf}$  = 0.009, Cohen's d = -0.969, n = 18) and between vertical-to-vertical and vertical-to-horizontal conditions (t = -5.910,  $p_{bonf} < 0.001$ , Cohen's d = -1.704, n = 18) (Table 8). The factor of unambiguous start configuration did not yield a significant difference (F = 2.306, df = 1, p = 10.147,  $\eta^2 p = 0.119$ , n = 18). The interaction effect of tACS and perceptual alteration revealed a significant effect (F = 2.524, df = 6, p = 0.026,  $\eta^2 p = 0.129$ , n = 18). Furthermore, a significant interaction effect of perceptual alteration and unambiguous start configuration was observed (F = 9.382, df = 3, p $< 0.001, \eta^2 p = 0.356, n = 18$ ).

All other effects of the RM-ANOVA showed no significant effect (Table 5 and 6).

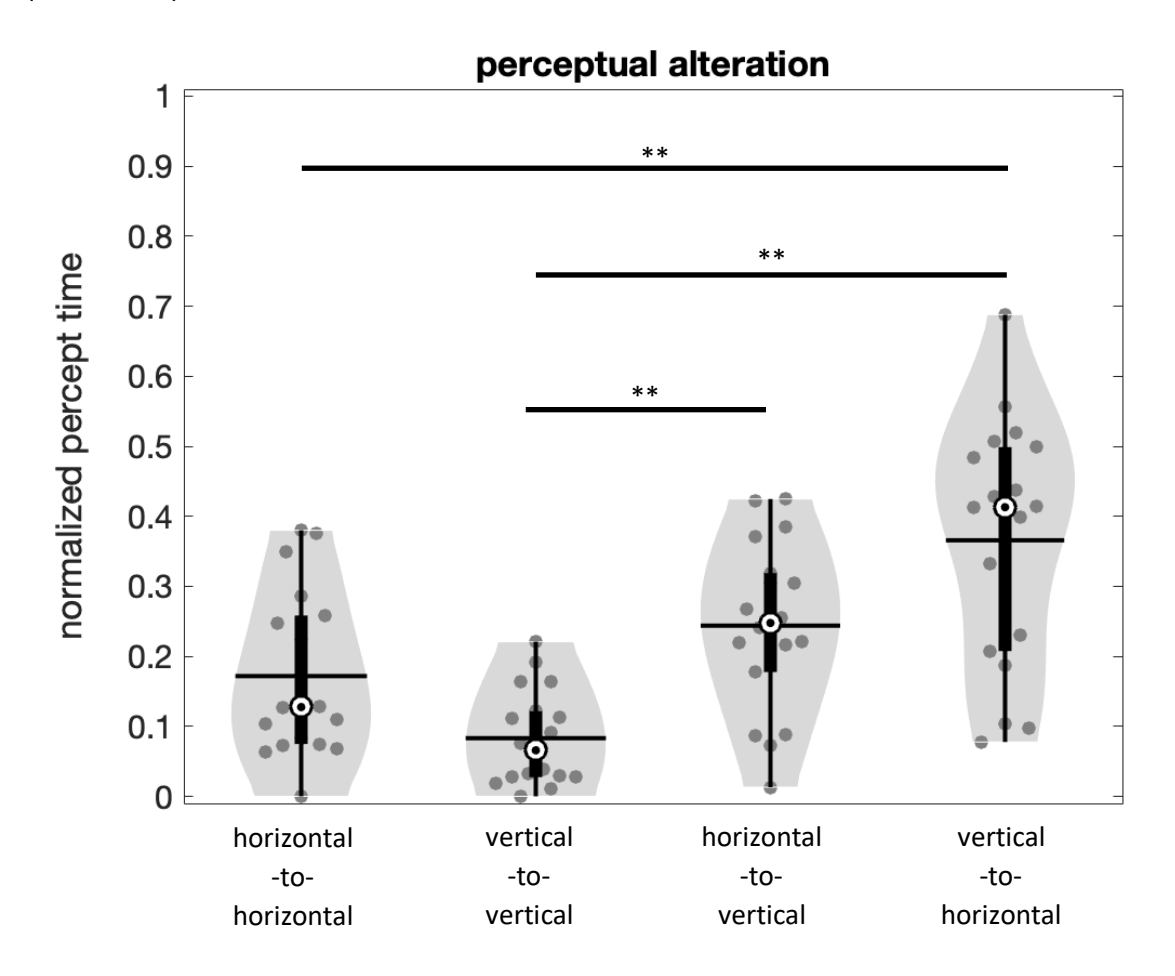
To resolve the multilevel, complex, significant interaction effects, nested RM-ANOVAs were conducted for each level of *perceptual alteration*. This approach resulted in four separate RM-ANOVAs, each corresponding to a specific level of the factor *perceptual alteration* (horizontal-to-horizontal, vertical-to-vertical, horizontal-to-vertical, vertical-to-horizontal).

Figure 18 – Violin plot – 3x4x2 RM-ANOVA Normalized percept time (NPT) – post hoc comparisons of *tACS conditions* (tactile SAM)



Effects of tACS condition on normalized percept time. The main factor of tACS revealed a significant (p = 0.027) effect of the tACS conditions. Bonferroni-corrected post hoc analyses did not reveal any significant differences (Table 7). Black dots represent each subject in the respective condition. The solid black horizontal lines indicate the mean value for the respective condition, the circular white marker with the inner black dot indicates the median value for the respective condition. Note. Results are averaged over the levels of perceptual alteration and unambiguous start configuration.

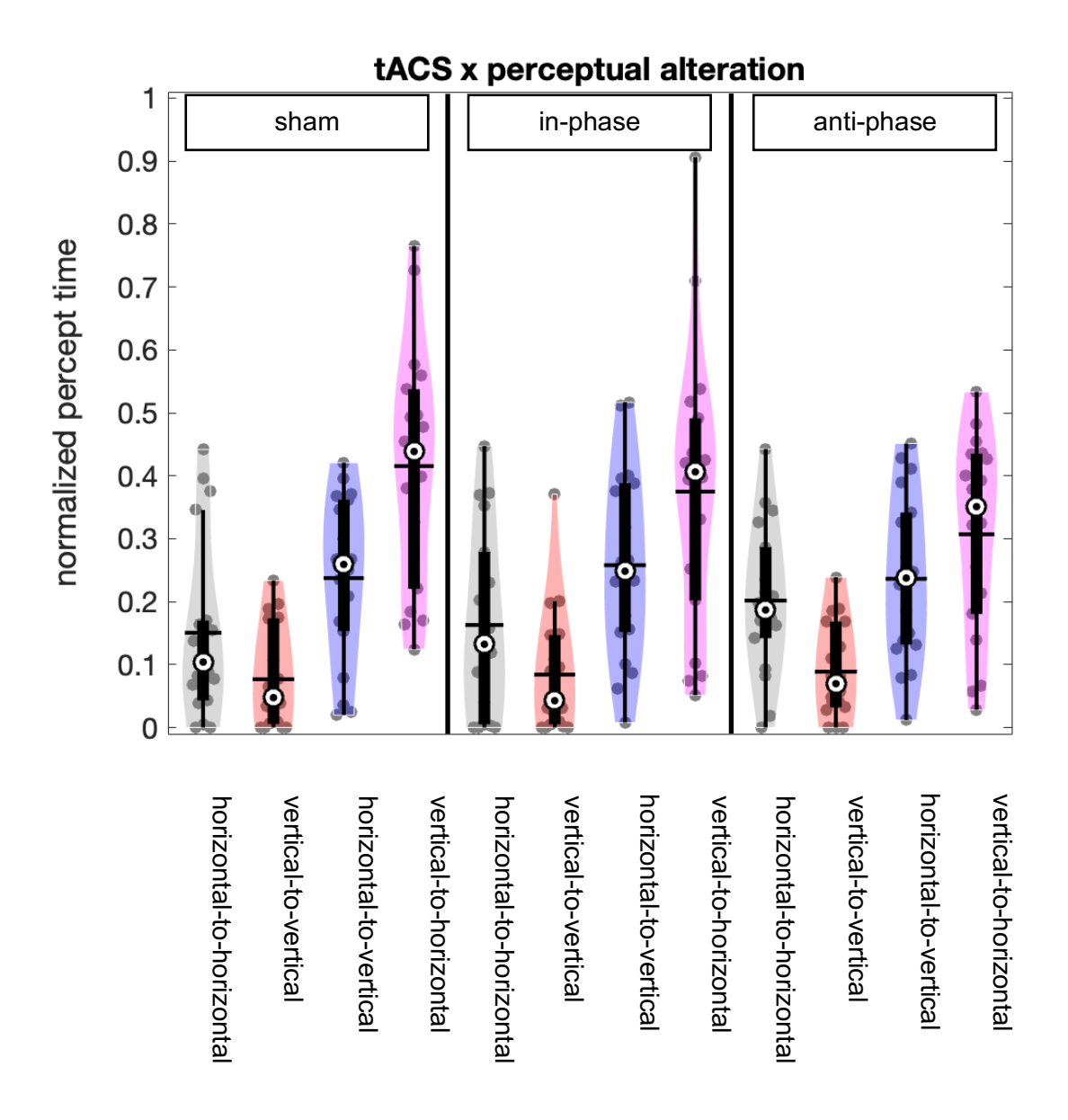
Figure 19 – Violin plot – 3x4x2 RM-ANOVA Normalized percept time (NPT) – *perceptual alteration* (tactile SAM)



Effects of *perceptual alteration* on normalized percept time (NPT). The factor of *perceptual alteration* revealed a highly significant (p < 0.001) effect. In the following Bonferroni-corrected post hoc analyses, significant differences between *horizontal-to-horizontal* and *vertical-to-horizontal* ( $p_{bonf} = 0.001$ ), as well as *vertical-to-vertical* and *horizontal-to-vertical* ( $p_{bonf} = 0.009$ ) and between *vertical-to-vertical* and *vertical-to-horizontal* ( $p_{bonf} < 0.001$ ) could be observed (Table 8). Each subject is represented by gray dots in the respective condition. The solid black horizontal lines indicate the mean value for the respective condition, while the circular white marker with the inner black dot indicates the median value for the respective condition.

Note. Results are averaged over the levels of tACS and unambiguous start configuration.

Figure 20 – Violin plot – 3x4x2 RM-ANOVA Normalized percept time (NPT) – Interaction of *tACS* and *perceptual alteration* (tactile SAM)

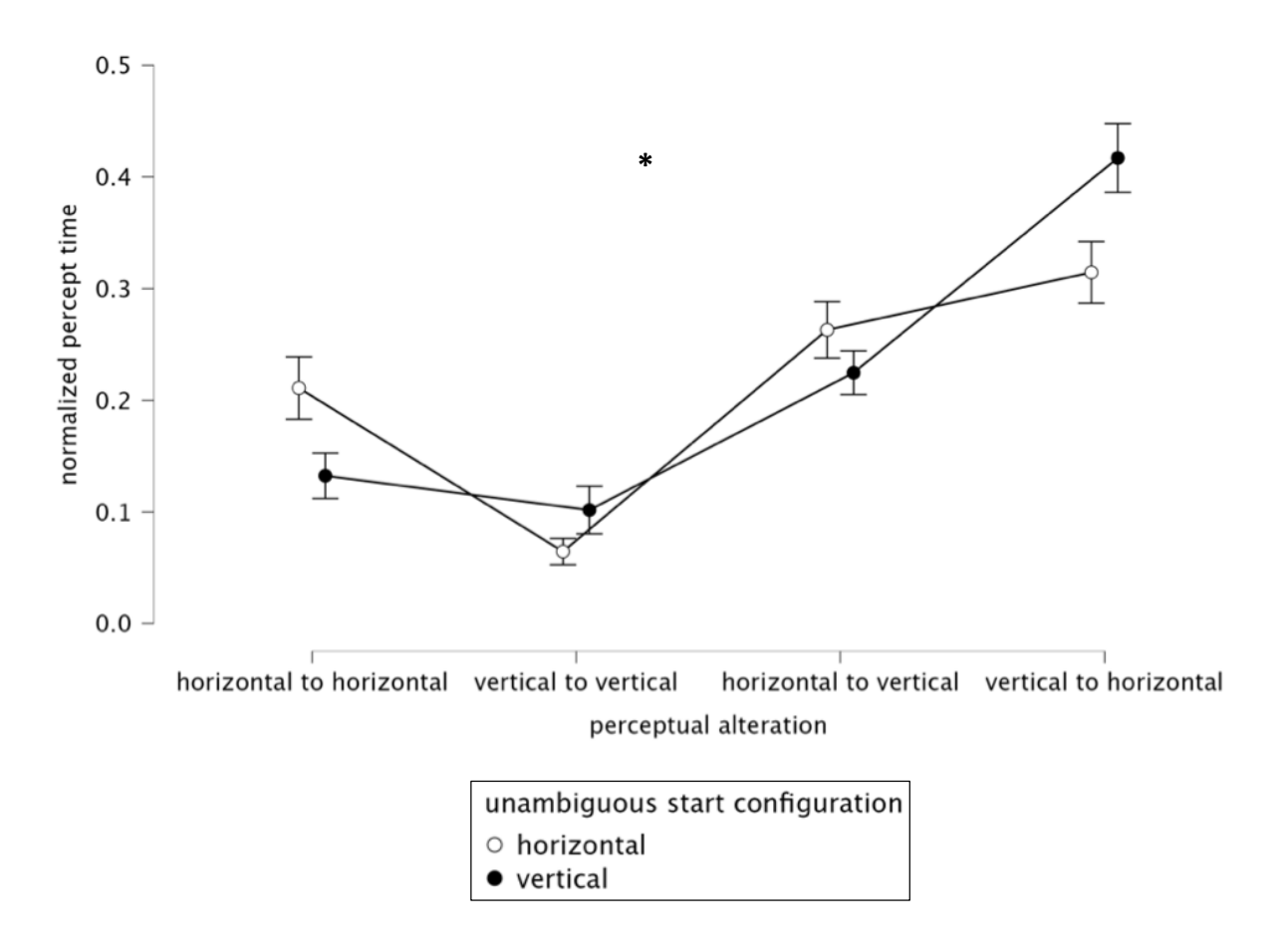


Interaction effect of *tACS* and *perceptual alteration* on normalized percept time (NPT). The RMANOVA revealed a significant interaction effect (p = 0.026) (Table 5).

Gray dots represent each subject in the respective condition. The solid black horizontal lines indicate the mean value for the respective condition, the circular white marker with the inner black dot indicates the median value for the respective condition. The color-coded violin plot represents the respective condition levels of the factor *perceptual alteration*.

*Note.* Results are averaged over the levels of *unambiguous start configuration*.

Figure 21 – Line plot – 3x4x2 RM-ANOVA Normalized percept time (NPT) – Interaction of *perceptual* alteration and unambiguous start configuration (tactile SAM)



Interaction effect of *perceptual alteration* and *unambiguous start condition* on normalized percept time (NPT). A significant effect was found for the interaction of *perceptual alteration* and *unambiguous start condition* (p < 0.001) (Table 5). Filled circular markers represent the *vertical unambiguous start condition*. Whereas unfilled circular markers represent the *horizontal unambiguous start condition*. Error bars indicate the standard error of the mean. *Note*. Results are averaged over the levels of *tACS*.

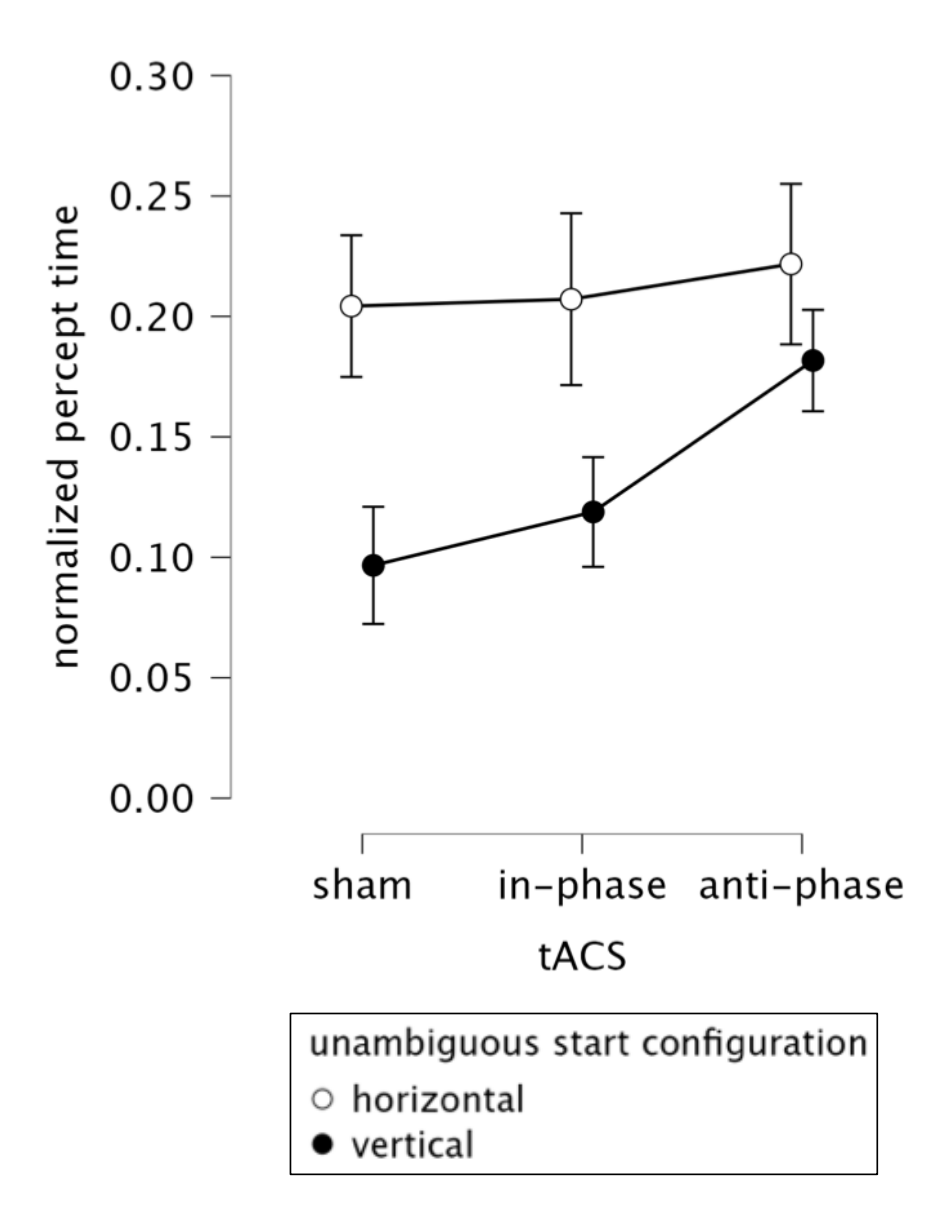
3.3.1.1.1. Normalized percept time (NPT) – 3x2 RM-ANOVA – *horizontal-to-horizontal* (Figure 22; Table 9-10)

tACS condition (3: [sham, in-phase, anti-phase])

start configuration of the unambiguous stimuli (2: [horizontal unambiguous, vertical unambiguous])

The analyses revealed a significant difference for the factor *unambiguous* start condition (F = 14.242, df = 1, p = 0.002,  $\eta^2 p = 0.456$ , n = 18). The *unambiguous horizontal* start condition resulted in higher NPTs compared to the *vertical unambiguous* start condition. All remaining effects were not significant.

Figure 22 – Line plot – 3x2 RM-ANOVA horizontal-to-horizontal – Normalized percept time (NPT) – Interaction of tACS and unambiguous start configuration (tactile SAM)



Line plot of normalized percept time (NPT) mean values within the condition of *horizontal-to-horizontal (perceptual alteration)* for the distinct *tACS conditions*.

Normalized percept times (NPTs) were significantly longer for the *horizontal unambiguous start* condition compared to the *vertical unambiguous start condition* (Table 9).

Filled circular markers represent the *vertical unambiguous start condition*. Whereas unfilled circular markers represent the *horizontal unambiguous start condition*. Error bars indicate the standard error of the mean.

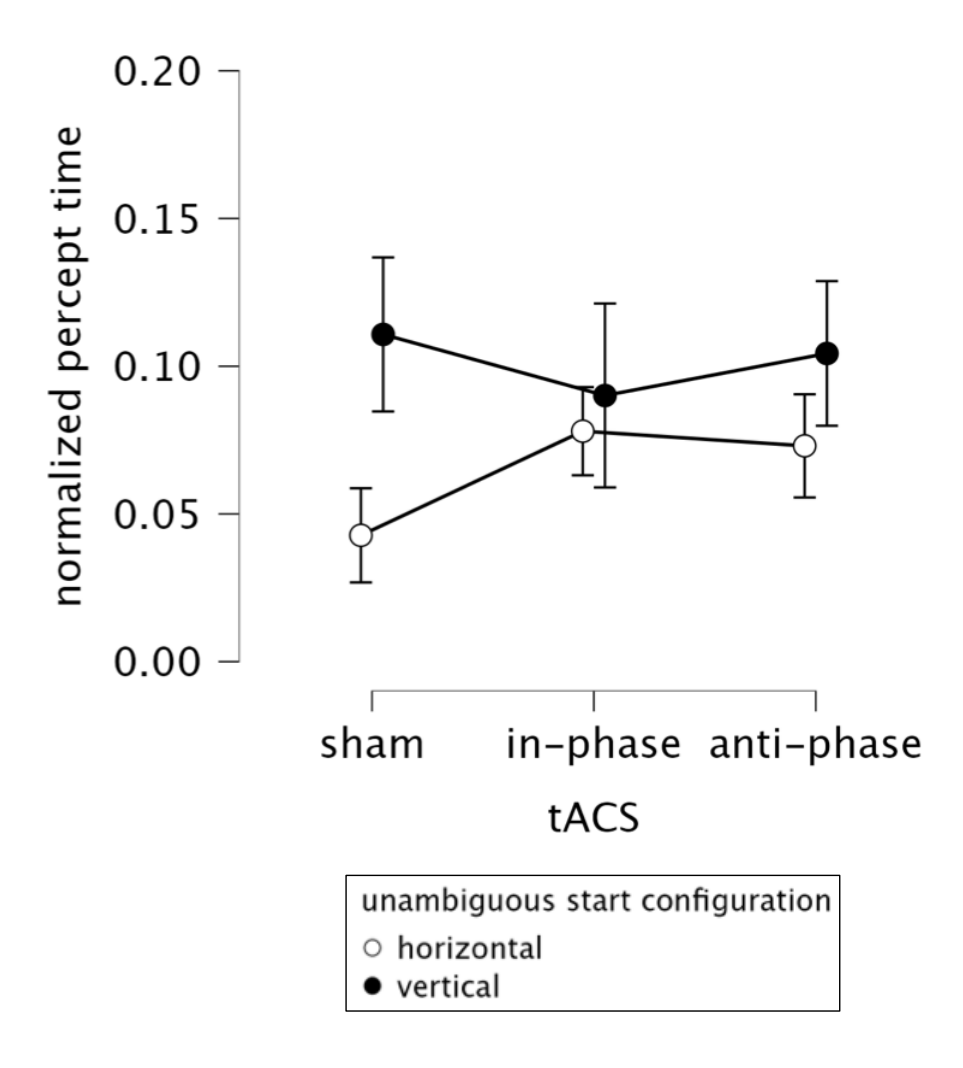
3.3.1.1.2. Normalized percept time (NPT) – 3x2 RM-ANOVA – *vertical-to-vertical* (Figure 23; Table 11-12)

tACS condition (3: [sham, in-phase, anti-phase])

start configuration of the unambiguous stimuli (2: [horizontal unambiguous, vertical unambiguous])

The analyses did not reveal any significant effect on NPTs.

Figure 22 – Line plot – 3x2 RM-ANOVA *vertical-to-vertical* – Normalized percept time (NPT) – Interaction of *tACS* and *unambiguous start configuration* (tactile SAM)



Line plot of NPT mean values within the condition of *vertical-to-vertical* (*perceptual alteration*) for the distinct *tACS conditions*. No significant effects could be observed (Table 11).

Filled circular markers represent the *vertical unambiguous* start condition. Whereas unfilled circular markers represent the *horizontal unambiguous* start condition. Error bars indicate the standard error of the mean.

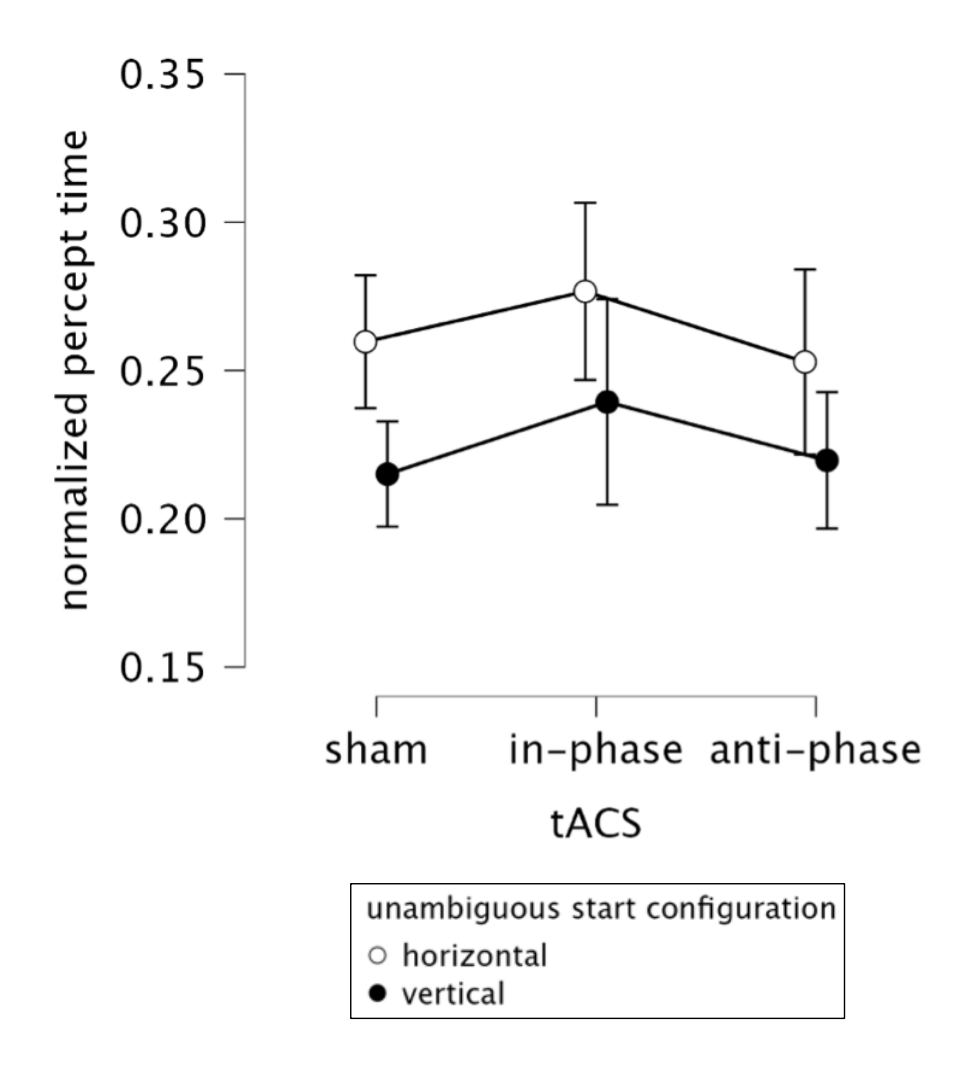
3.3.1.1.3. Normalized percept time (NPT) – 3x2 RM-ANOVA – horizontal-to-vertical (Figure 24; Table 13-14)

tACS condition (3: [sham, in-phase, anti-phase])

start configuration of the unambiguous stimuli (2: [horizontal unambiguous, vertical unambiguous])

The analyses did not reveal any significant effect on NPTs.

Figure 23 – Line plot – 3x2 RM-ANOVA horizontal-to-vertical – Normalized percept time (NPT) – Interaction of tACS and unambiguous start configuration (tactile SAM)



Line plot of NPT mean values within the condition of *horizontal-to-vertical* (*perceptual alteration*) for the distinct *tACS conditions*. No significant effects could be observed (Table 13).

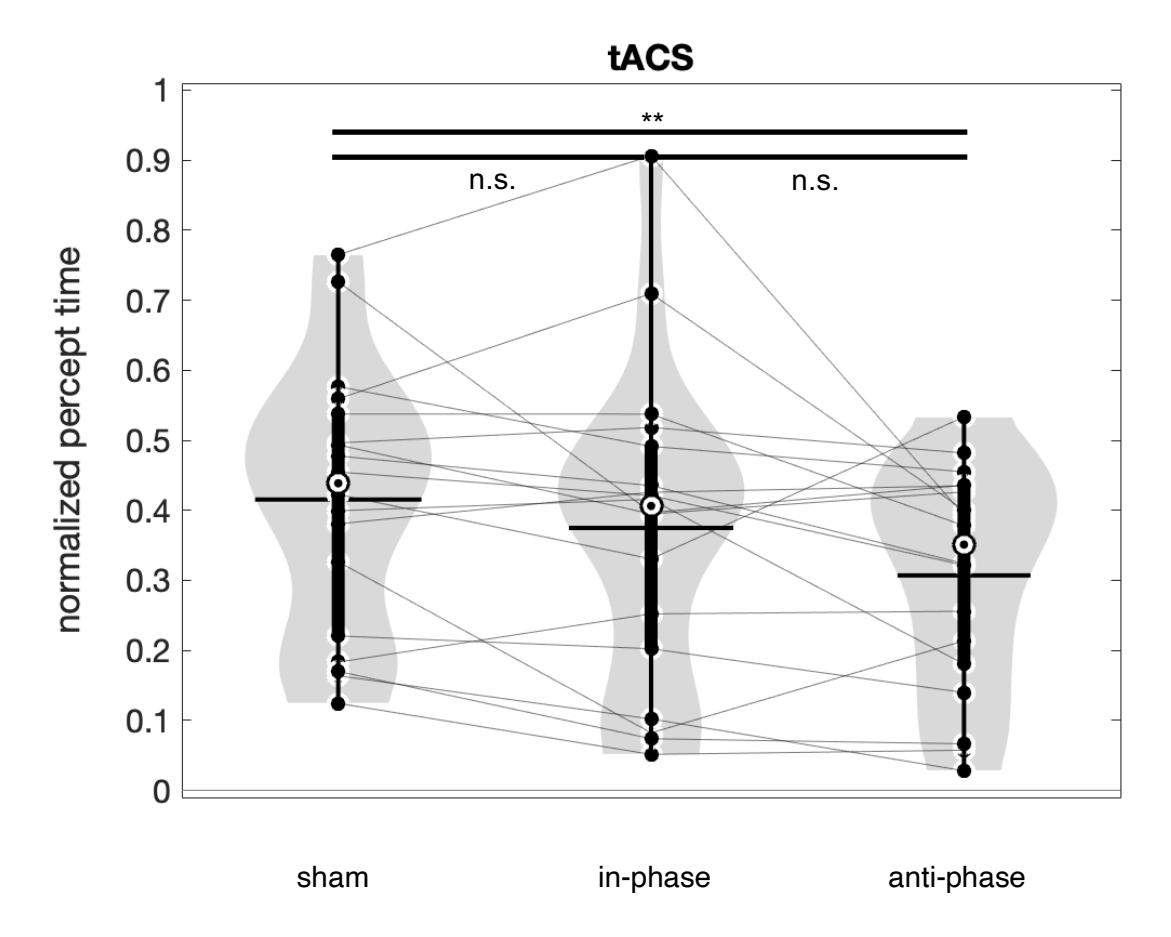
Filled circular markers represent the *vertical unambiguous* start condition. Whereas unfilled circular markers represent the *horizontal unambiguous* start condition. Error bars indicate the standard error of the mean.

3.3.1.1.4. Normalized percept time (NPT) – 3x2 RM-ANOVA – *vertical-to-horizontal* (Table 15-17)

tACS condition (3: [sham, in-phase, anti-phase])
start configuration of the unambiguous stimuli (2: [horizontal unambiguous,
vertical unambiguous])

The nested analyses revealed a significant effect for the factor tACS (F = 5.909, df = 2, p = 0.006,  $\eta^2 p = 0.258$ , n = 18). Bonferroni-corrected post hoc analyses revealed a highly significant difference between the *sham* and *anti-phase* condition (t = 3.406,  $p_{bonf} = 0.005$ ,  $Cohen's \ d = 0.505$ , n = 18). Whereas no significant difference between *sham* and *in-phase* (t = 1.274,  $p_{bonf} = 0.634$ ,  $Cohen's \ d = 0.189$ , n = 18) or *in-phase* and *anti-phase* (t = 2.128,  $p_{bonf} = 0.122$ ,  $Cohen's \ d = 0.316$ , n = 18) could be observed. In addition, a significant effect for the factor of *unambiguous* start condition (F = 14.919, df = 1, p = 0.001,  $\eta^2 p = 0.467$ , n = 18) was observed. The *unambiguous horizontal* start condition resulted in lower NPTs compared to the *vertical unambiguous* start condition.

Figure 24 – Violin plot – 3x2 RM-ANOVA *vertical-to-horizontal* – Normalized percept time (NPT) – post hoc comparisons of *tACS conditions* (tactile SAM)

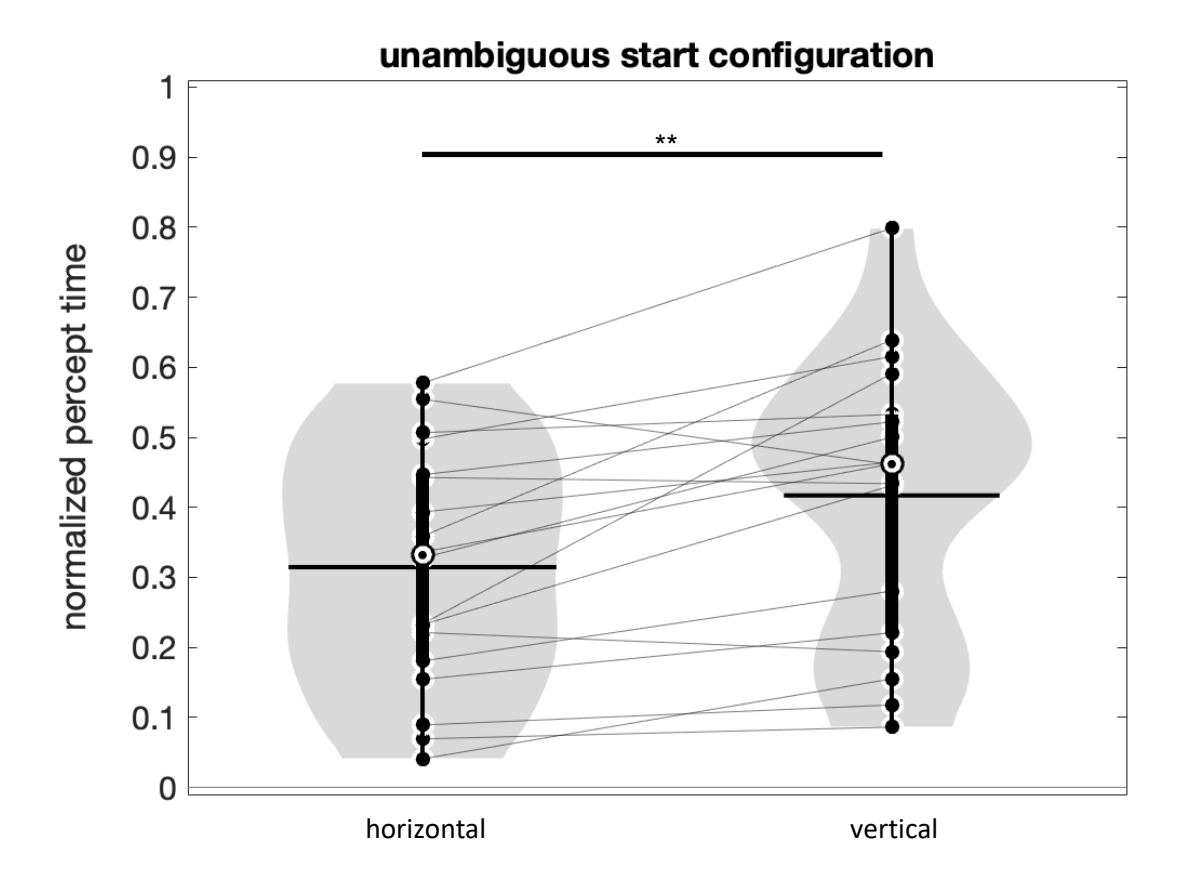


Effects of tACS conditions on normalized percept time (NPT) within the condition of vertical-to-horizontal (perceptual alteration). The main factor of tACS revealed a highly significant (p = 0.006) effect of the tACS conditions. Post hoc analyses resulted in highly significant ( $p_{bonf} = 0.005$ ) shorter horizontal normalized percept time in the anti-phase condition in relation to the sham condition (Table 17).

Black dots represent each subject in the respective condition. The solid black horizontal lines indicate the mean value for the respective condition, the circular white marker with the inner black dot indicates the median value for the respective condition.

*Note.* Results are averaged over the levels of *unambiguous start configuration*.

Figure 25 – Violin plot – 3x2 RM-ANOVA *vertical-to-horizontal* – Normalized percept time (NPT) – *unambiguous start configuration* (tactile SAM)



Effects of unambiguous start conditions on normalized percept time within the condition of vertical-to-horizontal (perceptual alteration). The main factor of unambiguous start condition revealed highly significant (p = 0.001) longer horizontal NPTs for the vertical unambiguous start condition (Table 16). Black dots represent each subject in the respective condition. The solid black horizontal lines indicate the mean value for the respective condition, the circular white marker with the inner black dot indicates the median value for the respective condition.

*Note.* Results are averaged over the levels of *tACS*.

### 3.3.1.2. Overview of results – Normalized percept time (NPT)

The analysis of Normalized Percept Times (NPT) investigated the effects of tACS conditions, perceived motion direction, unambiguous start configuration, and perceptual alterations on the duration of perceived motion. The 3x2x2 repeated measures ANOVA revealed significant effects of the tACS condition. Post hoc analyses demonstrated that the anti-phase condition resulted in significantly lower NPTs from both the in-phase and sham conditions. However, no significant difference was observed between the in-phase and sham conditions. This suggests that tACS phase may partially modulate perceptual stability. In addition, the perceived motion direction significantly influenced NPTs with horizontal motion patterns associated with longer NPTs compared to vertical motion patterns, suggesting a directional dependency in perceptual stability. The unambiguous start configuration, however, did not show a general effect on NPTs, and no significant interaction effects were observed between tACS condition, motion direction, and unambiguous start configuration.

An exploratory analysis incorporating *perceptual alterations, tACS conditions*, and *unambiguous start configuration* revealed significant effects for *tACS conditions, perceptual alterations*, and their interaction. However, the *unambiguous start configuration* alone had no significant effect. Nested analyses provided further insight into specific *perceptual alterations*. For *horizontal-to-horizontal alterations, the unambiguous start configuration* significantly influenced NPTs, with the *horizontal unambiguous start configuration* resulting in longer NPTs compared to *vertical unambiguous start configuration*. For *vertical-to-horizontal alterations*, significant lower NPTs for the *anti-phase* conditions was found (compared to sham). Notably, a significant effect of *unambiguous start configuration* emerged, showing that *horizontal unambiguous configurations* led to lower NPTs compared to *vertical unambiguous configurations*. No significant effects of *tACS* or *unambiguous start configuration* were found for *vertical-to-vertical* or *horizontal-to-vertical alterations*.

These findings suggest that *tACS*, particularly in the *anti-phase* condition, may exert a unique influence on perceptual stability during ambiguous motion perception in the tactile domain. *Horizontal motion* patterns appear to be more stable than *vertical* patterns, potentially reflecting differences in the underlying neural processing of these directions. The lack of interaction effects between *tACS*, *motion direction*, and *unambiguous start configuration* indicates that these factors influence NPTs largely independently. The significant interaction between *tACS conditions* and *perceptual alterations* highlights the role of *tACS* in modulating transitions between perceptual states, particularly in the *anti-*

*phase* condition. Overall, these results emphasize the impact of *anti-phase tACS* on perceptual stability, providing possible insight into the neural mechanisms underlying ambiguous motion perception.

#### 3.3.2. Button press per minute (BPM)

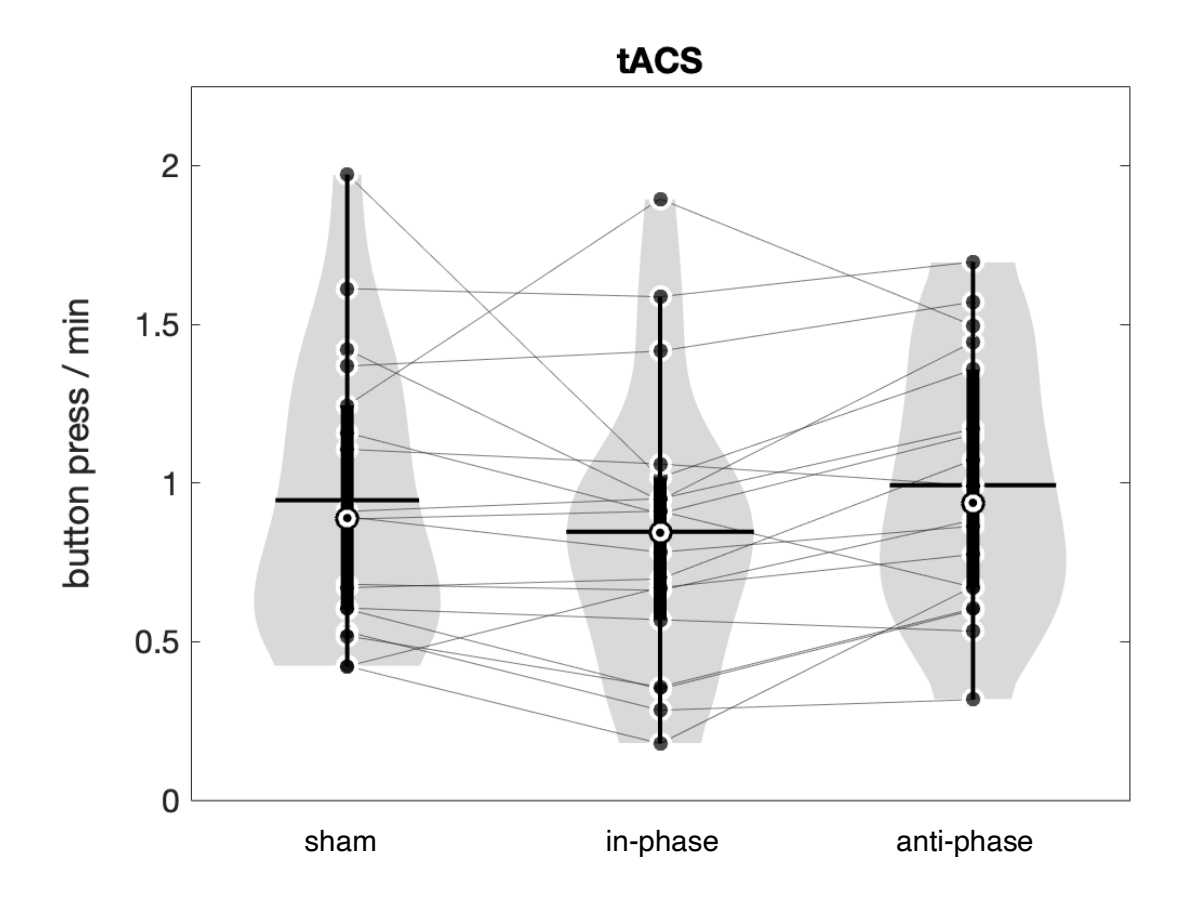
The relative number of buttons pressed per minute (BPM) was calculated for the *horizontal* and *vertical* button distinctively as:

$$BPM_{(horizontal \mid vertical)} = \frac{\sum absolute \ number \ of \ buttons \ pressed_{(horizontal \mid vertical)}}{total \ time \ of \ ambiguous \ stimulus \ configuration \ in \ seconds} \times 60$$

The RM-ANOVA (Table 18 and 19, Figure 27 -30) revealed a significant effect for the main factor of perceived motion direction (F = 8.681, df = 1, p = 0.009,  $\eta p^2 = 0.338$ , n = 18) and the interaction of perceived motion direction and unambiguous start configuration (F = 72.845, df = 1, p < 0.001,  $\eta p^2 = 0.811$ , n = 18). The main factor of tACS (F = 2.779, df = 2, p = 0.076,  $\eta p^2 = 0.140$ , n = 18), unambiguous start configuration (F = 0.115, df = 1, p = 0.738,  $\eta p^2 = 0.007$ , n = 18), the interaction between tACS condition and unambiguous start configuration (F = 0.555, df = 2, p = 0.579,  $\eta p^2 = 0.032$ , n = 18), the interaction effect between tACS condition and perceived motion direction (F = 0.423, df = 2, p = 0.658,  $\eta p^2 = 0.024$ , n = 18) and the interaction effect between tACS condition, perceived motion direction, and unambiguous start configuration (F = 0.446, df = 2, p = 0.644,  $\eta p^2 = 0.026$ , n = 18) revealed no significant difference.

Bonferroni-corrected post hoc comparisons of the interaction effect of *perceived motion direction* and *unambiguous start configuration* revealed a highly significant difference between the *horizontal perceived motion direction* in the *vertical unambiguous start configuration* and *vertical perceived motion direction* within the *vertical unambiguous start configuration* condition (t = 6.273,  $p_{bonf} < 0.001$ , Cohen's d = 1.067, n = 18). The comparison between the *horizontal perceived motion direction* and the *vertical perceived motion direction* within the *horizontal unambiguous start configuration* revealed no significant difference (t = -0.449,  $p_{bonf} = 0.659$ , Cohen's d = -0.080, n = 18).

Figure 26 – Violin plot – 3x2x2 RM-ANOVA Button press per minute (BPM) – post hoc comparisons of *tACS conditions* (tactile SAM)

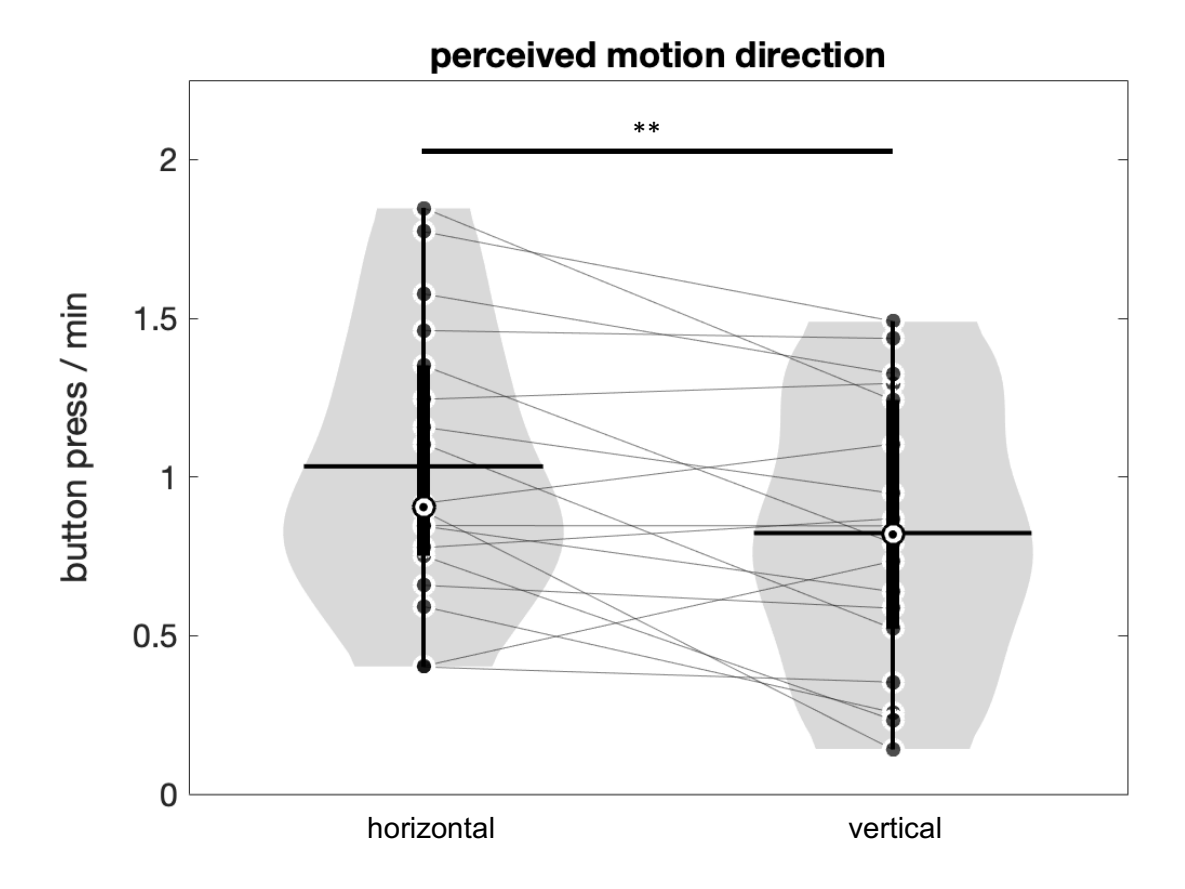


Effects of tACS conditions on button press per minute (BPM). The factor of tACS did not reach significance (p = 0.076) (Table 20).

Black dots represent each subject in the respective condition. The solid black horizontal lines indicate the mean value for the respective condition, the circular white marker with the inner black dot indicates the median value for the respective condition.

Note. Results are averaged over the levels of perceived motion direction and unambiguous start configuration.

Figure 27 – Violin plot – 3x2x2 RM-ANOVA Button press per minute (BPM) – *perceived motion direction* (tactile SAM)

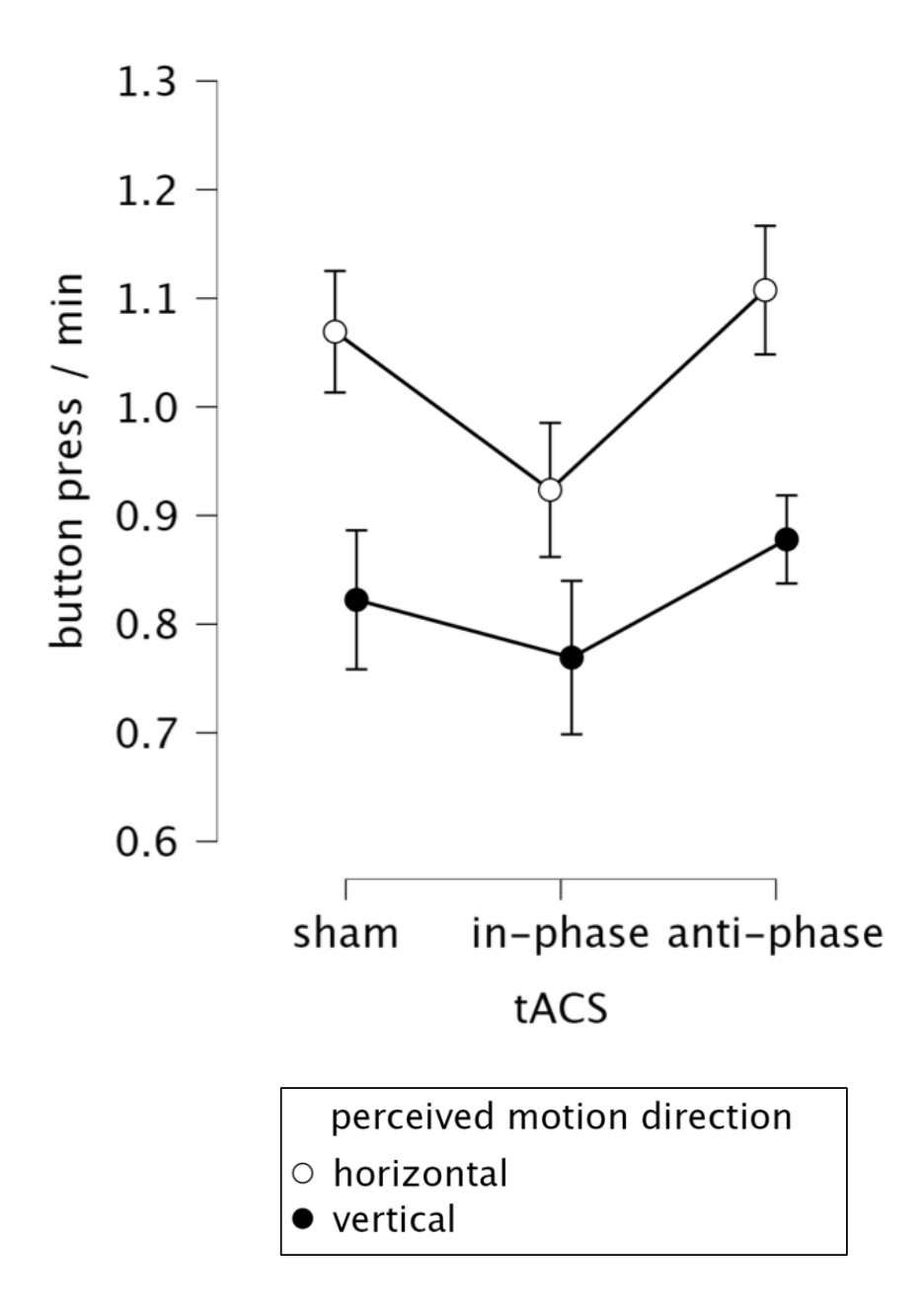


Effects of *perceived motion direction* on button press per minute (BPM). The button press rate for a *horizontal* (between forearm) motion pattern was significantly (p = 0.01) higher in relation to the button press rate for a *vertical* (within forearm) motion percept (Table 18).

Black dots represent each subject in the respective condition. The solid black horizontal lines indicate the mean value for the respective condition, the circular white marker with the inner black dot indicates the median value for the respective condition.

*Note.* Results are averaged over the levels of *tACS* and *unambiguous start configuration*.

Figure 28 – Line plot – 3x2x2 RM-ANOVA Button press per minute (BPM) – Interaction of *tACS* and *perceived motion direction* (tactile SAM)



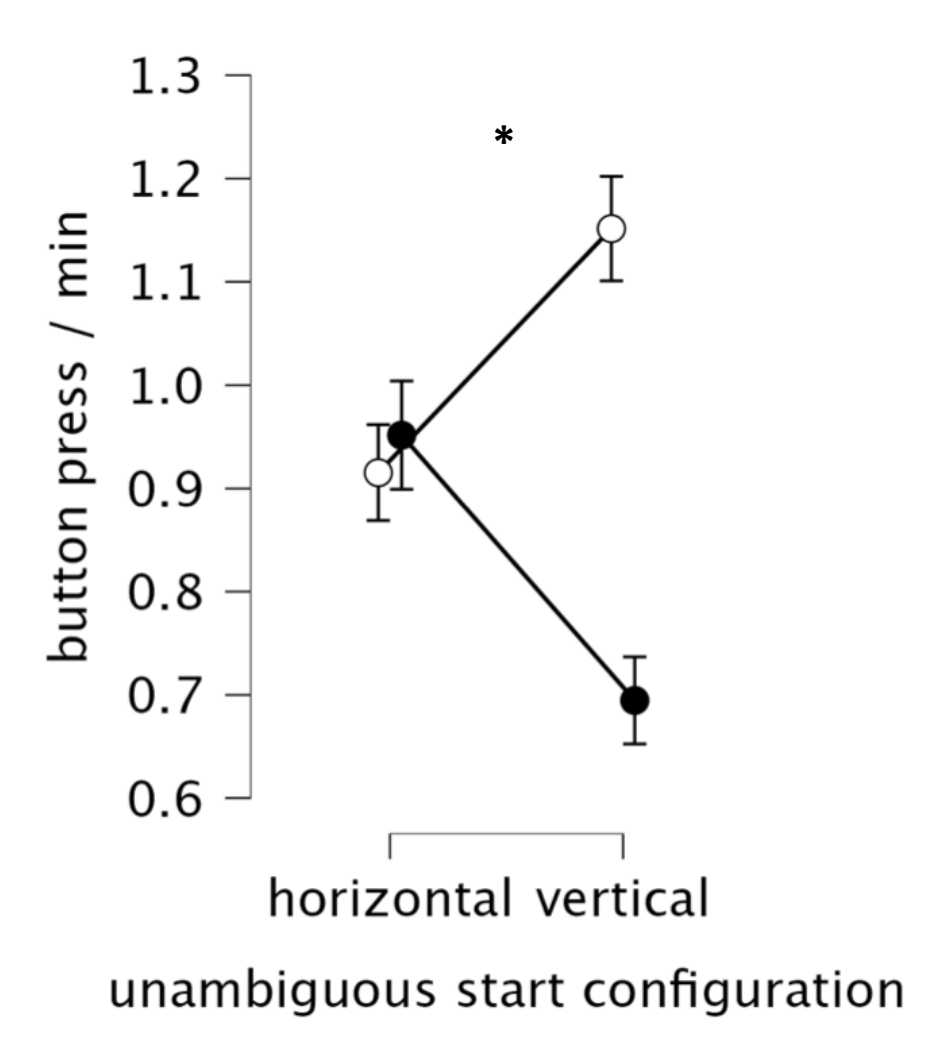
Interaction effect of *tACS* and *perceived motion direction* on the button press rate. The interaction effect did not reach significance (p = 0.658) (Table 18).

Error bars indicate the standard error of means. The filled black dots indicate the mean values across participants for the *vertical perceived motion direction*, whereas the white dots indicate the mean values across participants for the *horizontal perceived motion direction*.

*Note.* Results are averaged over the levels of *unambiguous start configuration*.

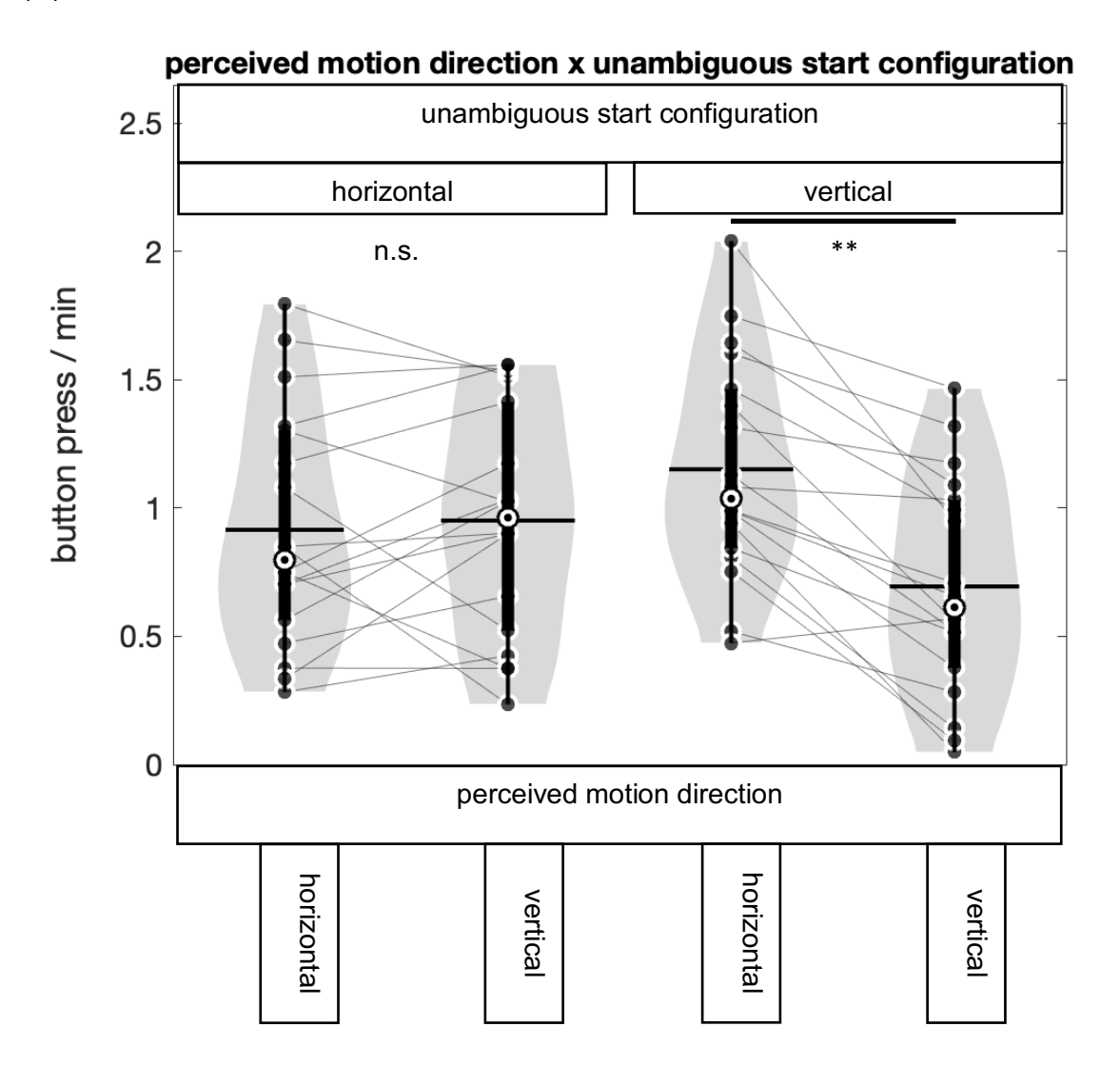
Figure 29 – Line plot and violin plot– 3x2x2 RM-ANOVA Button press per minute (BPM) – Interaction of *perceived motion direction* and *unambiguous start configuration* (tactile SAM)

(a.)



perceived motion direction

- horizontal
- vertical



(a.) – (b.) Interaction effect of perceived motion direction and unambiguous start configuration on button press per minute (BPM). The interaction effect was highly significant (p < 0.001) (Table 18). The significant interaction effect indicates that the effect of perceived motion direction on button presses per minute (BPM) is influenced by the level of unambiguous start configuration. For the horizontal unambiguous start configuration, no significant difference between the horizontal and vertical perceived motion direction is observed (p = 0.659), whereas the vertical unambiguous start configuration results in significant increased horizontal BPM rates and decreased vertical BPM rates ( $p_{bonf} < 0.001$ ).

- (a.) Error bars indicate the standard error of means. The filled black dots indicate the mean values across participants for the *vertical perceived motion direction*, whereas the white dots indicate the mean values across participants for the *horizontal perceived motion direction*.
- (b.) Black dots represent each subject in the respective condition. The solid black horizontal lines indicate the mean value for the respective condition, the circular white marker with the inner black dot indicates the median value for the respective condition.

*Note.* Results are averaged over the levels of *tACS*.

## 3.3.2.1. Overview of results – Button press per minute (BPM)

The analysis of button presses per minute (BPM) revealed that the perceived motion direction exerted a significant influence. Horizontal BPM rates were significantly higher compared to vertical BPM rates. Additionally, a significant interaction between perceived motion direction and the unambiguous start configuration was observed. Specifically, within the vertical unambiguous start configuration, horizontal BPM rates revealed significantly higher rates compared to vertical BPM rates. However, in the horizontal unambiquous start configuration, no significant difference regarding BPM rates were found between horizontal and vertical perceived motion Notably, the tACS condition itself did not show a significant effect on BPM rates, nor were significant interaction effects observed between tACS condition and the other factors. These results indicate that BPM is primarily influenced by the perceived motion direction and its interaction with the unambiguous start configuration. The higher BPM rates observed for horizontal motion in the vertical unambiguous configuration may indicate perceptual bias for horizontal motion perception. The absence of notable effects from tACS conditions on BPM may indicate that this behavioral measure may be less responsive to external neuromodulation, in contrast to other metrics such as NPTs. In conclusion, these results highlight the influence of directional and contextual factors on perceptual responses during ambiguous motion perception in the tactile domain.

## 3.3.3. Analyses of cumulative gamma distribution functions (gCDF) of NPTs

Interestingly, further investigations regarding the temporal dynamics of percept time distributions of bistable stimuli in different modalities indicate a resemblance to the gamma distribution (Kohler et al.,

2008; Pressnitzer & Hupé, 2006). Regarding the visual SAM stimulus, previous studies have demonstrated that percept time distributions fit the gamma probability density function (Kohler et al., 2008; Strüber et al., 2014).

The gamma distribution function is a right skewed distribution and is determined by the shape parameter a and the scale parameter b. The distribution characteristics regarding the tactile SAM stimulus have not been published before.

In order to validate and investigate the ambiguity characteristics of the applied tactile SAM stimulus, a series of distribution functions were fitted to the underlaying normalized percept time distribution (see Table 21 for the exact distributions). The fitted distribution functions of the normalized percept times were compared with other appropriate probability density distribution functions (see Table 21 for the exact distributions).

Normalized percept times were preferred over raw percept time data due to the variable jitter phase of the *unambiguous start configuration*, which was excluded from further analysis.

For the analyses, all normalized percept times were pooled for each subject in each condition. Parameters of the gamma distribution and gamma probability density function, as well as the gamma cumulative distribution function, were estimated using MATLABs gamfit, gampdf, and gamcdf functions (MATLAB, R2016b (9.1.0), The MathWorks Inc., Natick, MA, USA). The goodness of fit of known possible underlaying distributions for the normalized percept times was evaluated using MATLAB's mle function (maximum likelihood estimates function), which included a non-parametric distribution model using MATLAB's ksdensity (Kernel smoothing function estimate for univariate and bivariate data) function (MATLAB, R2016b (9.1.0), The MathWorks Inc., Natick, MA, USA). Log-likelihood values and Akaike Information Criterion (AIC; Akaike, 1973) values were evaluated as criteria for the best-fitting distribution model. The log-likelihood values and Akaike Information Criterion values for the gamma function revealed the highest log-likelihood and lowest Akaike Information Criterion values compared to the rest of the fitted distributions (Table 21). Consequently, the relation of the estimated values indicates, that the gamma distribution fit for the normalized percept time data has the best goodness of fit compared to the other suitable possible distribution functions (Table 21). The probability density function of the gamma distribution is defined as:

$$y = f(x|a,b) = \frac{1}{b^a \Gamma(a)} x^{a-1} e^{\frac{-x}{b}},$$

where  $\Gamma(\cdot)$  denotes the gamma function.

The gamma function is established for positive real values of x, where x > 0, according to the following definition:

$$\Gamma(x) = \int_0^\infty e^{-t} t^{x-1} dt$$

The cumulative distribution function of the gamma distribution is expressed by:

$$p = F(x|a,b) = \frac{1}{b^a \Gamma(a)} \int_{0}^{x} t^{a-1} e^{\frac{-t}{b}} dt.$$

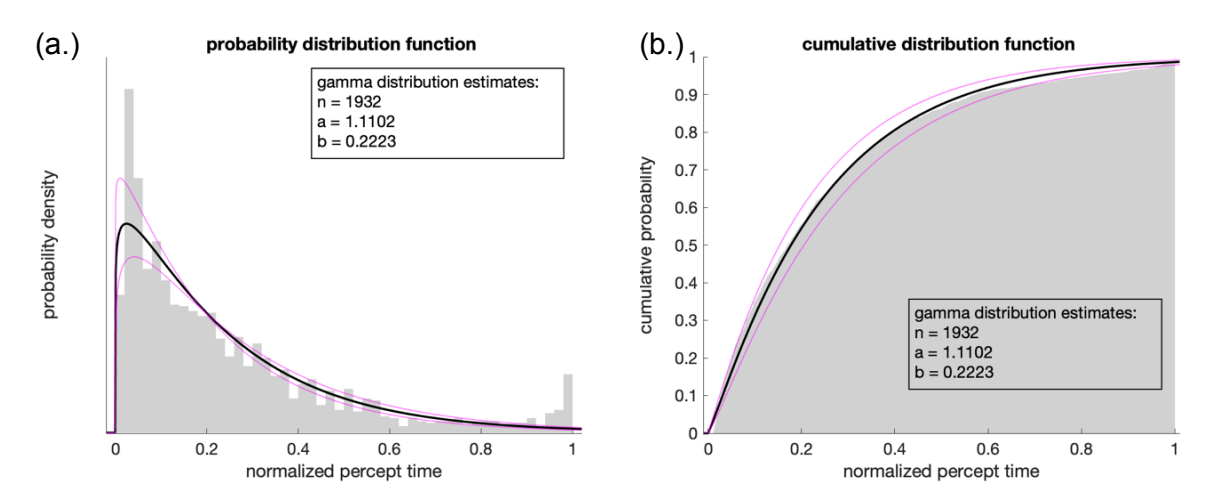
The result p is the probability that a single observation from the gamma distribution with parameters a and b falls in the interval of 0 and x (Figure 31).

Since distribution of the normalized percept times may depict and provide more diverse and advanced informative insights than mere comparisons of mean values of percept durations, a further non-parametric permutational statistical analysis was constructed.

This methodology provides an effective analysis of sensitive deviations in the shape of cumulative distribution functions that may not automatically be evident in significant contrasts of mean NPT values (Misselhorn et al., 2019).

Therefore, the gamma probability density function estimate was conducted by pooling normalized percept time data for the respective conditions. As a next step, gamma distribution parameter and subsequent the gamma cumulative distribution functions for the respective conditions were estimated based on the pooled data.

Figure 30— Gamma probability density distribution (a.) and gamma cumulative distribution function (gCDF) (b.)



n (pooled data across all conditions and all participants) = 1932, shape parameter a = 1.1102 [95% confidence interval: 1.0497, 1.1742], scale parameter b = 0.2223 [95% confidence interval: 0.2072, 0.2384].

The x-axis represents the normalized percept time. The y-axis represents the probability density in (a.) and the cumulative probability in (b.).

- (a.) Gamma probability density plot of normalized percept times with underlying histogram plot. The color-coded lines in magenta indicate the upper- and lower 95% confidence interval of the predicted gamma probability distribution function. The shaded gray area portrays a histogram of normalized percept time values across all participants in every condition.
- (b.) Cumulative distribution function plot of normalized percept times. The color-coded lines in magenta indicate the upper- and lower 95% confidence interval of the predicted gamma cumulative distribution function. The shaded gray area depicts the empirical cumulative density function estimate of normalized percept time values across all participants in every condition.

In general, shifts in the cumulative distribution functions can be interpreted in specific ways: a shift to the right of the x-axis (NPT) indicates a higher proportion of longer normalized percept times, whereas a shift to the left of the x-axis indicates a higher proportion of shorter normalized percept durations. Relations of the cumulative gamma distribution functions in different conditions can be represented by forming differences of the corresponding conditions.

For statistical comparison of gCDFs based on the conditions under investigation, the differences of gCDFs were directly statistically evaluated by comparing the empirically observed difference of the gCDFs under investigation with a H<sub>0</sub> distribution.

The H<sub>0</sub> distribution was calculated separately for each specific statistical comparison in a directly compared design. For this purpose, the individual values of the normalized percept times for each participant were randomly permuted to the respective condition labels. This procedure was followed by a re-estimation of the cumulative gamma distribution functions. In the following step, the difference from the two cumulated functions data was again formed based on the permuted NPT data.

In total, this computational procedure was applied 100,000 times, resulting in 100,000 permuted gCDF differences mapped across the x-axis from 0 to 1.

For determining statistical significance, confidence intervals (CIs) based on the  $H_0$  distribution were calculated. The *alpha* level was set at *alpha* = 0.05 and first adjusted for both sides of the distribution as *alpha* = 0.05/2. The adjusted *alpha* value was Bonferroni-corrected as *alpha/n<sub>c</sub>*, as  $n_c$  being the number of contrasts.

The alpha value obtained takes into account both the two-tailed analyses and the multiple comparisons resulting from the factorial design. Nevertheless, it does not account for multiple comparisons along the range of NPTs examined.

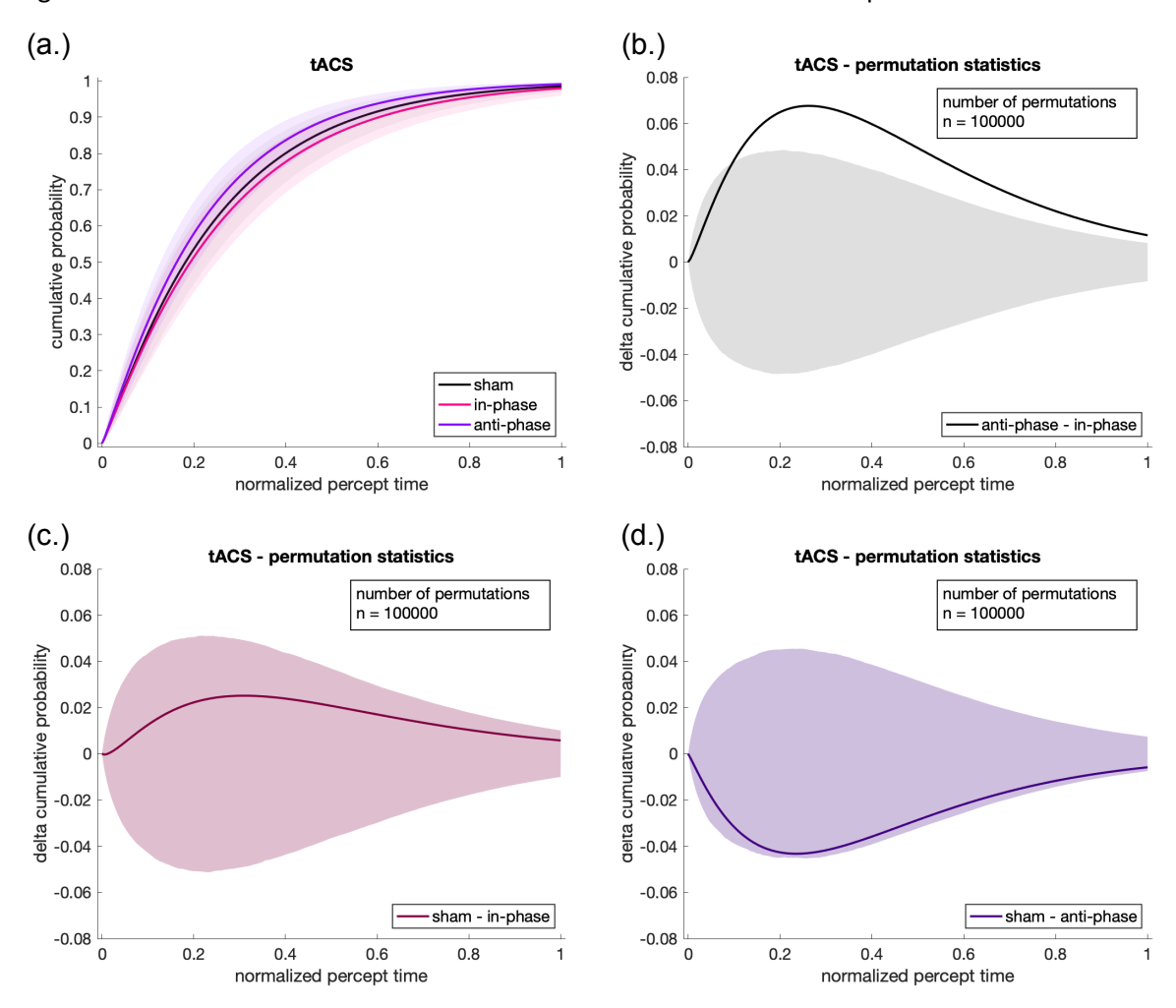
To account for multiple comparisons along the range of NPTs, a modified form of the extreme value-based correction (Cohen, 2017) was conducted. To that end, all values of  $alpha > 1 - (0.05/2/n_c)$  or  $alpha < (0.05/2/n_c)$  of the shuffled data set were identified for each permuted iteration. These extreme values over all permutations result in a distribution of extreme values. From this distribution, an upper and a lower threshold was determined that was consistent with the  $97.5^{th}$  or  $2.5^{th}$  percentile (corresponding to a two-tailed alpha of 0.05). Consequently, the resulting corrected CIs control for the global range of the data tested. Observed differences of the gamma CDFs in the respective conditions, that exceeded the corrected CI at any point were assessed as significant condition differences.

For statically evaluating the *tACS* effect three condition comparisons were conducted: sham - in-phase, sham - anti-phase, and anti-phase - in-phase (number of condition contrasts:  $n_c = 3$ ) (Figure 32). We observed statistically significant effect, for the difference between anti-phase - in-phase condition (significant cluster: anti-phase - in-phase, delta cumulative probability (y): 0.0443 - 0.0116, normalized

percept time (x): 0.1005 - 1). In concrete terms, in-phase tACS resulted in higher proportion of longer percept times in relation to anti-phase stimulation.

The other comparisons did not reveal a significant difference.

Figure 31 – Gamma cumulative distribution functions and statistical comparisons – tACS conditions



(a.) Cumulative gamma distribution function (gCDF) of normalized percept times (NPTs) for distinct *tACS conditions*. The color-coded lines represent the respective *tACS condition*. The underlying color-coded transparent area represents the 95% confidence interval (CI) of the gCDF estimate.

The *sham* condition lies between the *in-phase* and *anti-phase* condition. In relation to the *sham* condition the *in-phase* condition results in a rightward shift of the cumulative distribution function, indicating a higher proportion of longer normalized percept times. Conversely the *anti-phase* condition

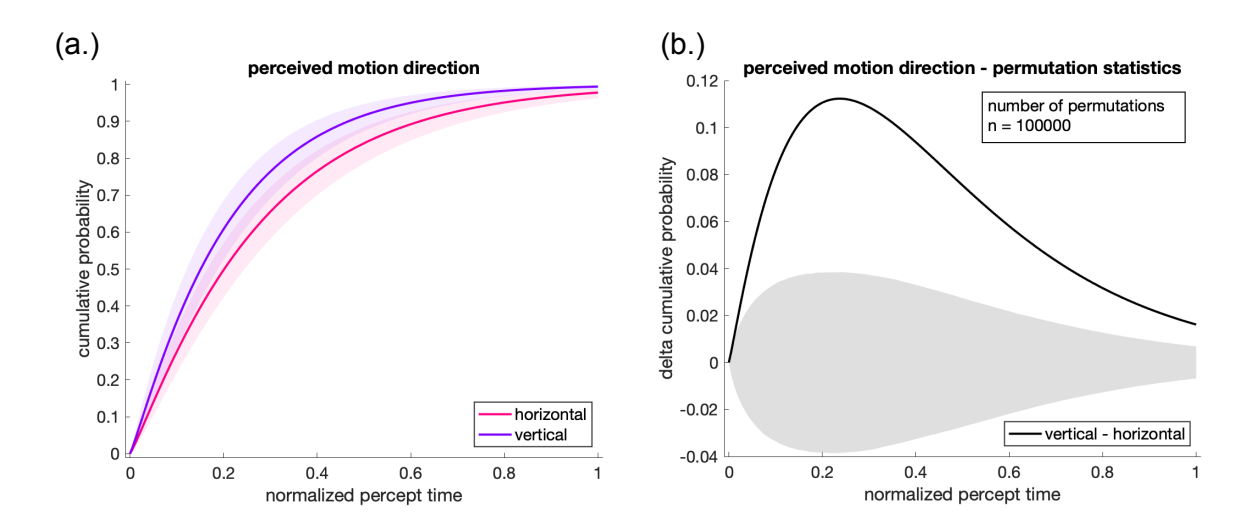
results in a shift to the left of the cumulative probability function indicating a higher proportion of shorter normalized percept times in relation to the *sham* condition.

- (b.) Permutation statistics for the difference in cumulative gamma distribution functions between *tACS* conditions. The color-coded shaded areas represent the corrected CI of the permutation statistic. The solid lines represent the respective empirical observed difference between the cumulative gamma distribution function. The difference between *anti-phase* and *in-phase tACS* condition shows a pronounced significant effect for the range of normalized percept times, indicating that the *in-phase* condition resulted in higher proportions of longer normalized percept times than the *anti-phase* condition.
- (c.) and (d.) All other comparisons did not reach significance.

Regarding the *perceived motion direction* pattern the permutation statistics (number of condition contrasts:  $n_c = 2$ ) revealed a significant effect (*significant cluster: vertical – horizontal, delta cumulative probability (y): 0.0097 – 0.0162, normalized percept time (x): 0.0100 – 1) (Figure 33).* 

For the *vertical motion direction* pattern, a significantly higher proportion of shorter percept times were observed compared to the *horizontal motion direction* pattern.

Figure 32 – Gamma cumulative distribution functions and statistical comparisons – *perceived motion direction* 

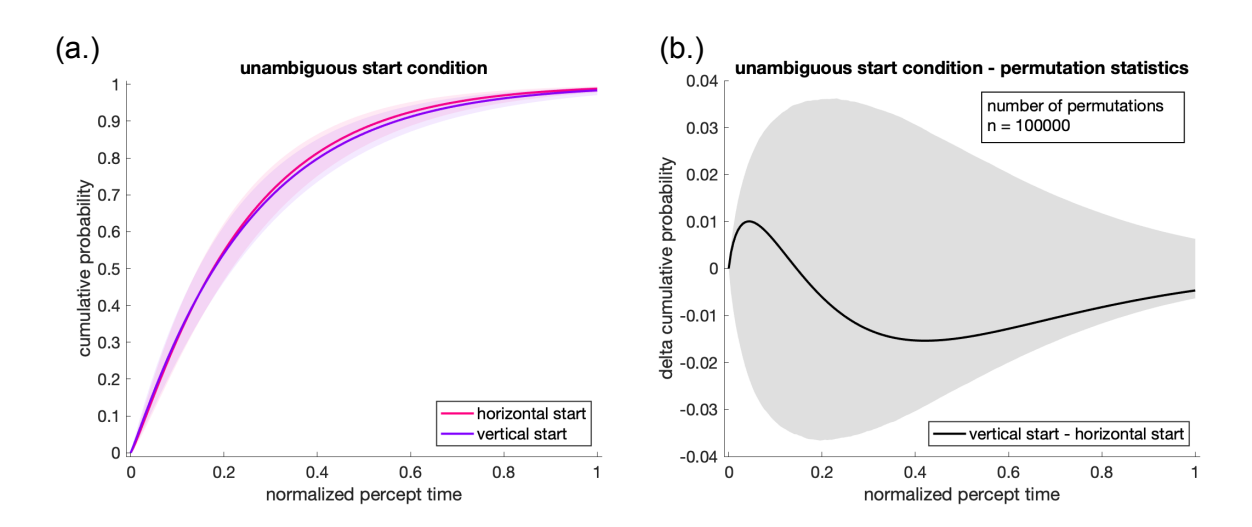


The x-axis represents the normalized percept time. The y-axis represents the cumulative probability in (a.) and the difference (delta) of the cumulative probability in (b.)

- (a.) Cumulative gamma distribution function (gCDF) of normalized percept times for distinct *perceived motion direction* conditions. The color-coded lines represent the respective *perceived motion direction* condition. The underlying color-coded transparent area represents the 95% confidence interval (CI) of the gCDF estimate.
- (b). Permutation statistics for the difference in cumulative gamma distribution functions between perceived motion directions. The shaded area represents the corrected CI of the permutation statistic. The solid line represents the respective empirically observed difference between the cumulative gamma distribution function. The difference between the vertical motion direction from the horizontal motion direction is significant. The positive values of the difference (gCDF perceived vertical motion direction gCDF perceived horizontal motion direction) indicate a significant higher proportion of increased normalized percept times (NPTs) for the horizontal motion direction.

For the factor of *unambiguous* start condition, no statically significant difference between the *vertical* start and *horizontal* start condition could be observed (number of condition contrasts:  $n_c = 2$ ) (Figure 34).

Figure 33 – Gamma cumulative distribution functions and statistical comparisons – *unambiguous start* condition



The x-axis represents the normalized percept time. The y-axis represents the cumulative probability in (a.) and the difference (delta) of the cumulative probability in (b.).

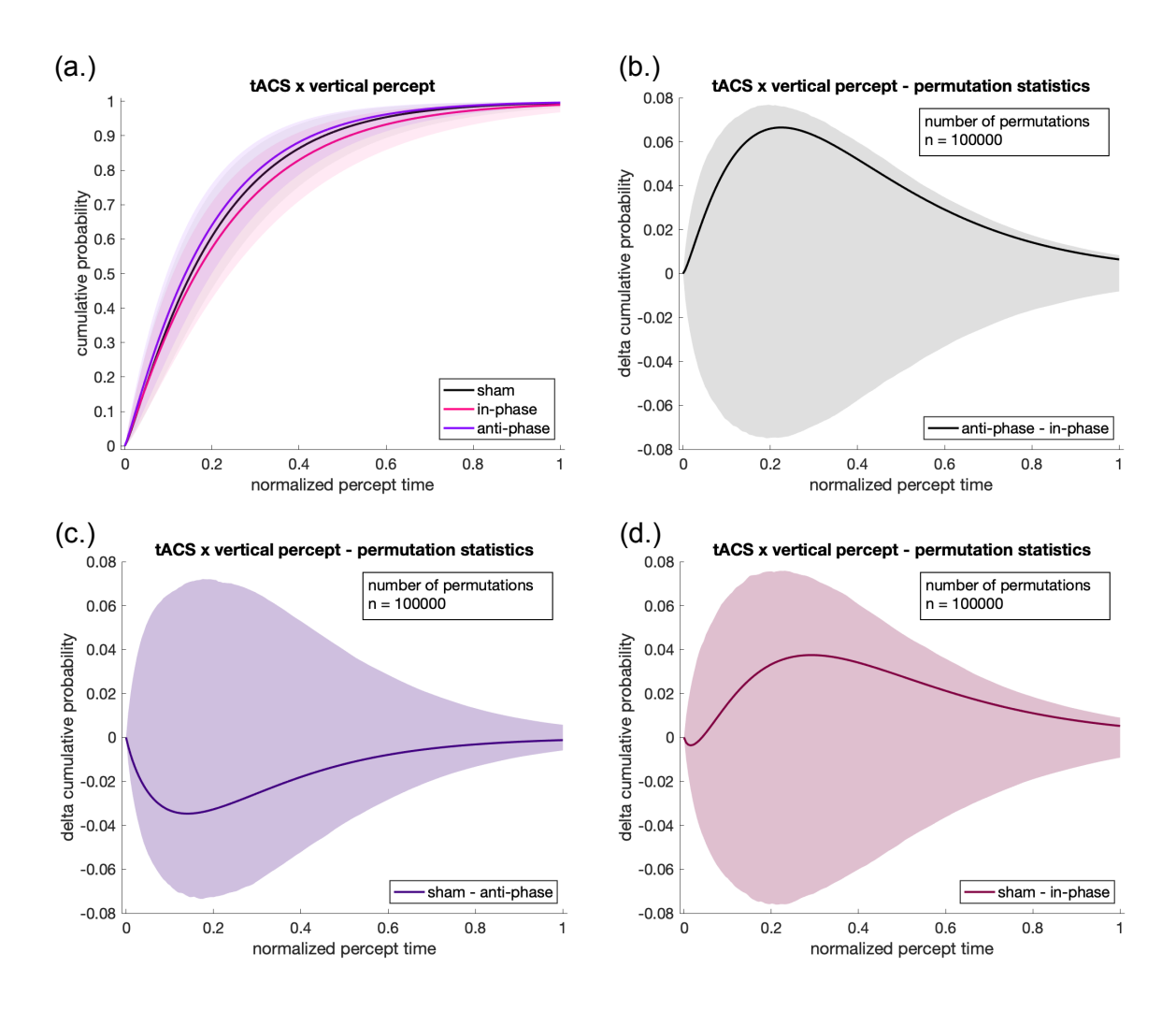
- (a.) Cumulative gamma distribution function (gCDF) of normalized percept times for the *unambiguous* start configuration. The color-coded lines represent the *unambiguous horizontal* or *vertical* start condition. The underlying color-coded transparent the 95% confidence interval (CI) of the estimated gCDFs.
- (b.) Permutation statistics for the difference in cumulative gamma distribution functions (gCDF) between the *unambiguous* start conditions. The shaded area represents the corrected CI of the permutation statistic. The solid line represents the respective empirical observed difference in the cumulative gamma distribution function. The difference between *unambiguous vertical* start condition and the *unambiguous horizontal* start condition is not significant.

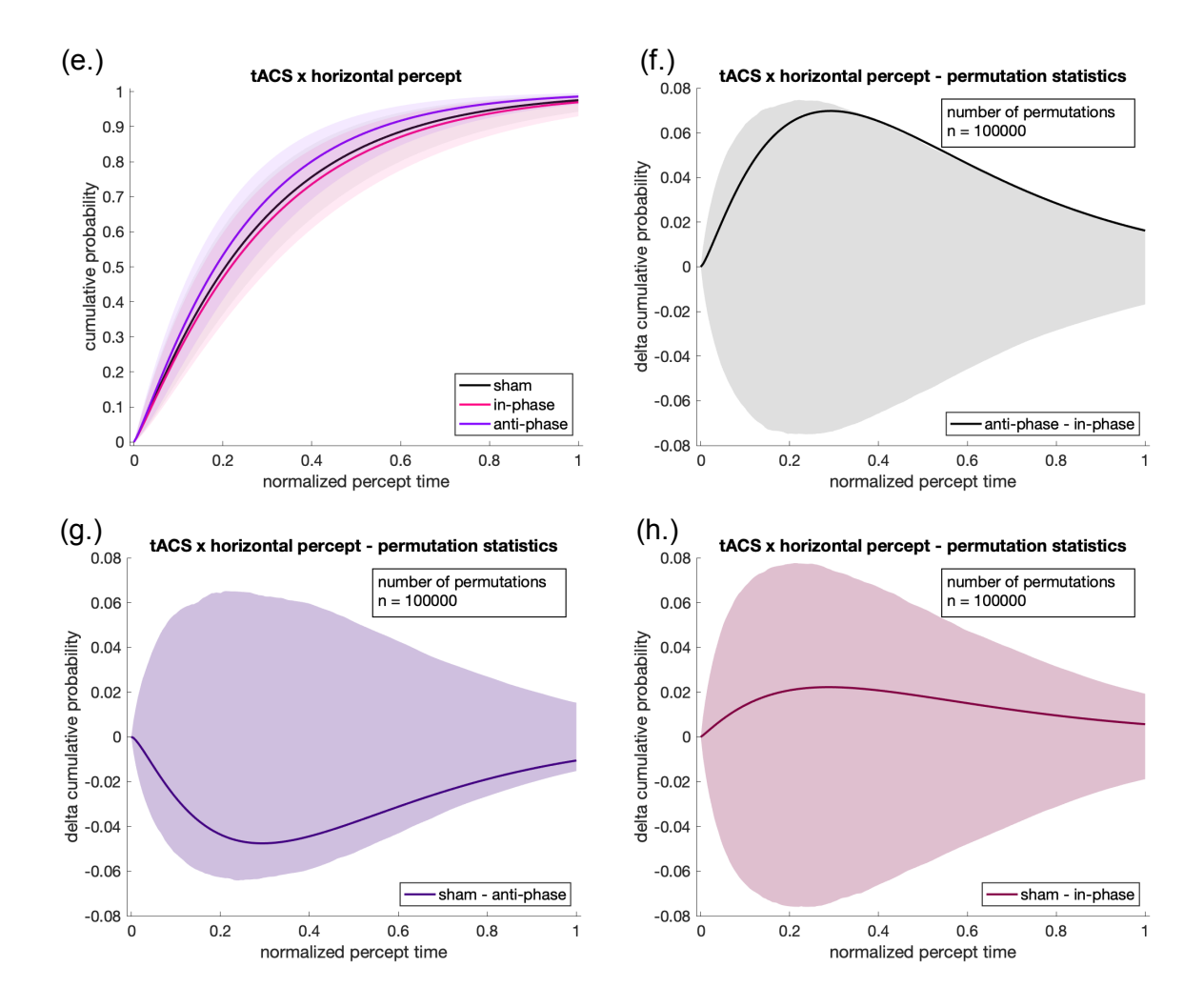
To further analyze phase specific *tACS* effects, interactional outcomes between the *tACS* conditions and the perceived motion direction were investigated (number of condition contrasts:  $n_c = 6$ ) (Figure

35). Within the perceived *vertical* NPTs, the *tACS* difference between *anti-phase* and *in-phase* did not reveal a significant difference.

However, within the perceived *horizontal motion direction*, a significant difference between the *in-phase* and *anti-phase* condition was observed (*significant cluster* [horizontal percept]: anti-phase - in-phase, delta cumulative probability (y): 0.0668 - 0.0355, normalized percept time (x): 0.3769 - 0.7136). This indicates that within the perceived *horizontal motion direction*,  $in-phase\ tACS$  resulted in a significant higher proportion of *horizontal* NPTs compared to *anti-phase tACS*. This effect could not be observed within the perceived *vertical motion direction*.

Figure 34 – Gamma cumulative distribution functions and statistical comparisons –  $tACS \times perceived$  motion direction





The x-axis represents the normalized percept time. The y-axis represents the cumulative probability in (a.) and (e.) and the difference (delta) of the cumulative probability in (b.) - (d.) and (f.) - (h.).

- (a.) Cumulative gamma distribution function (gCDF) of normalized percept times (NPTs) for distinct *tACS conditions* nested within the perceived *vertical motion direction* pattern. The color-coded lines depict the respective *tACS condition*. The underlying color-coded transparent represent the 95% confidence interval (CI) of the gCDF estimation.
- (b.) (d.) Adjusted permutation statistics for the difference of gCDFs between *tACS conditions* nested within the *vertical perceived motion direction* pattern. The solid lines represent the respective empirical observed difference between the gCDFs.

No significant difference between the *anti-phase* condition and *in-phase* condition, the *sham* condition and *anti-phase* condition as well as the *sham* condition and *in-phase* condition could be observed.

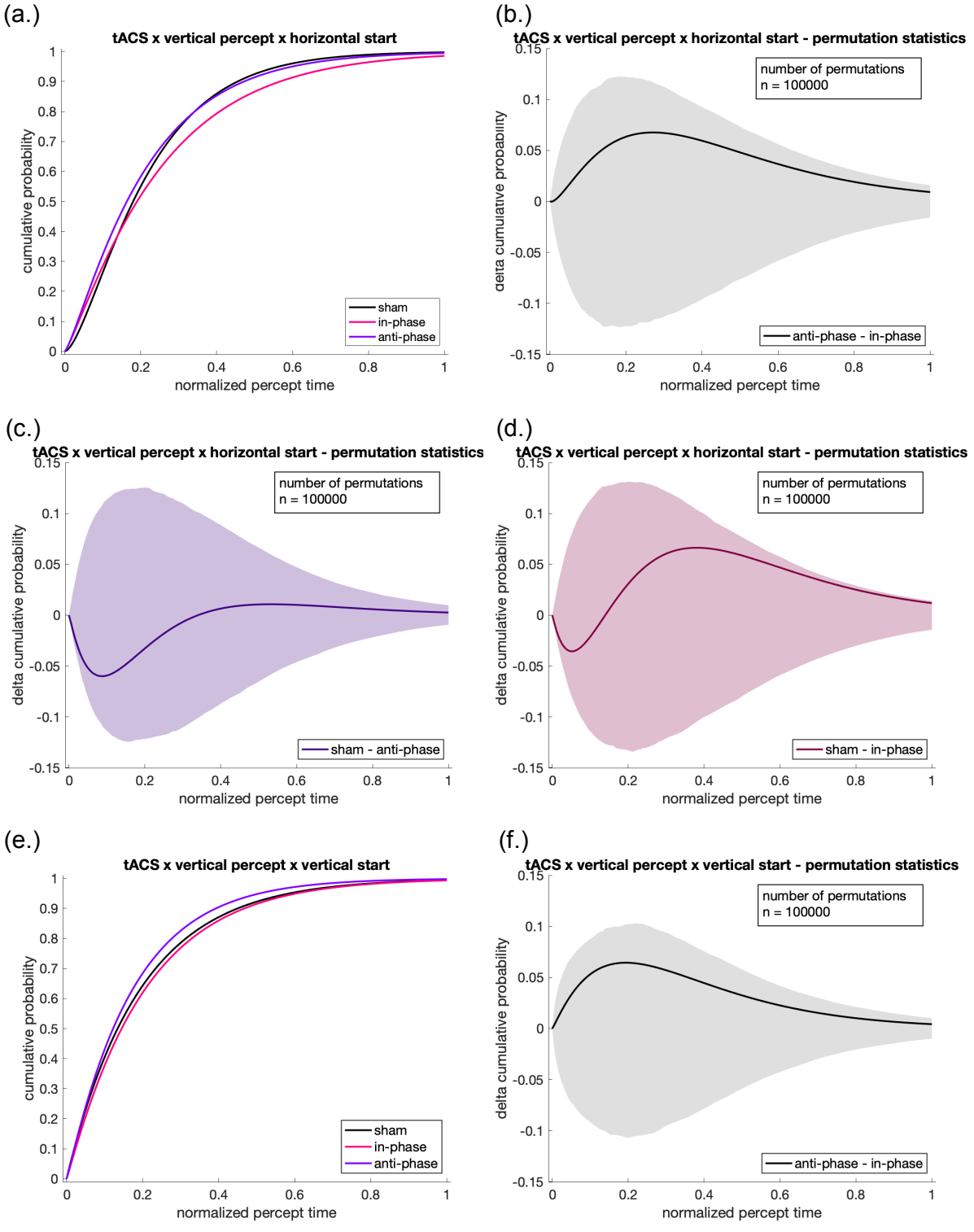
- (e.) Cumulative gamma distribution function (gCDF) of normalized percept times (NPTs) for distinct *tACS conditions* nested within the perceived *horizontal motion direction* pattern. The color-coded lines depict the respective *tACS condition*. The underlying color-coded transparent areas represent the 95% confidence interval of the gCDF estimation.
- (f.) (h.) Adjusted permutation statistics for the difference of gCDFs between tACS conditions nested within the horizontal perceived motion direction pattern. The solid lines represent the respective empirical observed difference between the gCDFs.
  - (f.) The difference between the *anti-phase* condition and *in-phase* condition revealed a significant effect.
  - (g.) (h.) No significant difference between the *sham* condition and *anti-phase* condition as well as the *sham* condition and *in-phase* condition could be observed.

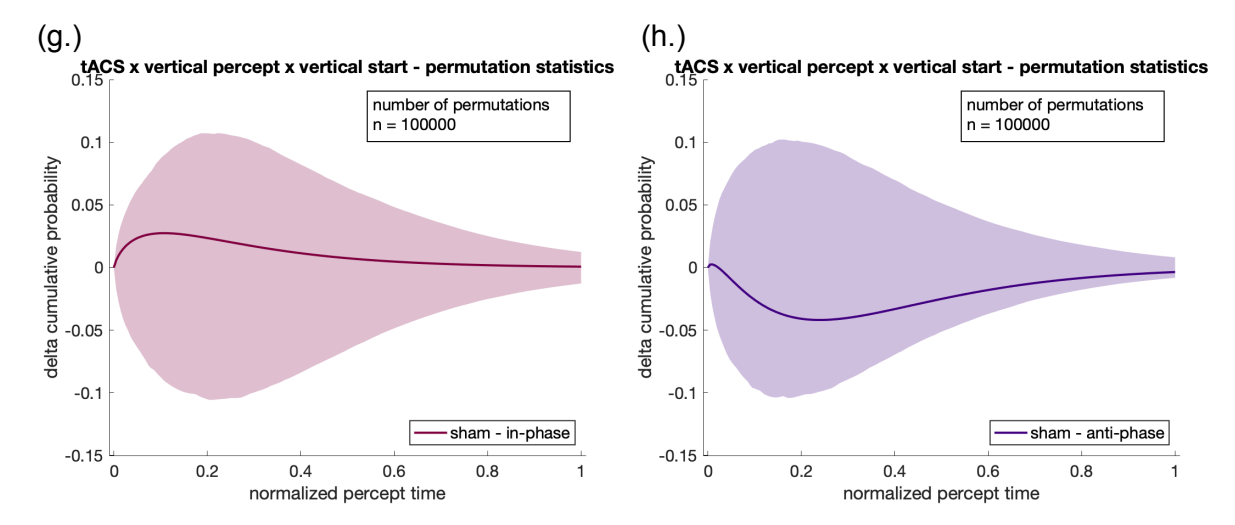
To further extend the statistical analyses of interaction effects, the *tACS* effect was statistically evaluated within the specific sub conditions of the *perceived motion direction* and the *unambiguous* start condition (number of condition contrasts:  $n_c = 12$ ).

Within the *vertical perceived motion direction* and the *horizontal unambiguous* start condition the permutation statistics did not reveal a significant effect between the compared *tACS conditions* (Figure 36). Similarly, within the *vertical perceived motion direction* and the *vertical unambiguous* start condition, the permutation statistics did not reveal a significant effect between the compared *tACS conditions* (Figure 36). Equally, within the *horizontal perceived motion direction* and the *horizontal unambiguous* start condition, the permutation statistics did not reveal a significant effect between the compared *tACS conditions* (Figure 37).

However, within the *horizontal perceived motion direction* and the *vertical unambiguous* start condition, the permutation statistics revealed a significant difference between the *in-phase* and *anti-phase* condition (*significant cluster [horizontal percept, vertical unambiguous start]: anti-phase – in-phase, delta cumulative probability (y): 0.1134 – 0.0819, normalized percept time (x): 0.2462 – 0.5176) (Figure 37). Regarding all other differences of the <i>tACS conditions*, no significant effect could be observed (Figure 37).

Figure 35 – Gamma cumulative distribution functions and statistical comparisons – *tACS x vertical* motion percept x unambiguous start condition





The x-axis represents the normalized percept time. The y-axis represents the cumulative probability in (a.) and (e.) and the difference (delta) of the cumulative probability in (b.) - (d.) and (f.) - (h.).

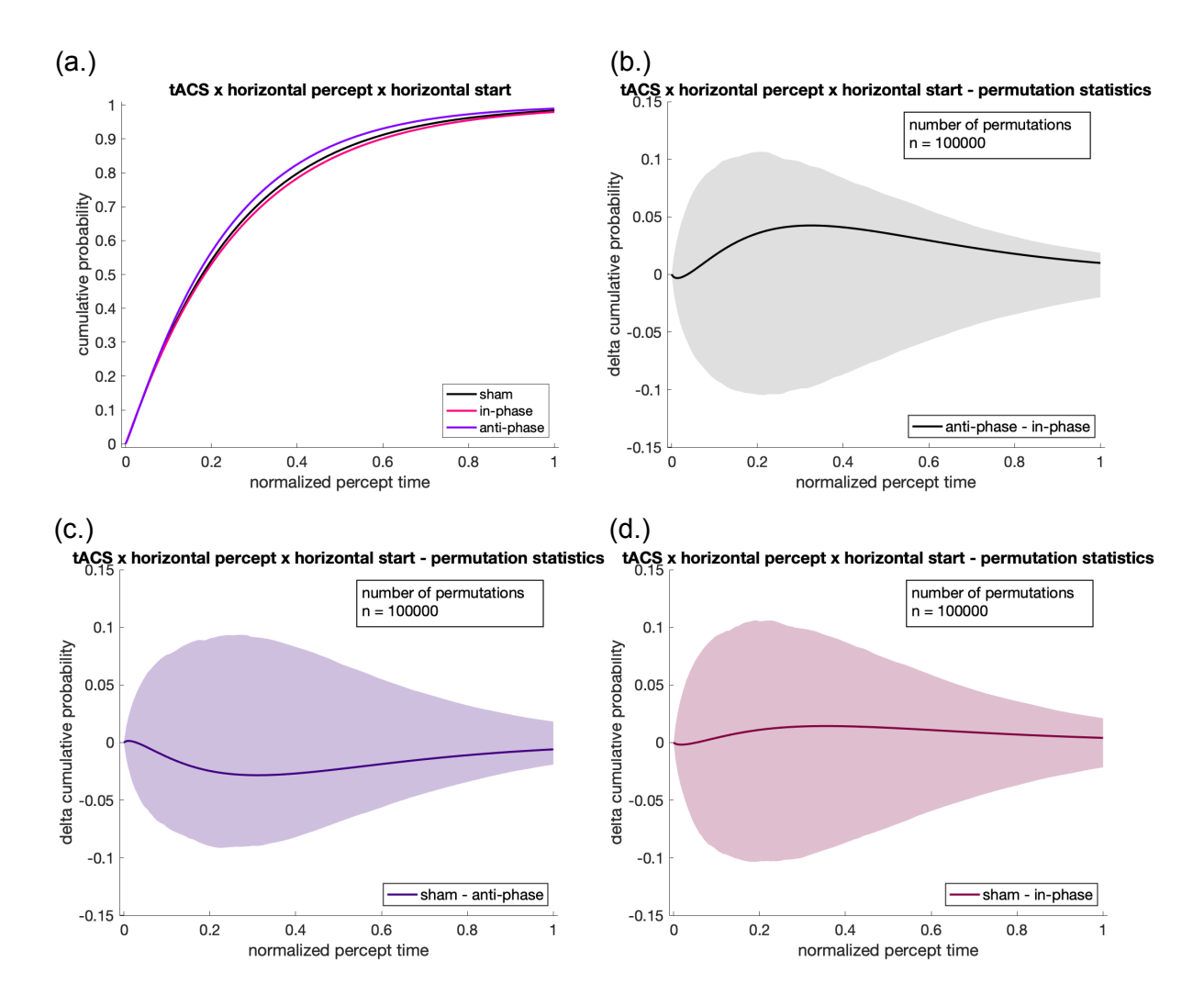
- (a.) Cumulative gamma distribution function (gCDF) of normalized percept times (NPTs) for distinct *tACS conditions* nested within the *perceived vertical motion direction* and *vertical unambiguous* start condition. The color-coded lines represent the respective *tACS condition*.
- (b.) (d.) Adjusted permutation statistics for the difference of gCDFs between *tACS conditions* nested within the *perceived vertical motion direction* and *horizontal unambiguous* start condition. The solid lines depict the respective empirical observed difference between the gCDFs.

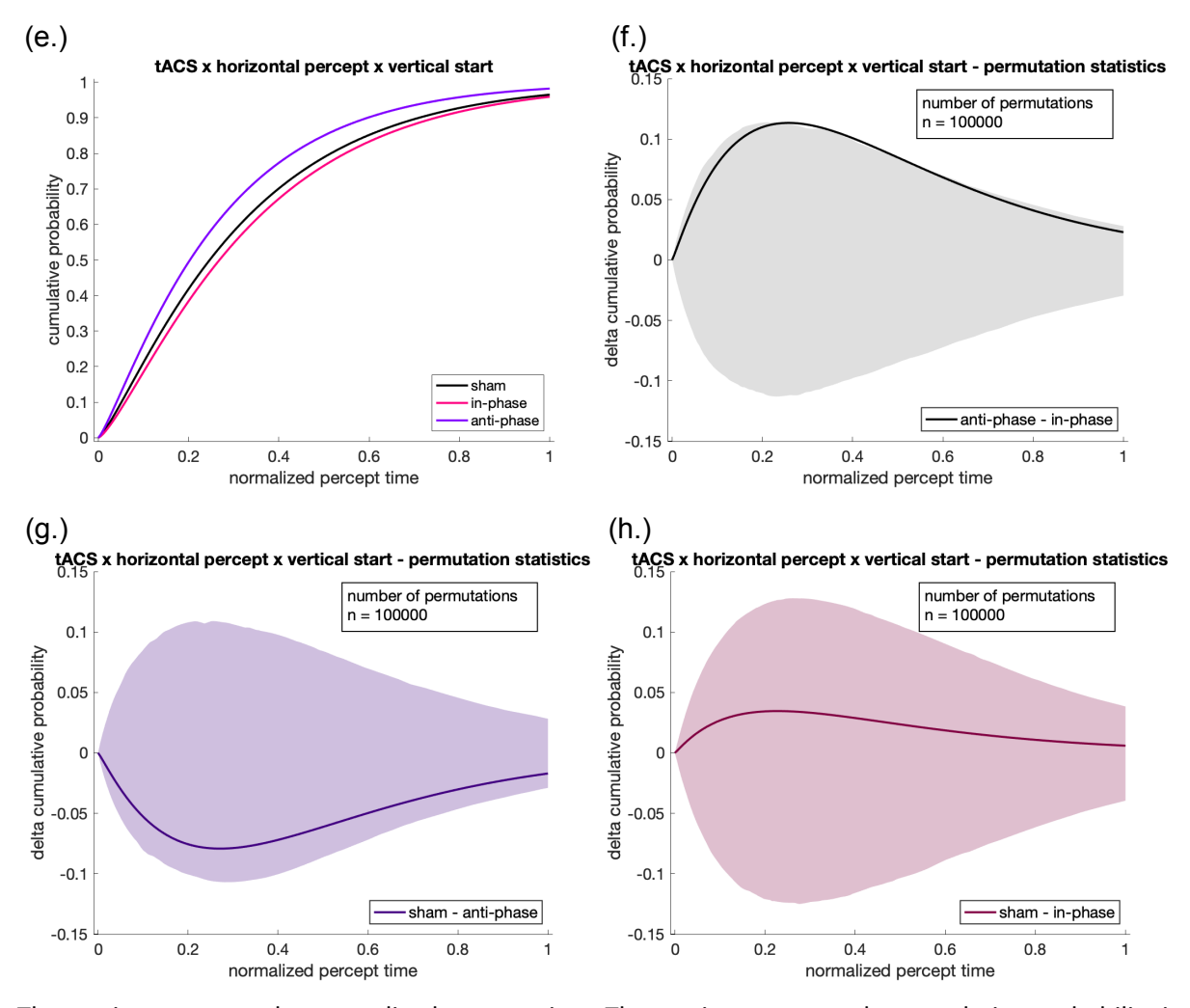
No significant difference between the *anti-phase* condition and *in-phase* condition, the *sham* condition and *anti-phase* condition as well as the *sham* condition and *in-phase* condition could be observed.

- (e.) Cumulative gamma distribution function (gCDF) of normalized percept times (NPTs) for distinct *tACS conditions* nested within the *perceived vertical motion direction* and *vertical unambiguous* start condition. The color-coded lines represent the respective *tACS condition*.
- (f.) (h.) Adjusted permutation statistics for the difference of gCDFs between *tACS conditions* nested within the *vertical perceived motion direction* nested within the *perceived vertical motion direction* and *vertical unambiguous* start condition. The solid lines represent the respective empirical observed difference between the gCDFs.

No significant difference between the *anti-phase* condition and *in-phase* condition, the *sham* condition and *anti-phase* condition as well as the *sham* condition and *in-phase* condition could be observed.

Figure 36 – Gamma cumulative distribution functions and statistical comparisons – *tACS x horizontal motion percept x unambiguous start condition* 





The x-axis represents the normalized percept time. The y-axis represents the cumulative probability in (a.) and (e.) and the difference (delta) of the cumulative probability in (b.) - (d.) and (f.) - (h.).

- (a.) Cumulative gamma distribution function (gCDF) of normalized percept times (NPTs) for distinct *tACS conditions* nested within the *perceived horizontal motion direction* and *horizontal unambiguous* start condition. The color-coded lines represent the respective *tACS condition*.
- (b.) (d.) Adjusted permutation statistics for the difference of gCDFs between *tACS conditions* nested within the *horizontal perceived motion direction* and *horizontal unambiguous* start condition. The solid lines represent the respective empirical observed difference between the gCDFs.

No significant difference between the *anti-phase* condition and *in-phase* condition, the *sham* condition and *anti-phase* condition as well as the *sham* condition and *in-phase* condition could be observed.

- (e.) Cumulative gamma distribution function (gCDF) of normalized percept times (NPTs) for distinct *tACS conditions* nested within the *perceived horizontal motion direction* and *vertical unambiguous* start condition. The color-coded lines represent the respective *tACS condition*.
- (f.) (h.) Adjusted permutation statistics for the difference of gCDFs between *tACS conditions* nested within the *horizontal perceived motion direction* and *vertical unambiguous* start condition. The solid lines represent the respective empirical observed difference between the gCDFs.
  - (f.). The difference between the *anti-phase* condition and *in-phase* condition revealed a significant effect.
  - (g.) (h.) No significant difference between the *sham* condition and *anti-phase* condition as well as the *sham* condition and *in-phase* condition could be observed.

## 3.3.3.1. Overview of results – cumulative gamma distribution functions

The analysis of cumulative gamma distribution functions investigated temporal dynamics of percept time distributions, focusing on their fit to a gamma distribution model. This novel application of gamma distributions to tactile stimuli aimed to validate the ambiguity characteristics of a tactile SAM stimulus. Normalized percept times were used to account for variable jitter phases in *unambiguous start configurations*, and data from all subjects and conditions were pooled for estimating gamma distributional parameters. Goodness-of-fit measures, including log-likelihood and Akaike Information Criterion (AIC), were calculated and demonstrated the superior fit of the gamma distribution compared to alternative models. Gamma cumulative distribution functions (gCDFs) were then calculated, offering a detailed view of percept time distributions across different conditions. This investigation revealed distinct shifts in the gamma cumulative distribution functions (gCDFs) under different experimental conditions. For the *tACS conditions*, significant effects were observed between *anti-phase* and *in-phase* stimulation. Specifically, *in-phase tACS* was associated with a higher proportion of longer percept times compared to *anti-phase tACS*, suggesting a phase-specific effect of *tACS* on perceptual stability.

The perceived *motion direction* also influenced percept time distributions. A significant difference emerged between *vertical* and *horizontal* motion patterns, with *horizontal* motion associated with a higher proportion of longer percept times. However, the *unambiguous start condition* (*horizontal* vs. *vertical*) did not yield statistically significant differences in percept time distributions.

Further analyses investigated the interaction between *tACS* conditions and *perceived motion direction*. Within the *horizontal* motion pattern, *in-phase tACS* resulted in significantly longer percept times compared to *anti-phase tACS*, whereas no significant differences were observed within the *vertical* motion pattern.

By further accounting for the *unambiguous start configuration, in-phase tACS* within the *vertical unambiguous start configuration* resulted in significantly longer percept times compared to *anti-phase tACS*.

These findings highlight the complex interplay between phase-specific effects of *tACS* and perceptual dynamics.

Statistical analyses employed a robust non-parametric permutation approach to account for potential deviations in the shape of cumulative distribution functions, providing a nuanced understanding of perceptual changes that might not be captured by mean comparisons alone (Misselhorn et al., 2019). This approach may highlight the value of applying gamma distribution models to tactile bistable stimuli, thereby providing novel insights into how *tACS* and perceptual conditions modulate temporal aspects of perception.

#### 3.3.4. Exploratory analyses of pupil dilatation

#### 3.3.4.1. Pupil amplitude time series analysis

For statistical comparison, non-parametric permutational analyses were conducted. To accomplish this, the observed pupil time course data for each participant in the *pressed* and *control* condition was randomly shuffled and reassigned to condition levels. This was followed by subtracting the permuted *pressed* condition data from the *control* condition data. We repeated this process for 100,000 permutations to generate a null distribution of mean differences expected by chance ( $H_0$  distribution). To conduct further analyses, confidence intervals (CIs) were constructed based on the  $H_0$  distribution of mean differences. For this purpose, *alpha* was set at *alpha* = 0.05/2 for a two-sided test.

To account for multiple comparisons, a modified form of the extreme value-based correction was conducted (Cohen, 2017). This involved identifying all values that were greater than the  $97.5^{th}$  percentile or less than the  $2.5^{th}$  percentile of the shuffled data set for each permuted iteration. These extreme values, considered over all permutations, result in a distribution of extreme values. From this distribution, an upper and lower threshold consistent of the  $97.5^{th}$  or  $2.5^{th}$  percentile (corresponding

to a two-tailed *alpha* of 0.05) was determined. Consequently, the resulting corrected CIs control for the global range of the tested data.

We conducted these analyses for the mean pupil time course including all participants and conditions, as well as for the distinct tACS conditions. The alpha level of significance for the analyses of the different tACS conditions was Bonferroni-adjusted by the number of condition contrasts  $(n_c = 3)$  as  $alpha = (0.05/2)/n_c = 0.0083$ .

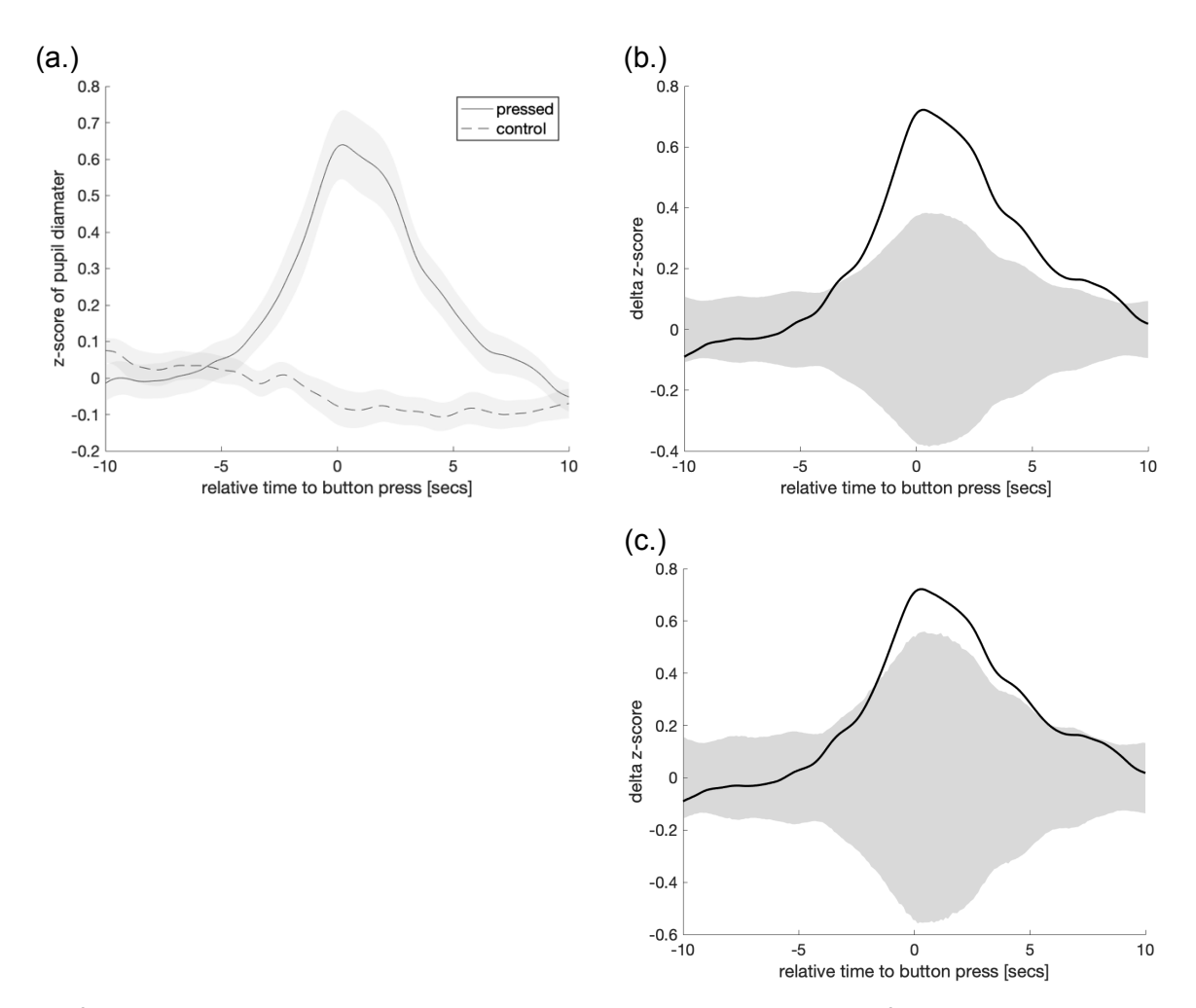
For observed values more extreme than the corrected Cls, significance was assumed.

The non-parametric permutational analyses revealed significant differences for the mean pupil time course (significant cluster: pressed – control, delta z-score (y): 0.3776-0.2149, relative time to button press (x): -1559-ms - +5678-ms) as well as for the pupil time course of the distinct tACS conditions (significant cluster, sham: pressed – control, delta z-score (y): 0.4650-0.4615, relative time to button press (x): -854-ms - +2663-ms; in-phase: pressed – control, delta z-score (y): 0.5736-0.5208, relative time to button press (x): -1155-ms - +4271-ms; anti-phase: pressed – control, delta z-score (y): 0.4136-0.3365, relative time to button press (x): -1256-ms - +3366-ms) (Figure 38 and 39).

Specifically, pupil dilation steadily increases around -5 seconds prior to the onset of a button press and peaking at the time of the button press, followed by a continues decrease in pupil diameter (Figure 38 and 39).

This observed pattern of pupil response was consistent across all subjects and conditions, as well as across the different *tACS conditions*.

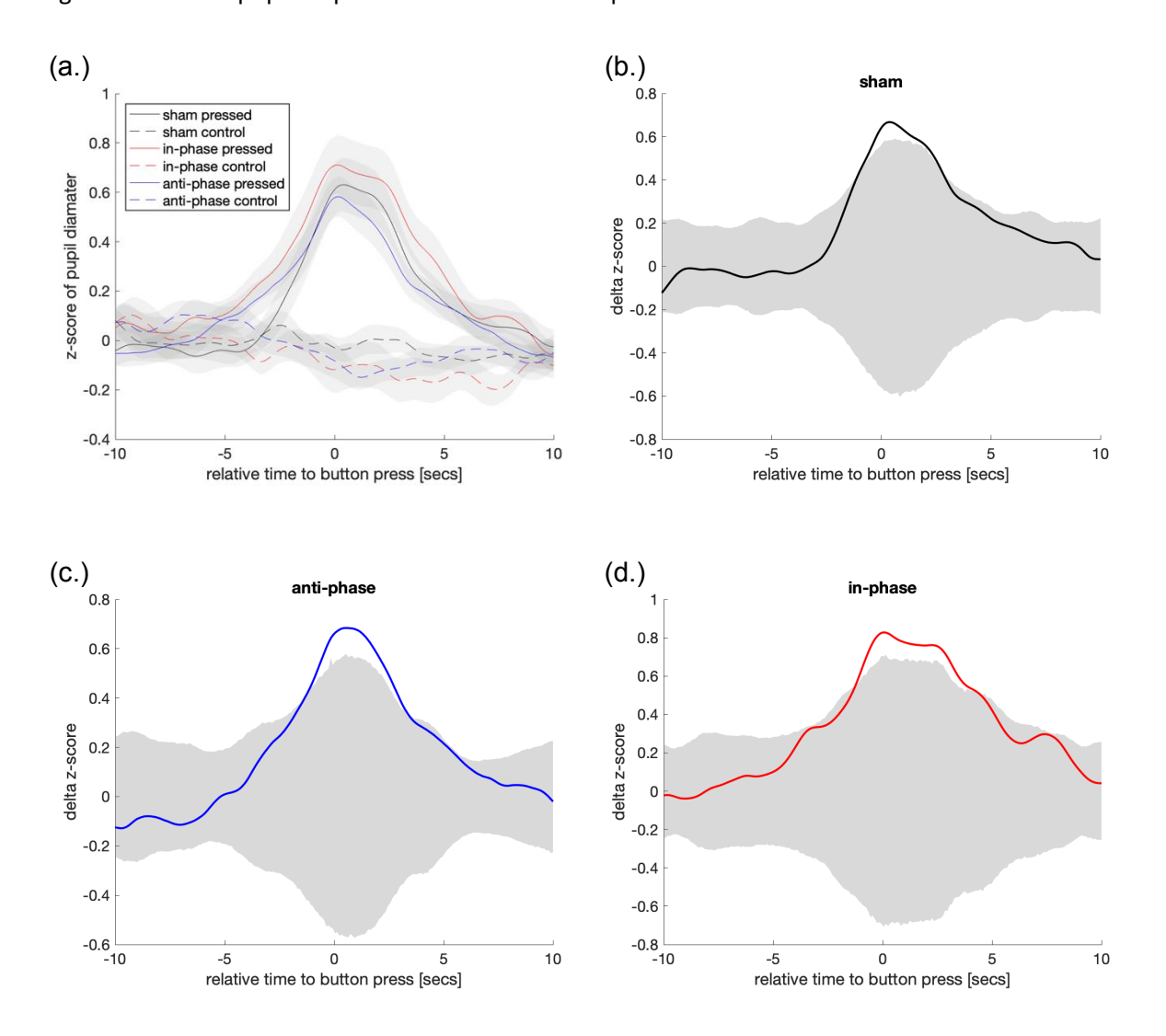
Figure 37 – Mean pupil amplitude time courses and permutation statistics for all participants and all conditions



The figure displays the mean pupil amplitude time course within a range of -10 seconds prior and + 10 seconds following the time point of a button press (beginning of a percept reported by participants). The x-axis delineates a time frame of -10 seconds prior and +10 seconds following the time point of a button press. The y-axis represents the z-scored pupil diameter in (a.) and the differences of the z-scored pupil diameter between the *pressed* and *control* condition (*pressed – control*) in (b.) and (c.). (a.) The solid line illustrates the mean pupil amplitude time course for the *pressed* condition, encompassing all participants and conditions. The dashed line represents the corresponding control condition (pupil time course without a button press). Shaded gray areas denote the standard error of the mean.

- (b.) Permutation statistics of the condition difference *pressed control*. The shaded gray area represents the confidence intervals (CIs) without considering multiple comparisons along the x-axis (alpha = 0.05 / 2). The solid line represents the observed pupil time course.
- (c.) Adjusted permutation statistics of the condition difference pressed control. The shaded gray area represents the confidence intervals (CIs) corrected for multiple comparisons along the x-axis (alpha = 0.05 / 2). The solid line represents the observed pupil time course.

Figure 38 – Mean pupil amplitude time courses and permutation statistics for distinct tACS conditions



Pupil amplitude time course within a range of -10 seconds prior to and + 10 seconds following the time point of a button press (beginning of a percept reported by participants). The x-axis encompasses a time frame of -10 seconds prior and +10 seconds following the time point of a button press. The y-axis represents the z-scored pupil diameter in (a.) and the differences of the z-scored pupil diameter between the *pressed* and *control* condition (*pressed* – *control*) in (b.) and (c.).

- (a.) The solid color-coded lines represent the mean pupil amplitude time course for the *pressed* condition of all participants for the distinct *tACS conditions* (*sham*: black, *in-phase*: red, *anti-phase*: blue). The dashed color-coded lines represent the respective *control* condition (pupil time course without a button press). Shaded gray areas represent the standard error of the mean across subjects. The y-axis represents the z-scored pupil diameter.
- (b.) Adjusted permutation statistics of the condition difference *pressed control* for the *sham* condition. The shaded gray area represents the confidence intervals (CIs) adjusted for multiple comparisons along the x-axis (alpha = [0.05/2]/3). The solid line represents the observed pupil time course. The y-axis represents the differences in z-scored pupil diameter.
- (c.) Same as (b.) Adjusted permutation statistics of the condition difference *pressed control* for the *in-phase* condition.
- (d.) Same as (b.) and (c.) Adjusted permutation statistics of the condition difference *pressed control* for the *anti-phase* condition.

# 3.3.4.2. Correlation patterns of pupil amplitude modulation (AM) and normalized percept time (NPT)

Existing studies in the visual modality have revealed that the amplitude of pupil dilation predict the stability (or in other words percept duration) of a subsequent percept for bistable stimuli (Einhäuser et al., 2008; Hupé et al., 2009; Kloosterman et al., 2015).

Nevertheless, neuroscientific research investigating the relationship between pupil dilation and bistable perception in the tactile modality is limited.

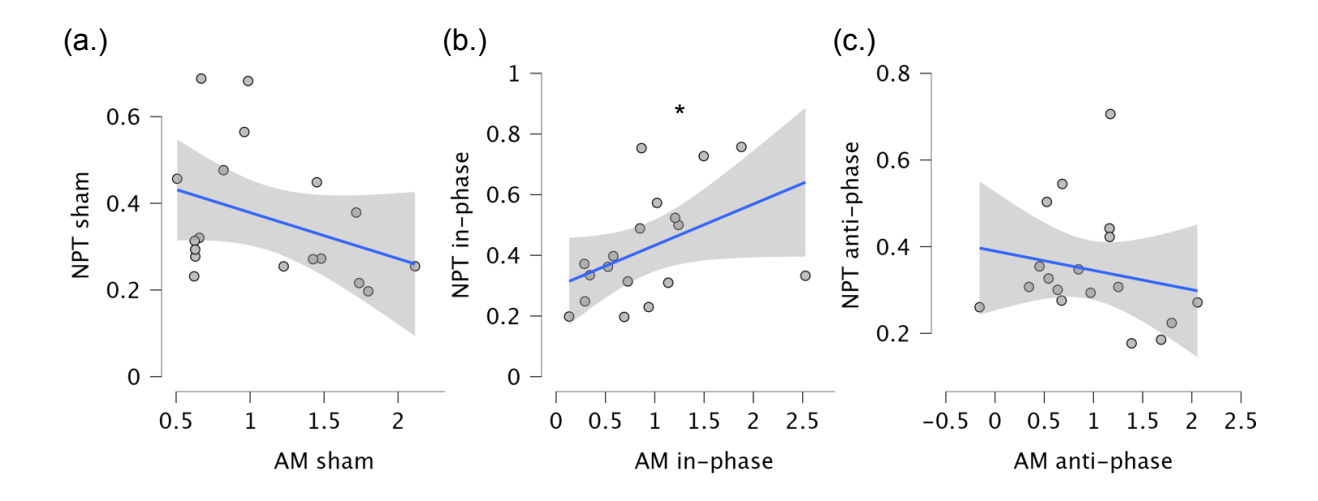
Therefore, we investigated this relationship by examining correlation patterns between the amplitude modulation of pupil dilation and the subsequent normalized percept time in the tactile bistable apparent motion paradigm.

Spearman correlation coefficients were calculated by using MATLAB's *corr* function to identify potential relationships between the pupil amplitude modulation (AM) and subsequent NPTs for the distinct tACS conditions (MATLAB, R2016b (9.1.0), The MathWorks Inc., Natick, MA, USA). The analyses revealed a significant positive correlation between amplitude modulation and subsequent normalized percept time within the *in-phase tACS* condition (Spearman's rho = 0.501, p = 0.036). Conversely, no statistically significant correlation was observed for the other tACS conditions (sham: Spearman's rho = -0.352, p = 0.152; anti-phase: Spearman's rho = -0.325, p = 0.188).

Furthermore, we conducted permutation statistics to determine significant differences between pupil amplitude modulation and NPTs across the *tACS conditions*.

No significant differences in amplitude modulations between *tACS conditions* were found (100,000 permutations, no correction for multiple comparison; sham – in-phase: p = 0.4168, sham – anti-phase. p = 0.4442, in-phase – anti-phase: p = 0.9170).

However, in correspondence with the previously analyzed results on NPTs, significant differences were observed between the *sham* and the *in-phase* as well as between the *in-phase* and the *anti-phase tACS* conditions (100,000 permutations, no correction for multiple comparisons; sham – in-phase: p = 0.0415, sham – anti-phase. p = 0.5268, in-phase – anti-phase: p = 0.0037).



Correlation patterns of amplitude modulation (AM) [x-axis] and normalized percept time (NPT) [y-axis] for the distinct *tACS conditions*.

Correlation coefficients were calculated as Spearman's rho and significance were assessed using MATLAB's *corr* function for the distinct *tACS conditions*.

Gray dots represent the corresponding values for each participant. The blue lines represent the linearly interpolated regression line based on the least squares method. The shaded gray areas represent the 95% confidence interval of the regression line estimate.

- (a.) For the *sham* condition, no significant correlation was observed (*sham: Spearman's rho = -0.352*, p = 0.152).
- (b.) For the *in-phase* condition, a significant positive correlation between AM and NPT was observed (Spearman's rho = 0.501, p = 0.036).
- (c.) For the *anti-phase* condition, no significant correlation was observed (anti-phase: Spearman's rho = -0.325, p = 0.188).

### 3.3.4.3. Overview of results – exploratory analyses of pupil dilatation

Non-parametric permutation analyses were conducted to compare pupil dilation time courses between conditions. The results revealed significant pupil dilation differences between the *pressed* and *control* conditions, as well as across *tACS conditions*. Notably, pupil dilation increased approximately five seconds before a button press, peaked at the press, and subsequently decreased gradually. This suggests a close link between pupil dynamics and behavioral responses.

Further analyses explored the relationship between pupil amplitude modulation (AM) and normalized percept time (NPT). A significant positive correlation was observed in the *in-phase tACS condition*, indicating that greater pupil dilation was associated with longer percept durations. This result may highlight a potential relationship between pupil response and perceptual stability.

However, no significant correlations were found for *sham* or *anti-phase* conditions, suggesting that the associated effect may be specific to *in-phase tACS*. Permutation testing revealed significant differences in NPTs between the *in-phase* condition and both the *sham* and *anti-phase* conditions but not between *sham* and *anti-phase* conditions. No significant differences were observed for AM between the three different *tACS conditions*. The results indicate that pupil dilation may serve as a physiological marker of perceptual and cognitive engagement, particularly under *in-phase tACS*. The correlation between increased amplitude modulation and prolonged perceptual durations suggests that *in-phase tACS* may enhance perceptual stability by regulating the same underlying mechanisms, which are engaged in pupil amplitude modulations. The lack of comparable effects in other conditions further highlights the

specificity of *in-phase* stimulation. These findings contribute to our understanding of the ways in which physiological and neural mechanisms interact to shape perceptual experiences.

#### 3.4. Discussion

This experiment investigated the potential neuromodulatory role of bihemispheric, phase-specific *tACS* on tactile motion perception. Therefore, we designed an ambiguous tactile stimulus setup inspired by the well-established Stroboscopic Alternative Motion (SAM) paradigm in the visual modality (Chardhuri & Glaser et al., 1991; Helfrich et al., 2014; Schiller, 1933; Strüber et al., 2014).

The experimental framework regarding the tactile stimuli was rooted in the original work of Schiller (Schiller, 1933) in the visual domain, where alternating sequential activation of diagonally arranged light dots created bistable apparent motion perceptions. Expanding upon this foundation, our tactile setup employed vibrotactile elements strategically positioned on participants' forearms (Liaci et al., 2016). Utilizing this tactile adaptation of the SAM stimulus allowed us to probe the dynamics of ambiguous tactile motion perception (Liaci et al., 2016).

A central advantage of bistable stimuli is their unique ability to allow transient perceptual mutually exclusive alterations while maintaining the physical stimulus constant (Blake & Logothetis, 2002; Helfrich et al., 2016). This characteristic provides a possible fertile ground for the investigation of perceptual states, their possible underlying neural activity as well as their reaction to phase and frequency specific *tACS* (Blake & Logothetis, 2002; Helfrich et al., 2014; Helfrich et al., 2016).

Following the established role of *tACS* in modulating neural oscillations and brain activity, our study aimed to investigate its impact on the perception of tactile ambiguous motion. We hypothesized that the current perceptual state of given subject is determined by the oscillatory synchronization of the primary somatosensory cortices. In an attempt to modulate these oscillatory fingerprints supposed to be correlated with perceptual states, multi electrode *tACS* was applied in phase- and frequency specific mode (Helfrich et al., 2014). To unravel whether *tACS* could effectively influence the perception of tactile apparent motion, we employed a bihemispheric, bilateral gamma *tACS* over primary somatosensory cortices, while subjects reported their current perceptual state.

The overall normalized percept time indicates that 88.29% (± 11.49% standard deviation) of the time the ambiguous stimulus configuration was presented, a clear ambiguous *vertical* or *horizontal motion direction* pattern was perceived by the participants.

For the presented timeframes of the *unambiguous horizontal* direction pattern, the control condition revealed that 86.19% (± 10.87% standard deviation) of the timeframe was accurately indicated as a *horizontal* percept across all participants. During the time of the *vertical unambiguous* stimulus configuration 70.06% (± 16.38% standard deviation) of the timeframe was correctly indicated across all participants. These results indicate that participants stayed attentive and focused on the tactile apparent motion pattern during the experimental trials.

#### 3.4.1. Phase specific *tACS* effect on normalized percept time (NPT)

#### 3.4.1.1. 3x2x2 RM-ANOVA

The 3x2x2 RM ANOVA was designed to analyze the complex interplay of multiple factors potentially influencing participants' perception of tactile ambiguous motion. The factors encompassed the *tACS condition*, the *perceived motion direction*, and the *unambiguous start configuration*. This comprehensive analysis enabled the dissection of potential interactions between these factors and an assessment of their individual contributions to the participants' tactile perceptual experiences. According to the results of the 3x2x2 RM-ANOVA, the factor of *tACS condition* had a significant effect on the dependent variable of NPT. Given our previously established hypotheses, this finding appears to be unexpected.

The underlying assumption for this experiment was that of hemispherical integration, which anticipated that *in-phase* gamma *tACS* would improve the functional oscillatory coupling between the primary somatosensory cortices of both hemispheres and thus result in a bias towards *horizontal* motion perception (between forearm motion), as suggested by an increase in *horizontal* percept time. Conversely, anti-phasic *tACS* was expected to hamper the functional coupling between the primary somatosensory areas of both hemispheres, leading to a bias towards *vertical* perception of motion, as indicated by an increase in *vertical* percept time. Consequently, we were expecting to observe a statistically significant interaction effect between the *tACS condition* and the perceived pattern of *motion direction*.

Notably, the RM-ANOVA analysis revealed a significant impact of the *tACS condition*. To further examine this impact, the Bonferroni-corrected post hoc comparison indicated that NPTs were significantly higher for the *in-phase* condition in relation to the *anti-phase* condition. In addition,

significantly higher NPTs were observed for the *sham* condition in comparison to the *anti-phase* condition.

These findings suggest that the application of *in-phase tACS condition* enhances normalized motion percept times, regardless of the *unambiguous start configuration* and the *perceived motion direction* pattern.

To explain these results further, the *in-phase* bihemispheric stimulation may enhance the formation of a tactile motion percept, including *horizontal* and *vertical* tactile perceptions. Additionally, *in-phase* gamma *tACS* may stabilize a current perceptual state, regardless of the apparent *motion direction* pattern. Conversely, *anti-phase* gamma *tACS* may destabilize the current perceptual state of perceived apparent motion.

Moreover, the RM-ANOVA revealed a significant difference between the *horizontal* and *vertical motion direction* patterns perceived by the participants. Since a balanced aspect ratio of AR~1.2 was introduced, no significant differences between the *perceived motion direction* patterns were expected (Liaci et al., 206). Nevertheless, participants indicated significantly longer NPTs for the *horizontal motion direction* pattern compared to *vertical motion direction* pattern. This observation was independent of the *unambiguous* starting configuration and *tACS condition*.

This result may indicate that in the tactile modality, the perception of a *horizontal* apparent motion pattern may be more effortlessly perceived than the perception of a *vertical* apparent motion pattern. Considering the hypothesis of bihemispheric integration, this finding is noteworthy and contrasts with the visual modality (Liaci et al., 2016). In the visual modality, the *perceived motion direction* pattern of the visual SAM stimulus has been shown to be determined by the introduced aspect ratio (Chardhuri & Glaser et al., 1991). Based on the experimental setup using an aspect ratio of AR  $\sim$  1.2, no distinct bias was expected for perceiving either a *horizontal* or a *vertical motion direction* pattern. (Helfrich et al., 2014; Strüber et al., 2014; Rose et al., 2005).

As expected, the main factor of *unambiguous start configuration* did not yield a significant difference in NPTs. This implies that the specific configuration of *unambiguous* stimuli, whether *horizontal* or *vertical*, did not have a significant impact on NPTs.

Furthermore, the interaction effects between *tACS condition*, *perceived motion direction*, and *unambiguous start configuration* did not yield a significant outcome. These results suggest that the interplay between these factors does not significantly influence NPTs.

Overall, the results of the analysis revealed two main effects with large effect sizes, highlighting their substantial impact on NPT (Miles & Shevlin, 2001). Primarily, the main effect of *tACS* indicates a pronounced influence of *tACS* conditions (sham, in-phase, anti-phase) on perceptual motion processing. Correspondingly, the main effect of perceived motion direction exerted a robust influence on NPTs. Post hoc comparisons of the *tACS* conditions revealed small effect sizes (Lachenbruch & Cohen, 1989).

#### 3.4.1.2. 3x4x2 RM-ANOVA

This section explores the complex interplay of factors that impact NPTs as unveiled by the 3x4x2 RM-ANOVA. This comprehensive analysis explored the impact of *tACS condition*, *perceptual alterations*, and the start configuration of *unambiguous* stimuli on participants' tactile ambiguous motion perception.

For this purpose, individual NPTs were categorized in dependence of the preceding percept. The RM-ANOVA showed a significant *tACS* effect with a medium effect size, indicating a meaningful difference among the *tACS* conditions (Miles & Shevlin, 2001). Nevertheless, it should be noted that Bonferroni-corrected post hoc comparisons only revealed a tendency towards significantly higher NPTs for the *in-phase* condition in relation to the *anti-phase* condition, as well as between the *sham* condition compared to the *anti-phase* condition.

These findings indicate the same statistical patterns described in the 3x2x2 RM-ANOVA.

The factor of *perceptual alteration* demonstrated a highly significant effect on NPTs, with large a effect size (Miles & Shevlin, 2001). Bonferroni-corrected post hoc analyses illuminated the nature of these effects: the condition of *vertical-to-horizontal* alteration showed the highest NPTs compared to NPTs for the *horizontal-to-horizontal* condition, and *vertical-to-vertical* condition. Additionally, the condition of *horizontal-to-vertical*, showed highly significant higher NPTs compared to the *vertical-to-vertical* condition.

This finding underscores the substantial role that *perceptual alterations* have on shaping the perceptual temporal dynamics of tactile ambiguous motion perception.

As expected, the factor of *unambiguous start configuration* did not produce a significant difference in NPTs. This implies that neither the *horizontal* nor the *vertical unambiguous* stimulus configuration, presented prior of the ambiguous tactile stimulus configuration, did exert a substantial influence on the temporal dynamics of ambiguous motion perception.

Interestingly, the interaction effect of *tACS* and *perceptual alteration*, along with *perceptual alteration* and *unambiguous start configuration*, produced significant results. These interactions underscore the complexity of the factors involved in modulating NPTs in tactile ambiguous apparent motion perception. The interaction between *tACS* and *perceptual alteration* had a small effect size (Miles & Shevlin, 2001). Nevertheless, the interaction implies that the influence of *tACS* on NPTs depends upon the specific prior *perceptual alteration* experienced by participants. Correspondingly, the interaction between *perceptual alteration* and *unambiguous start configuration* demonstrates the interplay between these factors in shaping participants' tactile perceptual experiences of tactile motion perception. The interaction of *perceptual alteration* and *unambiguous start configuration* demonstrated a large effect size (Miles & Shevlin, 2001) indicating its importance in shaping NPTs. In order to further simplify and interpret the significant interaction effects of *tACS* and *perceptual alteration*, four separate RM-ANOVAs (4 \* RM-ANOVA 3x2) were calculated for each level of *perceptual alteration*.

The significant *tACS* effect was observed exclusively in the sub analyses of the RM-ANOVA of the *vertical-to-horizontal* condition. *TACS* and *unambiguous start configuration* independently exerted strong effects on NPT, while their interaction had a negligible impact (Miles & Shevlin, 2001). The subsequent Bonferroni-corrected post hoc analyzes revealed highly significant lower *horizontal* NPTs for the *anti-phase* condition in relation to the *sham* condition with a medium effect size (Lachenbruch & Cohen, 1989). However, no significant difference was found between the *in-phase* and *anti-phase* condition.

This finding implies a possible phase specific *tACS* effect on NPTs in line with the stated hypothesis of interhemispheric integration (Helfrich et al., 2014; Strüber et al., 2014; Rose et al., 2005).

In concrete terms, this result suggests that *anti-phasic* bihemispheric *tACS* impedes the perceptual formation and stability of the perception of a *horizontal motion* pattern if the preceding perception was that of a *vertical motion* pattern.

In addition, for the sub-analyses of the *horizontal-to-horizontal* RM-ANOVA and the *vertical-to-horizontal* RM-ANOVA, a significant effect was found for the primary factor of *unambiguous start configuration*.

Regarding the sub analyses of *horizontal-to-horizontal* higher *horizontal* NPTs for the *unambiguous horizontal* start condition compared to the *unambiguous vertical* start condition was observed. On the

other hand, in the *vertical-to-horizontal* sub-analyses, highly significant *horizontal* NPTs were observed for the *unambiguous vertical start condition* compared to the *unambiguous horizontal start condition*.

#### 3.4.2. Phase specific *tACS* effect on button press per minute (BPM)

To gain a deeper understanding and interpretation of the presented findings, it is necessary to consider the dependent variable of button presses per minute (BPM). This is because NPTs only indicate the time of perception in relation to the total time of the ambiguous tactile stimulus. Therefore, NPTs only indicate the relative timing of apparent motion perception patterns without providing insights into the rate or dynamics of perceptual switches or the process of perceptual formation. The rate of button presses, as an additional measure, provides valuable insights into the dynamics of perceptual development and perceptual decrement of motion perception (Helfrich et al., 2014). By considering both NPTs and the rate of button presses, a more comprehensive understanding of the temporal dynamics of *perceptual alterations* during the experimental task can be achieved, contributing to a more nuanced interpretation of the findings.

Specifically, an analogous 3x2x2 RM-ANOVA design was used to explore the effects of *tACS condition*, perceived motion direction, and unambiguous start configuration on the button press rate of participants. In contrast to the significant effects for NPTs described above, the RM-ANOVA of the buttons pressed per minute (BPM) did not produce a statistically significant effect for the factor of *tACS*.

Nevertheless, a significant effect with a large effect size for the factor of *perceived motion direction* was observed (Miles & Shevlin, 2001). Particularly, the BPM rate was significantly higher for the perceived *horizontal motion* pattern compared to the *vertical motion* pattern. This finding aligns to the significant higher NPTs for the perceived *horizontal motion direction*. Together they suggest a bias for the *horizontal motion* perception in the tactile domain (given a fixed aspect ratio of AR ~1.2). Interestingly, a significant interaction effect with a large effect size regarding the factors of *perceived motion direction* pattern and *unambiguous start configuration* was also observed (Miles & Shevlin, 2001). This interaction effect suggests that the relationship between *perceived motion direction* and button press rates is modulated by the initial configuration of *unambiguous* stimuli. Specifically, when the initial start configuration was *vertically unambiguous*, subsequent *horizontal* BPM rates (during the

ambiguous tactile stimulus configuration) were significantly higher compared to *vertical* BPM rates. In contrast, we did not observe this effect for *horizontal unambiguous start configuration*.

The observed effects on perceptual dynamics may be explained to an extent by a general bias towards *horizontal motion* perception.

The main factor of *unambiguous start configuration*, and all other interaction effects (including *tACS condition* with *perceived motion direction*, *tACS condition* with *unambiguous start configuration*, and the three-way interaction) did not show any statistically significant differences. This implies that these factors did not significantly influence the participants' button press rates.

The summary statistics illustrate that the mean BPM across all conditions and subjects was 0.9283 (± 0.5233 standard deviation) button presses per minute.

Interestingly, for the visual modality, participants reported a higher switch rate of about 11.2 *perceptual alterations* per minute for the visual SAM stimulus (Helfrich et al., 2014).

This finding suggests that the tactile apparent motion quartet could have a meaningfully lower BPM rate compared to the visual motion quartet, indicating potential differences in perceptual dynamics between the tactile and visual sensory modalities.

Nevertheless, it is worth noting that these differences could also be attributed, at least in part, to variations in experimental settings across different studies. For example, some experiments using visual SAM stimulus did not include an option of "no percept" of a *motion direction* pattern. Overall, the reduced dynamic of motion pattern perception in the tactile modality appears to be consistent with findings from other tactile apparent motion paradigms (Carter et al., 2008; Conrad et al., 2012).

#### 3.4.3. Analyses of cumulated gamma distribution functions

Cumulative distribution functions (CDFs) are commonly utilized to describe the cumulated probability distribution of a particular variable. Additionally, CDFs can be used to analyze statistical properties, such as the mean, variance, and skewness of a distribution. Regarding normalized percept times (NPTs), the variable of interest is the normalized duration of a perceived *horizontal* or *vertical motion* pattern. Gamma CDFs regarding the dependent variable of NPTs for the respective conditions under investigation were predicted and calculated. In the following statistical evaluations non-parametric statistical differences based on differences between gamma CDFs were computed.

Non-parametric comparisons of cumulated distribution functions have the potential to detect slight differences that might not be detected by a mean comparison or ANOVAs (Misselhorn et al., 2019). Therefore, relative shifts of the cumulated gamma distribution functions can provide valuable insights into the differences of in the distributions of the respective condition. In general, relative shifts to the right of the x-axis of the gCDF indicate longer NPTs. Conversely, if the CDF for one experimental condition is relatively shifted to the left, compared to the other experimental condition, the pattern indicates that the NPTs for the respective condition are lower than those for the other condition. To investigate the impact of all relevant factors on NPTs, condition differences were analyzed in a full factorial design, including possible interactions of factor levels. The non-parametric analyses of cumulative gamma distribution functions for NPTs further revealed statistically significant differences. Statistical comparisons between tACS conditions revealed a significant tACS effect: in-phasic tACS relatively shifts the gamma CDF to the right compared to anti-phasic tACS, irrespective of the unambiguous start configuration as well as the motion direction. Descriptively, the CDF of the sham condition resides between both tACS conditions. Nevertheless, statistically significant differences regarding the stimulation and sham conditions could not be observed. In concrete terms, in-phasic tACS increased NPTs compared to anti-phasic tACS, regardless of the perceived motion pattern and unambiguous start condition.

Regarding the *perceived motion direction*, we observed a pronounced significant shift to the right of the x-axes for *horizontal* motion perception pattern compared to a *vertical* motion perception pattern. Specifically, the *vertical motion direction* pattern exhibited shorter NPTs compared to the *horizontal* direction. Regarding the *unambiguous start configuration*, there was no significant effect observed which suggests that the starting configuration did not significantly influence NPTs.

Additional investigation into the interaction effects between *tACS conditions* and *perceived motion direction* revealed significant differences among conditions. Within the *horizontal* NPTs, in-phasic *tACS* showed a significant shift towards longer NPTs compared to anti-phasic *tACS*. In the realm of *vertical* NPTs, the analysis revealed that the contrast between *anti-phase* and *in-phase tACS conditions* did not produce a significant difference.

These significant interactions emphasize the complexity of the factors involved in modulating NPTs in tactile ambiguous apparent motion perception. The relationship between *tACS* and *perceptual* 

alteration implies that in-phasic *tACS* stabilizes and stimulates longer *horizontal* NPTs. In the context, of *vertical* NPTs however, no difference between *tACS* condition was observed.

These findings partially support our primary hypothesis that perceived directional motion patterns can be modulated by gamma *tACS* in a phase-specific manner.

Finally, we considered complex interactions among all relevant factor levels in the non-parametric statistical assessment of cumulative distribution functions (CDFs). For this purpose, we considered all levels of *tACS conditions*, *perceived motion direction*, and *unambiguous start configuration* as relevant interaction factors.

Within the particular sub condition of *vertical perceived motion direction* and *horizontal unambiguous start configuration*, the permutation statistics did not uncover a significant effect between the various *tACS conditions*.

Similarly, within the specific sub condition of *vertical perceived motion direction* and *vertical unambiguous start configuration*, the permutation statistics did not produce a significant effect between the different *tACS conditions*.

From these results, it may be inferred that phase-specific gamma *tACS* does not significantly impact the perceived *vertical* NPTs with respect to the *horizontal* or *vertical unambiguous start configuration*. The analysis was further extended to encompass the sub condition of *horizontal perceived motion direction* and *horizontal unambiguous start configuration*. As observed in the previous contexts, the permutation statistics did not reveal any significant effects among the various *tACS conditions*. This indicates that, within this particular context, the modulation of tactile perception by phase specific *tACS* did not cause statistically significant alterations in the *perceived motion direction* patterns reflected in NPTs.

Intriguingly, within the sub conditions involving horizontal perceived motion direction and a vertical unambiguous start configuration, our permutation statistics revealed a significant difference between the in-phase and anti-phase tACS conditions. Specifically, in-phase tACS showed a significant shift towards longer horizontal NPTs compared to anti-phase tACS.

These results contribute to the understanding of the relationships between CDFs regarding *perceived motion direction* and *tACS*. Furthermore, they complement the results of the RM-ANOVA of NPTs for the sub-condition of *vertical-to-horizontal motion direction* and *tACS conditions* as well as the interaction between CDFs in terms of *horizontal motion direction* and *tACS conditions*.

Overall, these findings contribute and support the primary hypothesis that gamma *tACS* may phase-specifically modulate perceived directional tactile motion patterns.

#### 3.4.4. Pupil dilation is indicative prior to perceptual formation

Pupil dilation has received considerable attention as a potential indicator of cognitive and perceptual states (Einhäuser et al., 2008; Kloostermann et al., 2015). Recent studies have suggested that pupil dilation, as a physiological response, may provide valuable insights into the conscious perception of ambiguous stimuli (Einhäuser et al., 2008).

Exploratory analyses of the recorded pupil data within the experiential investigation of tactile ambiguous motion perception revealed differentiated aspects. As postulated and described in previous publications and investigations, we found a statistically significant increase in pupil dilation a priori of a *perceptual alteration* (Einhäuser et al., 2008; Hupé et al., 2009; Kloosterman et al., 2015).

Typically, pupil parameters were investigated at about 500ms prior and past to *perceptual alteration* (Einhäuser et al., 2008). Since most of experimental designs employed visually ambiguous stimuli, a generally higher dynamic of *perceptual alterations* of ambiguous stimuli may be hypothesized.

The pupil amplitude data observed in this experiment shows a remarkable pattern. About 5 seconds prior to the actual *perceptual alteration*, the pupil amplitude commences to increase steadily and reaches a peak at about the beginning of the perception of directional tactile motion pattern. In contrast to experimental investigations in the visual modality, the time frames for analyses span over 20 seconds compared to about 1-4 second duration used in experimental investigations in the visual modality. This difference may be partially explained to the more dynamic nature of *perceptual alterations* for visual ambiguous stimuli compared to tactile stimuli.

Moreover, this is the first research to discover the concept of pupil dilation in an apparent motion paradigm associated with tactile ambiguity spanning time frames of this extent.

Regarding the statistical evaluation, the non-parametric analyses revealed a significant cluster of increased pupil dilation for the condition of button *pressed* (and therefore, perception of a tactile *motion direction*) compared to the compared to the *control* condition (no button pressed). The differences between *tACS conditions*, *perceived motion direction* or *unambiguous start configuration* were not subjected to statistical analysis.

However, the experimental paradigm did not include a control condition with no motor response, which could be a confounding factor on pupil dilation of motor responses (Hupé et al., 2009). In conclusion, the results indicate that the increased dilation of the pupil time course may be indicative to the formation of a conscious tactile motion percept.

## 3.4.5. Pupil dilation predicts the following perceptual duration of a tactile percept within the *in-phase* condition

Furthermore, pupil dilation in the context of the respective *tACS condition* was investigated as a potential predictor variable for the subsequent duration of tactile perception. Therefore, the pupil amplitude modulations (de Gee et al., 2014; Kloostermann et al., 2015) were calculated subject wise and analyzed in terms of Spearman correlation coefficients for the distinctive *tACS conditions*.

Interestingly, a significant correlation between the amplitude modulation and the subsequent NPTs could be observed within the *in-phase tACS condition*. Nevertheless, a significant association in terms of Spearman correlations within the *sham* or *anti-phase tACS condition* could not be observed.

This finding may suggest a predictive value of the individual pupil amplitude modulation for the following NPTs for the *in-phase* condition. It should be noted that no statistically significant difference between pupil amplitude modulations regarding the different *tACS conditions* was observed. Nevertheless, regarding NPTs statistical differences between the *in-phase* and *anti-phase* condition were observed.

The fact that the significant correlation between amplitude modulation and NPTs could only be observed for the *in-phase tACS condition*, may imply a multifaceted interactional and modulatory effect between phase specific gamma *tACS* and neural networks involved in sensory and perceptual processing, as well as attentional processing concerning tactile ambiguous motion perception.

Regarding this investigation, the exact physiological mechanisms underpinning this predictive relationship remain speculative. Generally, it is believed that pupil dilation patterns are influenced by subcortical neuromodulatory systems, especially the locus coeruleus and its norepinephrine-related projections (de Gee et al., 2014; Kloostermann et al., 2015). One potential interpretation of the observed effects is that bihemispheric gamma *tACS* modulates cortical neuronal networks, resulting in complex interactions with subcortical neuromodulatory systems. These interactions may affect both the cognitive and perceptual processes in tactile ambiguous motion perception. Regarding the *in*-

*phase tACS* stimulation, cortical neuronal synchronization processes may interact with neuromodulatory systems to produce and stabilize a tactile motion percept.

#### 3.5. Conclusion

In summary, the experimental investigations on the tactile apparent motion quartet reveal complex and differentiated results regarding the effects of phase-specific, bihemispheric gamma tACS targeting somatosensory cortices. In general terms, the analyses of cumulated gamma distribution functions, as well as the RM-ANOVA of NPTs and button press rate, suggest that in-phase bihemispheric tACS stabilizes the perceptual formation of a motion pattern, irrespective of its direction. On the other hand, anti-phase bihemispheric tACS destabilizes the establishment and maintenance of tactile perceptual states. Nevertheless, the RM-ANOVA analyses did not establish a generalized effect in terms of the hypothesis of interhemispheric integration (Helfrich et al., 2014; Strüber et al., 2014; Rose et al., 2005). Two exceptions may indicate a phase-dependent impact of tACS on the perceived pattern of tactile motion direction. The investigation identified an exception in the sub-analyses of the RM-ANOVA regarding NPTs within the condition of perceiving a vertical-to-horizontal motion pattern: anti-phasic tACS decreases horizontal NPTs if the preceding percept was that of a vertical motion direction pattern. This finding suggests that anti-phase tACS my lead to reduced meaningful interhemispheric coupling, which in turn may be associated with decreased horizontal NPTs. The other exception pertains to the analyses of CDFs and their interactional effects. The pattern of significant results implies a phase specific tACS effect corresponding to the hypothesis of interhemispheric integration. For the interaction effect of tACS and perceived motion direction a significant phase-specific tACS effect was observed. In-phase tACS produced significantly longer percept durations for horizontal motion direction compared to anti-phase tACS. In contrast, no significant difference was observed between the in-phase tACS and anti-phase tACS conditions for the perceived vertical motion direction. This result suggests that in-phase tACS may increase meaningful interhemispheric coupling, which, in turn, may be associated with increased horizontal NPTs.

Nevertheless, previous publications regarding the visual SAM stimulus also discussed alternative hypothesis explaining the slight bias towards *vertical* motion perception. One possible explanation is our daily and routine experiences with gravity (Chaudhuri & Glaser, 1991). Frequent exposure to stimuli, that generate *vertical* trajectories on our sensory modalities may

establish a a priori "reference frame" for biased vertical motion perception during metastable stimuli (Chaudhuri & Glaser, 1991). Such perceptual biases may be formed via learning mechanisms (Chaudhuri & Glaser, 1991). Regarding the tactile SAM stimulus, previous experimental investigations revealed differentiated, in some parts counterintuitive and contradictory results (Liaci et al., 2016). Liaci et al. employed a similar tactile version of the SAM stimulus and revealed a bias towards vertical motion perception, whereas we observed a bias towards horizontal motion perception (between forearm motion) (Liaci et al., 2016). Furthermore, as an explanation of the differentiated results in the tactile modality, Liaci et al. speculated that tactile motion perception may necessitate alignment and integration of information from two "reference frames" (Liaci et al., 2016). They introduced the concept of a "somatotopic", "endogenous reference frame" as well as a "space-bases exogenous reference frame" (Liaci et al., 2016). Regarding the visual SAM stimulus, which solely involves the "exogenous reference frame", the bias towards vertical motion perception may be explained by the interhemispheric integration hypotheses and the vertical learning hypothesis (Liaci et al., 2016). Conversely, the tactile SAM stimulus on the other hand might operate in the domains of an "endogenous" and "exogenous reference frame" in order to form a coherent perception of an apparent motion direction. Moreover, the systems may require a mechanism to balance and adjust the information transmitted in these "reference frames" (Liaci et al., 2016). Inconsistent evidence from these different "reference frames" may cause variability in tactile motion perception as parameter ranges increase (Liaci et al., 2016). Subsequently, cognitive top-down modulations may influence the direction of perceived tactile motion (Liaci et al., 2016). Phase-specific bihemispheric gamma tACS may modulate the "endogenous" and "exogenous reference frames" in complex non-linear ways, resulting in intricate interactions in ambiguous tactile motion perception that could account for the diverse and heterogenous behavioral outcomes (Liaci et al., 2016). As a noteworthy phenomenon, the amplitude of pupil dilation steadily increases over a 5-second time period before peaking upon onset of the perception of a motion direction pattern. Notably, the modulation of pupil dilation amplitude is positively correlated and may thus have predictive value for the duration of the subsequent perceptual state (Einhäuser et al., 2008). However, this correlation pattern was only observed in the in-phase condition.

These findings indicate a potential interaction between global neuronal and cognitive and perceptual network states during multistable tactile apparent motion perception under the influence of *tACS*.

Overall, the effects of gamma *tACS* on tactile motion perception may be more complex than the predefined rudimental hypothesis predicts. Further investigations are required to determine the underlying mechanisms of the *tACS* effects on somatosensory perception and how they relate to the hypothesis of interhemispheric integration.

# 4. Modulation of *unambiguous* visuotactile apparent motion perception by *tACS*

#### 4.1. Introduction

This explorative, within subject designed, experiment aims to expand the understanding of *tACS* effects on unambiguous visuotactile apparent motion perception. The general approach of this experiment was to modulate unambiguous tactile apparent motion perception by applying frequency- and phase-specific sinusoidal *tACS* in a forced-choice visuotactile motion quartet paradigm.

#### 4.2. Materials and methods

#### 4.2.1. Participants

For this study twenty-one healthy subjects (n = 21, 10 males, 11 females, age range = 19-34 years, mean age = 25.5714 years, standard deviation = 3.7891) were recruited.

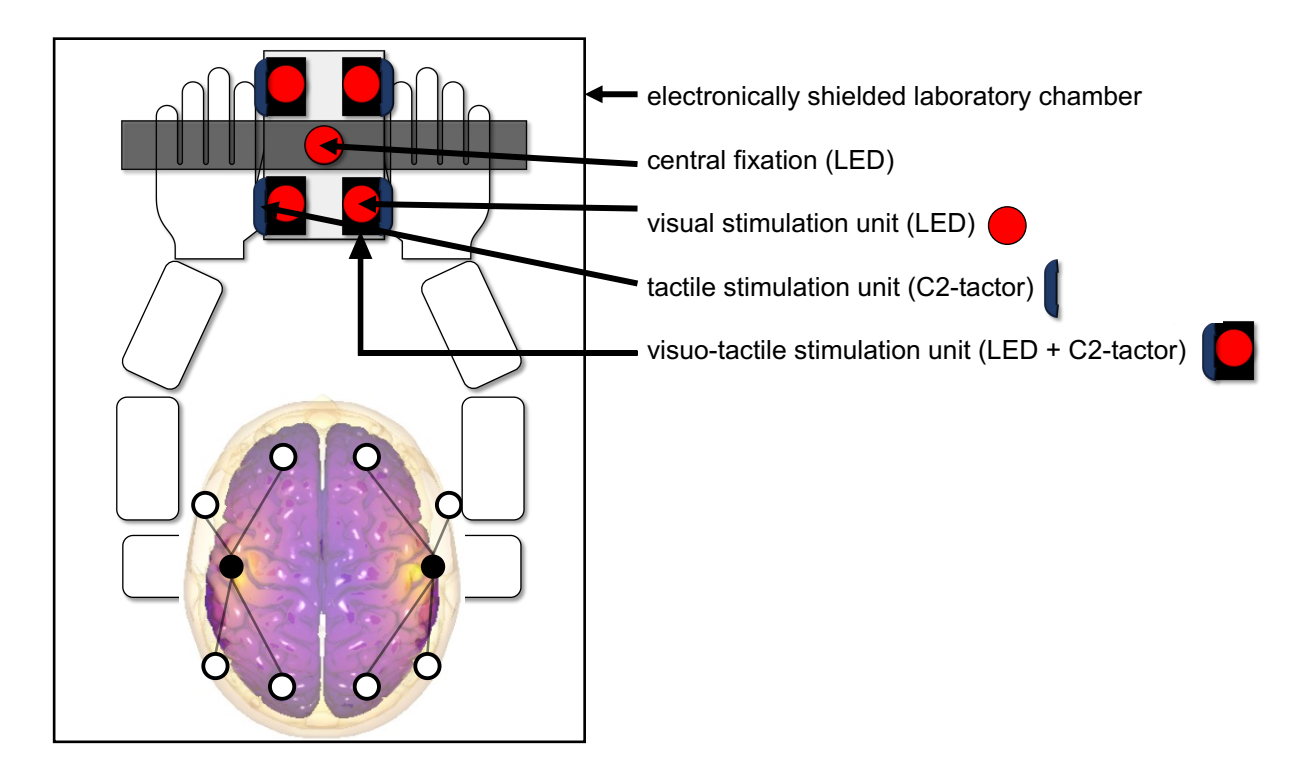
#### 4.2.2. Visuotactile stimuli

The general methods section contains a comprehensive description of the C-2 tactor stimulation units. Four C-2 tactors were attached perpendicularly to the *horizontal* plane within the frame of a rectangular cuboid. The visual stimulus consisted of four red light points (inner diameter of 2.8 mm, 0.03° visual angle), which were introduced in the experimental chamber by four fiber optic cables (inner diameter of 2.8 mm, 0.03°). Each fiber optic cable was threaded through pre-drilled holes through in one of the four adjustable cuboids. This stimulus setting allowed for colocalized multisensory stimulation of the visual and tactile modality in a spatially and temporally coupled manner. The visuotactile stimulation unit of the cuboid itself was mounted on an adjustable black plate, which was inclined at a 45° angle to the *horizontal* plane.

The cuboid units were positioned on the plate to form an imaginary rectangle. The *horizontal* distance of the stimuli was set to 7 cm (7.6° visual angle), and the *vertical* distance of the stimuli was set to 6 cm (6.4° visual angle). A stationary, white light point with an inner diameter of 2.8 mm (0.03° visual angle) was introduced and used as a fixational point for the participant, centrally located to the visuotactile apparent motion quartet.

Visual and tactile stimulus parameters, along with stimulus activation patterns, were controlled by a customized MATLAB (MATLAB, R2016b (9.1.0), The MathWorks Inc., Natick, MA, USA) script that was operated on a Microsoft computer, which was located outside the shielded chamber, where participants were seated.

Figure 39 – Schematic representation of the experimental design (visuotactile apparent motion perception)



Schematic representation of the experimental design for the unambiguous visuotactile apparent motion stimulus. Participants in the experiment were seated in an electronically shielded, light and sound attenuated laboratory room. The visuotactile stimulus unit consisted of C-2 tactors attached

with red LED lights and was positioned at fixed distances on a motion quartet grid in front of the participant.

## 4.2.3. Experimental paradigm of the unambiguous visuotactile apparent motion stimulus (Figure 41)

Participants were invited for two consecutive days with the aim of applying longer current stimulation times, as *tACS* was limited to 40 minutes per day for each subject.

Experimental conditions were randomized, while preserving the two specific *tACS conditions* (*in-phase* or *anti-phase* stimulation) in a block wise fashion.

Participants were seated comfortably in a chamber that was acoustically and visually insulated and electromagnetically shielded. This chamber was located in the laboratory area of the Department of Neurophysiology and Pathophysiology at the University Medical Center in Hamburg, Germany.

The visuotactile motion quartet was positioned on a table before the participants. The study participants were directed to position their hands on the outside edges of the visuo-tactile stimulation devices, leading to medial, proximal, and distal visuo-tactile stimulation locations for the index finger on both the right and left sides.

The multisensory apparent motion design allowed for bimodal stimulation in a temporally and spatially coupled manner.

Stimulation streams consisted of unambiguous visual and tactile apparent *motion direction* patterns, which were presented in the following *motion direction* conditions:

- 1. unimodal tactile horizontal motion
- 2. unimodal tactile vertical motion,
- 3. bimodal tactile incongruent horizontal motion,
- 4. bimodal tactile incongruent vertical motion,
- 5. bimodal tactile congruent horizontal motion, and
- 6. bimodal tactile congruent vertical motion.

One trial consisted of four stimulation frames, each containing visuotactile activation for 300 ms followed by an interstimulus interval of 200 ms. This resulted in 2 seconds of stimulus presentation in advance of an expected response for each trial. The total duration of the experiment was limited to 40 minutes, with the precise length dependent on the response latencies of each participant. After each

trial's sensory stimulus stream, participants were instructed to report their *perceived motion direction* pattern by activating one of two keys on a response device (Cedrus Response Pad, RB844, Cedrus Corporation, San Pedro, CA 90734, USA) with their right or left foot. The direction of the response pattern was counterbalanced across participants.

The right (respective left) button corresponds to a *horizontal* percept, whereas the left (respective right) button corresponds to a *vertical* percept.

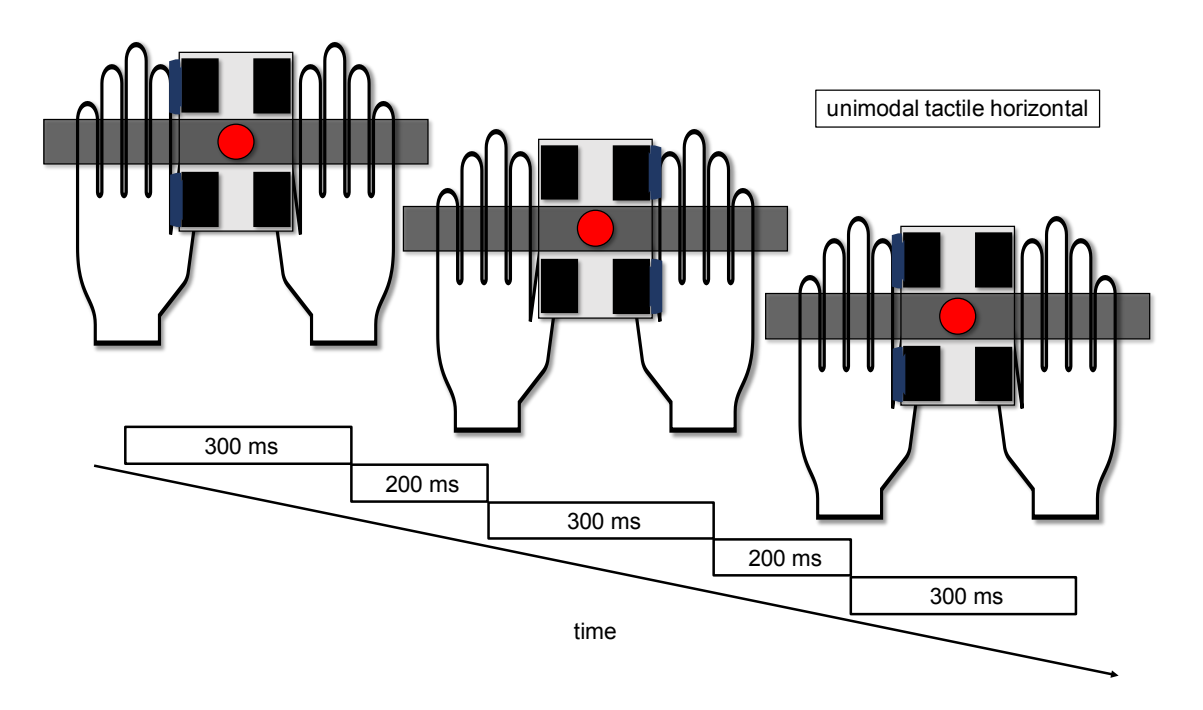
Subjects were explicitly instructed to report only their tactile percept as quickly and accurately as possible. The subsequent trial would commence only after participants indicated their choice via the response device (using a forced-choice experimental design).

In addition, participants were instructed to fixate on the introduced fixation point, which was centrally positioned between their hands throughout the entire duration of the study. Before commencing the experiment, participants received about ten minutes of training to familiarize themselves with the unambiguous visuotactile stimulus configurations. All participants were blinded with respect to the distinct non-invasive brain stimulation conditions and scientific hypotheses.

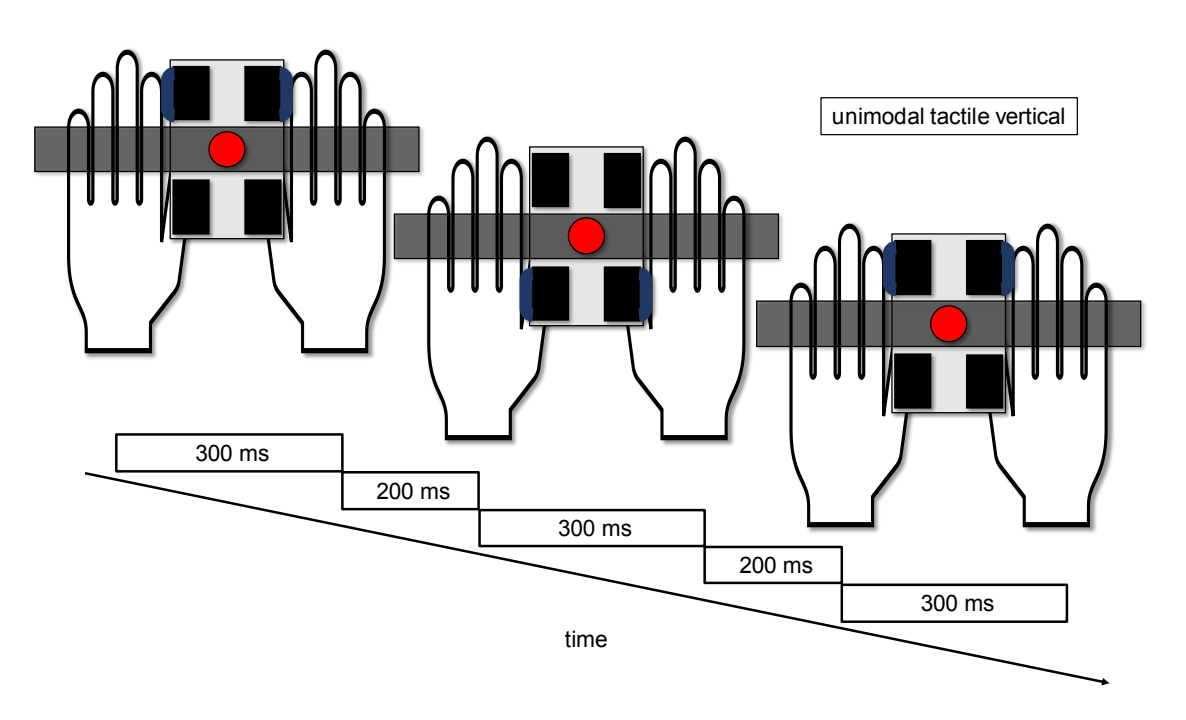
Figure 40 – Unambiguous visuotactile stimulus configuration

## (a.) – (b.) unimodal tactile conditions

### unimodal tactile horizontal

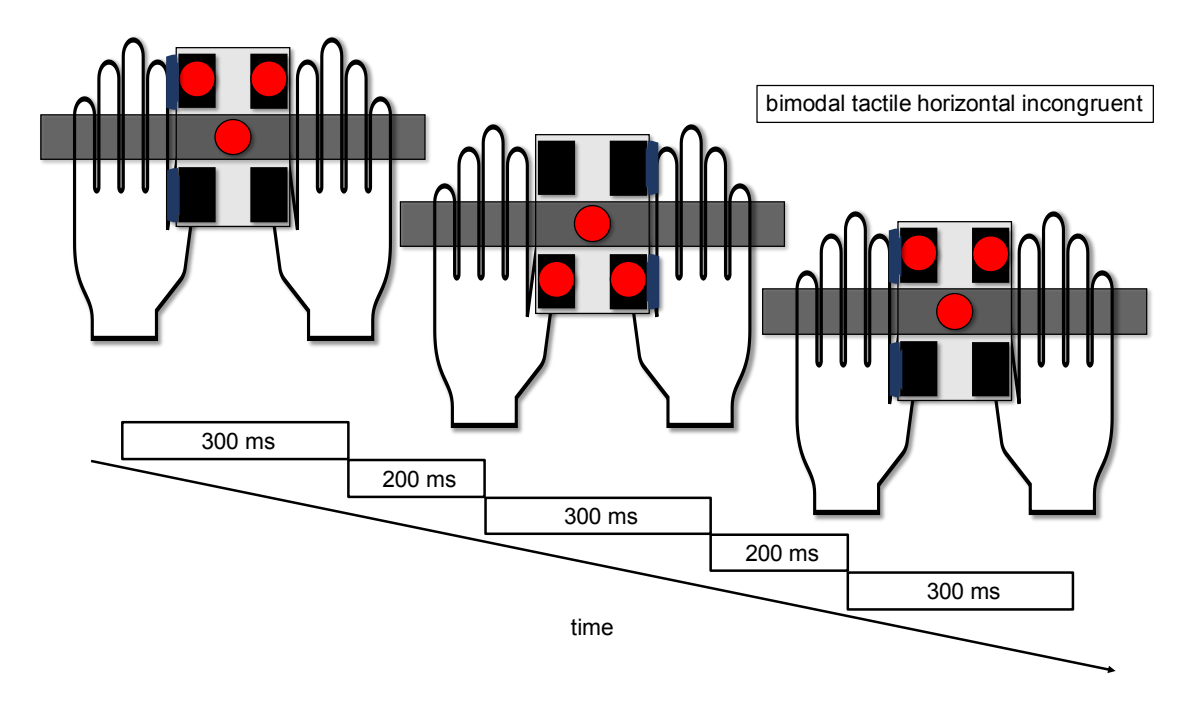


#### unimodal tactile vertical

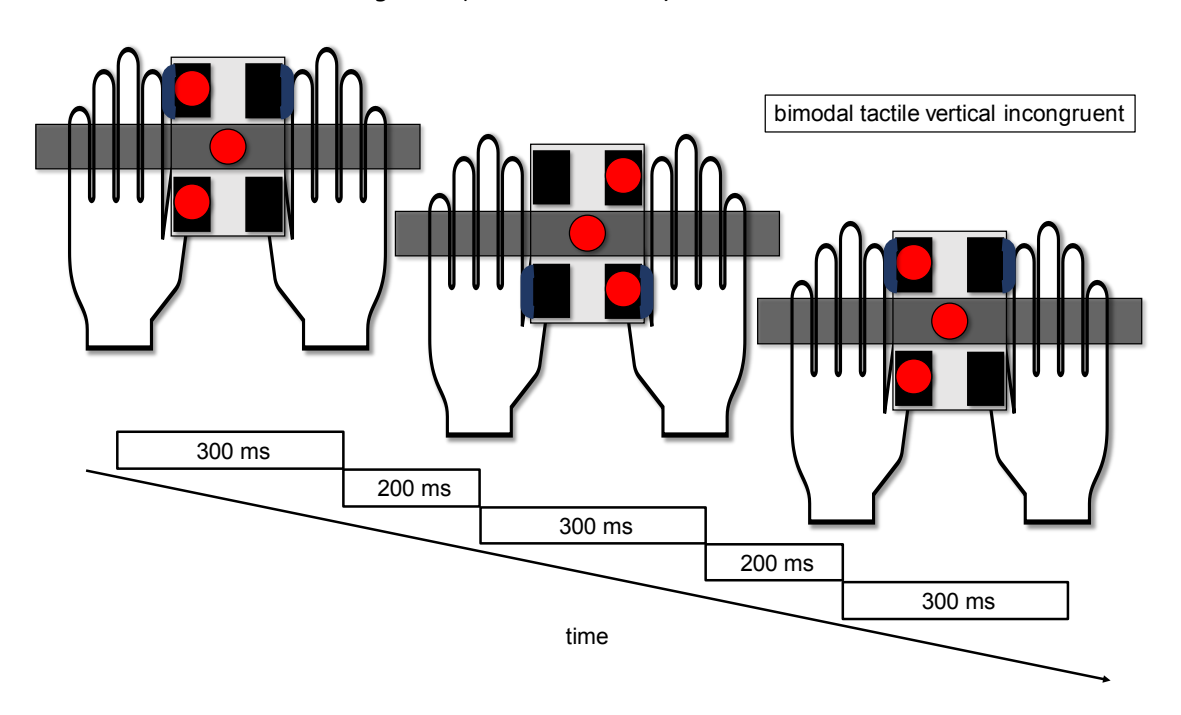


### (c.) – (d.) bimodal incongruent conditions

bimodal tactile horizontal incongruent (visual vertical) condition

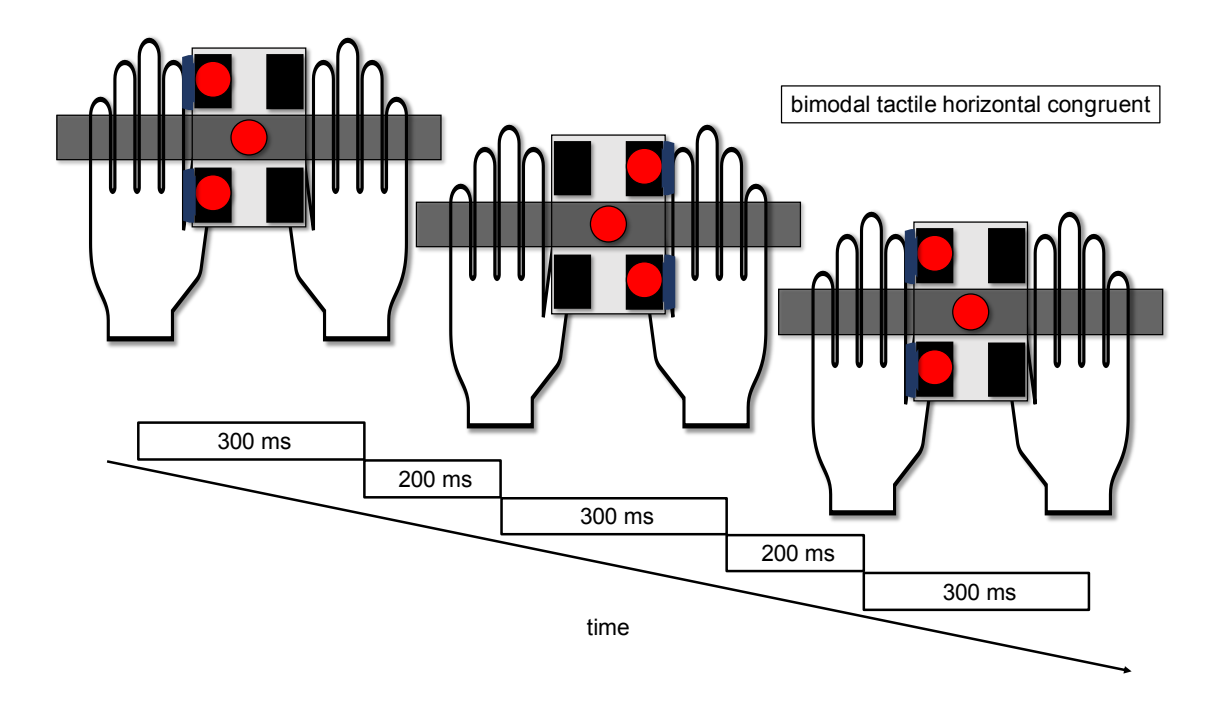


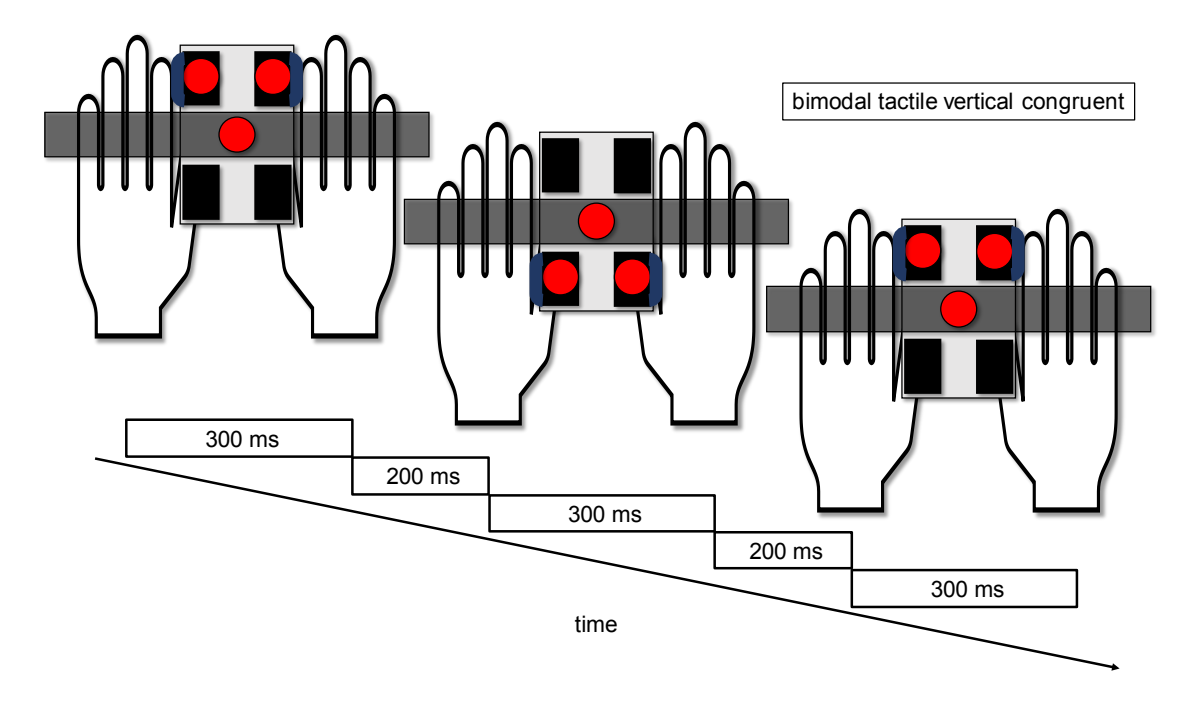
bimodal tactile vertical incongruent (visual horizontal) condition



(e.) – (f.) bimodal congruent conditions

bimodal tactile horizontal congruent (visual horizontal) condition





Experimental stimulus configurations were randomized, while preserving the two specific *tACS* conditions (in-phase or anti-phase stimulation) in a blockwise fashion. The multisensory apparent motion design allowed for bimodal stimulation of the proximal and distal index finger in a temporally and spatially coupled manner. Stimulation streams entailed unambiguous visual and tactile apparent motion direction patterns, which were presented in the eight following motion direction conditions: (a.) unimodal tactile horizontal motion, (b.) unimodal tactile vertical motion, (c.) bimodal tactile incongruent horizontal motion, (d.) bimodal tactile incongruent vertical motion, (e.) bimodal tactile congruent horizontal motion, and (f.) bimodal tactile congruent vertical motion.

One trial consisted of four stimulation frames, each containing (visuo)tactile activation for 300 ms followed by an interstimulus interval of 200 ms, resulting in a total of 2 seconds of (visuo)tactile stimulation.

#### 4.2.4. *TACS* protocol

While performing the unambiguous tactile apparent motion task, transcranial current stimulation was bilaterally applied by two accumulator powered stimulators (DC-Stimulator plus, NeuroConn, neuroCare Group GmbH, Munich, Germany). The current was continuously administered throughout

the entire experiment via ten Ag/AgCl electrodes (12 mm diameter, EASYCAP GmbH, Herrsching, Germany) in a 1-in-4 electrode configuration for each respective electrical stimulation site. The frequency and intensity of the alternating current stimulation was controlled by a customized MATLAB (MATLAB, R2016b (9.1.0), The MathWorks Inc., Natick, MA, USA) script on a Microsoft computer and adjusted to a frequency 40 Hz and an stimulation magnitude of 2 mA peak-to-peak.

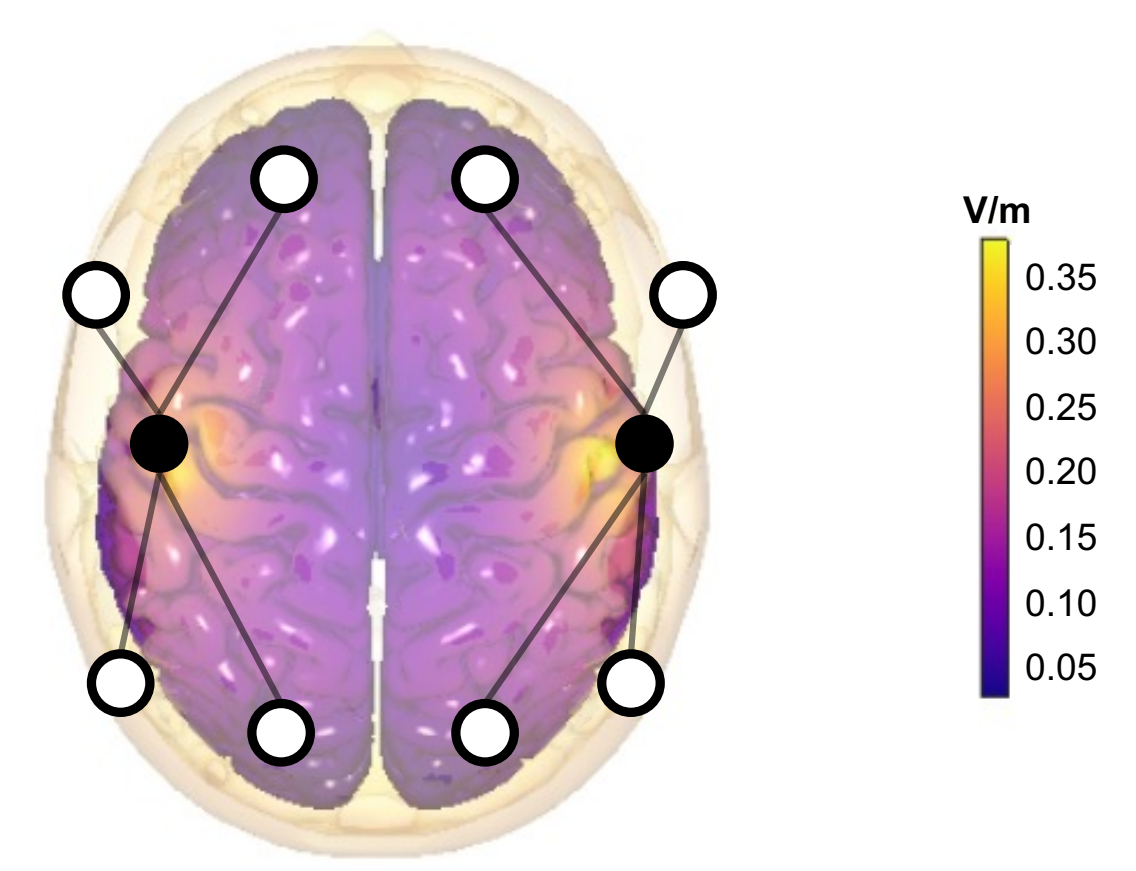
*TACS* was administered in a block wise experimental design, and the *tACS* conditions were preassigned and counterbalanced across and within participants.

At the beginning of the *in-phase* and *anti-phase tACS conditions*, the electrical stimulation intensity was increased sinusoidally (from 0 mA to the maximum of 2 mA intensity) for a ten-second-long segment, preceding the onset of the visuotactile stimulus in order to accustom participants to the electrical stimulation.

Prior to the non-invasive electrical stimulation, an electric field model was constructed, targeting the bihemispheric primary somatosensory cortex, ensuring that the chosen areas were within the trajectory of the propagating electrical field induced by *tACS* (refer to section 2.3) (Misselhorn et al., 2019).

Following the experiment, participants underwent a debriefing. None of the participants were able to discern between the two distinct *tACS conditions*.

Figure 41 – tACS setup (visuotactile apparent motion)



The experiment involved a two-sided, multi-electrode setup for bilateral *tACS*. The black and white dots represent stimulation electrodes at different polarities. The sinusoidal stimulation magnitude was adjusted to 2 mA peak-*to*-peak and a frequency of 40 Hz. An estimation of the maximum current intensities on the cortical surface was conducted (see section 2.3.). Subjects received bihemispheric *in-phase* and *anti-phase* alternating current stimulation, via two symmetrical adjusted 4-in-1 montages over somatosensory cortices.

The modeled cortical surface is color-coded to represent the simulated maximum field strength in plots per meter [V/m] (2 mA peak-to-peak).

Figure 42 – Electrical stimulation parameters – *anti-phase tACS condition* (visuotactile apparent motion)

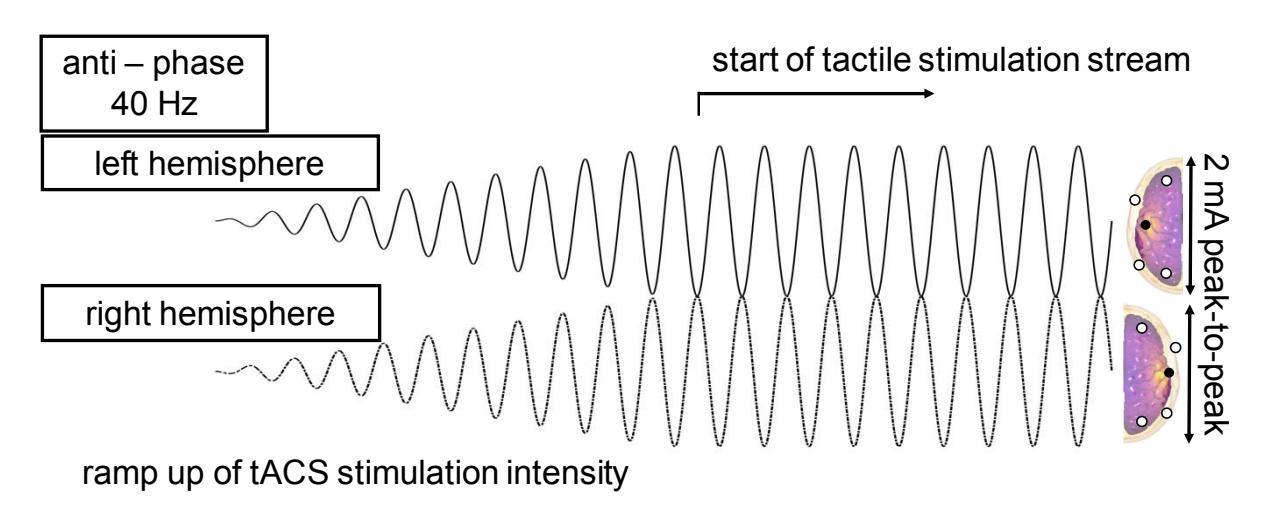
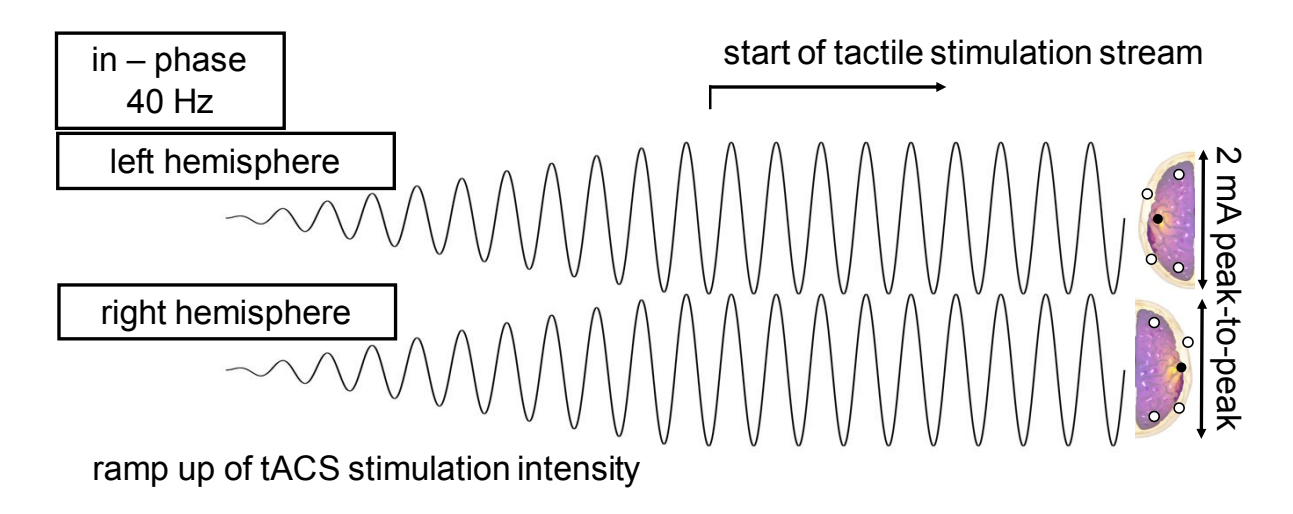


Figure 43 – Electrical stimulation parameters – *in-phase tACS condition* (visuotactile apparent motion)



Bilateral electrical stimulation was applied to participants while they performed the visuotactile apparent motion task. The electrical stimulation magnitude was adjusted to 2 mA peak-to-peak and a frequency of 40 Hz. The ramp up segment was fixed for 10 seconds before reaching maximum intensity, followed by the (visuo)tactile stimulation. It should be noted that a lower sinusoidal frequency was used in this figure for clarity.

#### 4.2.5. Hypothesis

Two distinct *tACS conditions* were defined as the independent variable under investigation: *in-phase* stimulation and *anti-phase* stimulation. The sequence of the two experimental conditions were randomly preassigned and balanced within and between participants. All participants were blinded with respect to the different non-invasive brain stimulation conditions and scientific hypotheses. In accordance with the hypotheses of interhemispheric integration, we hypothesize that the specific directional pattern of perceived *horizontal* and *vertical* tactile apparent motion is correlated with specific intra- and interhemispheric characteristic brain states. Moreover, the *tACS* design endeavors to modulate these neural brain states and the respective behavior in a causally and phase specific way. In concrete terms, we expected that *in-phase tACS* at 40 Hz would enhance the *horizontal* tactile percept, and that *anti-phase tACS* at 40 Hz would enhance the *vertical* tactile percept. This would be reflected in the respective accuracies, reaction times, and subsequent analyzed behavioral indices.

#### 4.3. Statistical analyses and results

Primary dependent variables examined in this experiment included accuracy (ACC), reaction time (RT), rate correct score (RCS), as well as Signal Detection Theory (SDT) parameters, including the sensitivity index d-prime (ď) and decision bias criterion (c). Statistical analyses were conducted using a RM-ANOVA design incorporating the factors of tACS stimulation (in-phase, anti-phase), motion direction (horizontal, vertical), and congruence (unimodal, incongruent, congruent). Additionally, post hoc contrasts were performed. The Greenhouse-Geisser correction was employed (when appropiate), and p-values along with degrees of freedom were adjusted using Bonferroni-correction. For further analyses, a non-parametric follow up analyses was conducted regarding only reaction times of correctly signified trials. Prior to the statistical analyses, an outlier analyses based on the intraindividual reaction time data was conducted. Therefore, trials with corresponding RTs above or below an absolute z-transformed reaction time value of 3 were excluded from further analysis for all dependent variables. In a following step, trials with an absolute RT value below 0.05 seconds (5 ms) and above 5 seconds (5000 ms) were excluded from further analyses. Overall, this approach excluded 4.8148 % of the dependent variables data for all trials. The submitted outlier analysis was performed independently for all predefined conditions.

Subsequently, the behavioral data of the dependent variables were concatenated subject wise for every respective condition.

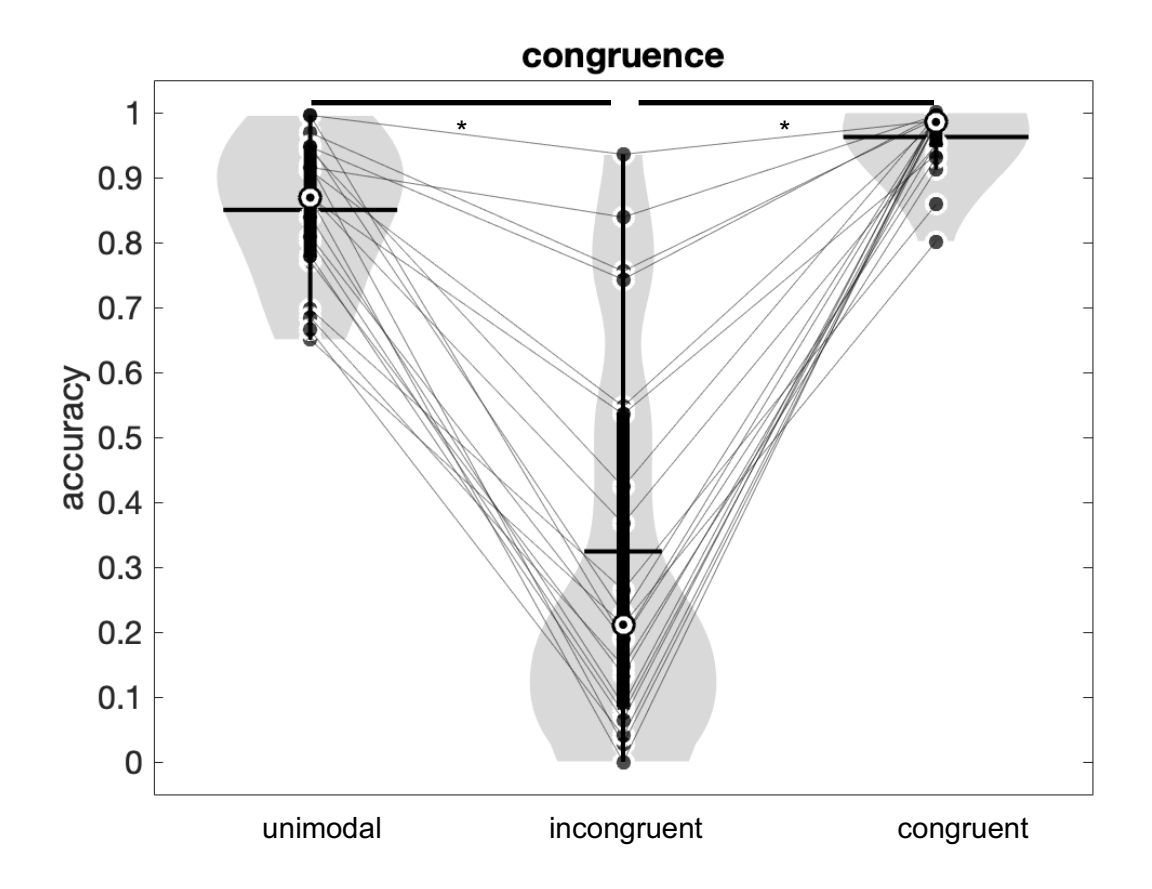
#### 4.3.1. Accuracies

Accuracies (ACC) were calculated on a subject wise basis for every condition separately and were defined as the proportion of correct responses given by the participant j including all trials in the respective condition i.

$$ACC_{i,j} = \frac{\sum_{k=1}^{n_{i,j}} absolute \ number \ of \ correct \ responses_{i,j}}{absoulte \ number \ of \ trials_{i,j}}$$

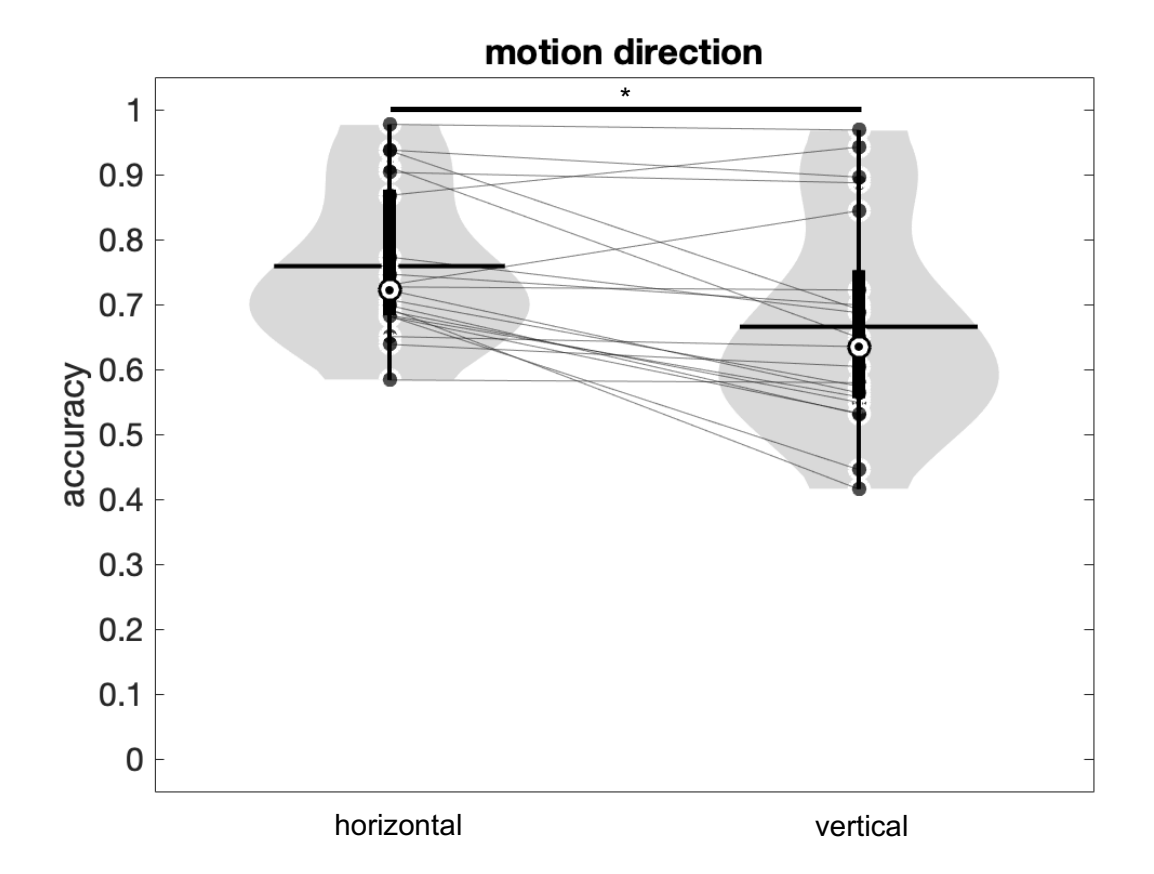
Participants were sufficiently trained in the task and contributed on average an accuracy rate of 0.7123 (71.23%) ( $\pm$  0.3519 standard deviation) across all trials and all conditions. For the dependent variable of *accuracy*, the RM-ANOVA (Table 24-25, Figure 45-48) revealed significant effects for the main factor of *congruence* (*Greenhouse-Geisser corrected*, F = 96.87, df = 1.113, p < 0.001,  $\eta^2 p = 0.829$ , n = 21), motion direction (F = 13.887, df = 1, p = 0.001,  $\eta^2 p = 0.410$ , n = 21) as well as a two-way significant interaction effect for *congruence* and *motion direction* (F = 15.438, df = 2.000, p < 0.001,  $\eta^2 p = 0.436$ , n = 21). All remaining effects, especially the hypothesized two-way interaction effect of *tACS* and *motion direction* (F = 0.506, df = 1, p = 0.485,  $\eta^2 p = 0.025$ , n = 21), did not reveal a significant effect (Table 24). The Bonferroni-corrected post hoc analyses for the factor *congruence* revealed a significant effect for the difference between the *unimodal* condition and the *incongruent* condition (t = 10.743,  $p_{bonf} < 0.001$ , *Cohen's* d = 2.510, n = 21) as well as the *incongruent* condition to the *congruent* condition (t = -13.037,  $p_{bonf} < 0.001$ , *Cohen's* d = -3.046, n = 21) (Table 26).

Figure 44 – Violin plot – 2x3x2 RM-ANOVA Accuracy (ACC) – post hoc comparisons of *congruence* (visuotactile apparent motion)



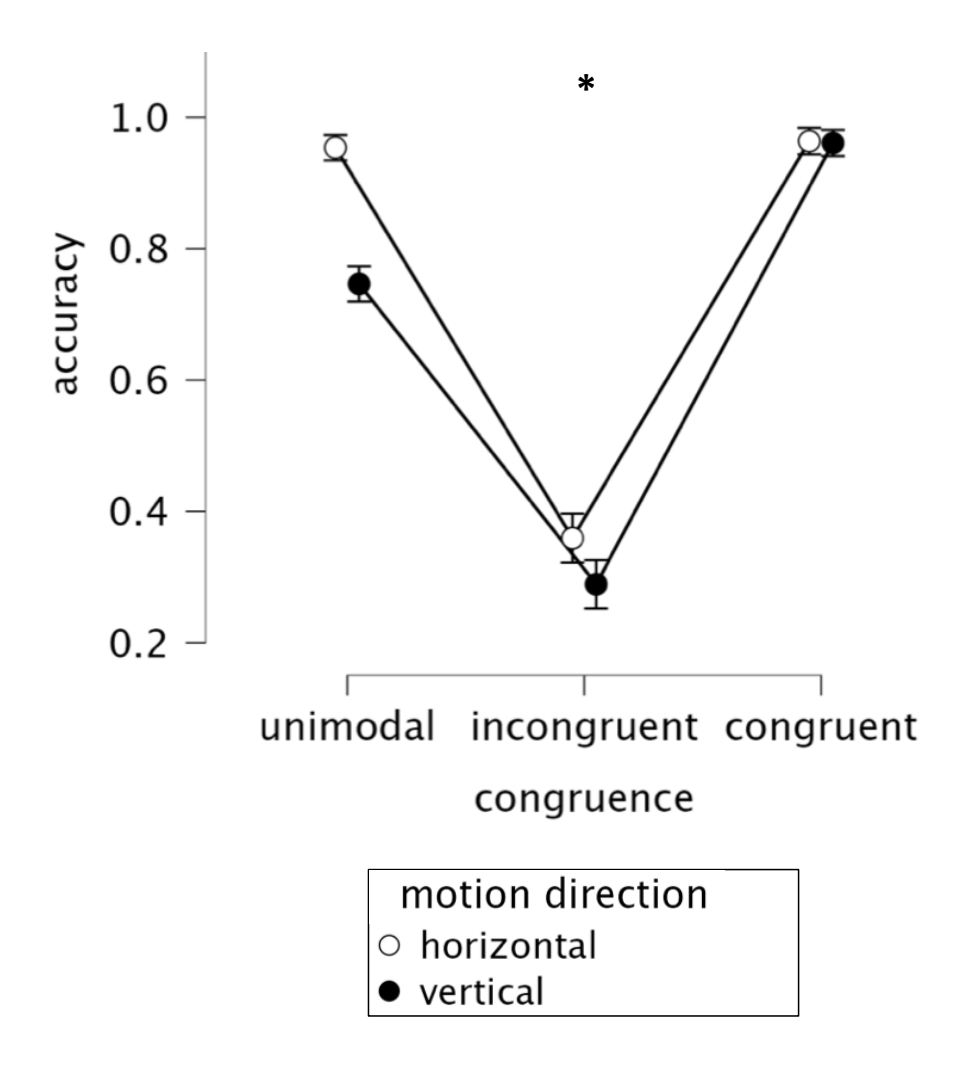
Effects of *Congruence* on accuracy. The effect of *congruence* produced significant results (p < 0.001). The post hoc analyses yielded highly significant increases in accuracy for the *congruent* condition (compared to the *incongruent* condition ( $p_{bonf} < 0.001$ )), and highly significant increases in accuracy for the *unimodal* condition (compared to the *incongruent* condition) ( $p_{bonf} < 0.001$ ) (Table 26). Interestingly, in the *incongruent* condition, several subjects achieved a mean accuracy rate below the chance level of < 0.5. Each subject in the respective condition is represented by black dots. The solid black *horizontal* lines show the mean value for each condition, while the circular white marker with the inner black dot indicates the median value. *Note.* results are averaged over the levels of *tACS* and *motion direction*.

Figure 45 – Violin plot – 2x3x2 RM-ANOVA Accuracy (ACC) – *motion direction* (visuotactile apparent motion)



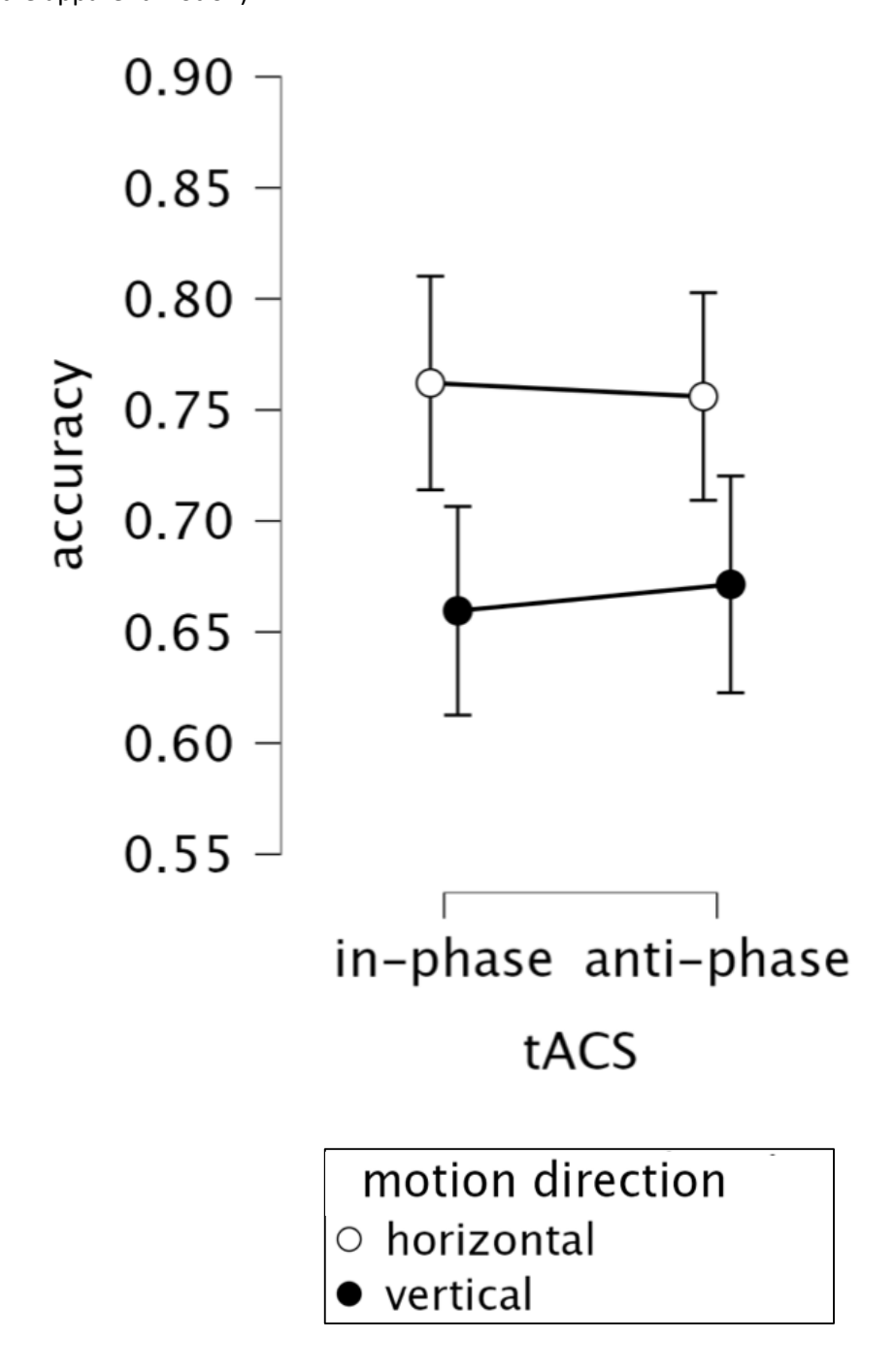
Effects of motion direction on accuracy. The main factor of motion direction revealed significant higher accuracies for the horizontal motion direction compared to the vertical motion direction (p < 0.001) (Table 24). Black dots represent each subject in the respective condition. The solid black horizontal lines indicate the mean value for the respective condition, the circular white marker with the inner black dot indicates the median value for the respective condition. Note. Results are averaged over the levels of tACS and congruence.

Figure 46 – Line plot – 2x3x2 RM-ANOVA Accuracy (ACC) – Interaction of *congruence* and *motion direction* (visuotactile apparent motion)



Interaction effect between *congruence* and *motion direction*. The RM-ANOVA revealed a significant interaction effect between *congruence* and *motion direction* on accuracy (p < 0.001) (Table 24). Error bars indicate the standard error of means. The filled black dots indicate the mean values across participants for the *vertical motion direction*, whereas the white dots indicate the mean values across participants for the *horizontal motion direction*. *Note*. Results are averaged over the levels of *tACS*.

Figure 47 – Line plot – 2x3x2 RM-ANOVA Accuracy (ACC) – Interaction of *tACS* and *motion direction* (visuotactile apparent motion)



Interaction effect between tACS and motion direction. The RM-ANOVA did not reveal a significant interaction effect between tACS stimulation condition and motion direction (p = 0.485) (Table 24). Error bars indicate the standard error of means. The filled black dots indicate the mean values across participants for the vertical motion direction, whereas the white dots indicate the mean values across participants for the vertical motion direction. vertical vertica

#### 4.3.1.1. Overview of results – accuracy

The proportion of correct responses across all trials was used to calculate the accuracy of each participant and condition. The mean accuracy achieved by participants was 71%. The analysis yielded significant main effects of congruence and motion direction, as well as a significant interaction between congruence and motion direction. Post hoc comparisons revealed that accuracy was significantly higher in the *congruent* condition than in the *incongruent* condition, and also higher in the *unimodal* condition than in the *incongruent* condition. It is noteworthy that some participants in the *incongruent* condition demonstrated accuracy levels below the chance level. With regard to motion direction, horizontal motion resulted in significantly higher accuracy compared to vertical motion. However, the hypothesized interaction between phase-specific tACS stimulation and motion direction was not significant, indicating no notable influence of tACS on performance accuracy. These findings highlight the importance of stimulus congruence and motion direction in shaping performance accuracy. The superior accuracy in *congruent* and *unimodal* conditions suggests that perceptual alignment between stimuli facilitates task performance, while incongruence introduces a perceptual conflict. The horizontal motion advantage may reflect inherent differences in how horizontal and vertical motion are processed. The lack of tACS effects on accuracy indicates that, in this context, tACS does not appear to modulate participants' ability to make correct responses.

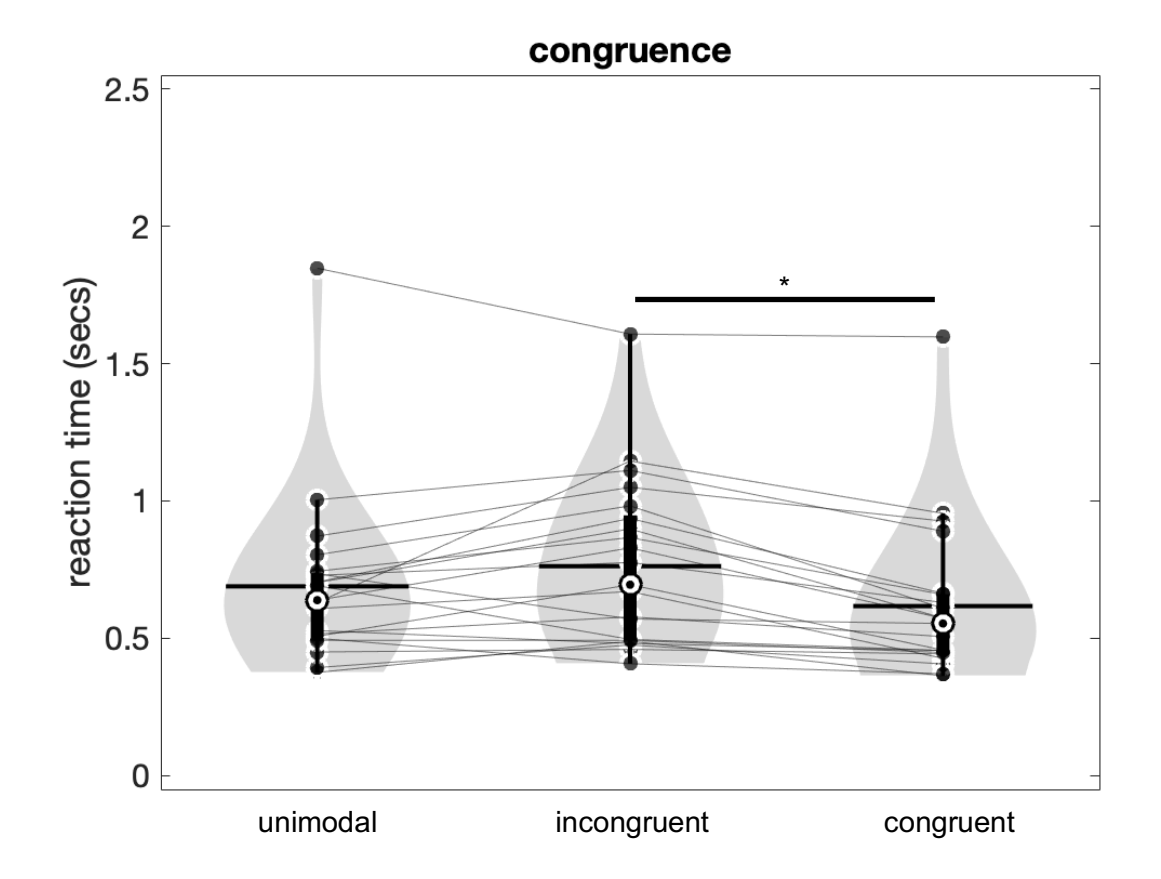
#### 4.3.2. Reaction times

In accordance with the RM-ANOVA for accuracies, mean reaction time (RT) data were congregated subject wise for every condition separately encompassing all trials in the respective condition. This method resulted in a RM-ANOVA design incorporating the factors of *tACS Stimulation (in-phase, anti-phase), motion direction (horizontal, vertical)*, and *congruence (unimodal, incongruent, congruent)*.

The mean reaction time for all subjects and all conditions was 0.7123 seconds (± 0.3519 standard deviation).

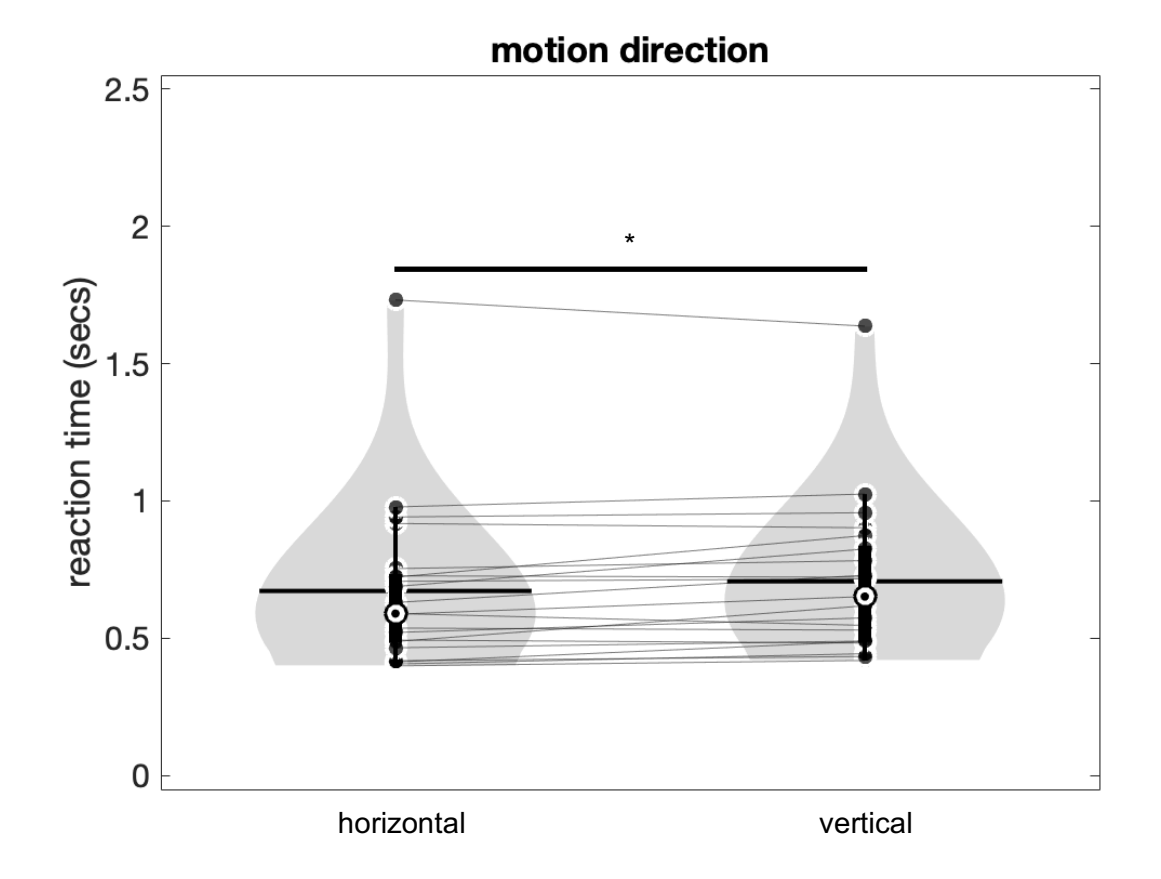
The results of the RM-ANOVA (Table 27-28, Figure 49-52) indicated significant effects regarding the dependent variable of reaction times. Significant effects encompassed the main factor of *congruence* (Greenhouse-Geisser corrected, F = 11.855, df = 1.570, p < 0.001,  $\eta^2 p = 0.372$ , n = 21), motion direction (F = 6.969, df = 1, p < 0.016,  $\eta^2 p = 0.258$ , n = 21) as well as a two-way significant interaction effect for congruence and motion direction (Greenhouse-Geisser corrected, F = 4.106, df = 1.443, p = 0.039,  $\eta^2 p = 0.170$ , n = 21). All remaining effects, especially the hypothesized two-way interaction effect of *tACS* and motion direction, did not reach significance (F = 1.046, df = 1, p < 0.319,  $\eta^2 p = 0.025$ , n = 21) (Table 27). The Bonferroni-corrected post hoc analyses for the factor *congruence* revealed a significant difference between the *incongruent* condition and *congruent* condition (t = 4.869,  $p_{bonf} < 0.001$ , t = 0.432, t = 0.4

Figure 48 – Violin plot – 2x3x2 RM-ANOVA Rection times (RT) – post hoc comparisons of *congruence* (visuotactile apparent motion)



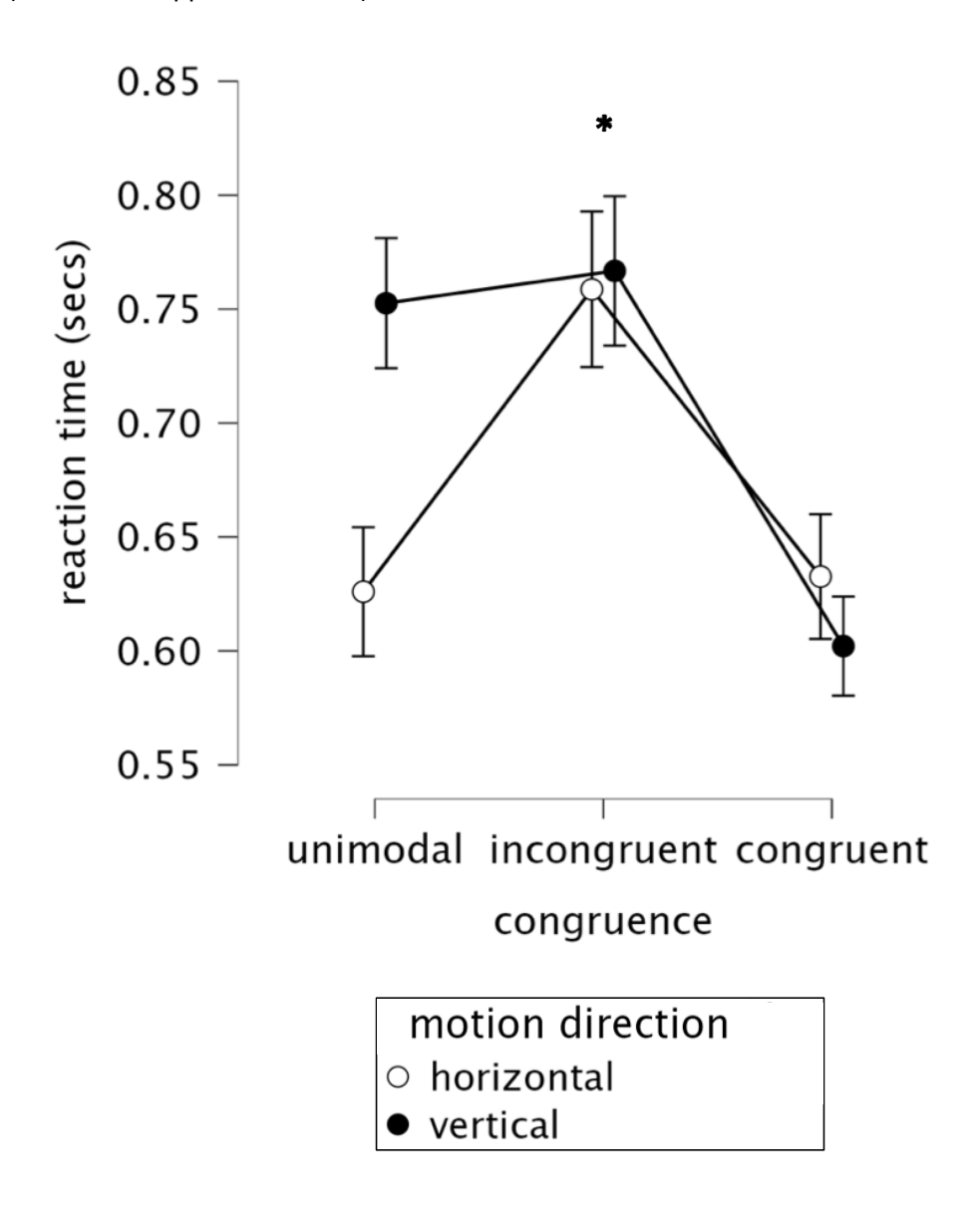
Effects of *congruence* on reaction time. The main factor of *congruence* revealed a highly significant (p < 0.001) effect. Post hoc analyses resulted in highly significantly ( $p_{bonf} < 0.001$ ) lower reaction times for the *congruent* condition compared to the *incongruent* condition (Table 29). Black dots represent each subject in the respective condition. The solid black *horizontal* lines indicate the mean value for the respective condition, the circular white marker with the inner black dot indicates the median value for the respective condition. *Note*. Results are averaged over the levels of *tACS* and *motion direction*.

Figure 49 – Violin plot – 2x3x2 RM-ANOVA Reaction times (RT) – *motion direction* (visuotactile apparent motion)



Effects of *motion direction* on reaction time. The main factor of *motion direction* revealed significant lower reaction times for the *horizontal motion direction* compared to the *vertical motion direction* (*p* = 0.016). Black dots represent each subject in the respective condition. The solid black *horizontal* lines indicate the mean value for the respective condition, the circular white marker with the inner black dot indicates the median value for the respective condition. *Note*. Results are averaged over the levels of *tACS* and *congruence*.

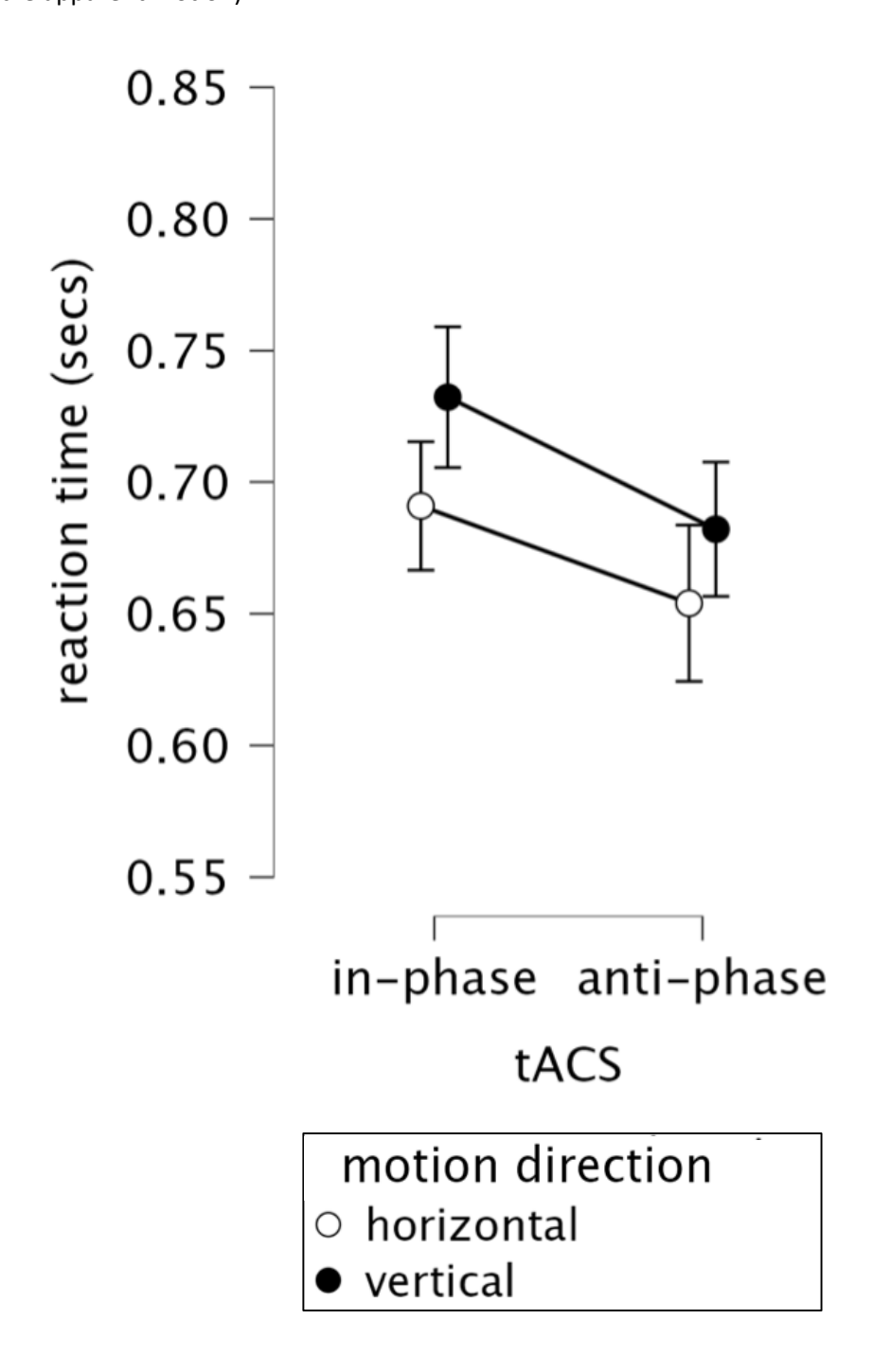
Figure 50 – Line plot – 2x3x2 RM-ANOVA Reaction times (RT) – Interaction of *congruence* and *motion direction* (visuotactile apparent motion)



Interaction effect between *congruence* and *motion direction*. The RM-ANOVA revealed a significant interaction effect between *congruence* and *motion direction* on reaction time (p = 0.039). Error bars indicate the standard error of means. The filled black dots indicate the mean values across participants

for the *vertical motion direction*, whereas the white dots indicate the mean values across participants for the *horizontal motion direction*. *Note*. Results are averaged over the levels of *tACS*.

Figure 51 – Line plot – 2x3x2 RM-ANOVA Reaction times (RT) – Interaction of *tACS* and *motion direction* (visuotactile apparent motion)



Interaction effect between *tACS* and *motion direction*. The RM-ANOVA did not reveal a significant interaction effect between *tACS* stimulation condition (*in-phase*, *anti-phase*) and *motion direction* (*horizontal*, *vertical*). Error bars indicate the standard error of means. The filled black dots indicate the mean values across participants for the *vertical motion direction*, whereas the white dots indicate the mean values across participants for the *horizontal motion direction*. *Note*. Results are averaged over the levels of *congruence*.

### 4.3.2.1. Overview of results – reaction times

The analysis of reaction times revealed significant effects of *congruence* and *motion direction*, as well as an interaction between these two factors. The results demonstrated that reaction times were significantly faster in the *congruent* condition compared to the *incongruent* condition, indicating that stimuli that are aligned or match facilitate quicker responses. Furthermore, reaction times were found to be faster when the *motion direction* was *horizontal* than when it was *vertical*, which suggests that *horizontal motion* may be processed more efficiently. However, the interaction between *tACS* stimulation and *motion direction* did not yield significant effects, indicating that *tACS* did not exert an influence on reaction times across conditions.

These findings indicate that reaction times are predominantly influenced by the *congruence* of stimuli and the direction of *motion*, rather than by *tACS stimulation*. The faster responses in *congruent* conditions provide support for the notion that perceptual alignment facilitates behavioral performance (Soto-Faraco et al., 2004). The observed advantage of *horizontal motion* may be attributed to underlying differences in the perception and processing of *horizontal* and *vertical motion*. The lack of *tACS* effects indicates that, while *tACS* may affect other aspects of perception or cognition, it does not markedly influence reaction time in this task.

#### 4.3.3. Rate Correct Score

In neuroscientific investigations, it is typical to instruct participants to respond as rapidly as possible without compromising the accuracy of the response. This principle is acknowledged in the concept of the speed-accuracy trade-off (Liesefeld & Janczyk, 2018). This conception describes the tendency for decision speed (reaction time) to covary with the accuracy of the response (Liesefeld & Janczyk, 2018). In concrete terms, the speed-accuracy tradeoff model describes the relationship between reaction

speed and accuracy while processing a task (Liesefeld & Janczyk, 2018). In many experimental designs, accuracy increases at lower speed and decreases at higher speed (Liesefeld & Janczyk, 2018). The speed-accuracy tradeoff can vary across experiments, participants, and conditions (Liesefeld & Janczyk, 2018).

One consequence of the participants' behavior could be that experiment results may emerge in an unforeseen behavioral pattern through reaction times (RTs) or accuracy rates (Liesefeld & Janczyk, 2018). Possible more challenging issues could arise from effects that are not genuine, possibly due to variations in the speed-accuracy tradeoff (Liesefeld & Janczyk, 2018). Solutions to this problem have been elaborated in combining RTs with accuracies (Liesefeld & Janczyk, 2018).

In the further analyses, we utilized the rate correct score (RCS) (Liesefeld & Janczyk, 2018; Woltz & Was, 2006). The RCS relates the absolute number of correct responses (NC) of participant i in condition j to summed RTs of participant i in condition j as:

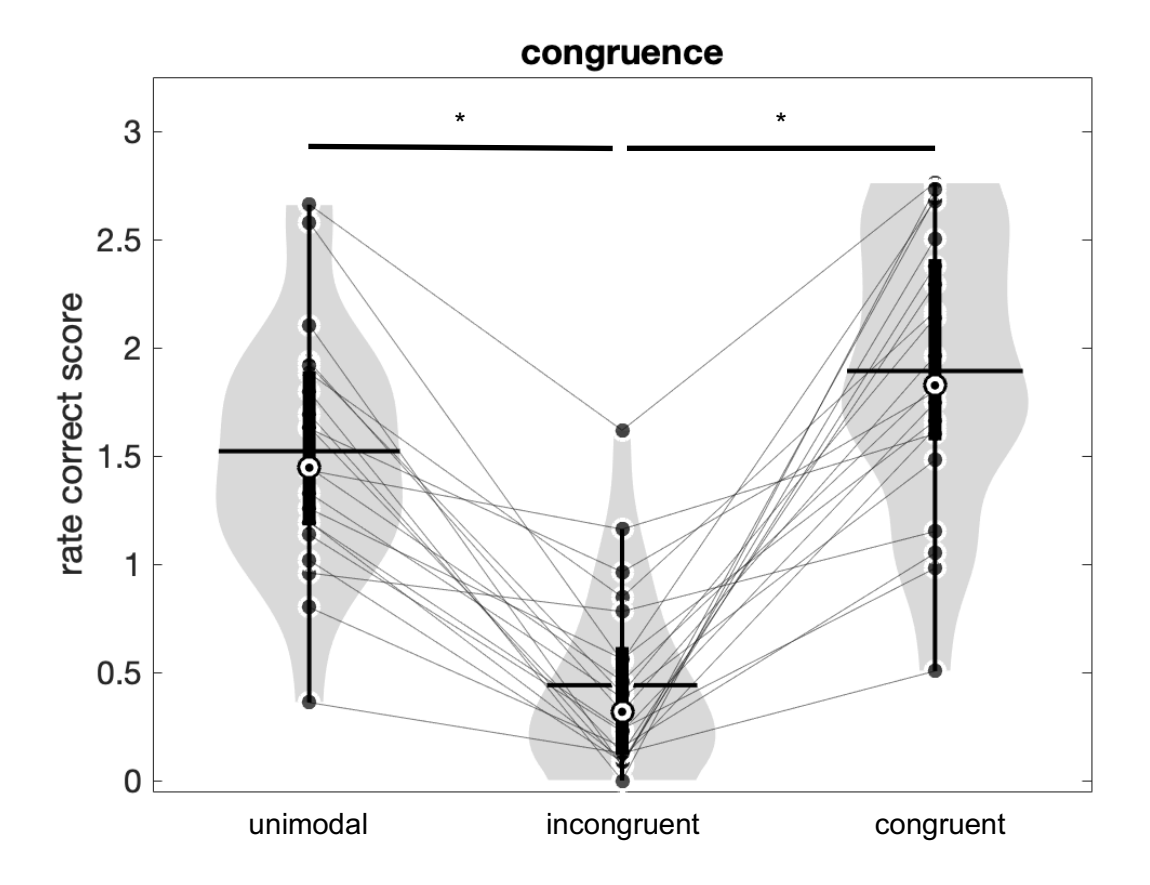
$$RCS_{i,j} = \frac{{}^{NC_{i,j}}}{\sum_{k=1}^{n_{i,j}} {}^{RT}_{i,j,k}}$$
 (Woltz & Was, 2006).

According to Woltz & Was, the RCS "can be interpreted directly as number of correct responses per unit time" (Woltz & Was, 2006). The mean RCS values across all participants and all conditions was 1.2848 ( $\pm$  0.9261 standard deviation). In accordance with previous statistical analyses, a 3x2x2 RM-ANOVA (Table 30-31, Figure 53-56) model with the factors of *tACS Stimulation (in-phase, anti-phase), motion direction (horizontal, vertical)*, and *congruence (unimodal, incongruent, congruent)* was utilized to evaluate for statistical effects of the RCS. The RM-ANOVA revealed significant effects for the main factor of *congruence (Greenhouse-Geisser corrected, F = 74.329, df = 1.302, p < 0.001, \eta^2 p = 0.788, n = 21),* and *motion direction (F = 14.368, df = 1, p = 0.001, \eta^2 p = 0.418, n = 21),* as well as a two-way significant interaction effect for *congruence* and *motion direction (F = 13.461, df = 2.000, p < 0.001, \eta^2 p = 0.402, n = 21). All remaining effects, especially the hypothesized two-way interaction effect of <i>tACS* and *motion direction (F = 0.019, df = 1, p = 0.891, \eta^2 p = 9.654 \times 10^4, n = 21),* did not reveal a significant effect (Table 30).

The Bonferroni-corrected post hoc analyses for the factor *congruence* revealed a significant effect for the difference between the *unimodal* condition and the *incongruent* condition (t = 8.737,  $p_{bonf} < 0.001$ , *Cohen's* d = 1.598, n = 21), between the *unimodal* condition and the *congruent* condition (t = -2.996,

 $p_{bonf} = 0.014$ , Cohen's d = -0.548, n = 21), as well as between the *incongruent* condition and the congruent condition (t = -11.733,  $p_{bonf} < 0.001$ , Cohen's d = -2.147, n = 21) (Table 32).

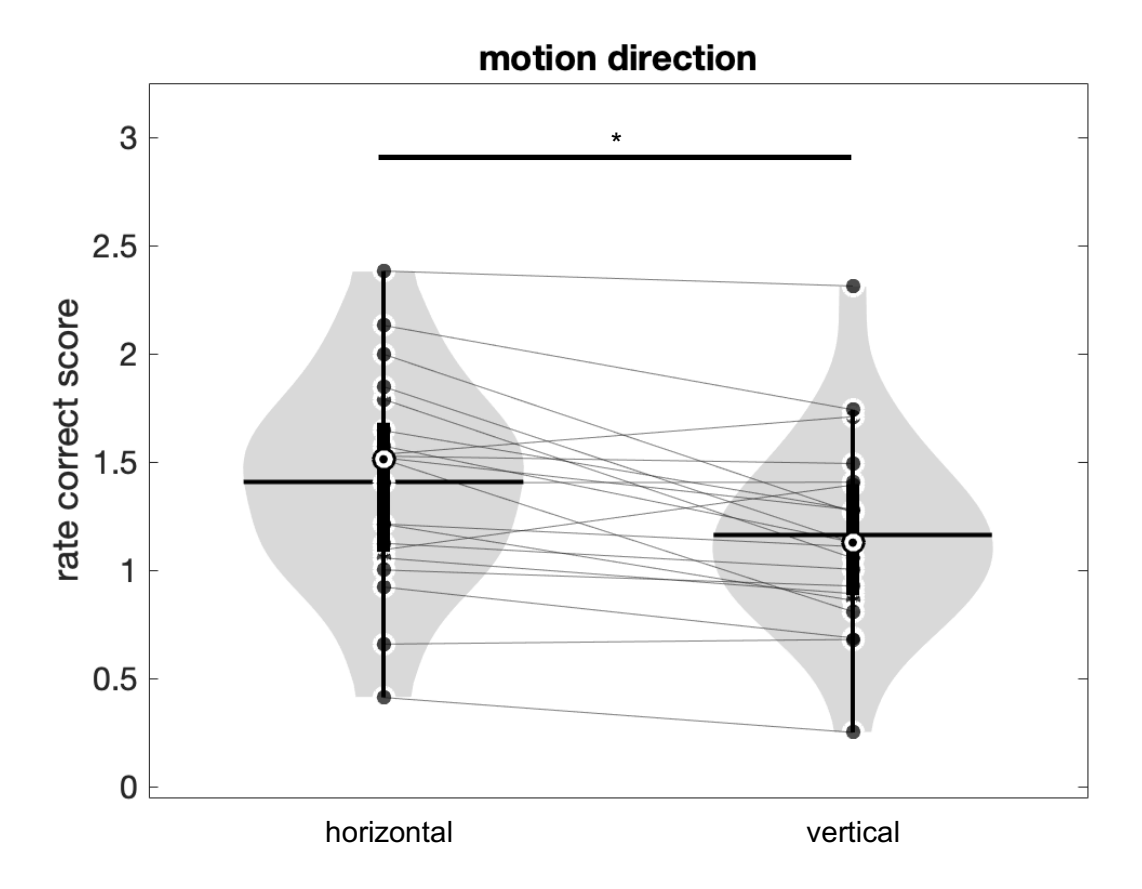
Figure 52 – Violin plot – 3x2x2 RM-ANOVA Rate Correct Score (RCS) – post hoc comparisons of *congruence* (visuotactile apparent motion)



Effects of *congruence* on Rate Correct Score (RCS). The main factor of *congruence* revealed a highly significant (p < 0.001) effect. Post hoc analyses resulted in significantly ( $p_{bonf} < 0.001$ ) higher accuracies for the *congruent* condition compared to the *incongruent* condition, as well as a significant higher RCS for the *unimodal* condition compared to the *incongruent* condition ( $p_{bonf} < 0.001$ ) and significant higher RCS for the *congruent* condition compared to the *unimodal* condition ( $p_{bonf} = 0.014$ ) (Table 32). Black dots represent each subject in the respective condition. The solid black *horizontal* lines indicate the mean value for the respective condition, the circular white marker with the inner black dot indicates

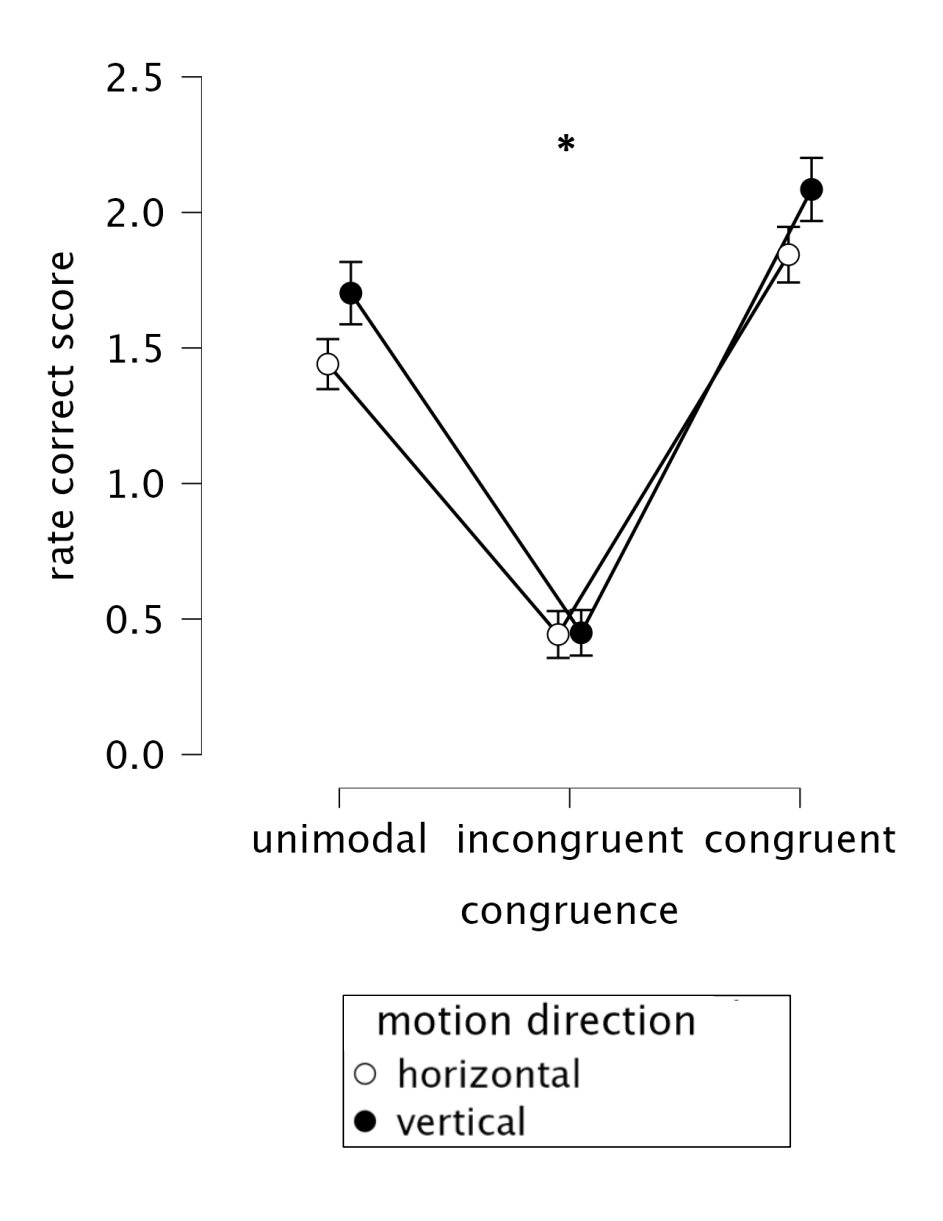
the median value for the respective condition. *Note.* Results are averaged over the levels of *tACS* and *motion direction*.

Figure 53 – Violin plot – 2x3x2 RM-ANOVA Rate Correct Score (RCS) – *motion direction* (visuotactile apparent motion)



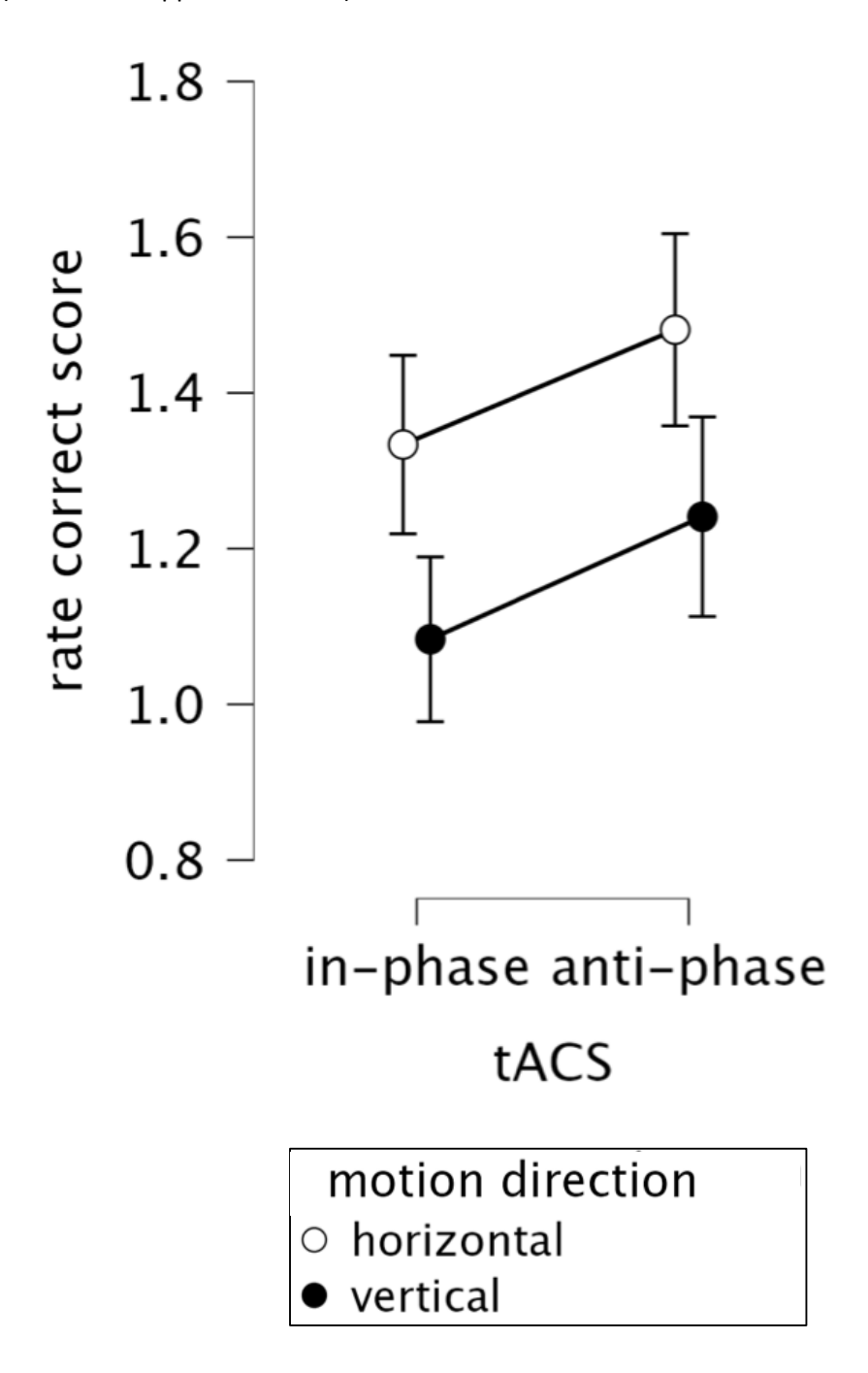
Effects of *motion direction* on rate correct score (RCS). The main factor of *motion direction* revealed significant higher RCS for the *horizontal motion direction* compared to the *vertical motion direction* (*p* = 0.001). Black dots represent each subject in the respective condition. The solid black *horizontal* lines indicate the mean value for the respective condition, the circular white marker with the inner black dot indicates the median value for the respective condition. *Note*. Results are averaged over the levels of *tACS* and *congruence*.

Figure 54 – Line plot – 2x3x2 RM-ANOVA Rate Correct Score (RCS) – Interaction of *congruence* and *motion direction* (visuotactile apparent motion)



Interaction effect of *congruence* and *motion direction*. The RM-ANOVA revealed a significant interaction effect of *congruence* and *motion direction* on RCS (p < 0.001). Error bars indicate the standard error of means. The filled black dots indicate the mean values across participants for the *vertical motion direction*, whereas the white dots indicate the mean values across participants for the *horizontal motion direction*. *Note*. Results are averaged over the levels of *tACS*.

Figure 55 – Line plot – 2x3x2 RM-ANOVA Rate Correct Score (RCS) – Interaction of *tACS* and *motion direction* (visuotactile apparent motion)



Interaction effect of *tACS* and *motion direction* for RCS. The RM-ANOVA did not reveal a significant interaction effect between *tACS* stimulation condition (*in-phase*, *anti-phase*) and *motion direction* (*horizontal*, *vertical*). Error bars indicate the standard error of means. The filled black dots indicate the mean values across participants for the *vertical motion direction*, whereas the white dots indicate the mean values across participants for the *horizontal motion direction*. *Note*. Results are averaged over the levels of *congruence*.

### 4.3.3.1. Overview of results – rate correct score

The analysis of the rate correct score (RCS) (Woltz & Was, 2006), a combined measure of accuracy and reaction time, revealed significant effects of *congruence* and *motion direction*, as well as their interaction. The results demonstrated that the *congruent* condition exhibited higher RCS values compared to the *incongruent* condition. Additionally, the *unimodal* condition demonstrated superior performance compared to the *incongruent* condition. This indicates that colocalized stimuli not only improve accuracy but also facilitate more rapid correct responses. Moreover, the *horizontal motion* direction yielded higher RCS values than the *vertical motion* direction, indicating superior performance for the former. Nevertheless, no significant interaction between *tACS* stimulation and *motion direction* was identified, indicating that tACS did not impact RCSs. These findings underscore the pivotal role of stimulus *congruence* and *motion direction* in optimizing performance. It can be posited that *congruent* and *unimodal* stimuli reduce the cognitive processing demands placed upon the subject, thereby facilitating faster and more accurate responses. The observed advantage of *horizontal motion*. The absence of *tACS* effects on RCS indicates that *tACS* does not affect the RCSs in the context of this experiment.

### 4.3.4. Signal Detection Theory parameters: sensitivity (d') and bias (c)

Furthermore, the behavioral data was analyzed in the context of Signal Detection Theory (SDT). SDT is a method that is found to be useful to assess sensitivity and bias in decision making processes (Macmillan & Creelman, 2004; Anderson, 2015). Originally the theory was advanced by radar researchers (Anderson, 2015). In the further course cognitive neuroscience transferred the principles of SDT hypotheses to decision-making processes (Anderson, 2015; Macmillan & Creelman, 2004). SDT can be incorporated into any decision-making processes involving a binary decision circumstance

(Anderson, 2015; Macmillan & Creelman, 2004). It allows for evaluating quantitative analyses of perceptional processes in human and animals (Anderson, 2015). The universal hypothesis of SDT posits that decisions are based within a framework of uncertainty (Anderson, 2015). The decision maker's objective is to filter out the background noise or interference from the actual target signal. In this context, the underlying response behavior in experimental contexts can be categorized into a fourfield matrix of hits, misses, false alarms, and correct rejections (Anderson, 2015; Macmillan & Creelman, 2004). A correct identification of a target signal is referred to as a hit (in medical terms: sensitivity) (Anderson, 2015; Macmillan & Creelman, 2004). On the other hand, a miss indicates that the target signal was not recognized (Anderson, 2015; Macmillan & Creelman, 2004). False alarms indicates that the background noise was mistakenly recognized by the decision maker as a target signal (Anderson, 2015; Macmillan & Creelman, 2004). Finally, correctly recognizing background noise as such is termed as a correct rejection (in medical terms: specificity) (Anderson, 2015; Macmillan & Creelman, 2004). The stimulus response matrix for a decision task produces independent measures resulting from the SDT framework (Anderson, 2015; Macmillan & Creelman, 2004). In the SDT context, sensitivity is defined as the relative difference between the mean of the signal distribution and the noise distribution, assuming they follow a normal gaussian distribution (Anderson, 2015; Macmillan & Creelman, 2004). This specific distance between the mean of the signal and noise distribution is usually denoted as d' (d prime) (Anderson, 2015; Macmillan & Creelman, 2004). Furthermore, the second relevant parameter of SDT framework is the individual strategy of the decision maker. Based on the individual (possible biased) decision threshold (also termed decision boundary), the decision maker may tend to give generally more positive or negative responses relative to an "ideal" observer (Anderson, 2015; Macmillan & Creelman, 2004). The decision boundary is termed criterion c and is defined by the distance of the decision boundary of the decision maker from the boundary of the "ideal" observer (Macmillan & Creelman, 2004). SDT implies that the sensitivity measure d' and the decision boundary criterion c in decision-making processes can be expressed as a normalized function of hit and false alarm rates (Macmillan & Creelman, 2004). Based on these assumptions, the following formula for calculating the relevant parameters from experimental data can be obtained as (Macmillan & Creelman, 2004):

sensitivity:  $d' = z(hit) - z(false\ alarm)$ 

criterion: 
$$c = -\frac{1}{2}x [z(hit) + z(false alarm)]$$

Where z(hit) or z(false alarm) corresponds to the inverse of the standard normal cumulative distribution function (CDF), evaluated at the probability values of hit or false alarm (Macmillan & Creelman, 2004). Regarding the parameter of d', a high value implies more proficient ability to discriminate between target signal and background noise (Macmillan & Creelman, 2004). For the individual decision boundary, a criterion of c = 0 corresponds to an ideal unbiased observer (Macmillan & Creelman, 2004). A criterion of c < 0 would suggest a tendency towards a liberal decision-making process, whereas a criterion of c > 0 implies a tendency towards a conservative decision-making process (Macmillan & Creelman, 2004). Advantageous of SDT is that it provides independent measures decision bias in unitless sensitivity and а measure (Anderson, 2015). In the framework of STD, the underlying response behavior of the unambiguous bimodal experiment can be classified into a four-field panel as (see Table 33):

Hit: tactile horizontal motion indicated while tactile horizontal stimulus configuration present.

Miss: tactile vertical motion indicated while tactile horizontal motion configuration presented.

False Alarm: tactile horizontal motion indicated while tactile vertical motion configuration presented.

Correct Rejection: tactile vertical motion indicated while tactile vertical motion configuration presented.

Table 1 – Signal Detection Theory – classification of response behavior

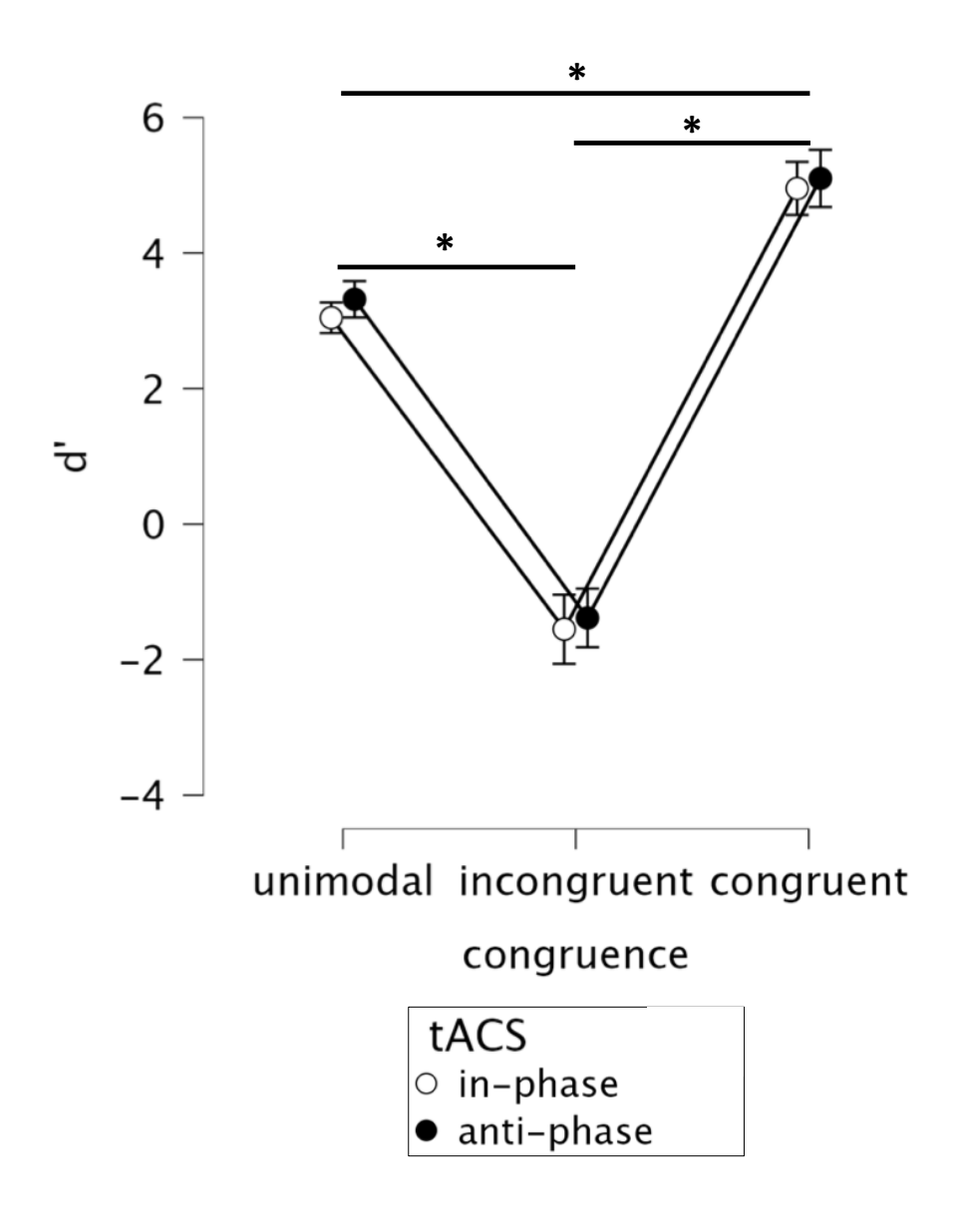
Objective tactile	Perceptual process:				
stimulus configuration	perceived motion by participant				
	Horizontal	Vertical			
Horizontal	Hit	Miss			
Vertical	False Alarm	Correct Rejection			

MATLABs norminv function was used to calculate and derive d' and c from the behavioral data (MATLAB, R2016b (9.1.0), The MathWorks Inc., Natick, MA, USA). In the circumstance of hit values or false alarm values of exactly 0 or 1, we implemented the correction by adjusting the extreme values (Stanislaw & Todorov, 1999). This commonly used correction method replaces the value of 0 with (0.5 / n), where n represents the absolute number of signal or noise trials (Stanislaw & Todorov, 1999). Furthermore, exact values of 1 are replaced with (n-0.5)/n, where n represents the number of signal or noise trials (Stanislaw & Todorov, 1999). In light of the hypothesis of interhemispheric integration, specific hypotheses in the context of signal detection parameters regarding the investigated stimulus configurations and experimental conditions have been formulated. Within the particular context of the stimulus configurations investigated, it is theorized that in-phase tACS could enhance sensitivity indices (d') relative to anti-phase tACS. Nevertheless, as the sensitivity index (d') is conceptualized as a parameter of discriminatory ability, phase specific nuanced tACS effects may not be reflected in the sensitivity index (d'). This is because anti-phase tACS is believed to also enhance correct rejection rates, ultimately leading to decreased false alarm rates. As a result, decreased false alarm rates subsequently produce elevated sensitivity scores (d'). Furthermore, in-phase tACS is believed to decrease the decision boundary (criterion c) compared to anti-phase tACS. The decrease indicates a perceptual inclination to perceive horizontal motion within the particular framework of SDT and the specific experimental conditions. Conversely, an increase in the decision boundary (criterion c) would imply a reduced bias towards horizontal motion perception. It should be highlighted that, the parameters of d' and criterion (c) are conceptualized as independent measures within the framework of SDT.

### 4.3.4.1. Sensitivity index d'

Statistical analyses were conducted to examine the sensitivity index d', utilizing a 2x3 RM-ANOVA design which incorporated the factors of tACS Stimulation (in-phase, anti-phase) and congruence (unimodal, incongruent, congruent). The mean d' scores across all participants and all conditions was 2.2479 ( $\pm$  3.4685 standard deviation). The RM-ANOVA (Table 34-35, Figure 57) indicated significant effects for the main factor of congruence (Greenhouse-Geisser corrected, F = 78.912, df = 1.182, p < 0.001,  $\eta^2p = 0.798$ , n = 21). All remaining effects did not reveal a significant difference (Table 34). The Bonferroni-corrected post hoc analyses for the factor congruence revealed a significant effect for the difference between the unimodal condition and the incongruent condition (t = 8.723,  $p_{bonf} < 0.001$ , Cohen's d = 2.150, n = 21), as well as between the incongruent condition and congruent condition (t = -12.191,  $p_{bonf} < 0.001$ , Cohen's d = -3.004, n = 21), and between the unimodal condition and congruent condition (t = -3.468,  $p_{bonf} = 0.004$ , Cohen's d = -0.855, n = 21) (Table 36).

Figure 56 – Line plot – 2x3 RM-ANOVA sensitivity d' – Interaction of *congruence* and *tACS* (visuotactile apparent motion)



Effects of *congruence* on sensitivity (d', sensitivity index). The main factor of *congruence* revealed a highly significant (p < 0.001) effect. Post hoc analyses resulted in significantly ( $p_{bonf} < 0.001$ ) higher sensitivity (d') for the *congruent* condition compared to the *incongruent* condition, as well as a significant higher sensitivity (d') for the *unimodal* condition compared to the *incongruent* condition

 $(p_{bonf} < 0.001)$  and significant higher sensitivity (d') for the *congruent* condition compared to the *unimodal* condition  $(p_{bonf} = 0.004)$ . The RM-ANOVA did not reveal a significant interaction effect of *congruence* and *tACS*. Error bars represent the standard error of means. The filled black dots represent the mean values across participants for the *anti-phase tACS stimulation*, whereas the white dots represent the mean values across participants for the *in-phase tACS stimulation*.

### 4.3.4.2. Overview of results (sensitivity index d')

The analysis of the sensitivity index (d'), a measure of a participant's ability to distinguish signal from noise independent of response bias, revealed significant effects of stimulus *congruence*. The highest level of sensitivity was observed in the *congruent* condition, followed by the *unimodal* condition, and the lowest level was observed in the *incongruent* condition. This suggests that *congruent* visuotactile stimuli facilitate enhanced discrimination abilities relative to *incongruent* or *unimodal* stimuli. It is noteworthy that the *congruent* condition demonstrated superior performance compared to the *unimodal* condition, indicating that multisensory integration enhances perceptual sensitivity when stimuli are aligned across modalities. Nevertheless, no significant interaction between *tACS* stimulation and stimulus *congruence* was observed, suggesting that *tACS* did not affect participants' sensitivity. These findings underscore the significance of stimulus *congruence* in enhancing perceptual sensitivity. It is probable that *congruent* stimuli facilitate more efficient sensory processing by reducing ambiguity and increasing coherence across modalities (Soto-Faraco & Väljamäe, 2012). The absence of *tACS* effects indicates that *tACS*, at least under the conditions tested, may not modulate the neural mechanisms underlying sensitivity to *congruent* and *incongruent* stimuli.

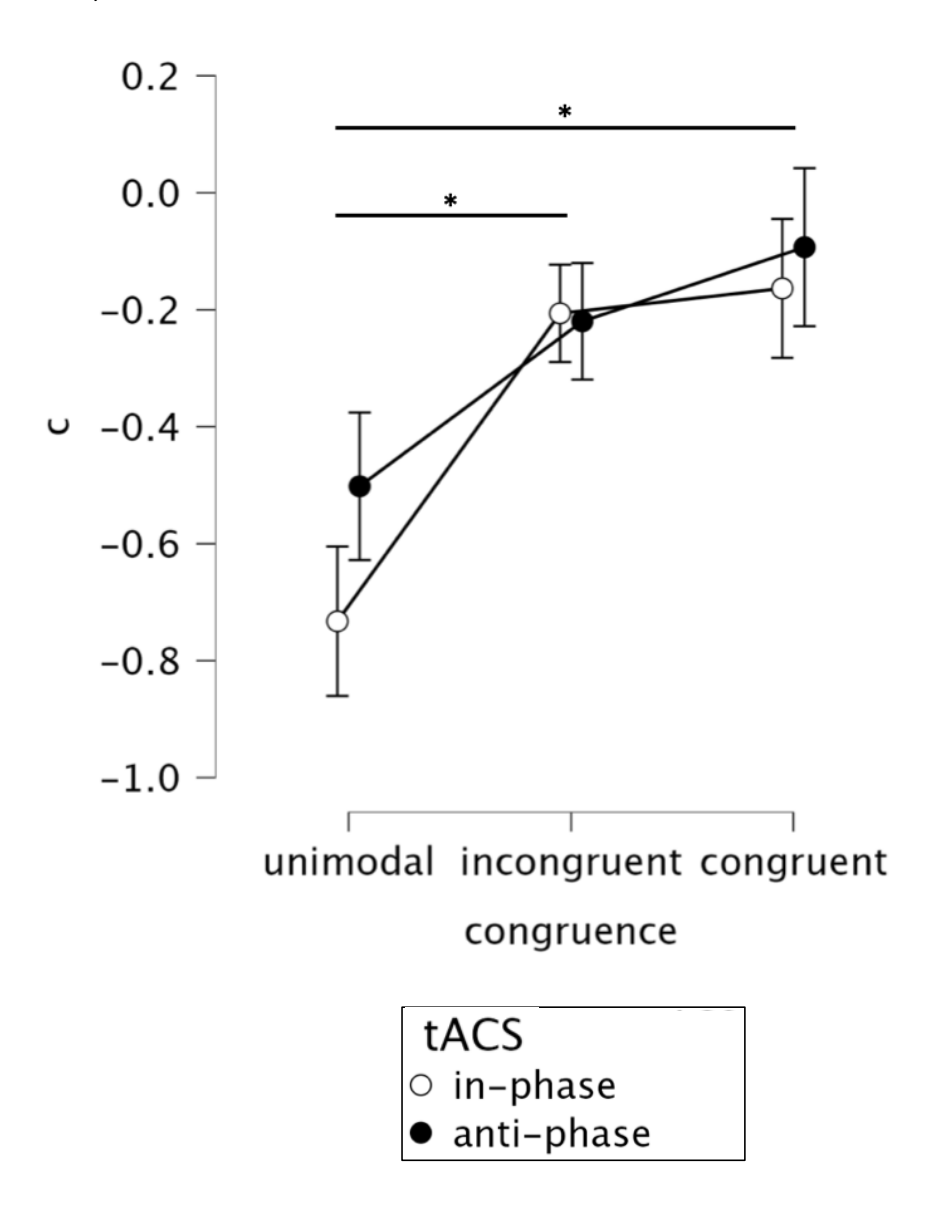
### 4.3.4.3. Criterion c

Statistical analyses were conducted to examine the criterion variable c utilizing a 2x3 RM-ANOVA (Table 37-38, Figure 58) design which entailed the factors of *tACS stimulation (in-phase, anti-phase)* and *congruence (unimodal, incongruent, congruent)*. Notably, the analysis identified significant effects for the main factor of *congruence (F = 7.828, df = 2, p = 0.001, \eta^2 p = 0.281, n = 21)*. However, all remaining effects did not demonstrate any significant differences (Table 37, Figure 58).

The Bonferroni-corrected post hoc analyses for the factor *congruence* revealed a significant effect on the difference between the *unimodal* condition and the *incongruent* condition (t = -3.061,  $p_{bonf} = 0.012$ ,

Cohen's d = -0.640, n = 21), as well as the difference between the *unimodal* condition and the *congruent* condition  $(t = -3.702, p_{bonf} = 0.002 Cohen's d = -0.775, n = 21)$  (Table 39).

Figure 57 – Line plot – 2x3 RM-ANOVA criterion c – Interaction of *congruence* and *tACS* (visuotactile apparent motion)



Effects of *congruence* on criterion c (bias parameter). The main factor of *congruence* revealed a highly significant (p < 0.001) effect. Post hoc analyses resulted in in a significantly lower criterion for the

unimodal condition compared to the *incongruent* condition ( $p_{bonf} = 0.012$ ) and significantly lower criterion for the *unimodal* condition compared to the *congruent* condition ( $p_{bonf} = 0.002$ ). The RM-ANOVA did not reveal a significant interaction effect of *congruence* and *tACS*. The standard error of means is indicated by the error bars. The filled black dots represent the mean values across participants for the *anti-phase tACS stimulation*, whereas the white dots represent the mean values across participants for the *in-phase tACS stimulation*.

### 4.3.4.4. Overview of results – response bias c

The analysis of the response bias criterion (c), which indicates a participant's tendency to favor one type of response over another, revealed a significant effect of stimulus *congruence*. In the *unimodal* condition, participants exhibited a negative bias in comparison to both the *incongruent* and *congruent* conditions, indicating a heightened propensity to respond as if a signal (in this case *horizontal motion*) was present despite uncertainty. Nevertheless, no significant interaction between *tACS* stimulation and *congruence* was identified, indicating that *tACS* did not exert an influence on response bias. These findings indicate that stimulus *congruence* is a pivotal factor in influencing decision-making tendencies. The negative bias towards the *horizontal motion* direction observed in the *unimodal* condition may be attributed to the absence of cross-modal contextual cues. The absence of *tACS* effects indicates that the stimulation did not modulate the decision-making processes underlying the bias towards *horizontal motion* perception, at least under the conditions investigated.

### 4.3.5. Non-parametric permutational statistical analyses of reaction time distributions

For the dependent variable of correct reaction time (cRT), a non-parametric permutational statistical analysis was conducted based on the comparison of distributions of correct RTs. To achieve this, cumulative distribution functions (CDFs) for the correct RT data were estimated using a Gaussian kernel estimator through a customized MATLAB script (Botev et al., 2010). This analytical approach offers a robust and sensitive investigation into subtle differences in RT data as reflected in the shape of cumulative distributions. Such differences may not always be apparent when examining mean RT values, as typically done in RM-ANOVAs (Misselhorn et al., 2019).

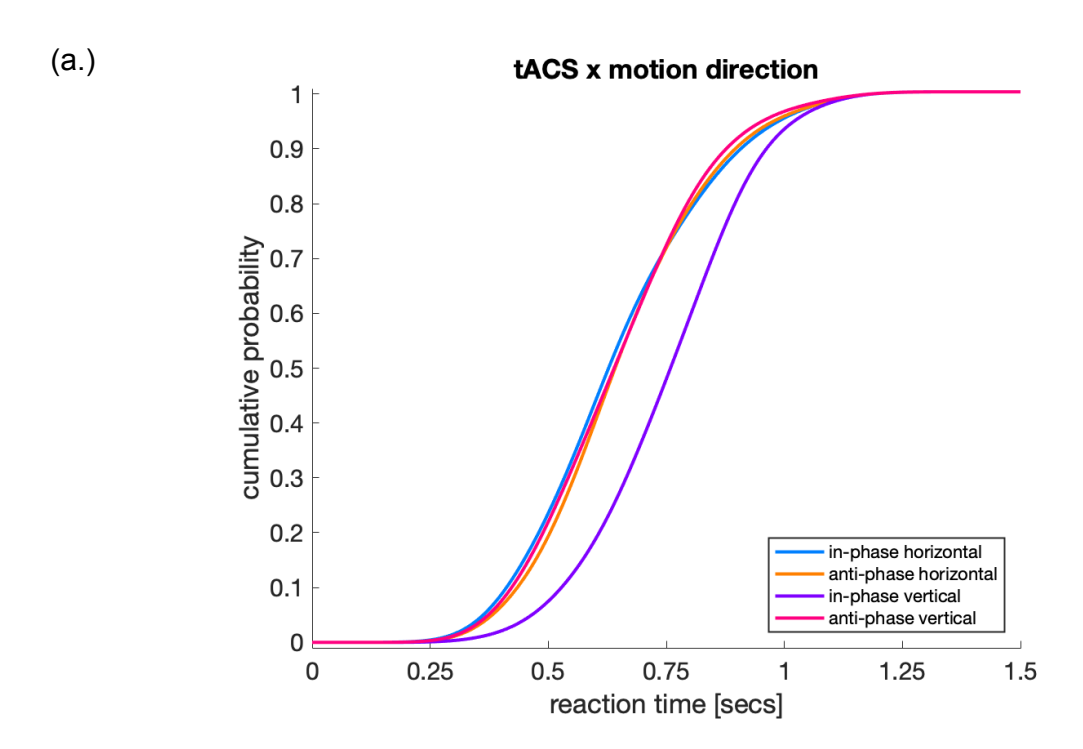
In general, alterations in cumulative distribution functions convey specific insights. A rightward shift along the x-axis (representing correct RTs) indicates a higher proportion of longer correct RTs, while a

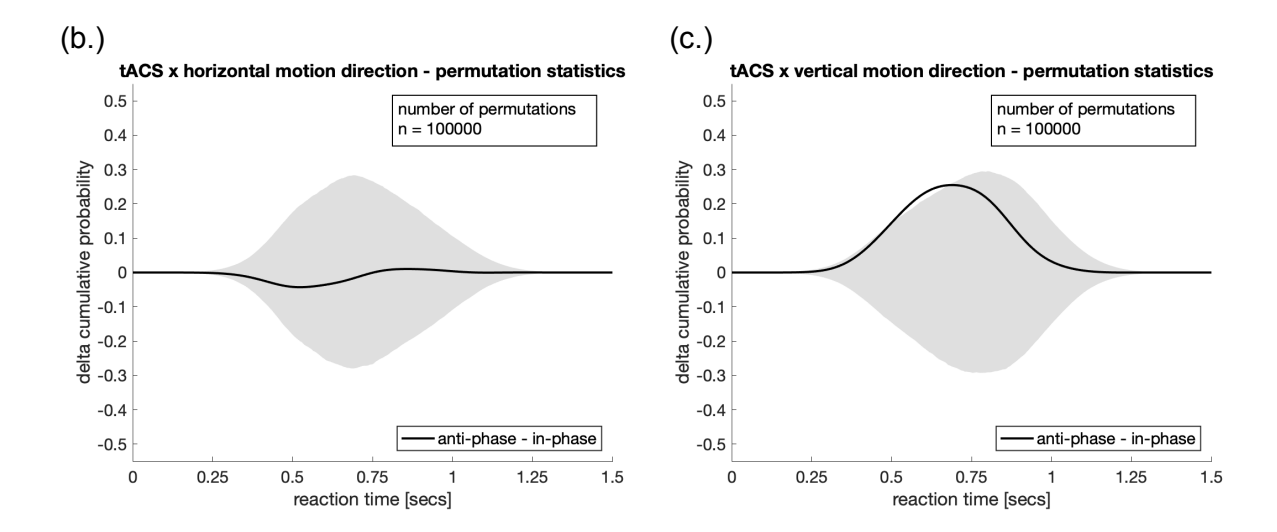
leftward shift suggests a higher proportion of shorter correct RTs. The relationship between cumulative distribution functions across different conditions can be elucidated by computing differences between the corresponding conditions under examination. We hypothesized a phase specific tACS effect on correct RTs in dependance of the motion direction. Basically, lower correct RTs imply a better performance. Therefore, the subconditions of interest were defined as the interaction effect between tACS and motion direction. In concrete terms, we hypothesized significant lower correct RTs for the inphase condition compared to the anti-phase condition within the horizontal motion direction. Similarly, within the vertical motion direction, significant lower correct RTs for the anti-phase condition compared to the in-phase condition were hypothesized. CDFs were computed using 256 bins for each subject and subcondition under investigation. Subsequently, differences between CDFs were constructed based on the congregated and averaged (across participants) correct RT data. To evaluate statistically significant contrasts between CDFs, confidence intervals (CIs) were computed by permutation statistics. To that end, we randomly permuted the correct RT data of the given interaction into two respective sets, estimated the CDFs, and computed the differences. This procedure was replicated for 100.000 times (100.000 permutations). The resulting differences produce a H<sub>0</sub> distribution, which represents the shuffled computed differences of CDFs under the assumption of random positive or negative variabilities of CDF differences expected by chance. To account for multiple testing, we implemented corrections for multiple comparison due to condition contrasts as well as due to the range of values of correct RTs, based on a modified form of the extreme value-based correction method (Cohen, 2017).

For that purpose, we determined two-sided confidence intervals (CI) by employing percentiles at the Bonferroni-corrected (two comparisons) alpha level of alpha = (0.05/2)/2 = 0.0125 (lower threshold: alpha, upper threshold: 100 - alpha). In a next step, all values exceeding the upper or lower threshold of the shuffled data set for each permutation were identified. Those extreme values over all permutations result in a distribution of extreme values. From the resulting distribution, an upper and a lower threshold consisting of percentiles of alpha (lower threshold:  $1,25^{th}$  percentile), and 100 - alpha (upper threshold  $98,75^{th}$  percentile) was determined. Consequently, the resulting corrected Cls control on the one hand for the absolute number of condition contrasts through Bonferroni correction, as well as for the global range of the tested cRT data. For observed values more extreme than the corrected Cls, significance between conditions was assumed. Regarding the *horizontal motion* 

direction, no statistical difference between the *anti-phase* and *in-phase tACS condition* was observed. Regarding the *vertical motion direction*, a significant difference between *anti-phase* and *in-phase* could be observed in the sense that the *in-phase* condition significantly prolonged correct reaction times compared to the *anti-phase* condition (significant range of cRT, x-axis: *anti-phase – in-phase*: 505.9 ms – 670.6 ms; y-axis: 0.151 – 0.254). Furthermore, we conducted the identical analyses using the full set of rection time data, irrespective of the allocation of correct RT or incorrect RT. These analyses did not reveal any significant differences within the compared contrasts of *anti-phase* and *in-phase* conditions within the respective *motion direction (horizontal, vertical)*.

Figure 58 – Permutational statistical analyses of correct reaction time distributions



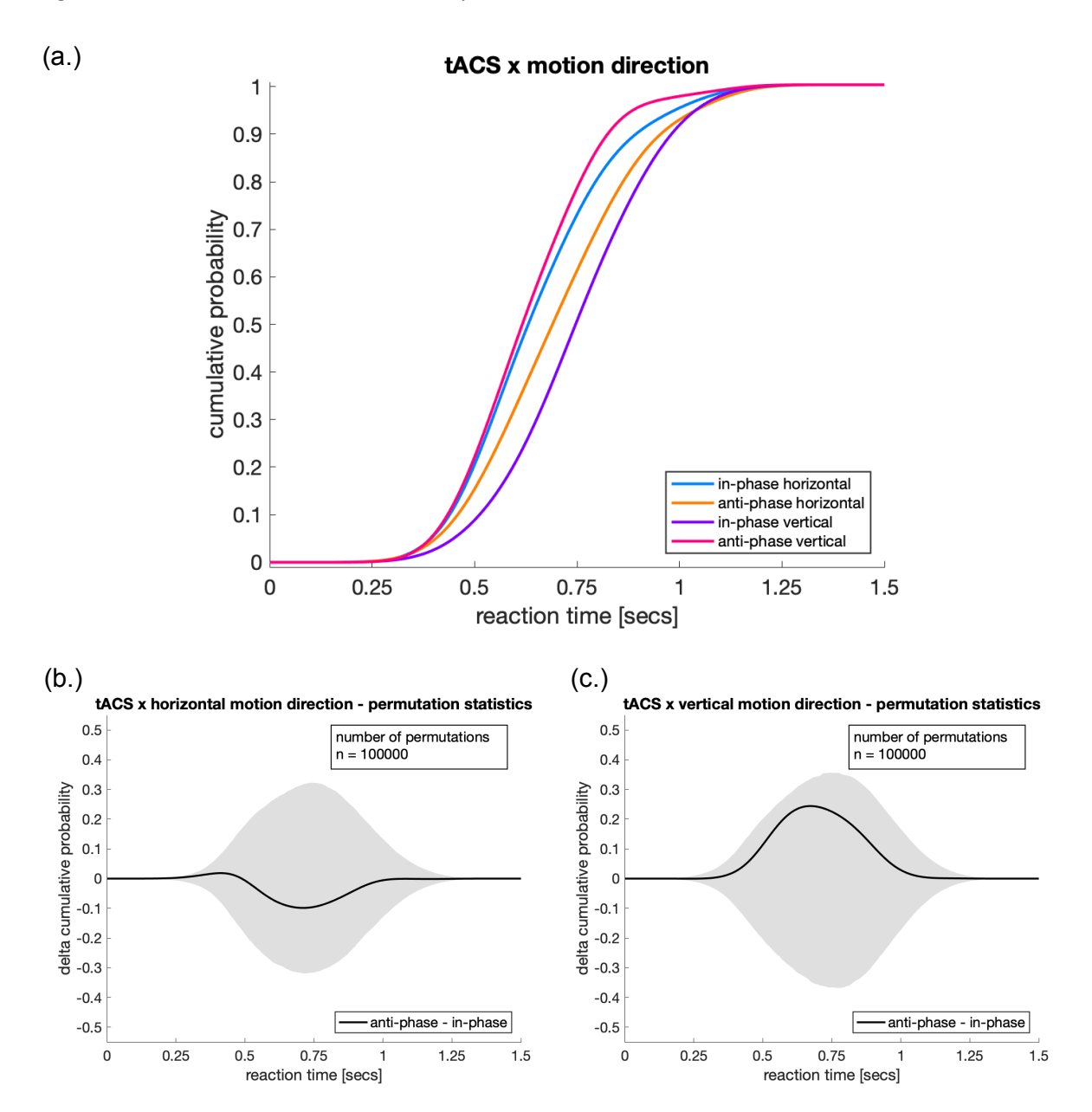


Cumulative distribution functions of correct RT and statistical comparisons – interaction of *tACS* and *motion direction* 

The x-axis represents correct RTs ranging of 0 to 1.5 seconds. The y-axis represents the cumulative probability in (a.) and the difference (delta) between the cumulative probability functions in (b.) – (c.). The shaded gray area represents the confidence intervals (CIs) corrected for multiple comparisons (b.) – (c.).

- (a.) The solid color-coded lines illustrate the cumulative distribution function for the respective conditions under investigation. Within the *vertical motion direction*, the *in-phase tACS condition* results in a rightward shift compared to the *anti-phase* condition.
- (b.) Adjusted permutation statistics of the condition difference within the *horizontal motion direction* between *anti-phase tACS* and *in-phase tACS (anti-phase in-phase)*. The solid line represents the observed differences of *anti-phase tACS in-phase tACS* within the *horizontal motion direction*. No significant difference was observed.
- (c.) Adjusted permutation statistics of the condition difference within the *vertical motion direction* between *anti-phase tACS* and *in-phase tACS (anti-phase in-phase)*. The solid line represents the observed differences of *anti-phase tACS in-phase tACS* within the *vertical motion direction*. A significant difference was observed (significant range of cRT, x-axis: anti-phase in-phase: 505.9 ms 670.6 ms; y-axis: 0.151 0.254), indicating a longer correct RT for the *anti-phase* condition in relation to the *in-phase* condition within the *vertical motion direction*.

Figure 59 – Permutational statistical analyses of reaction time distributions



Cumulative distribution functions including all RTs and statistical comparisons – interaction of *tACS* and *motion direction*.

The x-axis delineates the RTs within a range of 0 to 1.5 seconds. The y-axis represents the cumulative probability in (a.) and the difference (delta) of the cumulative probability in (b.) – (c.). The shaded gray area represents the confidence intervals (CIs) corrected for multiple comparisons (b.) – (c.).

- (a.) The solid color-coded lines illustrate the cumulative distribution function of the respective conditions under investigation.
- (b.) Adjusted permutation statistics of the condition difference within the *horizontal motion direction* between *anti-phase tACS* and *in-phase tACS (anti-phase in-phase)*. The solid line represents the observed differences of *anti-phase tACS in-phase tACS* within the *horizontal motion direction*. No significant difference was observed.
- (c.) Adjusted permutation statistics of the condition difference within the *vertical motion direction* between *anti-phase tACS* and *in-phase tACS (anti-phase in-phase)*. The solid line represents the observed differences of *anti-phase tACS in-phase tACS* within the *vertical motion direction*. No significant difference was observed.

## 4.3.5.1. Overview of results – non-parametric permutational statistical analyses of rection time distributions

The analysis of correct reaction times (cRT) using non-parametric permutation-based statistical methods revealed that *tACS* influenced reaction times in a manner that was dependent on the presented *motion direction*. In particular, in the case of *vertical motion*, correct reaction times were found to be longer when *in-phase tACS* was applied, in comparison to *anti-phase tACS*. In contrast, no significant difference was identified between *in-phase* and *anti-phase tACS* with respect to *horizontal motion*. This suggests that the *phase* of *tACS* stimulation exerts a direction-dependent effect on reaction time performance. A further analysis, which included both correct and incorrect reaction times, demonstrated no significant differences between the *tACS conditions* for either *motion direction*. This suggests that *tACS* did not influence overall task performance when considering both correct and incorrect responses. These findings indicate that *tACS* exerts a more nuanced, direction-specific influence on correct reaction times. This may indicate that *tACS* interacts with the neural processing associated with specific types of motion perception, but its effects may not extend to broader measures of task performance.

### 4.4. Discussion

In this experiment, the potential neuromodulatory role of bihemispheric, phase specific *tACS* on an unambiguous visuotactile motion perception paradigm was investigated. Therefore, we administered bilateral gamma *tACS* over primary somatosensory cortices while subjects performed a visuotactile motion perception task.

We hypothesized that the current perceptual state is determined by the state of oscillatory synchronization of the primary somatosensory cortices. In an attempt to modulate these oscillatory patterns (which are supposed to be correlated with perceptual states) multi electrode *tACS* was applied in a phase- and frequency specific approach.

# 4.4.1. No phase specific *tACS* effect for accuracies (ACC), reaction times (RT), Rate Correct Score (RCS), sensitivity index (d') and decision boundary (criterion c)

Since we hypothesized a phase specific effect of tACS on the perception of motion direction, we conducted separate RM-ANOVAs for each dependent variable under investigation. In concrete terms, in-phase tACS was hypothesized to improve performance parameters for horizontal motion direction stimulus configurations, whereas anti-phase tACS was theorized to enhance performance scores for the vertical motion direction (Helfrich et al., 2014). Conversely, in-phase tACS was hypothesized to impair performance scores for the vertical motion direction, whereas anti-phase tACS was theorized to impair performance scores in regard of the horizontal motion direction (Helfrich et al., 2014). In statistical terms, significant interaction effects between the phase specific tACS conditions and motion direction for the dependent variables of accuracy (ACC), reaction time (RT) and rate correct score (RCS) were hypothesized. In addition, regarding the signal detection theory parameters of the sensitivity index (d'), significant higher sensitivity scores for the in-phase condition compared to the anti-phase condition were assumed (Macmillan & Creelman, 2004). Furthermore, in terms of the decision boundary (criterion c), a significant lower boundary and therefore a significant bias for the horizontal motion direction within the in-phase condition compared to the anti-phase condition was theorized (Macmillan & Creelman, 2004). There were no significant interaction effects between the phasespecific tACS conditions and motion direction concerning the dependent variables of accuracy (ACC), reaction time (RT), and rate correct score (RCS) (Woltz & Was, 2006). Nevertheless, patterns of significant differences were consistently observed concerning the factors of congruence and motion

direction. The congruent condition consistently showed significantly better performance indices in terms of accuracies, reaction times, and rate correct scores as compared to the *incongruent* condition. Moreover, post hoc comparisons for the dependent variable of accuracy established significantly greater accuracy for the congruent condition in comparison to the unimodal condition. In the domain of rate correct scores (RCS), post hoc comparisons revealed significantly higher scores for the congruent condition when compared to both the incongruent and unimodal conditions, as well as higher scores for the unimodal condition compared to the incongruent condition. Moreover, motion direction emerged as significant factor impacting accuracies (ACC), reaction times (RT), and rate correct scores (RCS). Interestingly, even though, the stimulus design incorporated exclusively unambiguous motion stimuli, the overall pattern of significance indicates that performance scores are superior for the horizontal motion direction than for the vertical motion direction. These findings indicate a bias towards the perception of horizontal motion direction, whereas the hypothesis of interhemispheric integration implies a bias towards vertical motion direction (Chaudhuri & Glaser 1991; Helfrich et al., 2014; Liaci et al., 2016). Importantly, regarding the dependent variables of ACC, RT, and RCS a two-way interaction between congruence and motion direction was observed. This underscores the nuanced relationship between these factors. This interaction highlights the complex interplay between perceptual congruence and the direction of perceived motion in shaping perceptual integration processes.

Overall, large effect sizes were observed for the factors congruence and motion direction across the dependent variables of ACC and RCS (Miles & Shevlin, 2001). Specifically, congruence demonstrated a very strong effect on ACC and a strong effect on RCS, highlighting its robust influence on both measures. Motion direction also exhibited a large effect on both ACC and RCS, suggesting that it substantially impacted these dependent variables. Furthermore, the interaction between congruence and motion direction showed a medium to large effect size on ACC and a moderate effect on RCS, indicating a notable interaction between these factors in influencing performance (Miles & Shevlin, 2001). Medium effect sizes were found for the interaction between congruence and motion direction on reaction times (Miles & Shevlin, 2001). The interaction suggests that while these factors have a meaningful effect, their influence is weaker compared to the main effects of congruence and motion direction (Miles & Shevlin, 2001). Post hoc comparisons for the factor congruence revealed large effect sizes for the differences between incongruent and congruent conditions on ACC and RCS indicating a

highly significant difference favoring *congruent* conditions (Lachenbruch & Cohen, 1989). Similarly, large effect sizes were found for the comparison between *unimodal* and *incongruent* conditions on RCS, emphasizing a significant impact favoring *unimodal* conditions (Lachenbruch & Cohen, 1989). Additionally, a medium effect size was observed for the comparison between *unimodal* and *congruent* conditions on RCS (Lachenbruch & Cohen, 1989). In summary, the findings indicate that *congruence* and *motion direction* are powerful factors influencing performance, particularly in ACC and RCS ratings, with significant interactions and post hoc comparisons highlighting their importance in shaping the results.

In the context of signal detection theory parameters, the sensitivity index d' was statistically explored, assuming possible phase specific tACS differences (Macmillan & Creelman, 2004). In the specific experimental context, in-phase tACS was presumed to increase sensitivity, while anti-phase tACS was anticipated to decrease sensitivity. Nevertheless, as the sensitivity index d' is conceptualized as a score of discriminative performance within stimulus configurations, another possible assumption may arise. Anti-phase tACS could potentially facilitate the increase of correct rejection rates, consequently leading to lower false alarm rates. Therefore, lower false alarm rates result in a relative increase of d' values. Overall, the sensitivity index d' may not capture nuanced phase specific tACS effects. The exploratory RM-ANOVA for the sensitivity index showed significantly higher sensitivity scores for the congruent condition compared to the incongruent and unimodal conditions. Additionally, higher sensitivity scores were observed for the *unimodal* condition compared to the *incongruent* condition. Furthermore, no significant differences were found between the *in-phase* and *anti-phase* conditions. This suggests that, within the parameters of this study, tACS may not exert a significant modulatory effect on participants' sensory discrimination abilities. Nevertheless, for the factor of congruence and its respective post hoc comparisons large to medium effect sizes were observed (Lachenbruch & Cohen, 1989; Miles & Shevlin, 2001).

Regarding the decision boundary (criterion c), otherwise also conceptualized as perceptual bias, the RM-ANOVA did not indicate a significant difference between the *in-phase* and *anti-phase* conditions (Macmillan & Creelman, 2004). However, *congruence* levels significantly impacted participants' decision boundary with moderate effect sizes (Lachenbruch & Cohen, 1989; Miles & Shevlin, 2001). Post hoc analyses further elucidated these effects, demonstrating that the *unimodal* condition showed a significantly lower decision boundary with moderate effect sizes, indicating an increased perceptual

bias towards the perception of horizontal motion direction compared to the incongruent and congruent conditions (Lachenbruch & Cohen, 1989). Our results align with previous research, emphasizing the pivotal role of congruence and incongruence in multimodal motion perception (Conrad et al., 2012; Soto-Faraco & Väljamäe, 2012). These findings correspond to experimental neuroscientific studies exploring behavioral effects of multisensory perception, as congruent presentation of visual and tactile motion direction results in enhanced behavioral performance compared to a unimodal or even incongruent visuotactile stimulus configurations (Soto-Faraco & Väljamäe, 2012).

Furthermore, it should be noted that ACCs and the sensitivity index scores for the incongruent condition indicated that the performance of a few participants performed below chance level, or even achieved a score of zero (indicating that they did not correctly detect any trials). In terms of SDT, some participants displayed negative d' values for the incongruent condition. Negative sensitivity values indicate that "noise" trials were more likely to be recognized and classified as "signal" trials than the opposite (Macmillan & Creelman, 2004). Interestingly, this pattern of results indicates that, even with attentional focus exclusively on the tactile modality, the presented incongruent visual motion direction biases and dominates the resulting tactile perception. This finding strongly implies a robust effect of visual motion stimulus dominance over the tactile domain. Remarkably, the factor of motion direction emerged as a significant variable for the dependent variables of ACC, RT, and RCS. The results indicate higher performance scores for the horizontal motion direction in comparison to the vertical motion direction, suggesting a perceptional bias. This bias becomes more pronounced when analyzing the performance scores for horizontal and vertical motion perception in dependance of the different levels of congruence (RM-ANOVA interaction effect). Especially in the unimodal tactile condition, the most pronounced performance differences (and therefore perceptual bias) are evident between motion direction levels towards the perception of horizontal motion. As for the bimodal stimulus conditions, the differences in performance favoring horizontal motion perception decrease. This finding suggests a dominance of the unambiguous visual stimulus. To further elucidate the afore mentioned horizontal bias, the analyses of the criterion variable c in the context of SDT provides further insights between the relationship of the investigated factors. The significantly lower levels observed for the unimodal condition compared to the bimodal conditions are consistent with the results seen for ACC, RT, and RCS. Lower levels of the decision boundary (criterion c) correspond to a more liberal decision

boundary, which, according to the constructed model, indicates a bias towards *horizontal* motion perception (Macmillan & Creelman, 2004).

### 4.4.2. Phase specific tACS effect for correct reaction time data

A novel aspect of our study involved the non-parametric analysis of cumulative distribution differences in correct reaction time data. This approach revealed a significant phase specific effect of tACS. Implementing non-parametric analyses of cumulated distribution differences of reaction time data provide the potential to detect subtle effects in distribution differences, which are not naturally depicted in analyses of mean comparisons like RM-ANOVAs (Misselhorn et al., 2019). In the domain of correct RTs, a significant effect for the difference between anti-phase and in-phase within the vertical motion direction was observed. Specifically, the in-phase condition led to prolonged reaction times compared to the anti-phase condition. This shift is visually illustrated by a rightward shift in the CDF plot. On the other hand, for the horizontal motion direction, no significant difference between in-phase and anti-phase was evident. An additional analysis that included all RT data, irrespective of correctness, did not reveal any significant differences between the anti-phase and inphase tACS conditions within their respective motion directions (horizontal, vertical). Overall, in the domain of correct RTs within the vertical stimulus configuration, in-phase tACS significantly decreases performance compared to anti-phase condition. The non-parametric permutational analysis of RT distributions provide a nuanced perspective on the interaction between tACS and motion direction in multisensory perception tasks. The significant difference observed in the vertical motion direction highlights the impact of tACS phase on correct reaction times, with the inphase condition leading to slower responses. In contrast, the absence of a significant difference in the horizontal motion direction indicates that tACS might not exert a substantial influence on RT distributions in all sub conditions. This discrepancy might underscore the importance of considering the parameter space of non-invasive brain stimulation research (Bland & Sale, 2019). The usefulness of CDFs in revealing these effects underscores their importance in analyzing RT data beyond mean based values (Misselhorn et al., 2019). Overall, our findings advance the understanding of the effects of tACS and motion direction on RT distributions in multisensory perception, with potential implications for research in cognitive neuroscience.

### 4.5. Conclusion

This investigation aimed to provide critical insights into the interplay between bihemispheric, phasespecific tACS, neural oscillations, and the complex processes governing multisensory perception. Therefore, the experimental paradigm of bilateral gamma tACS was administered over the primary somatosensory cortices while participants engaged in a visuotactile motion perception task. The overarching hypothesis centered on the notion that perceptual states are intricately linked to oscillatory synchronization patterns within the primary somatosensory cortices. To probe this hypothesis, we employed a multi-electrode tACS approach that controlled phase and frequency specificity to modulate neural activity. The first set of analyses revolved around the notion of phasespecific tACS effects on accuracy, reaction times, rate correct score, the sensitivity index (d'), and the decision boundary (criterion c) (Macmillan & Creelman, 2004). Although our hypotheses suggested distinct outcomes of in-phase and anti-phase tACS on horizontal and vertical motion perception, the results disclosed differential aspects. No significant effects emerged between tACS phase and motion direction across these dependent variables. Instead, spatial, and temporal congruence between visual and tactile stimuli emerged as a dominant determinant, with congruent stimulus configurations yielding significantly improved behavioral performance scores. In addition, motion direction and the interaction of congruence and motion direction emerged as fundamental factors shaping performance. Furthermore, the findings highlight a bias towards horizontal motion perception, even in the presence of unambiguous motion stimuli. The relationship between congruence and motion direction proved intricate, shaping perceptual integration processes in nuanced ways.

Signal detection theory parameters, d' and criterion c, provided insights into the complex relationship between *tACS*, sensory discrimination abilities and decisional bias (Macmillan & Creelman, 2004). These analyses showed that *tACS* may not exert substantial modulatory effects in this context. It was noteworthy that some participants performed below chance levels for *incongruent* conditions, emphasizing the dominant influence of visual motion stimuli on tactile perception, even when attention was predominantly focused on the tactile modality. The second facet of the experimental investigation delved into the non-parametric analysis of cumulative distribution differences in the domain of correct reaction time data (Misselhorn et al., 2019). This approach revealed a significant phase-specific effect of *tACS*, but only within the *vertical motion direction*. The *in-phase tACS condition* led to prolonged reaction times in this context, challenging the expectation that *tACS* would uniformly

influence reaction times across all subconditions. These findings suggest that *tACS* effects may be context dependent (Bland & Sale, 2019). The use of non-parametric permutational analysis and cumulative distribution functions proved effective in uncovering subtle differences in RT data beyond mean values (Misselhorn at al., 2019). In conclusion, our investigation advances comprehension of the complex interplay between bihemispheric, phase-specific *tACS*, and the multifaceted processes underlying multisensory perception. While our initial hypotheses yielded nuanced results, the absence of significant *tACS* effects, in regard to *motion direction*, emphasizes the complexity of these processes. Perceptual biases, particularly towards *horizontal* motion perception, as well as *congruence* emerged as influential factors. Moreover, our exploration into *tACS* effects in sensory discrimination, decisional bias and its effects on correct reaction times underlines the complexity of *tACS* as a neuromodulatory technique.

This study provides a foundation for future research into the mechanisms of bihemispheric *tACS*, perceptual biases, and multisensory integration. The newfound insights provide approaches for further investigations regarding multimodal motion perception and the potential modulation of neural oscillations through *tACS*.

### 5. General Discussion

Transcranial Alternating Current Stimulation (*tACS*) is considered a valuable instrument in experimentally exploring and modulating neural oscillations and their role in multisensory perception (Bland & Sale, 2019; Herrmann et al., 2016). Neural oscillations, particularly in the gamma frequency range, have long been associated with sensory perception (Engel & Fries, 2016). The conducted experimental investigations aimed to explore the role of gamma band oscillations in tactile motion perception and their modulation using *tACS*. Our hypothesis states that the perception state is contingent upon the oscillatory synchronization state in primary somatosensory cortices. The initial segment of this study examined the impact of *tACS* on ambiguous tactile motion perception, whereas the second experimental design focused on unambiguous visuotactile motion perception. Both experiments applied a 40 Hz sinusoidal electrical stimulation to the primary somatosensory cortices. Furthermore, phase specific conditions of bihemispheric, multielectrode *tACS*, was applied. The overreaching hypothesis as founded in the assumption of interhemispheric integration, where *horizontal* perceptual states within the tactile modality were believed to be correlated with increased

interhemispheric coupling in gamma band frequencies, while *vertical* perceptual states were assumed to be associated with reduced coupling in this frequency range (Helfrich et al., 2014). One notable observation was the differential impact of *in-phase* and *anti-phase tACS* on the perception of ambiguous tactile motion perception. *In-phasic tACS* demonstrated a capacity to increase normalized percept times (NPTs) in contrast to *anti-phasic tACS*. Interestingly, this effect was observed irrespective of the *perceived motion direction*. More detailed analyses suggest a phase-dependent effect contingent upon the *perceived motion direction*, supporting the hypothesis of interhemispheric integration (Chaudhuri & Glaser 1991; Helfrich et al., 2014).

In the RM-ANOVA sub analyses of NPTs in dependence of the proceeding percept (vertical-tohorizontal), anti-phasic gamma tACS reduces NPTs for horizontal motion direction. Furthermore, nonparametric comparisons of cumulated gamma distribution differences revealed a significant interaction effect between tACS and perceived motion direction. In-phase tACS produced significantly longer perceived durations for horizontal motion direction compared to anti-phase tACS. In contrast, no significant difference was observed between the in-phase tACS and anti-phase tACS conditions for the perceived vertical motion direction. These effect patterns suggest a significant modulatory role of tACS ambiguous tactile perceptual processes (Helfrich 2014). et al., The experimental investigation of modulating visuotactile apparent motion perception by tACS revealed notable results. In correspondence with the hypothesis of interhemispheric integration, a significant difference between in-phase tACS and anti-phase tACS within the domain of correct reaction times was observed. Specifically, the in-phase condition led to prolonged reaction times condition, within compared to the anti-phase the vertical motion perception. On the other hand, no significant difference was found between in-phase and anti-phase for the horizontal motion direction, indicating subtle interactions between tACS phase and motion direction. The perceived direction of tactile motion emerged as another significant factor. Participants exhibited better performance scores as well as longer percept times for the horizontal motion direction. Notably, our study revealed a bias towards horizontal motion perception. Both experiments consistently demonstrated a preference for horizontal motion patterns, contradicting our initial hypothesis of a bias toward vertical motion. This unexpected horizontal bias may underline the complex neural basis of tactile motion perception and tACS. Our findings indicate that the tactile domain may have a stronger inclination towards horizontal tactile motion perception. However, it is essential to note that

in the framework of visuotactile conditions, the dominance of visual stimuli dampened this preference (Soto-Faraco & Väljamäe, 2012). Relevant disparities between the tactile and visual modality are evident. The tactile modality operates with a considerably lower degree of dynamism when compared to the dynamic nature of the visual modality (Helfrich et al., 2014). Moreover, the tactile sense appears to be easily influenced and even dominated by the visual modality (Soto-Faraco & Väljamäe, 2012). From an evolutionary perspective, it is worth considering the tendency for perceiving motion in a horizontal direction within the tactile modality. This preference for horizontal motion may have biologically founded roots. It can be argued that this preference is sensible from an evolutionary standpoint (Liaci et al., 2016). In the tactile modality, having perceptual sensitivity to motion along a horizontal trajectory could have provided a significant advantage. Given our bilateral and symmetrical arm and hand configuration, it is inherently more likely to encounter and interact with objects or stimuli in the space between our arms and hands (Liaci et al., 2016). Therefore, it is plausible that the human tactile system has developed a heightened sensitivity to horizontal motion patterns as they naturally align with the typical haptic interactions experienced in daily life (Liaci et al., 2016). Consequently, motion perception between a horizontal trajectory might be perceived more naturally than towards a vertical trajectory, contrary to the visual modality. Furthermore, the somatosensory cortex and associated neural mechanisms for processing tactile motion perception may contribute to an inherent tendency for horizontal motion patterns (Liaci et al., 2016).

Overall, the data do not conclusively support a coherent pattern of results that would support the overarching hypothesis of interhemispheric integration. The exploratory investigations, instead, provide a unique perspective on the potential of *tACS* to modulate tactile motion perception. To advance a broader comprehension of the results, it is important to acknowledge the extensive range of parameters that govern non-invasive brain stimulation. These parameters include stimulation frequency, sites, parameters, and control conditions (Bland & Sale 2019; Herrmann et al., 2016). These numerous variables significantly contribute to the observed variability in results within the *tACS* research field (Bland & Sale 2019; Herrmann et al., 2016). In our specific investigation, we primarily focused on distinct parameters of *tACS* and their effects on tactile motion perception. Nevertheless, it is vital to acknowledge the broader *tACS* research landscape, which explore numerous possibilities within this parameter space (Bland & Sale 2019; Herrmann et al., 2016). The interplay of these parameters with intricate neural networks may lead to a wide variability of outcomes. This complex

web of interactions may account for the context-dependent nature of *tACS* effects, which sometimes yields varying results across different studies (Bland & Sale 2019; Herrmann et al., 2016). Potential variability in this specific investigation could be due to the distinctive operation of the tactile modality in comparison to the visual modality. It is plausible that the features of the tactile system make it less likely to be affected by generalized patterns of interhemispheric integration, but our study did not definitively corroborate this hypothesis. Additionally, the specifics of the applied experimental setup should be taken into consideration (Bland & Sale 2019; Herrmann et al., 2016). For the purposes of experimental investigations into *tACS*, examining the finer details (from stimulus parameters to experimental conditions) may prove essential given the limitations that these intricacies present when extrapolating *tACS* effects to a broader interpretative level.

Preliminary analysis of the detailed nature of oscillatory signatures in tactile motion perception could potentially offer more specific insights into the targets of *tACS* modulation. The parameter space regarding *tACS* stimulation details is extensive, and the precise oscillatory networks involved in tactile motion perception within these stimulus configurations have yet to be fully explored. Additionally, the role of the stimulation site warrants discussion. Evidence supports human middle temporal area (hMT) as a target area for motion perception, despite its traditional connection to visual motion perception (Amemiya et al., 2017; Van Kemenade et al., 2014). Tactile motion perception studies uncovered hMT activation patterns, indicating its potential as a supramodal motion perception area, that may be susceptible of non-invasive brain stimulation (Amemiya et al., 2017; Van Kemenade et al., 2014).

In summary, our study emphasizes the necessity of considering the extensive parameter space of non-invasive brain stimulation within *tACS* research. This space envelopes multiple factors that can significantly affect *tACS* study outcomes. Hence, though our research offers valuable insights, recognizing the broader complexities in the field is crucial in accounting for the variable results observed in *tACS* investigations. In conclusion, this comprehensive analysis underlines the complex interplay between *tACS* and visuotactile motion perception. Furthermore, the utility of non-parametric analysis of cumulative distribution differences in studying multisensory perception deserves further exploration, as it offers a nuanced perspective of data analyses. Overall, these findings contribute to the understanding of multisensory perception and provide insights into the potential applications of *tACS* in modulating sensory and perceptual processes.

### 6. General Summary

This dissertation investigates the potential role of gamma-band neural oscillations in tactile and visuotactile motion perception, focusing on their modulation through transcranial alternating current stimulation (tACS). Neural oscillations, particularly in the gamma frequency range, have long been associated with sensory processing and perception (Engel & Fries, 2016). The overarching hypothesis of this work proposed that interhemispheric gamma-band synchronization plays a critical role in determining perceptual states, with in-phase and anti-phase tACS differentially affecting these states. Two experimental paradigms were employed: one examining ambiguous tactile motion perception and another investigating unambiguous visuotactile motion perception. Both experiments utilized 40 Hz sinusoidal electrical stimulation applied to the primary somatosensory cortices.

The first experiment explored the impact of *tACS* on ambiguous tactile motion perception. It revealed significant phase-dependent effects, with *in-phase tACS* increasing normalized percept times (NPTs) for *horizontal motion* compared to *anti-phase tACS*. This effect was consistent regardless of the perceived motion direction. Further analysis indicated that *anti-phase tACS* specifically reduced NPTs for *horizontal motion* in *vertical-to-horizontal* percept transitions, suggesting a differential impact of *tACS phase* on perceptual processes. Interestingly, contrary to the initial hypothesis, participants exhibited a bias toward *horizontal motion* perception, which persisted across experimental conditions. This unexpected *horizontal* preference highlights the complex interplay of neural mechanisms in tactile motion processing and may reflect an inherent sensitivity of the somatosensory system to *horizontal motion* trajectories (Liaci et al., 2016).

The second experiment focused on visuotactile motion perception, examining how *tACS* modulates perception when tactile stimuli are locally and timely paired with visual motion cues. A significant phase-dependent effect was observed in correct reaction times for vertical motion perception, with *in-phase tACS* leading to prolonged reaction times compared to *anti-phase tACS*. However, for *horizontal motion* perception, no significant differences were found between the two *tACS* conditions. The findings suggest subtle interactions between the *tACS* phase and perceived *motion direction* in multisensory contexts. Notably, participants demonstrated better performance for *horizontal motion* patterns. However, in visuotactile scenarios, the dominance of visual stimuli appeared to dampen this tactile preference, reflecting the hierarchical influence of the visual modality on multisensory integration.

While the present study provides valuable insights into the modulatory potential of *tACS* on motion perception, the findings do not conclusively support the hypothesis of interhemispheric gamma-band integration as a determinant of perceptual states. The variability in results underscores the complexity of *tACS* effects, which are highly dependent on parameters such as stimulation frequency, site, phase, and other experimental conditions. These factors interact with the intricate dynamics of neural oscillations and sensory networks, contributing to the observed inconsistencies in *tACS* research.

This dissertation underscores the necessity for a more systematic exploration of the extensive parameter space in *tACS* research. Fine-tuning stimulation parameters, identifying precise oscillatory networks, and considering individual variability in neural responses are essential for advancing the understanding of *tACS* effects.

In conclusion, this study emphasises the potential of *tACS* as a tool for modulating sensory and perceptual processes while acknowledging the challenges inherent in interpreting its effects. The findings contribute to the growing body of research on multisensory perception and provide a foundation for future investigations into the neural mechanisms underlying tactile and visuotactile motion perception.

Diese Dissertation untersucht die potenzielle Rolle von neuronalen Oszillationen im Gamma-Band bei der taktilen und visuotaktilen Bewegungswahrnehmung und konzentriert sich auf deren Modulation durch transkranielle Wechselstromstimulation (tACS). Neuronale Oszillationen, insbesondere im Gamma-Frequenzbereich, werden seit langem mit sensorischer Verarbeitung und Wahrnehmung in Verbindung gebracht (Engel & Fries, 2016). Die übergreifende Hypothese dieser Arbeit besagt, dass die interhemisphärische Gamma-Band-Synchronisation eine entscheidende Rolle bei der Bestimmung von Wahrnehmungszuständen spielt, wobei phasengleiche und gegenphasige tACS diese Zustände unterschiedlich beeinflussen. Es wurden zwei experimentelle Paradigmen verwendet: eines zur Untersuchung ambiger taktilen Bewegungswahrnehmung und ein anderes zur Untersuchung der unambiger visuotaktilen Bewegungswahrnehmung. In beiden Experimenten wurden die primären somatosensorischen Hirnareale mit einer sinusförmigen elektrischen Stimulation von 40 Hz stimuliert.

Das erste Experiment untersuchte die Auswirkungen von *tACS* auf die Wahrnehmung ambiger taktiler Bewegungen. Es zeigte signifikante phasenabhängige Effekte, wobei phasengleiche *tACS* die normalisierten Wahrnehmungszeiten (NPTs) für horizontale Bewegungen im Vergleich zu gegenphasigen *tACS* erhöhten. Dieser Effekt war unabhängig von der wahrgenommenen Bewegungsrichtung konsistent. Weitere Analysen ergaben, dass gegenphasige *tACS* die NPTs für horizontale Bewegungen bei Übergängen von vertikaler zu horizontaler Wahrnehmung spezifisch reduzierten, was auf einen differenzierten Einfluss der *tACS*-Phase auf Wahrnehmungsprozesse hindeutet. Interessanterweise zeigten die Teilnehmer entgegen der ursprünglichen Hypothese eine Vorliebe für die Wahrnehmung horizontaler Bewegungen, die über alle Versuchsbedingungen hinweg anhielt. Diese unerwartete horizontale Präferenz unterstreicht das komplexe Zusammenspiel neuronaler Mechanismen bei der taktilen Bewegungsverarbeitung und könnte eine inhärente Empfindlichkeit des somatosensorischen Systems für horizontale Bewegungsbahnen widerspiegeln (Liaci et al., 2016).

Das zweite Experiment konzentrierte sich auf die visuell-taktile Bewegungswahrnehmung und untersuchte, wie tACS die Wahrnehmung moduliert, wenn taktile Reize lokal und zeitlich mit visuellen Bewegungsmustern gepaart sind. Ein signifikanter phasenabhängiger Effekt wurde bei korrekten Reaktionszeiten für die vertikale Bewegungswahrnehmung beobachtet, wobei phasengleiche tACS im Vergleich zu gegenphasigen tACS zu verlängerten Reaktionszeiten führten. Bei der Wahrnehmung horizontaler Bewegungen wurden jedoch keine signifikanten Unterschiede zwischen den beiden tACS-Bedingungen festgestellt. Die Ergebnisse deuten auf subtile Interaktionen zwischen der tACS-Phase und der wahrgenommenen Bewegungsrichtung in multisensorischen Kontexten hin. Insbesondere zeigten die Teilnehmer eine bessere Leistung bei horizontalen Bewegungsmustern. In visuell-taktilen Szenarien schien die Dominanz der visuellen Stimuli diese taktile Präferenz jedoch zu dämpfen, was den hierarchischen Einfluss der visuellen Modalität auf die multisensorische Integration widerspiegelt. Obwohl die vorliegende Studie wertvolle Einblicke in das modulatorische Potenzial von tACS auf die Bewegungswahrnehmung liefert, unterstützen die Ergebnisse nicht schlüssig die Hypothese der interhemisphärischen Gamma-Band-Integration als Determinante der Wahrnehmungszustände. Die Variabilität der Ergebnisse unterstreicht die Komplexität der tACS-Effekte, die in hohem Maße von Parametern wie der Stimulationsfrequenz, dem Ort der Stimulation, der Stimulations-Phase und anderen experimentellen Bedingungen abhängig sind. Diese Faktoren interagieren mit der

komplizierten Dynamik neuronaler Oszillationen und sensorischer Netzwerke und tragen zu den beobachteten Unstimmigkeiten in der *tACS*-Forschung bei.

Diese Dissertation unterstreicht die Notwendigkeit einer systematischeren Erforschung des umfangreichen Parameterraums in der *tACS*-Forschung. Die Feinabstimmung von Stimulationsparametern, die Identifizierung präziser oszillatorischer Netzwerke und die Berücksichtigung der individuellen Variabilität neuronaler Reaktionen sind für ein besseres Verständnis der *tACS*-Effekte unerlässlich.

Zusammenfassend unterstreicht diese Studie das Potenzial von *tACS* als Instrument zur Modulation sensorischer und wahrnehmungsbezogener Prozesse und räumt gleichzeitig die Herausforderungen ein, die mit der Interpretation ihrer Auswirkungen verbunden sind. Die Ergebnisse tragen zu den wachsenden Forschungsergebnissen über multisensorische Wahrnehmung bei und bieten eine Grundlage für zukünftige Untersuchungen der neuronalen Mechanismen, die der taktilen und visuotaktilen Bewegungswahrnehmung zugrunde liegen.

### 7. Supplementary Material – Tables

### 7.1. Modulation of ambiguous tactile apparent motion perception by *tACS*

Table 2 – Randomization list and basic information about the participants (tactile SAM)

participant	tACS randomization			age	sex
1	sham	in-phase	anti-phase	28	male
2	sham	anti-phase	in-phase	22	female
3	in-phase	anti-phase	sham	29	female
4	in-phase	sham	anti-phase	26	male
5	anti-phase	in-phase	sham	23	male
6	anti-phase	sham	in-phase	21	female
7	sham	in-phase	anti-phase	19	female
8	sham	anti-phase	in-phase	27	male
9	in-phase	anti-phase	sham	26	male
10	in-phase	sham	anti-phase	23	female
11	anti-phase	in-phase	sham	21	female
12	anti-phase	sham	in-phase	27	female
13	sham	in-phase	anti-phase	34	male
14	sham	anti-phase	in-phase	26	female
15	in-phase	anti-phase	sham	21	male
16	in-phase	sham	anti-phase	32	male
17	anti-phase	in-phase	sham	26	male
18	anti-phase	sham	in-phase	28	female

Randomization table and demographic characteristics of subjects participating in the ambiguous tactile apparent motion study.

Table 3 – 3x2x2 RM-ANOVA – Normalized percept time (NPT) (tactile SAM)

RM-ANOVA – n	ormalized percep	ot time (NPT)	– Within Su	bjects Effe	cts		
Cases	Sphericity Correction	Sum of Squares	df	Mean Square	F	р	η²p
tACS	None	0.027	2.000	0.013	5.595	0.008	0.248
	Greenhouse- Geisser	0.027	1.601	0.017	5.595	0.013	0.248
Residuals	None	0.081	34.000	0.002			
	Greenhouse- Geisser	0.081	27.213	0.003			
perceived motion direction	None	2.494	1.000	2.494	8.430	0.010	0.331
Residuals	None	5.029	17.000	0.296			
unambiguous start configuration	None	0.002	1.000	0.002	1.626	0.219	0.087
Residuals	None	0.025	17.000	0.001			
tACS *	None	0.035	2.000	0.018	0.736	0.487	0.041
perceived motion direction	Greenhouse- Geisser	0.035	1.736	0.020	0.736	0.470	0.041
Residuals	None	0.812	34.000	0.024			

	Greenhouse-	0.812	29.504	0.028			
	Geisser						
tACS *	None	5.506×10 <sup>-4</sup>	2.000	2.753×10 <sup>-4</sup>	0.454	0.639	0.026
unambiguous							
start							
configuration							
	Greenhouse- Geisser	5.506×10 <sup>-4</sup>	1.887	2.918×10 <sup>-4</sup>	0.454	0.628	0.026
Residuals	None	0.021	34.000	6.063×10 <sup>-4</sup>			
	Greenhouse- Geisser	0.021	32.074	6.427×10 <sup>-4</sup>			
perceived	None	0.002	1.000	0.002	0.075	0.787	0.004
motion							
direction *							
unambiguous							
start							
configuration							
Residuals	None	0.420	17.000	0.025			
tACS *	None	0.018	2.000	0.009	0.344	0.712	0.020
perceived	Greenhouse-	0.018	1.852	0.010	0.344	0.696	0.020
motion	Geisser						
direction *							
unambiguous							
start							
configuration							
Residuals	None	0.889	34.000	0.026			

Greenhouse-	0.889	31.492	0.028		
Geisser					

Table 4 – 3x2x2 RM-ANOVA – Test of Sphericity – Normalized percept time (NPT) (tactile SAM)

Test of Sphericity	Mauchly's	Approx.	df	p-value	Greenhouse-	Huynh-	Lower
	W	X <sup>2</sup>			Geisser ε	Feldt ε	Bound ε
tACS	0.751	4.590	2	0.101	0.800	0.871	0.500
tACS * perceived	0.848	2.645	2	0.266	0.868	0.958	0.500
motion direction							
tACS *	0.940	0.991	2	0.609	0.943	1.000	0.500
unambiguous start							
configuration							
tACS * perceived	0.920	1.328	2	0.515	0.926	1.000	0.500
motion direction *							
unambiguous start							
configuration							

Table 5 - 3x2x2 RM-ANOVA – Normalized percept time (NPT) – post hoc comparisons of *tACS* conditions (tactile SAM)

Post Hoc Comparisons -	Mean	SE	t	pbonf	Cohen's d
tACS	Difference				
sham – in-phase	-0.004	0.008	-0.436	1.000	-0.018
sham – anti-phase	0.022	0.008	2.655	0.036*	0.110

in-phase – anti-phase	0.025	0.008	3.090	0.012*	0.128
-----------------------	-------	-------	-------	--------	-------

<sup>\*</sup> p < .05

*Note.* P-value adjusted for comparing a family of 3.

Note. Results are averaged over the levels: perceived motion direction, unambiguous start configuration.

Table 6 – 3x4x2 RM-ANOVA – Normalized percept time (NPT) (tactile SAM)

RM-ANOVA 3x4	lx2 – normalized p	percept time (I	NPT) – Witl	hin Subjects	Effects		
Cases	Sphericity Correction	Sum of Squares	df	Mean Square	F	р	η²p
tACS	None	0.013	2.000	0.006	4.025	0.027	0.191
	Greenhouse- Geisser	0.013	1.788	0.007	4.025	0.032	0.191
Residuals	None	0.054	34.000	0.002			
	Greenhouse- Geisser	0.054	30.393	0.002			
perceptual	None	4.623°	3.000ª	1.541ª	12.485ª	< .001ª	0.423°
alteration	Greenhouse- Geisser	4.623	2.119	2.181	12.485	< .001	0.423
Residuals	None	6.295	51.000	0.123			
	Greenhouse- Geisser	6.295	36.027	0.175			
unambiguous start configuration	None	0.003	1.000	0.003	2.306	0.147	0.119
Residuals	None	0.025	17.000	0.001			

			,				,
tACS *	None	0.268	6.000	0.045	2.524	0.026	0.129
perceptual	Greenhouse-	0.268	4.385	0.061	2.524	0.043	0.129
alteration	Geisser						
Residuals	None	1.806	102.000	0.018			
	Greenhouse-	1.806	74.545	0.024			
	Geisser						
tACS *	None	5.510×10 <sup>-5</sup>	2.000	2.755×10 <sup>-5</sup>	0.039	0.962	0.002
unambiguous	Greenhouse-	5.510×10 <sup>-5</sup>	1.830	3.012×10 <sup>-5</sup>	0.039	0.952	0.002
start	Geisser						
configuration							
Residuals	None	0.024	34.000	7.095×10 <sup>-4</sup>			
	Greenhouse-	0.024	31.104	7.756×10 <sup>-4</sup>			
	Geisser						
perceptual	None	0.524	3.000	0.175	9.382	< .001	0.356
alteration *	Greenhouse-	0.524	2.601	0.201	9.382	< .001	0.356
unambiguous	Geisser						
start							
configuration							
Residuals	None	0.949	51.000	0.019			
	Greenhouse-	0.949	44.209	0.021			
	Geisser						
tACS *	None	0.063	6.000	0.010	0.600	0.730	0.034
perceptual	Greenhouse-	0.063	3.347	0.019	0.600	0.636	0.034
alteration *	Geisser						
unambiguous							

start configuration						
Residuals	None	1.781	102.000	0.017		
	Greenhouse- Geisser	1.781	56.894	0.031		

Table 7 – 3x4x2 RM-ANOVA – Test of Sphericity – Normalized percept time (NPT) (tactile SAM)

Test of Sphericity	Mauchly's W	Approx.	df	p-value	Greenhouse- Geisser ε	Huynh- Feldt ε	Lower Bound ε
tACS	0.881	2.021	2	0.364	0.894	0.992	0.500
perceptual alteration	0.288	19.582	5	0.002	0.706	0.810	0.333
tACS * perceptual alteration	0.270	19.368	20	0.510	0.731	1.000	0.167
tACS * unambiguous start configuration	0.907	1.564	2	0.458	0.915	1.000	0.500
perceptual alteration * unambiguous start configuration	0.805	3.404	5	0.639	0.867	1.000	0.333

 $<sup>^{\</sup>rm a}$  Mauchly's test of sphericity indicates that the assumption of sphericity is violated (p < .05).

tACS * perceptual	0.139	29.169	20	0.091	0.558	0.711	0.167
alteration *							
unambiguous start							
configuration							

Table 8 – 3x4x2 RM-ANOVA – Normalized percept time (NPT) – post hoc comparisons of *tACS* conditions (tactile SAM)

Post Hoc Comparisons - tACS	Mean Difference	SE	t	pbonf	Cohen's d
sham – in-phase	4.096×10 <sup>-5</sup>	0.005	0.009	1.000	2.470×10 <sup>-4</sup>
sham – anti-phase	0.012	0.005	2.462	0.057	0.070
in-phase – anti-phase	0.012	0.005	2.453	0.058	0.070

Note. P-value adjusted for comparing a family of 3.

*Note.* Results are averaged over the levels of *perceptual alteration, unambiguous start configuration*.

Table 9 – 3x4x2 RM-ANOVA – Normalized percept time (NPT) – post hoc comparisons of *perceptual alteration* (tactile SAM)

Post Hoc Compariso	ons –	Mean	SE	t	pbonf	Cohen's d
perceptual alteration		Difference				
	vertical-to-	0.089	0.048	1.852	0.419	
	vertical					0.534
horizontal-to-	horizontal-to-	-0.072	0.048	-1.510	0.823	
horizontal	vertical					-0.435
	vertical-to-	-0.194	0.048	-4.058	0.001**	
	horizontal					-1.170

	horizontal-to-	-0.161	0.048	-3.362	0.009**	
vertical-to-vertical	vertical					-0.969
	vertical-to-	-0.283	0.048	-5.910	<.001***	
	horizontal					-1.704
horizontal-to-	vertical-to-	-0.122	0.048	-2.548	0.083	
vertical	horizontal					-0.735

Note. Results are averaged over the levels of: tACS, unambiguous start configuration.

*Note.* P-value adjusted for comparing a family of 6.

Table 10 – 3x2 RM-ANOVA horizontal-to-horizontal – Normalized percept time (NPT) (tactile SAM)

RM-ANOVA 3x2	2 – horizontal-to-h	<i>orizontal</i> – no	rmalized p	ercept time	(NPT) – V	Vithin Sul	ojects
Effects							
Cases	Sphericity	Sum of	df	Mean	F	р	η²p
	Correction	Squares		Square			
tACS	None	0.051	2.000	0.026	1.783	0.184	0.095
	Greenhouse- Geisser	0.051	1.846	0.028	1.783	0.187	0.095
Residuals	None	0.490	34.000	0.014			
	Greenhouse- Geisser	0.490	31.389	0.016			
unambiguous	None	0.167	1.000	0.167	14.242	0.002	0.456
start							
configuration							
Residuals	None	0.199	17.000	0.012			
	None	0.022	2.000	0.011	0.694	0.507	0.039

<sup>\*</sup> p < .05, \*\* p < .01, \*\*\* p < .001.

tACS *	Greenhouse-	0.022	1.675	0.013	0.694	0.483	0.039
unambiguous	Geisser						
start							
configuration							
Residuals	None	0.534	34.000	0.016			
	Greenhouse-	0.534	28.472	0.019			
	Geisser						

Table 11 – 3x2 RM-ANOVA *horizontal-to-horizontal* – Test of Sphericity – Normalized percept time (NPT) (tactile SAM)

Test of Sphericity	Mauchly's	Approx.	df	p-value	Greenhouse-	Huynh-	Lower
	W	X <sup>2</sup>			Geisser ε	Feldt ε	Bound ε
tACS	0.917	1.389	2	0.499	0.923	1.000	0.500
tACS *	0.806	3.454	2	0.178	0.837	0.918	0.500
unambiguous start							
configuration							

Table 12 – 3x2 RM-ANOVA *vertical-to-vertical* – Normalized percept time (NPT) (tactile SAM)

RM-ANOVA 3x2 – <i>vertical-to-vertical</i> – normalized percept time (NPT) – Within Subjects Effects											
Cases	Sphericity Correction	Sum of Squares	df	Mean Square	F	р	η²p				
tACS	None	0.003	2.000	0.001	0.157	0.856	0.009				
	Greenhouse- Geisser	0.003	1.773	0.001	0.157	0.831	0.009				

Residuals	None	0.282	34.000	0.008			
	Greenhouse-	0.282	30.135	0.009			
	Geisser						
unambiguous	None	0.037	1.000	0.037	3.139	0.094	0.156
start							
configuration							
Residuals	None	0.202	17.000	0.012			
tACS *	None	0.015	2.000	0.007	0.855	0.434	0.048
unambiguous	Greenhouse-	0.015	1.852	0.008	0.855	0.427	0.048
start	Geisser						
configuration							
Residuals	None	0.289	34.000	0.009			
	Greenhouse-	0.289	31.492	0.009			
	Geisser						

Table 13 – 3x2 RM-ANOVA *vertical-to-vertical* – Test of Sphericity – Normalized percept time (NPT) (tactile SAM)

Test of Sphericity	Mauchly's	Approx.	df	p-value	Greenhouse-	Huynh-	Lower
	W	X <sup>2</sup>			Geisser ε	Feldt ε	Bound ε
tACS	0.872	2.196	2	0.334	0.886	0.982	0.500
tACS *	0.920	1.328	2	0.515	0.926	1.000	0.500
unambiguous start							
configuration							

Table 14 – 3x2 RM-ANOVA horizontal-to-vertical – Normalized percept time (NPT) (tactile SAM)

RM-ANOVA 3x2	2 – horizontal-to-v	<i>ertical</i> – norm	alized perc	cept time (N	PT) – Wit	hin Subje	cts Effects
Cases	Sphericity Correction	Sum of Squares	df	Mean Square	F	р	η²p
tACS	None	0.011ª	2.000ª	0.005ª	0.394ª	0.678ª	0.023ª
	Greenhouse- Geisser	0.011	1.464	0.007	0.394	0.615	0.023
Residuals	None	0.466	34.000	0.014			
	Greenhouse- Geisser	0.466	24.880	0.019			
unambiguous start configuration	None	0.040	1.000	0.040	2.696	0.119	0.137
Residuals	None	0.251	17.000	0.015			
tACS *	None	6.056×10 <sup>-4</sup>	2.000	3.028×10 <sup>-4</sup>	0.025	0.975	0.001
unambiguous start configuration	Greenhouse- Geisser	6.056×10 <sup>-4</sup>	1.600	3.784×10 <sup>-4</sup>	0.025	0.954	0.001
Residuals	None	0.409	34.000	0.012			
	Greenhouse- Geisser	0.409	27.206	0.015			

 $<sup>^{\</sup>rm a}$  Mauchly's test of sphericity indicates that the assumption of sphericity is violated (p < .05).

Table 15 – 3x2 RM-ANOVA *horizontal-to-vertical* – Test of Sphericity – Normalized percept time (NPT) (tactile SAM)

Test of Sphericity	Mauchly's	Approx.	df	p-value	Greenhouse-	Huynh-	Lower
	W	X <sup>2</sup>			Geisser ε	Feldt ε	Bound ε
tACS	0.633	7.306	2	0.026	0.732	0.783	0.500
tACS *	0.750	4.597	2	0.100	0.800	0.870	0.500
unambiguous start							
configuration							

Table 16 – 3x2 RM-ANOVA *vertical-to-horizontal* – Normalized percept time (NPT) (tactile SAM)

RM-ANOVA 3x2	2 – vertical-to-hori	<i>zontal</i> – norm	alized perc	cept time (N	PT) – Wit	hin Subje	cts Effects
Cases	Sphericity	Sum of	df	Mean	F	р	η²p
	Correction	Squares		Square			
tACS	None	0.216	2.000	0.108	5.909	0.006	0.258
	Greenhouse- Geisser	0.216	1.655	0.131	5.909	0.010	0.258
Residuals	None	0.622	34.000	0.018			
	Greenhouse- Geisser	0.622	28.139	0.022			
unambiguous	None	0.283	1.000	0.283	14.919	0.001	0.467
start							
configuration							
Residuals	None	0.323	17.000	0.019			
	None	0.026	2.000	0.013	0.770	0.471	0.043

tACS *	Greenhouse-	0.026	1.669	0.016	0.770	0.451	0.043
unambiguous	Geisser						
start							
configuration							
Residuals	None	0.573	34.000	0.017			
	Greenhouse-	0.573	28.380	0.020			
	Geisser						

*Note.* Type III Sum of Squares

Table 17 – 3x2 RM-ANOVA *vertical-to-vertical* – Test of Sphericity – Normalized percept time (NPT) (tactile SAM)

Test of Sphericity	Mauchly's	Approx.	df	p-value	Greenhouse-	Huynh-	Lower
	W	X <sup>2</sup>			Geisser ε	Feldt ε	Bound ε
tACS	0.792	3.737	2	0.154	0.828	0.906	0.500
tACS *	0.802	3.531	2	0.171	0.835	0.915	0.500
unambiguous start							
configuration							

Table 18 – 3x2 RM-ANOVA *vertical-to-horizontal* – Normalized percept time (NPT) – post hoc comparisons of *tACS conditions* (tactile SAM)

Post Hoc Comparisons - tACS	Mean Difference	SE	t	pbonf	Cohen's d
sham – in-phase	0.041	0.032	1.274	0.634	0.189
sham – anti-phase	0.108	0.032	3.402	0.005**	0.505
in-phase – anti-phase	0.068	0.032	2.128	0.122	0.316

Note. P-value adjusted for comparing a family of 3.

*Note.* Results are averaged over the levels of *unambiguous start configuration*.

Table 19 – 3x2x2 RM-ANOVA – Button press per minute (BPM) (tactile SAM)

Cases	Sphericity	Sum of	df	Mean	F	р	η²p
	Correction	Squares		Square			
tACS	None	0.804	2.000	0.402	2.779	0.076	0.140
	Greenhouse- Geisser	0.804	1.702	0.472	2.779	0.086	0.140
Residuals	None	4.920	34.000	0.145			
	Greenhouse- Geisser	4.920	28.938	0.170			
perceived	None	2.387	1.000	2.387	8.681	0.009	0.338
motion							
direction							
Residuals	None	4.674	17.000	0.275			
unambiguous	None	0.006	1.000	0.006	0.115	0.738	0.007
start							
configuration							
Residuals	None	0.855	17.000	0.050			
tACS *	None	0.087	2.000	0.043	0.423	0.658	0.024
perceived	Greenhouse-	0.087	1.826	0.048	0.423	0.640	0.024
motion	Geisser						
direction							
Residuals	None	3.493	34.000	0.103			

	Greenhouse-	3.493	31.039	0.113			
	Geisser						
tACS *	None	0.076	2.000	0.038	0.555	0.579	0.032
unambiguous							
start							
configuration							
	Greenhouse- Geisser	0.076	1.883	0.040	0.555	0.569	0.032
Residuals	None	2.312	34.000	0.068			
	Greenhouse- Geisser	2.312	32.004	0.072			
perceived	None	3.283	1.000	3.283	72.845	< .001	0.811
motion							
direction *							
unambiguous							
start							
configuration							
Residuals	None	0.766	17.000	0.045			
tACS *	None	0.047	2.000	0.023	0.446	0.644	0.026
perceived	Greenhouse-	0.047	1.761	0.027	0.446	0.620	0.026
motion	Geisser						
direction *							
unambiguous							
start							
configuration							
Residuals	None	1.790	34.000	0.053			

Greenhouse-	1.790	29.944	0.060		
Geisser					

 $<sup>^{\</sup>rm a}$  Mauchly's test of sphericity indicates that the assumption of sphericity is violated (p < 0.05).

Table 20 – 3x2x2 RM-ANOVA – Test of Sphericity – Button press per minute (BPM) (tactile SAM)

Test of Sphericity	Mauchly's	Approx.	df	p-value	Greenhouse-	Huynh-	Lower
	W	X <sup>2</sup>			Geisser ε	Feldt ε	Bound ε
tACS	0.825	3.077	2	0.215	0.851	0.936	0.500
tACS * perceived	0.905	1.604	2	0.448	0.913	1.000	0.500
motion direction							
tACS *	0.938	1.030	2	0.597	0.941	1.000	0.500
unambiguous start							
configuration							
tACS * perceived	0.865	2.329	2	0.312	0.881	0.975	0.500
motion direction *							
unambiguous start							
configuration							

Table 21 - 3x2x2 RM-ANOVA – Button press per minute (BPM) – post hoc comparisons of *tACS* conditions (tactile SAM)

Post Hoc Comparisons -	Mean	SE	t	pbonf	Cohen's d
tACS	Difference				
sham – in-phase	0.099	0.063	1.568	0.379	0.197
sham – anti-phase	-0.047	0.063	-0.741	1.000	-0.093
in-phase – anti-phase	-0.146	0.063	-2.309	0.082	-0.289

*Note.* P-value adjusted for comparing a family of 3.

Table 22 – Log-likelihood values and Akaike Information Criterion values for considered modelled distributions

Distribution name	Log-liklihood	Akaike Information Criterion
gamma	777.9669	-1551.9337
weibull	774.7382	-1545.4764
generalized pareto	772.7095	-1541.4190
exponential	771.4651	-1540.9301
lognormal	765.9045	-1527.8089
non-parametric kernel	732.6055	35399.6751
inversegaussian	732.0097	-1460.0193
loglogistic	710.6040	-1417.2080
nakagami	708.8595	-1413.7190
gev	674.3390	-1342.6779
beta	188.0033	-372.0065
tlocationscale	170.4168	-334.8335
logistic	114.0960	-224.192
uniform	23.27240	-42.5449
normal	20.60970	-37.2194
rayleigh	-163.4606	328.9212
rician	-163.4606	330.9213

Note. Results are averaged over the levels of perceived motion direction, unambiguous start configuration.

Table 23 – Spearman's correlation – normalized percept time (NPT) and amplitude modulation (AM)

Spearman's correlation – normalized percept time (NPT) and amplitude modulation (AM)							
normalized percept time (NPT)		amplitude modulation (AM)					
		AM sham	AM in-phase	AM anti-phase			
NPT sham	Spearman's rho	-0.352					
	p-value	0.152					
NPT in-phase	Spearman's rho		0.501				
	p-value		0.036*				
NPT anti-phase	Spearman's rho			-0.325			
	p-value			0.188			

## 7.2. Modulation of unambiguous visuotactile apparent motion perception by *tACS*Table 24 – Randomization list and basic information about the participants (visuotactile apparent motion perception)

participant	tACS rando	mization	age	sex
1	in-phase	anti-phase	28	male
2	anti-phase	in-phase	22	female
3	in-phase	anti-phase	29	female
4	anti-phase	in-phase	26	male
5	in-phase	anti-phase	23	male

6	anti-phase	in-phase	21	female
7	in-phase	anti-phase	19	female
8	anti-phase	in-phase	27	male
9	in-phase	anti-phase	26	male
10	anti-phase	in-phase	23	female
11	in-phase	anti-phase	21	female
12	anti-phase	in-phase	27	female
13	in-phase	anti-phase	34	male
14	anti-phase	in-phase	26	female
15	in-phase	anti-phase	21	male
16	anti-phase	in-phase	32	male
17	in-phase	anti-phase	26	male
18	anti-phase	in-phase	28	female
19	in-phase	anti-phase	24	female
20	anti-phase	in-phase	25	male
21	in-phase	anti-phase	29	female

Randomization table and demographic characteristics of subjects participating in the unambiguous visuotactile apparent motion study.

Table 25 – 2x3x2 RM-ANOVA – Accuracy (ACC) (visuotactile apparent motion)

RM-ANOVA – Accuracy – Within Subjects Effects							
Cases	Sphericity Correction	Sum of Squares	df	Mean Square	F	p	η²p
tACS	None	5.318×10 <sup>-4</sup>	1.000	5.318×10 <sup>-4</sup>	0.036	0.851	0.002

Residuals	None	0.295	20.000	0.015			
congruence	None	19.506ª	2.000ª	9.753°	96.873ª	< .001ª	0.829
	Greenhouse-	19.506	1.113	17.533	96.873	< .001	0.829
	Geisser						
Residuals	None	4.027	40.000	0.101			
	Greenhouse-	4.027	22.251	0.181			
	Geisser						
motion	None	0.551	1.000	0.551	15.438	< .001	0.436
direction							
Residuals	None	0.714	20.000	0.036			
tACS *	None	0.010ª	2.000°	0.005ª	0.560ª	0.576ª	0.027
congruence	Greenhouse-	0.010	1.369	0.007	0.560	0.513	0.027
	Geisser						
Residuals	None	0.346	40.000	0.009			
	Greenhouse-	0.346	27.383	0.013			
	Geisser						
tACS *	None	0.005	1.000	0.005	0.506	0.485	0.025
motion							
direction							
Residuals	None	0.202	20.000	0.010			
congruence *	None	0.457	2.000	0.229	10.388	< .001	0.342
motion	Greenhouse-	0.457	1.670	0.274	10.388	< .001	0.342
direction	Geisser						
Residuals	None	0.881	40.000	0.022			

	Greenhouse-	0.881	33.400	0.026			
	Geisser						
tACS *	None	0.011	2.000	0.005	1.403	0.258	0.066
congruence *	Greenhouse-	0.011	1.827	0.006	1.403	0.258	0.066
motion	Geisser						
direction							
Residuals	None	0.156	40.000	0.004			
	Greenhouse-	0.156	36.545	0.004			
	Geisser						

Table 26 – 2x3x2 RM-ANOVA – Test of Sphericity – Accuracy (ACC) (visuotactile apparent motion)

Test of	Mauchly's	Approx.	df	p-value	Greenhouse-	Huynh-	Lower
Sphericity	W	X <sup>2</sup>			Geisser ε	Feldt ε	Bound ε
congruence	0.202	30.358	2	< .001	0.556	0.566	0.500
tACS *	0.539	11.734	2	0.003	0.685	0.718	0.500
congruence							
congruence *	0.802	4.183	2	0.123	0.835	0.902	0.500
motion direction							
tACS *	0.905	1.887	2	0.389	0.914	1.000	0.500
congruence *							
motion direction							

 $<sup>^{\</sup>rm a}$  Mauchly's test of sphericity indicates that the assumption of sphericity is violated (p < 0.05).

Table 27 – 2x3x2 RM-ANOVA – Accuracy (ACC) – post hoc comparisons of *congruence* (visuotactile apparent motion)

Post Hoc Comparisons -	Mean	SE	t	pbonf	Cohen's d
congruence	Difference				
unimodal – incongruent	0.526	0.049	10.743	<.001***	2.510
unimodal – congruent	-0.112	0.049	-2.294	0.081	-0.536
incongruent – congruent	-0.638	0.049	-13.037	<.001***	-3.046

<sup>\*</sup> p < .05, \*\*\* p < .001

Note. P-value adjusted for comparing a family of 3.

*Note.* Results are averaged over the levels of: *tACS, motion direction.* 

Table 28 – 2x3x2 RM-ANOVA – Reaction times (RT) (visuotactile apparent motion)

RM-ANOVA – Re	eaction times – W	ithin Subjects E	ffects				
Cases	Sphericity	Sum of	df	Mean	F	р	η²p
	Correction	Squares		Square			
tACS	None	0.120	1.000	0.120	0.712	0.409	0.034
Residuals	None	3.356	20.000	0.168			
congruence	None	0.887ª	2.000°	0.444ª	11.855ª	< .001ª	0.372
	Greenhouse- Geisser	0.887	1.570	0.565	11.855	< .001	0.372
Residuals	None	1.497	40.000	0.037			
	Greenhouse- Geisser	1.497	31.404	0.048			
motion direction	None	0.076	1.000	0.076	6.969	0.016	0.258

Residuals	None	0.218	20.000	0.011			
tACS *	None	0.007ª	2.000°	0.004ª	0.523ª	0.597ª	0.025
congruence	Greenhouse- Geisser	0.007	1.451	0.005	0.523	0.541	0.025
Residuals	None	0.274	40.000	0.007			
	Greenhouse- Geisser	0.274	29.018	0.009			
tACS * motion direction	None	0.003	1.000	0.003	1.046	0.319	0.050
Residuals	None	0.053	20.000	0.003			
congruence *	None	0.281ª	2.000ª	0.141ª	4.106ª	0.024ª	0.170
motion direction	Greenhouse- Geisser	0.281	1.443	0.195	4.106	0.039	0.170
Residuals	None	1.371	40.000	0.034			
	Greenhouse- Geisser	1.371	28.863	0.048			
tACS *	None	0.008ª	2.000ª	0.004ª	0.442ª	0.646ª	0.022
congruence * motion direction	Greenhouse- Geisser	0.008	1.509	0.005	0.442	0.592	0.022
Residuals	None	0.373	40.000	0.009			
	Greenhouse- Geisser	0.373	30.181	0.012			

 $^{\rm a}$  Mauchly's test of sphericity indicates that the assumption of sphericity is violated (p < 0.05).

Table 29 – 2x3x2 RM-ANOVA – Test of Sphericity – Reaction times (RT) (visuotactile apparent motion)

Test of	Mauchly's	Approx.	df	p-value	Greenhouse-	Huynh-	Lower
Sphericity	W	X <sup>2</sup>			Geisser ε	Feldt ε	Bound ε
congruence	0.726	6.076	2	0.048	0.785	0.840	0.500
tACS *	0.622	9.036	2	0.011	0.725	0.767	0.500
congruence							
congruence *	0.614	9.263	2	0.010	0.722	0.763	0.500
motion direction							
tACS *	0.675	7.478	2	0.024	0.755	0.803	0.500
congruence *							
motion direction							

Table 30 - 2x3x2 RM-ANOVA – Reaction times (RT) – post hoc comparisons of *congruence* (visuotactile apparent motion)

Post Hoc Comparisons - congruence	Mean Difference	SE	t	pbonf	Cohen's d
unimodal – incongruent	-0.073	0.030	-2.460	0.055	-0.218
unimodal – congruent	0.072	0.030	2.409	0.062	0.214
incongruent – congruent	0.145	0.030	4.869	<.001***	0.432

<sup>\*\*\*</sup>p < .001

Note. P-value adjusted for comparing a family of 3.

*Note.* Results are averaged over the levels of: *tACS, motion direction.* 

Table 31 – 2x3x2 RM-ANOVA – Rate Correct Score (RCS) (visuotactile apparent motion)

RM-ANOVA – Ra	ate Correct Score	– Within Subje	cts Effects				
Cases	Sphericity Correction	Sum of Squares	df	Mean Square	F	р	η²p
tACS	None	1.464	1.000	1.464	1.700	0.207	0.078
Residuals	None	17.222	20.000	0.861			
congruence	None	95.571ª	2.000ª	47.786ª	74.329ª	< .001ª	0.788
	Greenhouse- Geisser	95.571	1.302	73.409	74.329	< .001	0.788
Residuals	None	25.716	40.000	0.643			
	Greenhouse- Geisser	25.716	26.038	0.988			
motion direction	None	3.785	1.000	3.785	14.368	0.001	0.418
Residuals	None	5.269	20.000	0.263			
tACS *	None	0.679ª	2.000ª	0.340ª	2.252ª	0.118ª	0.101
congruence	Greenhouse- Geisser	0.679	1.170	0.580	2.252	0.144	0.101
Residuals	None	6.030	40.000	0.151			
	Greenhouse- Geisser	6.030	23.404	0.258			
tACS * motion	None	0.002	1.000	0.002	0.019	0.891	9.654×10 <sup>-</sup>
Residuals	None	1.597	20.000	0.080			

congruence *	None	3.934ª	2.000°	1.967ª	13.461ª	< .001ª	0.402
motion direction	Greenhouse-	3.934	1.823	2.157	13.461	< .001	0.402
airection	Geisser						
Residuals	None	5.845	40.000	0.146			
		5.845	36.468	0.160			
tACS *	None	0.075ª	2.000ª	0.038ª	0.688ª	0.509ª	0.033
congruence *	Greenhouse-	0.075	1.225	0.061	0.688	0.444	0.033
motion	Geisser						
direction							
Residuals	None	2.184	40.000	0.055			
	Greenhouse-	2.184	24.506	0.089			
	Geisser						

Table 32 – 2x3x2 RM-ANOVA – Test of Sphericity – Rate Correct Score (RCS) (visuotactile apparent motion)

Test of	Mauchly's	Approx.	df	p-value	Greenhouse-	Huynh-	Lower
Sphericity	W	X <sup>2</sup>			Geisser ε	Feldt ε	Bound ε
congruence	0.464	14.598	2	< .001	0.651	0.678	0.500
tACS *	0.291	23.461	2	< .001	0.585	0.599	0.500
congruence							
congruence *	0.903	1.936	2	0.380	0.912	0.998	0.500
motion direction							

 $<sup>^{\</sup>rm a}$  Mauchly's test of sphericity indicates that the assumption of sphericity is violated (p < 0.05).

tACS *	0.368	19.008	2	< .001	0.613	0.632	0.500
congruence *							
motion direction							

Table 33 – 2x3x2 RM-ANOVA – Rate Correct Score (RCS) – post hoc comparisons of *congruence* (visuotactile apparent motion)

Post Hoc Comparisons – Rate Correct Score	Mean Difference	SE	t	pbonf	Cohen's d
unimodal –incongruent	1.081	0.124	8.737	<.001***	1.598
unimodal – congruent	-0.371	0.124	-2.996	0.014*	-0.548
incongruent – congruent	-1.452	0.124	-11.733	<.001***	-2.147

<sup>\*</sup> p < .05, \*\*\* p < .001

Note. P-value adjusted for comparing a family of 3.

*Note.* Results are averaged over the levels of: *tACS, motion direction.* 

Table 34 – 2x3 RM-ANOVA – sensitivity d' (visuotactile apparent motion)

RM-ANOVA – se	RM-ANOVA – sensitivity d' – Within Subjects Effects						
Cases	Sphericity Correction	Sum of Squares	df	Mean Square	F	р	η²p
		5400.00		oquu. c			
tACS	None	1.208	1.000	1.208	0.483	0.495	0.024
Residuals	None	50.050	20.000	2.502			
congruence	None	941.280ª	2.000°	470.640°	78.912ª	< .001ª	0.798
	Greenhouse- Geisser	941.280	1.182	796.084	78.912	< .001	0.798
Residuals	None	238.563	40.000	5.964			

	Greenhouse- Geisser	238.563	23.648	10.088			
tACS *	None	0.094	2.000	0.047	0.070	0.933	0.003
congruence	Greenhouse- Geisser	0.094	1.661	0.057	0.070	0.903	0.003
Residuals	None	27.066	40.000	0.677			
	Greenhouse- Geisser	27.066	33.227	0.815			

Table 35 – 2x3 RM-ANOVA – Test of Sphericity – sensitivity d' (visuotactile apparent motion)

Test of	Mauchly's	Approx.	df	p-value	Greenhouse-	Huynh-	Lower
Sphericity	W	X <sup>2</sup>			Geisser ε	Feldt ε	Bound ε
congruence	0.309	22.344	2	< .001	0.591	0.607	0.500
tACS *							
congruence	0.796	4.331	2	0.115	0.831	0.897	0.500

Table 36 – 2x3 RM-ANOVA – sensitivity d' – post hoc comparisons of *congruence* (visuotactile apparent motion)

Post Hoc Comparisons – congruence	Mean Difference	SE	t	pbonf	Cohen's d
unimodal – incongruent	4.649	0.533	8.723	<.001***	2.150
unimodal – congruent	-1.848	0.533	-3.468	0.004**	-0.855
incongruent – congruent	-6.497	0.533	-12.191	<.001***	-3.004

 $<sup>^{\</sup>rm a}$  Mauchly's test of sphericity indicates that the assumption of sphericity is violated (p < .05).

Note. Results are averaged over the levels of: tACS.

*Note.* P-value adjusted for comparing a family of 3.

\*\* p < .01, \*\*\* p < .001

Table 37 – 2x3 RM-ANOVA –criterion c (visuotactile apparent motion)

RM-ANOVA – criterion c – Within Subjects Effects							
Cases	Sphericity	Sum of	df	Mean	F	р	η²p
	Correction	Squares		Square			
tACS	None	0.290	1.000	0.290	0.894	0.356	0.043
Residuals	None	6.479	20.000	0.324			
congruence	None	5.735	2.000	2.868	7.828	0.001	0.281
	Greenhouse- Geisser	5.735	1.922	2.983	7.828	0.002	0.281
Residuals	None	14.652	40.000	0.366			
	Greenhouse- Geisser	14.652	38.448	0.381			
tACS *	None	0.324	2.000	0.162	0.881	0.422	0.042
congruence	Greenhouse- Geisser	0.324	1.919	0.169	0.881	0.419	0.042
Residuals	None	7.355	40.000	0.184			
	Greenhouse- Geisser	7.355	38.373	0.192			

*Note.* Sphericity corrections not available for factors with 2 levels.

 $<sup>^{\</sup>rm a}$  Mauchly's test of sphericity indicates that the assumption of sphericity is violated (p < .05).

Table 38 – 2x3 RM-ANOVA – Test of Sphericity – criterion c (visuotactile apparent motion)

Test of	Mauchly's	Approx.	df	p-value	Greenhouse-	Huynh-	Lower
Sphericity	W	X <sup>2</sup>			Geisser ε	Feldt ε	Bound ε
congruence	0.960	0.783	2	0.676	0.961	1.000	0.500
tACS *							
congruence	0.958	0.823	2	0.663	0.959	1.000	0.500

Table 39 – 2x3 RM-ANOVA – criterion c – post hoc comparisons of *congruence* (visuotactile apparent motion)

Post Hoc Comparisons – congruence	Mean Difference	SE	t	pbonf	Cohen's d
unimodal – incongruent	-0.404	0.132	-3.061	0.012*	-0.640
unimodal – congruent	-0.489	0.132	-3.702	0.002**	-0.775
incongruent – congruent	-0.085	0.132	-0.641	1.000	-0.134

Note. Results are averaged over the levels of: tACS.

*Note.* P-value adjusted for comparing a family of 3.

<sup>\*</sup> p < .05, \*\* p < .01, \*\*\* p < .001

## 8. List of abbreviations

ACC	accuracy
AIC	Akaike information criterion
AM	amplitude modulation
AR	aspect ratio
BPM	button pressed per minute
CDF	cumulative distribution function
CI	confidence interval
criterion (c)	decision bias / decision threshold / decision boundary
d-prime (d')	sensitivity index
EEG	electroenecephaolgraphy
fMRI	functional magnetic resonance imaging
gCDF	cumulative gamma distribution function
HD	high-density
hMT	human middle temporal (brain area)
Hz	Hertz
kΩ	kilo ohm
LTD	long-term depression
LTP	long-term potentiation
mA	milliampere
MEG	magnetoencephalography
mm	millimeter
ms	miliseconds
NPT	normalized percept time
RCS	rate correct score
RM-ANOVA	repeated measures analysis of variance
RT	reaction time
rTMS	repetitve transcranial magnetic stimulation
SAM	stroboscopic alternative motion

SDT	Signal Detection Theory
STDP	spike timing-dependent plasticity
tACS	transcranial alternating current stimulation
tDCS	transcranial direct current stimulation
tES	transcranial electric stimulation

## 9. List of illustrations

Figure 1 – C-2 tactor used in both experiments	36
Figure 2 – DC-Stimulator plus	39
Figure 3 – EASYCAP Equipment	39
Figure 4 – <i>tAC</i> S setup ( <i>in-phase</i> modeled current)	40
Figure 5 – Schematic representation of the experimental design (tactile SAM)	46
Figure 6 – Schematic representation of tACS conditions and study concept (tactile SAM)	47
Figure 7 – Detailed trial description (tactile SAM)	47
Figure 8 – <i>Unambiguous</i> tactile stimulus configuration (tactile SAM)	48
Figure 9 – Ambiguous tactile stimulus configuration (tactile SAM)	49
Figure 10 – tACS setup (in-phase modeled current, tactile SAM)	51
Figure 11 – Electrical stimulation parameters – anti-phase tACS condition (tactile SAM)	52
Figure 12 – Electrical stimulation parameters – in-phase tACS condition (tactile SAM)	52
Figure 13 – Electrical stimulation parameters – <i>sham</i> condition (tactile SAM)	53
Figure 14 $-$ Normalized percept time (NPT) in dependence of the preceding percept (tactile SAM) $$	58
Figure $15 - Violin plot - 3x2x2$ RM-ANOVA Normalized percept time (NPT) – post hoc comparisons	of
tACS conditions (tactile SAM)	61
Figure $16 - \text{Line plot} - 3x2x2 \text{ RM-ANOVA Normalized percept time (NPT)} - Interaction of \textit{tACS} and$	
perceived motion direction (tactile SAM)	62
Figure 17 – Violin plot – 3x2x2 RM-ANOVA Normalized percept time (NPT) – perceived motion	
direction (tactile SAM)	63
Figure $18 - \text{Violin plot} - 3x4x2 \text{ RM-ANOVA Normalized percept time (NPT)} - \text{post hoc comparisons}$	of
tACS conditions (tactile SAM)	65
Figure 19 – Violin plot – 3x4x2 RM-ANOVA Normalized percept time (NPT) – perceptual alteration	
(tactile SAM)	66
Figure 20 – Violin plot – $3x4x2$ RM-ANOVA Normalized percept time (NPT) – Interaction of <i>tACS</i> and	d
perceptual alteration (tactile SAM)	67
Figure $21 - \text{Line plot} - 3x4x2$ RM-ANOVA Normalized percept time (NPT) $- \text{Interaction of } \textit{perceptuce}$	וו
alteration and unambiguous start configuration (tactile SAM)	68

Figure 22 – Line plot – 3x2 RM-ANOVA horizontal-to-horizontal – Normalized percept time (NPT) –
Interaction of tACS and unambiguous start configuration (tactile SAM)
Figure 23 – Line plot – 3x2 RM-ANOVA <i>vertical-to-vertical</i> – Normalized percept time (NPT) –
Interaction of tACS and unambiguous start configuration (tactile SAM)
Figure 24 – Line plot – 3x2 RM-ANOVA horizontal-to-vertical – Normalized percept time (NPT) –
Interaction of tACS and unambiguous start configuration (tactile SAM)73
Figure 25 – Violin plot – 3x2 RM-ANOVA <i>vertical-to-horizontal</i> – Normalized percept time (NPT) –
post hoc comparisons of tACS conditions (tactile SAM)
Figure 26 – Violin plot – 3x2 RM-ANOVA <i>vertical-to-horizontal</i> – Normalized percept time (NPT) –
unambiguous start configuration (tactile SAM) condition
Figure 27 – Violin plot – 3x2x2 RM-ANOVA Button press per minute (BPM) – post hoc comparisons of
tACS conditions (tactile SAM)
Figure 28 – Violin plot – 3x2x2 RM-ANOVA Button press per minute (BPM) – perceived motion
direction (tactile SAM)80
Figure 29 – Line plot – 3x2x2 RM-ANOVA Button press per minute (BPM) – Interaction of tACS and
perceived motion direction (tactile SAM)81
Figure 30 – Line plot and violin plot– 3x2x2 RM-ANOVA Button press per minute (BPM) – Interaction
of perceived motion direction and unambiguous start configuration (tactile SAM)83
Figure 31– Gamma probability density distribution (a.) and gamma cumulative distribution function
(gCDF) (b.)88
Figure 32 – Gamma cumulative distribution functions and statistical comparisons – perceived motion
direction
Figure 33 – Gamma cumulative distribution functions and statistical comparisons – unambiguous
start condition93
Figure 34 – Gamma cumulative distribution functions and statistical comparisons – $tACS \times perceived$
motion direction94
Figure 35 – Gamma cumulative distribution functions and statistical comparisons – $tACS \times vertical$
motion percept x unambiguous start condition97
Figure 36 – Gamma cumulative distribution functions and statistical comparisons – $tACS \times horizontal$
motion percent x unambiguous start condition

Figure 37 – Mean pupil amplitude time courses and permutation statistics for all participants and all	ı
conditions	)4
Figure 38 – Mean pupil amplitude time courses and permutation statistics for distinct tACS condition	ns
	)5
Figure 39 – Schematic representation of the experimental design (visuotactile apparent motion	
perception)	23
Figure $40 - Unambiguous visuotactile stimulus configuration (a.) - (b.) unimodal tactile conditions 12$	26
(c.) – (d.) bimodal incongruent conditions	27
(e.) – (f.) bimodal congruent conditions	28
Figure 41 – tACS setup (visuotactile apparent motion)	31
Figure 42 – Electrical stimulation parameters – anti-phase tACS condition (visuotactile apparent	
motion)	32
Figure 43 – Electrical stimulation parameters – <i>in-phase tACS condition</i> (visuotactile apparent	
motion)	32
Figure 44 – Violin plot – 2x3x2 RM-ANOVA Accuracy (ACC) – post hoc comparisons of <i>congruence</i>	
(visuotactile apparent motion)	35
Figure 45 – Violin plot – 2x3x2 RM-ANOVA Accuracy (ACC) – motion direction (visuotactile apparent	
motion)	36
Figure 46 – Line plot – 2x3x2 RM-ANOVA Accuracy (ACC) – Interaction of congruence and motion	
direction (visuotactile apparent motion)	37
Figure 47 – Line plot – 2x3x2 RM-ANOVA Accuracy (ACC) – Interaction of tACS and motion direction	
(visuotactile apparent motion)	38
Figure 48 – Violin plot – 2x3x2 RM-ANOVA Rection times (RT) – post hoc comparisons of congruence	2
(visuotactile apparent motion)	41
Figure 49 – Violin plot – 2x3x2 RM-ANOVA Reaction times (RT) – motion direction (visuotactile	
apparent motion)14	42
Figure 50 – Line plot – 2x3x2 RM-ANOVA Reaction times (RT) – Interaction of congruence and motio	n
direction (visuotactile apparent motion)	43
Figure 51 – Line plot – 2x3x2 RM-ANOVA Reaction times (RT) – Interaction of tACS and motion	
direction (visuotactile apparent motion)	45

Figure 52 – Violin plot – 3x2x2 RM-ANOVA Rate Correct Score (RCS) – post hoc comparisons of	
congruence (visuotactile apparent motion)	148
Figure 53 – Violin plot – 2x3x2 RM-ANOVA Rate Correct Score (RCS) – motion direction (visuotac	ctile
apparent motion)	149
Figure 54 – Line plot – 2x3x2 RM-ANOVA Rate Correct Score (RCS) – Interaction of <i>congruence</i> a	ınd
motion direction (visuotactile apparent motion)	150
Figure 55 – Line plot – $2x3x2$ RM-ANOVA Rate Correct Score (RCS) – Interaction of <i>tACS</i> and <i>mo</i>	tion
direction (visuotactile apparent motion)	151
Figure 56 – Line plot – 2x3 RM-ANOVA sensitivity d' – Interaction of congruence and tACS	
(visuotactile apparent motion)	157
Figure 57 – Line plot – $2x3$ RM-ANOVA criterion c – Interaction of congruence and tACS (visuota	ctile
apparent motion)	159
Figure 58 – Permutational statistical analyses of correct reaction time distributions	162
Figure 59 – Permutational statistical analyses of reaction time distributions	164

## 10. List of tables

Table 1 – Signal Detection Theory – classification of response behavior1	55
Table 2 – Randomization list and basic information about the participants (tactile SAM)1	80
Table 3 – 3x2x2 RM-ANOVA – Normalized percept time (NPT) (tactile SAM)1	81
Table 4 $-$ 3x2x2 RM-ANOVA $-$ Test of Sphericity $-$ Normalized percept time (NPT) (tactile SAM) 18	83
Table 5 – 3x2x2 RM-ANOVA – Normalized percept time (NPT) – post hoc comparisons of <i>tACS</i>	
conditions (tactile SAM)18	83
Table 6 – 3x4x2 RM-ANOVA – Normalized percept time (NPT) (tactile SAM)1	84
Table 7 – 3x4x2 RM-ANOVA – Test of Sphericity – Normalized percept time (NPT) (tactile SAM) 18	86
Table 8 – 3x4x2 RM-ANOVA – Normalized percept time (NPT) – post hoc comparisons of <i>tACS</i>	
conditions (tactile SAM)18	87
Table 9 $-$ 3x4x2 RM-ANOVA $-$ Normalized percept time (NPT) $-$ post hoc comparisons of <i>perceptual</i>	
alteration (tactile SAM)13	87
Table 10 – 3x2 RM-ANOVA <i>horizontal-to-horizontal</i> – Normalized percept time (NPT) (tactile SAM)	
1	88
Table 11 – 3x2 RM-ANOVA <i>horizontal-to-horizontal</i> – Test of Sphericity – Normalized percept time	
(NPT) (tactile SAM)	89
Table 12 – 3x2 RM-ANOVA <i>vertical-to-vertical</i> – Normalized percept time (NPT) (tactile SAM) 18	89
Table $13 - 3x2$ RM-ANOVA <i>vertical-to-vertical</i> – Test of Sphericity – Normalized percept time (NPT)	
(tactile SAM)19	90
Table 14 – 3x2 RM-ANOVA <i>horizontal-to-vertical</i> – Normalized percept time (NPT) (tactile SAM) 1	91
Table $15-3x2$ RM-ANOVA horizontal-to-vertical – Test of Sphericity – Normalized percept time (NP	'T)
(tactile SAM)19	92
Table 16 – 3x2 RM-ANOVA <i>vertical-to-horizontal</i> – Normalized percept time (NPT) (tactile SAM) 1	92
Table $17 - 3x2$ RM-ANOVA <i>vertical-to-vertical</i> – Test of Sphericity – Normalized percept time (NPT)	
(tactile SAM)19	93
Table 18 – 3x2 RM-ANOVA <i>vertical-to-horizontal</i> – Normalized percept time (NPT) – post hoc	
comparisons of <i>tACS condition</i> s (tactile SAM)19	93
Table 19 – 3x2x2 RM-ANOVA – Button press per minute (BPM) (tactile SAM)19	94
Table 20 – 3x2x2 RM-ANOVA – Test of Sphericity – Button press per minute (BPM) (tactile SAM) 1	97

Table 21 – 3x2x2 RM-ANOVA – Button press per minute (BPM) – post hoc comparisons of <i>tACS</i>
conditions (tactile SAM)
Table 23 – Spearman's correlation – normalized percept time (NPT) and amplitude modulation (AM)
199
Table 24 – Randomization list and basic information about the participants (visuotactile apparent
motion perception)
Table 25 – 2x3x2 RM-ANOVA – Accuracy (ACC) (visuotactile apparent motion)
Table 26 – 2x3x2 RM-ANOVA – Test of Sphericity – Accuracy (ACC) (visuotactile apparent motion) 202
Table 27 – 2x3x2 RM-ANOVA – Accuracy (ACC) – post hoc comparisons of <i>congruence</i> (visuotactile
apparent motion)
Table 28 – 2x3x2 RM-ANOVA – Reaction times (RT) (visuotactile apparent motion)
Table 29 – 2x3x2 RM-ANOVA – Test of Sphericity – Reaction times (RT) (visuotactile apparent motion)
Table 30 – 2x3x2 RM-ANOVA – Reaction times (RT) – post hoc comparisons of <i>congruence</i>
(visuotactile apparent motion)
Table 31 – 2x3x2 RM-ANOVA – Rate Correct Score (RCS) (visuotactile apparent motion) 206
Table 32 – 2x3x2 RM-ANOVA – Test of Sphericity – Rate Correct Score (RCS) (visuotactile apparent
motion)
Table 33 – 2x3x2 RM-ANOVA – Rate Correct Score (RCS) – post hoc comparisons of <i>congruence</i>
(visuotactile apparent motion)
Table 34 – 2x3 RM-ANOVA – sensitivity d' (visuotactile apparent motion)
Table 35 – 2x3 RM-ANOVA – Test of Sphericity – sensitivity d' (visuotactile apparent motion) 209
Table $36 - 2x3$ RM-ANOVA – sensitivity d' – post hoc comparisons of <i>congruence</i> (visuotactile
apparent motion)
Table 37 – 2x3 RM-ANOVA –criterion c (visuotactile apparent motion)
Table 38 – 2x3 RM-ANOVA – Test of Sphericity – criterion c (visuotactile apparent motion) 211
Table 39 – 2x3 RM-ANOVA – criterion c – post hoc comparisons of <i>congruence</i> (visuotactile apparent
motion)

## 11. Bibliography

- Aggelopoulos, N. C. (2015). Perceptual inference. *Neuroscience & Biobehavioral Reviews*, *55*, 375–392. https://doi.org/10.1016/j.neubiorev.2015.05.001
- AKAIKE, H. (1973). Maximum likelihood identification of Gaussian autoregressive moving average models. *Biometrika*, 60(2), 255–265. https://doi.org/10.1093/biomet/60.2.255
- Amemiya, T., Beck, B., Walsh, V., Gomi, H., & Haggard, P. (2017). Visual area V5/hMT+ contributes to perception of tactile motion direction: a TMS study. *Scientific Reports*, 7(1). https://doi.org/10.1038/srep40937
- Anderson, N. D. (2015). Teaching signal detection theory with pseudoscience. *Frontiers in Psychology*, 6. https://doi.org/10.3389/fpsyg.2015.00762
- Antal, A., & Herrmann, C. (2016). Transcranial alternating current and random noise stimulation: possible mechanisms. *Neural Plasticity*, 2016, 1–12. https://doi.org/10.1155/2016/3616807
- Berger, H. (1929). Über das Elektrenkephalogramm des Menschen. *Archiv Für Psychiatrie Und Nervenkrankheiten*, *87*(1), 527–570. https://doi.org/10.1007/bf01797193
- Bikson, M., Esmaeilpour, Z., Adair, D., Kronberg, G., Tyler, W. J., Antal, A., Datta, A., Sabel, B. A.,
  Nitsche, M. A., Loo, C., Edwards, D., Ekhtiari, H., Knotkova, H., Woods, A. J., Hampstead, B.
  M., Badran, B. W., & Peterchev, A. V. (2019). Transcranial electrical stimulation
  nomenclature. *Brain Stimulation*, 12(6), 1349–1366.
  https://doi.org/10.1016/j.brs.2019.07.010
- Biswas, A., Manivannan, M., & Srinivasan, M. A. (2015). Vibrotactile Sensitivity Threshold: Nonlinear Stochastic Mechanotransduction Model of the Pacinian Corpuscle. *IEEE Transactions on Haptics*, 8(1), 102–113. https://doi.org/10.1109/toh.2014.2369422
- Blake, R., & Logothetis, N. K. (2002). Visual competition. *Nature Reviews Neuroscience*, *3*(1), 13–21. https://doi.org/10.1038/nrn701
- Bland, N. S., & Sale, M. V. (2019). Current challenges: the ups and downs of tACS. *Experimental Brain Research*, 237(12), 3071–3088. https://doi.org/10.1007/s00221-019-05666-0

- Boring, E. G. (1930). A New Ambiguous Figure. *The American Journal of Psychology*, 42(3), 444. https://doi.org/10.2307/1415447
- Botev, Z. I., Grotowski, J. F., & Kroese, D. P. (2010). Kernel density estimation via diffusion. *The Annals of Statistics*, *38*(5). https://doi.org/10.1214/10-aos799
- Brascamp, J. W., Van Ee, R., Pestman, W. R., & Van Den Berg, A. V. (2005). Distributions of alternation rates in various forms of bistable perception. *Journal of Vision*, *5*(4), 1. https://doi.org/10.1167/5.4.1
- Buzsáki, G. (2002). Theta Oscillations in the Hippocampus. *Neuron*, *33*(3), 325–340. https://doi.org/10.1016/s0896-6273(02)00586-x
- Calvert, G., Spence, D. E. P. C., Department of Experimental Psychology Charles Spence, Stein, P. C. B. E., & Stein, B. C. A. E. (2004). *The Handbook of Multisensory Processes*. Amsterdam University Press.
- Carter, O., Konkle, T., Wang, Q., Hayward, V., & Moore, C. (2008). Tactile Rivalry Demonstrated with an Ambiguous Apparent-Motion Quartet. *Current Biology*, *18*(14), 1050–1054. https://doi.org/10.1016/j.cub.2008.06.027
- Chaudhuri, A., & Glaser, D. A. (1991). Metastable motion anisotropy. *Visual Neuroscience*, *7*(5), 397–407. https://doi.org/10.1017/s0952523800009706
- Clayton, M. S., Yeung, N., & Cohen Kadosh, R. (2018). The many characters of visual alpha oscillations. *European Journal of Neuroscience*, *48*(7), 2498–2508. https://doi.org/10.1111/ejn.13747
- Cohen, M. X. (2017). 15. Nonparametric Statistics. In *MATLAB for Brain and Cognitive Scientists*. MIT Press.
- Crick, F., & Koch, C. (2003). A framework for consciousness. *Nature Neuroscience*, *6*(2), 119–126. https://doi.org/10.1038/nn0203-119
- Darki, F., & Rankin, J. (2021). Perceptual rivalry with vibrotactile stimuli. *Attention, Perception, & Psychophysics*, 83(6), 2613–2624. https://doi.org/10.3758/s13414-021-02278-1

- De Gee, J. W., Knapen, T., & Donner, T. H. (2014). Decision-related pupil dilation reflects upcoming choice and individual bias. *Proceedings of the National Academy of Sciences of the United States of America*, 111(5). https://doi.org/10.1073/pnas.1317557111
- Desikan, R. S., Ségonne, F., Fischl, B., Quinn, B. T., Dickerson, B. C., Blacker, D., Buckner, R. L., Dale, A. M., Maguire, R. P., Hyman, B. T., Albert, M. S., & Killiany, R. J. (2006). An automated labeling system for subdividing the human cerebral cortex on MRI scans into gyral based regions of interest. *NeuroImage*, *31*(3), 968–980. https://doi.org/10.1016/j.neuroimage.2006.01.021
- Einhäuser, W., Stout, J., Koch, C., & Carter, O. (2008). Pupil dilation reflects perceptual selection and predicts subsequent stability in perceptual rivalry. *Proceedings of the National Academy of Sciences of the United States of America*, 105(5), 1704–1709. https://doi.org/10.1073/pnas.0707727105
- Engel, A. K., & Fries, P. (2010). Beta-band oscillations—signalling the status quo? *Current Opinion in Neurobiology*, 20(2), 156–165. https://doi.org/10.1016/j.conb.2010.02.015
- Engel, A. K., & Fries, P. (2016). Neuronal Oscillations, Coherence, and Consciousness. *The Neurology of Conciousness*, 49–60. https://doi.org/10.1016/b978-0-12-800948-2.00003-0
- Engel, A. K., Fries, P., & Singer, W. (2001). Dynamic predictions: Oscillations and synchrony in top—down processing. *Nature Reviews Neuroscience*, *2*(10), 704–716. https://doi.org/10.1038/35094565
- Engel, A. K., König, P., Kreiter, A. K., & Singer, W. (1991). Interhemispheric Synchronization of Oscillatory Neuronal Responses in Cat Visual Cortex. *Science*, *252*(5009), 1177–1179. https://doi.org/10.1126/science.252.5009.1177
- Feldman, D. C. (2012). The spike-timing dependence of plasticity. *Neuron*, *75*(4), 556–571. https://doi.org/10.1016/j.neuron.2012.08.001
- Fertonani, A., Ferrari, C., & Miniussi, C. (2015). What do you feel if I apply transcranial electric stimulation? Safety, sensations and secondary induced effects. *Clinical Neurophysiology*, 126(11), 2181–2188. https://doi.org/10.1016/j.clinph.2015.03.015

- Fries, P. (2005). A mechanism for cognitive dynamics: neuronal communication through neuronal coherence. *Trends in Cognitive Sciences*, *9*(10), 474–480. https://doi.org/10.1016/j.tics.2005.08.011
- Fries, P. (2009). Neuronal Gamma-Band Synchronization as a Fundamental Process in Cortical Computation. *Annual Review of Neuroscience*, *32*(1), 209–224. https://doi.org/10.1146/annurev.neuro.051508.135603
- Fries, P. (2015). Rhythms for Cognition: Communication through Coherence. *Neuron*, *88*(1), 220–235. https://doi.org/10.1016/j.neuron.2015.09.034
- Fröhlich, F. (2014). Endogenous and exogenous electric fields as modifiers of brain activity: rational design of noninvasive brain stimulation with transcranial alternating current stimulation.

  Dialogues in Clinical Neuroscience, 16(1), 93–102.

  https://doi.org/10.31887/dcns.2014.16.1/ffroehlich
- Gazzaniga, M. S. (1987). Perceptual and attentional processes following callosal section in humans. *Neuropsychologia*, *25*(1), 119–133. https://doi.org/10.1016/0028-3932(87)90048-0
- Goldstein, E. B. (2009). Encyclopedia of Perception. SAGE Publications.
- Goodale, M. A., & Milner, A. (1992). Separate visual pathways for perception and action. *Trends in Neurosciences*, 15(1), 20–25. https://doi.org/10.1016/0166-2236(92)90344-8
- Harmony, T. (2013). The functional significance of delta oscillations in cognitive processing. *Frontiers* in *Integrative Neuroscience*, 7. https://doi.org/10.3389/fnint.2013.00083
- Harrar, V., & Harris, L. R. (2007). Multimodal Ternus: Visual, Tactile, and Visuo Tactile Grouping in Apparent Motion. *Perception*, *36*(10), 1455–1464. https://doi.org/10.1068/p5844
- HARRAR, V., WINTER, R., & HARRIS, L. R. (2008). Visuotactile apparent motion. *Perception & Psychophysics*, 70(5), 807–817. https://doi.org/10.3758/pp.70.5.807
- Herrmann, C. S., Fründ, I., & Lenz, D. (2010). Human gamma-band activity: A review on cognitive and behavioral correlates and network models. *Neuroscience & Biobehavioral Reviews*, *34*(7), 981–992. https://doi.org/10.1016/j.neubiorev.2009.09.001

- Herrmann, C. S., Strüber, D., Helfrich, R. F., & Engel, A. K. (2016). EEG oscillations: From correlation to causality. *International Journal of Psychophysiology*, *103*, 12–21. https://doi.org/10.1016/j.ijpsycho.2015.02.003
- Herweg, N. A., Solomon, E. A., & Kahana, M. J. (2020). Theta Oscillations in Human Memory. *Trends in Cognitive Sciences*, *24*(3), 208–227. https://doi.org/10.1016/j.tics.2019.12.006
- Hipp, J. F., Engel, A. K., & Siegel, M. (2011). Oscillatory Synchronization in Large-Scale Cortical Networks Predicts Perception. *Neuron*, 69(2), 387–396. https://doi.org/10.1016/j.neuron.2010.12.027
- Holmes, N. P., & Tamè, L. (2019). Locating primary somatosensory cortex in human brain stimulation studies: systematic review and meta-analytic evidence. *Journal of Neurophysiology*, *121*(1), 152–162. https://doi.org/10.1152/jn.00614.2018
- Hupé, J., Lamirel, C., & Lorenceau, J. (2009). Pupil dynamics during bistable motion perception. *Journal of Vision*, *9*(7), 10. https://doi.org/10.1167/9.7.10
- Kandel, E. R., Schwartz, J. H., Jessell, T. M., Siegelbaum, S. A., & Hudspeth, A. J. (2012). *Principles of Neural Science (Principles of Neural Science (Kandel))* (5.). McGraw-Hill Education Ltd.
- Kasten, F. H., Dowsett, J., & Herrmann, C. (2016). Sustained Aftereffect of  $\alpha$ -tACS Lasts Up to 70 min after Stimulation. *Frontiers in Human Neuroscience*, 10. https://doi.org/10.3389/fnhum.2016.00245
- Kersten, D., Mamassian, P., & Yuille, A. (2004). Object Perception as Bayesian Inference. *Annual Review of Psychology*, 55(1), 271–304. https://doi.org/10.1146/annurev.psych.55.090902.142005
- Kim, E. J., Juavinett, A. L., Kyubwa, E. M., Jacobs, M., & Callaway, E. M. (2015). Three types of cortical layer 5 neurons that differ in brain-wide connectivity and function. *Neuron*, *88*(6), 1253–1267. https://doi.org/10.1016/j.neuron.2015.11.002
- Klimesch, W. (2012). Alpha-band oscillations, attention, and controlled access to stored information.

  \*Trends in Cognitive Sciences, 16(12), 606–617. https://doi.org/10.1016/j.tics.2012.10.007

- Kloosterman, N. A., Meindertsma, T., Van Loon, A. M., Lamme, V. a. F., Bonneh, Y., & Donner, T. H. (2015). Pupil size tracks perceptual content and surprise. *European Journal of Neuroscience*, *41*(8), 1068–1078. https://doi.org/10.1111/ejn.12859
- Knyazev, G. G. (2012). EEG delta oscillations as a correlate of basic homeostatic and motivational processes. *Neuroscience & Biobehavioral Reviews*, *36*(1), 677–695. https://doi.org/10.1016/j.neubiorev.2011.10.002
- Kohler, A., Haddad, L., Singer, W., & Muckli, L. (2008). Deciding what to see: The role of intention and attention in the perception of apparent motion. *Vision Research*, *48*(8), 1096–1106. https://doi.org/10.1016/j.visres.2007.11.020
- Kornmeier, J., & Bach, M. (2012). Ambiguous Figures What Happens in the Brain When Perception

  Changes But Not the Stimulus. *Frontiers in Human Neuroscience*, 6.

  https://doi.org/10.3389/fnhum.2012.00051
- Kornmeier, J., Hein, C. M., & Bach, M. (2009). Multistable perception: When bottom-up and top-down coincide. *Brain and Cognition*, *69*(1), 138–147. https://doi.org/10.1016/j.bandc.2008.06.005
- Kraus, F., Tune, S., Obleser, J., & Herrmann, B. (2023). Neural α Oscillations and Pupil Size
  Differentially Index Cognitive Demand under Competing Audiovisual Task Conditions. *The Journal of Neuroscience*, 43(23), 4352–4364. https://doi.org/10.1523/jneurosci.2181-22.2023
- Krause, M. R., Vieira, P., Csorba, B. A., Pilly, P. K., & Pack, C. C. (2019). Transcranial alternating current stimulation entrains single-neuron activity in the primate brain. *Proceedings of the National Academy of Sciences*, *116*(12), 5747–5755. https://doi.org/10.1073/pnas.1815958116
- Lachenbruch, P. A., & Cohen, J. (1989). Statistical Power Analysis for the Behavioral Sciences (2nd ed.). *Journal of the American Statistical Association*, *84*(408), 1096. https://doi.org/10.2307/2290095
- Larsen, R. S., & Waters, J. (2018). Neuromodulatory correlates of pupil dilation. *Frontiers in Neural Circuits*, 12. https://doi.org/10.3389/fncir.2018.00021

- Lewis, J. D., Beauchamp, M. S., & DeYoe, E. A. (2000). A Comparison of Visual and Auditory Motion Processing in Human Cerebral Cortex. *Cerebral Cortex*, *10*(9), 873–888. https://doi.org/10.1093/cercor/10.9.873
- Liaci, E., Bach, M., Tebartz Van Elst, L., Heinrich, S. P., & Kornmeier, J. (2016). Ambiguity in Tactile

  Apparent Motion Perception. *PLOS ONE*, *11*(5), e0152736.

  https://doi.org/10.1371/journal.pone.0152736
- Liesefeld, H. R., & Janczyk, M. (2018). Combining speed and accuracy to control for speed-accuracy trade-offs(?). *Behavior Research Methods*, *51*(1), 40–60. https://doi.org/10.3758/s13428-018-1076-x
- Liu, A., Vöröslakos, M., Kronberg, G. M., Henin, S., Krause, M. R., Huang, Y., Opitz, A., Mehta, A. D., Pack, C. C., Krekelberg, B., Berényi, A., Parra, L. C., Melloni, L., Devinsky, O., & Buzsáki, G. (2018). Immediate neurophysiological effects of transcranial electrical stimulation. *Nature Communications*, 9(1). https://doi.org/10.1038/s41467-018-07233-7
- Macmillan, N. A., & Creelman, C. D. (2004). Detection Theory. *Detection Theory*. https://doi.org/10.4324/9781410611147
- Maunsell, J. H. R., & Van Essen, D. C. (1987). Topographic organization of the middle temporal visual area in the macaque monkey: Representational biases and the relationship to callosal connections and myeloarchitectonic boundaries. *The Journal of Comparative Neurology*, 266(4), 535–555. https://doi.org/10.1002/cne.902660407
- Maunsell, J. H., & Van Essen, D. C. (1983). Functional properties of neurons in middle temporal visual area of the macaque monkey. I. Selectivity for stimulus direction, speed, and orientation. *Journal of Neurophysiology*, 49(5), 1127–1147. https://doi.org/10.1152/jn.1983.49.5.1127
- Miles, J., & Shevlin, M. (2001) Applying Regression and Correlation: A Guide for Students and Researchers. *Sage:London*.
- Misselhorn, J., Schwab, B. C., Schneider, T. R., & Engel, A. K. (2019). Synchronization of Sensory Gamma Oscillations Promotes Multisensory Communication. *Eneuro*, *6*(5), ENEURO.0101-19.2019. https://doi.org/10.1523/eneuro.0101-19.2019

- Necker, L. (1832). LXI. Observations on some remarkable optical phænomena seen in Switzerland; and on an optical phænomenon which occurs on viewing a figure of a crystal or geometrical solid. *The London, Edinburgh, and Dublin Philosophical Magazine and Journal of Science*, 1(5), 329–337. https://doi.org/10.1080/14786443208647909
- Nolte, G., & Dassios, G. (2005). Analytic expansion of the EEG lead field for realistic volume conductors. *Physics in Medicine and Biology*, *50*(16), 3807–3823. https://doi.org/10.1088/0031-9155/50/16/010
- Noury, N., Hipp, J. F., & Siegel, M. (2016). Physiological processes non-linearly affect electrophysiological recordings during transcranial electric stimulation. *NeuroImage*, *140*, 99–109. https://doi.org/10.1016/j.neuroimage.2016.03.065
- Pascual-Marqui, R. D., Lehmann, D., Koukkou, M., Kochi, K., Anderer, P., Saletu, B., Tanaka, H., Hirata, K., John, E. R., Prichep, L., Biscay-Lirio, R., & Kinoshita, T. (2011). Assessing interactions in the brain with exact low-resolution electromagnetic tomography. *Philosophical Transactions of the Royal Society A: Mathematical, Physical and Engineering Sciences, 369*(1952), 3768–3784. https://doi.org/10.1098/rsta.2011.0081
- Patel, J., Bansal, V., Minha, P., Ho, J., Datta, A., & Bikson, M. (2009). High-Density Transcranial Direct Current Stimulation (HD-tDCS): Skin Safety and Comfort. *Journal of Medical Devices*, *3*(2). https://doi.org/10.1115/1.3147486
- Pressnitzer, D., & Hupé, J. M. (2006). Temporal Dynamics of Auditory and Visual Bistability Reveal Common Principles of Perceptual Organization. *Current Biology*, *16*(13), 1351–1357. https://doi.org/10.1016/j.cub.2006.05.054
- Radman, T., Ramos, R. L., Brumberg, J. C., & Bikson, M. (2009). Role of cortical cell type and morphology in subthreshold and suprathreshold uniform electric field stimulation in vitro.

  \*Brain Stimulation\*, 2(4), 215-228.e3. https://doi.org/10.1016/j.brs.2009.03.007
- Reato, D., Rahman, A., Bikson, M., & Parra, L. C. (2010). Low-intensity electrical stimulation affects network dynamics by modulating population rate and spike timing. *The Journal of Neuroscience*, *30*(45), 15067–15079. https://doi.org/10.1523/jneurosci.2059-10.2010

- Regan, D. (1977). Steady-state evoked potentials. *Journal of the Optical Society of America*, *67*(11), 1475. https://doi.org/10.1364/josa.67.001475
- Ress, D., Backus, B. T., & Heeger, D. J. (2000). Activity in primary visual cortex predicts performance in a visual detection task. *Nature Neuroscience*, *3*(9), 940–945. https://doi.org/10.1038/78856
- Rose, M. (2005). Neural Coupling Binds Visual Tokens to Moving Stimuli. *Journal of Neuroscience*, 25(44), 10101–10104. https://doi.org/10.1523/jneurosci.2998-05.2005
- Sanchez, G., Hartmann, T., Fuscà, M., Demarchi, G., & Weisz, N. (2020). Decoding across sensory modalities reveals common supramodal signatures of conscious perception. *Proceedings of the National Academy of Sciences*, *117*(13), 7437–7446. https://doi.org/10.1073/pnas.1912584117
- Saturnino, G. B., Madsen, K. H., Siebner, H. R., & Thielscher, A. (2017). How to target inter-regional phase synchronization with dual-site Transcranial Alternating Current Stimulation.

  NeuroImage, 163, 68–80. https://doi.org/10.1016/j.neuroimage.2017.09.024
- Schwab, B. C., Misselhorn, J., & Engel, A. (2019). Modulation of large-scale cortical coupling by transcranial alternating current stimulation. *Brain Stimulation*, *12*(5), 1187–1196. https://doi.org/10.1016/j.brs.2019.04.013
- Schwartz, J. L., Grimault, N., Hupé, J. M., Moore, B. C. J., & Pressnitzer, D. (2012). Multistability in perception: binding sensory modalities, an overview. *Philosophical Transactions of the Royal Society B: Biological Sciences*, *367*(1591), 896–905. https://doi.org/10.1098/rstb.2011.0254
- Siegel, M., Donner, T. H., & Engel, A. K. (2012). Spectral fingerprints of large-scale neuronal interactions. *Nature Reviews Neuroscience*, *13*(2), 121–134. https://doi.org/10.1038/nrn3137
- Skedung, L., Arvidsson, M., Chung, J. Y., Stafford, C. M., Berglund, B., & Rutland, M. W. (2013). Feeling Small: Exploring the Tactile Perception Limits. *Scientific Reports*, *3*(1). https://doi.org/10.1038/srep02617
- Soto-Faraco, S., Lyons, J., Gazzaniga, M., Spence, C., & Kingstone, A. (2002). The ventriloquist in motion: Illusory capture of dynamic information across sensory modalities. *Cognitive Brain Research*, *14*(1), 139–146. https://doi.org/10.1016/s0926-6410(02)00068-x

- Soto-Faraco, S., Spence, C., & Kingstone, A. (2004). Cross-Modal Dynamic Capture: Congruency Effects in the Perception of Motion Across Sensory Modalities. *Journal of Experimental Psychology: Human Perception and Performance*, *30*(2), 330–345. https://doi.org/10.1037/0096-1523.30.2.330
- Soto-Faraco, S., Väljamäe, A. (2012). Multisensory Interactions during Motion Perception: From Basic Principles to Media Applications. In: Murray MM, Wallace MT, editors. *The Neural Bases of Multisensory Processes. Boca Raton (FL): CRC Press/Taylor & Francis*. Chapter 29. PMID: 22593897.
- Spitzer, B., & Haegens, S. (2017). Beyond the Status Quo: A Role for Beta Oscillations in Endogenous Content (Re)Activation. *Eneuro*, 4(4), ENEURO.0170-17.2017. https://doi.org/10.1523/eneuro.0170-17.2017
- Spruston, N. (2008). Pyramidal neurons: dendritic structure and synaptic integration. *Nature Reviews Neuroscience*, *9*(3), 206–221. https://doi.org/10.1038/nrn2286
- Stanislaw, H., & Todorov, N. (1999). Calculation of signal detection theory measures. *Behavior Research Methods, Instruments, &Amp; Computers, 31*(1), 137–149. https://doi.org/10.3758/bf03207704
- Strüber, D., Rach, S., Trautmann-Lengsfeld, S. A., Engel, A. K., & Herrmann, C. S. (2014). Antiphasic 40 Hz Oscillatory Current Stimulation Affects Bistable Motion Perception. *Brain Topography*, 27(1), 158–171. https://doi.org/10.1007/s10548-013-0294-x
- Ulrich, D. (2002). Dendritic resonance in rat neocortical pyramidal cells. *Journal of Neurophysiology*, 87(6), 2753–2759. https://doi.org/10.1152/jn.2002.87.6.2753
- Urai, A. E., Braun, A., & Donner, T. H. (2017). Pupil-linked arousal is driven by decision uncertainty and alters serial choice bias. *Nature Communications*, 8(1). https://doi.org/10.1038/ncomms14637
- Van Kemenade, B. M., Seymour, K., Wacker, E., Spitzer, B., Blankenburg, F., & Sterzer, P. (2014).

  Tactile and visual motion direction processing in hMT+/V5. *NeuroImage*, *84*, 420–427.

  https://doi.org/10.1016/j.neuroimage.2013.09.004

- Vöröslakos, M., Takeuchi, Y., Brinyiczki, K., Zombori, T., Oliva, A., Fernández-Ruiz, A., Kozák, G., Kincses, Z. T., Iványi, B., Buzsáki, G., & Berényi, A. (2018). Direct effects of transcranial electric stimulation on brain circuits in rats and humans. *Nature Communications*, *9*(1). https://doi.org/10.1038/s41467-018-02928-3
- Vossen, A., Gross, J., & Thut, G. (2015). Alpha power increase after transcranial alternating current stimulation at alpha frequency (A-TACs) reflects plastic changes rather than entrainment.

  Brain Stimulation, 8(3), 499–508. https://doi.org/10.1016/j.brs.2014.12.004
- Vosskuhl, J., Strüber, D., & Herrmann, C. (2018). Non-invasive Brain Stimulation: a paradigm shift in understanding brain oscillations. *Frontiers in Human Neuroscience*, *12*. https://doi.org/10.3389/fnhum.2018.00211
- Weinrich, C. A., Brittain, J., Nowak, M., Salimi-Khorshidi, R., Brown, P., & Stagg, C. J. (2017).

  Modulation of long-range connectivity patterns via frequency-specific stimulation of human cortex. *Current Biology*, *27*(19), 3061-3068.e3. https://doi.org/10.1016/j.cub.2017.08.075
- Wischnewski, M., Alekseichuk, I., & Opitz, A. (2023). Neurocognitive, physiological, and biophysical effects of transcranial alternating current stimulation. *Trends in Cognitive Sciences*, *27*(2), 189–205. https://doi.org/10.1016/j.tics.2022.11.013
- Woltz, D. J., & Was, C. A. (2006, April 1). Availability of related long-term memory during and after attention focus in working memory. SpringerLink. Retrieved October 17, 2022, from https://link.springer.com/article/10.3758/BF03193587?error=cookies\_not\_supported&code =17b74793-9853-4a6a-88fd-321f3411e1d6
- Zaehle, T., Rach, S., & Herrmann, C. (2010). Transcranial alternating current stimulation enhances individual alpha activity in human EEG. *PLOS ONE*, *5*(11), e13766. https://doi.org/10.1371/journal.pone.0013766

## 12. Declaration of the personal contribution

The work was carried out at the Institute of Neurophysiology and Pathophysiology under the supervision of Prof Andreas K. Engel, MD. The study was designed in collaboration with Prof. Dr. med. Andreas K. Engel and Darius Zokai.

After familiarization by laboratory members (Jonas Misselhorn, Bettina Schwab), I carried out the experiments independently. The statistical analysis was carried out by myself.

I confirm that I wrote the manuscript independently under the supervision of Andreas K. Engel and that I did not use any sources other than those specified by me.

Hamburg, 12.01.2025

Signature

13. Eidesstattliche Versicherung

Ich versichere ausdrücklich, dass ich die Arbeit selbständig und ohne fremde Hilfe, insbesondere ohne

entgeltliche Hilfe von Vermittlungs- und Beratungsdiensten, verfasst, andere als die von mir

angegebenen Quellen und Hilfsmittel nicht benutzt und die aus den benutzten Werken wörtlich oder

inhaltlich entnommenen Stellen einzeln nach Ausgabe (Auflage und Jahr des Erscheinens), Band und

Seite des benutzten Werkes kenntlich gemacht habe. Das gilt insbesondere auch für alle Informationen

aus Internetquellen.

Soweit beim Verfassen der Dissertation KI-basierte Tools ("Chatbots") verwendet wurden, versichere

ich ausdrücklich, den daraus generierten Anteil deutlich kenntlich gemacht zu haben. Die

"Stellungnahme des Präsidiums der Deutschen Forschungsgemeinschaft (DFG) zum Einfluss

generativer Modelle für die Text- und Bilderstellung auf die Wissenschaften und das Förderhandeln

der DFG" aus September 2023 wurde dabei beachtet.

Ferner versichere ich, dass ich die Dissertation bisher nicht einem Fachvertreter an einer anderen

Hochschule zur Überprüfung vorgelegt oder mich anderweitig um Zulassung zur Promotion beworben

habe.

Ich erkläre mich damit einverstanden, dass meine Dissertation vom Dekanat der Medizinischen

Fakultät mit einer gängigen Software zur Erkennung von Plagiaten überprüft werden kann.

12.01.2025

Datum

Unterschrift

232

14. Acknowledgement

At this point I would like to express my sincere gratitude to all those who have encouraged and

supported me during the writing of this dissertation.

Firstly, I would like to express my gratitude to Prof. Andreas Karl Engel, MD, who supervised my

dissertation.

I would also like to thank the entire neurophysiology team for their encouragement and constructive

impulses during the development of this dissertation.

I would also like to thank the management of the Collaborative Research Centre 936 for their financial

support.

Special thanks are also due to all the participants in both experiments, without whose co-operation

this work would not have been possible.

Finally, I would like to express my special thanks to both my parents, who have supported me

throughout my studies and my doctorate.

Hamburg, 12.01.2025

Darius Zokai

233